

Future Residential Energy System Design

Zur Erlangung des akademischen Grades eines

Doktors der Ingenieurwissenschaften

(Dr.-Ing.)

von der KIT-Fakultät für Wirtschaftswissenschaften
des Karlsruher Instituts für Technologie (KIT)

genehmigte

Dissertation

von

Max Kleinebrahm, M.Sc.

Tag der mündlichen Prüfung: 28.02.2024

Referent: Prof. Dr. Wolf Fichtner

Korreferent: Prof. Dr. Veit Hagenmeyer

Acknowledgments

This dissertation would not have been possible without the guidance, support, and encouragement of my colleagues, friends, and family.

Firstly, I sincerely thank my doctoral supervisor, Prof. Wolf Fichtner. You create a welcoming atmosphere at the IIP, marked by constructive, open, and friendly exchanges, which makes working here a great experience. I would also like to thank Prof. Hagenmeyer for co-reviewing my dissertation, and Prof. Nickel and Prof. Terzidis for serving as committee members.

I also would like to thank my long-time group leader, Armin, for many valuable discussions. Similarly, I owe a heartfelt thank you to Russell for not only offering initial guidance but also for his infectious enthusiasm for topics like energy self-sufficiency and household energy demand, which ignited my interest in these research areas. Thank you also for finding the right words, even in difficult times.

My deepest appreciation is extended to Jann, for the immense support throughout this dissertation. As a friend and a scientific discussion partner, your calm, constructive, and occasionally ironic approach has given me the necessary perspective on my work, especially during moments of doubt.

Elias, my long-term office mate, best discussion partner on residential building topics, and friend deserves a huge thank you. I looked forward to sitting with you in the office every day and talking for hours about the craziest topics. I am sure that the 'IIP Kicker Champion' title will not be the only thing that bonds us forever.

I am also profoundly grateful to all my colleagues and friends at the IIP for their discussions, support, coffee breaks, and multiple kicker sessions. Special thanks to Christoph, Daniel, Elias, Emil, Felix, Florian, Hans, Jann, Joris, Katrin, Manuel, Nina, Rafael, Richard, Thomas, Thorsten, Viktor, and Ümit. Additionally, a big thanks goes out to my research group, including Leandra, Tim, Anthony, and Thomas, for their understanding and support, particularly during the crucial final phase of my dissertation. I look forward to continuing working with you.

Over the past seven years, I have had the privilege of meeting many incredible individuals in Karlsruhe who have made my time here unforgettable. A heartfelt thank you to Jakob, Jonas, Kay, Marit, Razan, Rebecca, and all my friends at KTV and DJK! Thanks also to the Siegburg/Cologne crew. Time spent with you is always special, and I look forward to "coming home" more often in the future.

Lastly, but most importantly, I must acknowledge the unconditional support of my family. You mean the world to me. Thank you to my mum Maria, my dad Michael, and my brother Malte for everything.

Abstract

The objective of greenhouse gas-neutral economies and associated advancements in low-carbon technologies lead to a transformation of the way electricity and heat are supplied and consumed. Across the residential sector, rising energy procurement costs alongside decreasing capital costs for renewable energy technologies have driven recent trends toward individual and independent energy supply systems. Further, the electrification of mobility and heating will fundamentally change the structure of electricity demand. A comprehensive understanding of the underlying drivers that shape residential energy demand and supply is essential for designing future energy systems. Models representing fundamental connections that shape energy supply and demand and extrapolate techno-economic framework conditions are needed to predict future dissemination and impacts of building energy systems.

In this thesis, neural network-based approaches from the field of natural language processing are introduced to the field of behavioral modeling. The proposed methodology enables the generation of synthetic activity and mobility schedules of household occupants, which form the basis for a consistent simulation of residential electricity, heat, and mobility demand. Based on a detailed understanding of residential energy demand, a bottom-up framework for determining the cost-minimal design and operation of residential energy systems is presented for analyzing buildings under diverse techno-economic framework conditions. Finally, a building owner's microeconomic perspective is expanded by a central planner's macroeconomic perspective to comprehensively analyze the transformation of residential building stocks within the transformation of the surrounding municipal and national energy systems. Through the detailed representation of the heterogeneity and temporal inertia of local building stocks, existing shortcomings of a highly aggregated building stock representation are overcome.

The bottom-up framework is applied to evaluate the potential of a self-sufficient energy supply for 41 million single-family buildings in the European building stock. Cost-minimal and self-sufficient energy systems are calculated for 4,000 representative buildings on a high-performance computing cluster. Finally, surrogate models transfer the results to the entire building stock. The results show that under current techno-economic conditions, 53% of the 41 million buildings can technically supply themselves by only using local rooftop solar irradiation. If building owners would be willing to pay a premium of up to 50% compared with grid-dependent systems with electrified heat supplies, over two million buildings could leave the grid by 2050. Results for municipal building stock transformations from the perspective of a central planner for the exemplary city of Karlsruhe indicate that an increase of the retrofit rate to 2% per year and substantial electrification of the heat supply in the building sector is economically and ecologically beneficial.

List of included articles

1. Kleinebrahm, Max; Torriti, Jacopo; McKenna, Russell; Ardone, Armin; Fichtner, Wolf (2021): Using neural networks to model long-term dependencies in occupancy behavior. In *Energy and Buildings* 240 (3–4), Article 110879. DOI: [10.1016/j.enbuild.2021.110879](https://doi.org/10.1016/j.enbuild.2021.110879).
2. Kleinebrahm, Max; Weinand, Jann Michael; Naber, Elias; McKenna, Russell; Ardone, Armin; Fichtner, Wolf (2023b): Two million European single-family homes could abandon the grid by 2050. In *Joule* 7 (11), pp. 2485–2510. DOI: [10.1016/j.joule.2023.09.012](https://doi.org/10.1016/j.joule.2023.09.012).
3. Kleinebrahm, Max; Weinand, Jann Michael; Naber, Elias; McKenna, Russell; Ardone, Armin (2023a): Analysing municipal energy system transformations in line with national greenhouse gas reduction strategies. In *Applied Energy* 332, Article 120515. DOI: [10.1016/j.apenergy.2022.120515](https://doi.org/10.1016/j.apenergy.2022.120515).

Table of contents

- Acknowledgments..... i**
- Abstract..... iii**
- List of included articles.....v**
- Table of contents..... vii**
- List of figures ix**
- List of tables xi**
- Part I Overview1**
- 1 Introduction3**
- 2 Background.....7**
 - 2.1 Residential energy demand7
 - 2.1.1 Residential energy demand composition7
 - 2.1.2 Evolution of residential energy demand9
 - 2.1.3 Flexibility and timing of residential energy demand11
 - 2.1.4 Discussion and research needs.....15
 - 2.2 Residential energy system design17
 - 2.2.1 Economic framework conditions18
 - 2.2.2 Investment motives21
 - 2.2.3 The definition of self-sufficiency21
 - 2.2.4 Self-sufficient residential energy supply23
 - 2.2.5 Discussion and research needs.....26
 - 2.3 Municipal energy system transformation.....27
 - 2.3.1 Energy political framework conditions.....27
 - 2.3.2 Discussion and research needs.....30
- 3 Methodology31**
 - 3.1 Residential energy demand modeling31
 - 3.2 Residential activity modeling.....33
 - 3.2.1 Markov chain approach34
 - 3.2.2 Hierarchical regression approach.....36
 - 3.2.3 Neural network approach.....36

| | |
|--|-----------|
| 3.3 Residential building stock energy system optimization..... | 39 |
| 3.3.1 Synthetic building stock | 41 |
| 3.3.2 Energy system design | 42 |
| 3.3.3 Complexity reduction | 43 |
| 3.4 Municipal energy system transformation..... | 45 |
| 3.4.1 Municipal energy system optimization..... | 46 |
| 3.4.2 Residential building stock transformation | 47 |
| 4 Summaries of papers and results..... | 49 |
| 4.1 Paper A: Using neural networks to model long-term dependencies in occupancy behavior ... | 49 |
| 4.1.1 Objective and significance..... | 50 |
| 4.1.2 Methodology..... | 50 |
| 4.1.3 Key findings and discussion | 51 |
| 4.2 Paper B: Two million European single-family homes could abandon the grid by 2050 | 51 |
| 4.2.1 Objective and significance..... | 52 |
| 4.2.2 Methodology..... | 53 |
| 4.2.3 Key findings and discussion | 53 |
| 4.3 Paper C: Analysing municipal energy system transformations in line with national greenhouse gas reduction strategies | 54 |
| 4.3.1 Objective and significance..... | 55 |
| 4.3.2 Methodology..... | 56 |
| 4.3.3 Key findings and discussion | 56 |
| 5 Critical reflection | 59 |
| 6 Summary, conclusion, and outlook..... | 65 |
| 7 References | 69 |
| Part II Research Papers..... | 83 |
| Paper A Using neural networks to model long-term dependencies in occupancy behavior | 85 |
| Paper B Two million European single-family homes could abandon the grid by 2050..... | 107 |
| Paper C Analysing municipal energy system transformations in line with national greenhouse gas reduction strategies | 175 |

List of figures

| | |
|---|----|
| Figure 1: Composition of final energy consumption and greenhouse gas emissions in Germany. | 8 |
| Figure 2: Composition of the final energy demand of a German household in 2021 and 2045. | 11 |
| Figure 3: Daily household electricity supply, demand, and activity profiles. | 13 |
| Figure 4: Current and projected (2045) variations in household electricity demand. | 14 |
| Figure 5: European small-scale photovoltaic and residential battery storage capacity. | 18 |
| Figure 6: German economic framework conditions for PV-battery systems. | 19 |
| Figure 7: Definition of the system boundary of a residential building energy system. | 23 |
| Figure 8: Levelized Cost of Electricity of PV-battery systems in Germany in 2050. | 24 |
| Figure 9: Photovoltaic supply, electricity demand, and the degree of self-sufficiency. | 26 |
| Figure 10: Development of greenhouse gas emissions in the EU-27 member states. | 28 |
| Figure 11: Historical and future targeted renewable capacity expansion in Germany. | 29 |
| Figure 12: Bottom-up residential energy demand modeling framework. | 33 |
| Figure 13: Activity and mobility schedules from time use survey and mobility panel data. | 34 |
| Figure 14: Representation of the sequence generation process with different model approaches. | 35 |
| Figure 15: Explanation of the concept of an embedding layer. | 37 |
| Figure 16: Neural network architecture and the information flow during training process. | 38 |
| Figure 17: A framework for the evaluation of residential energy systems. | 41 |
| Figure 18: Overview of the energy system components represented in the optimization model. | 43 |
| Figure 19: Composition of the municipal energy system optimization objective function. | 47 |
| Figure 20: Stochastic process for the generation of residential building transformation scenarios. | 48 |
| Figure 21: Two-step approach for the generation of weekly activity schedules. | 49 |
| Figure 22: Municipal energy system components and energy carrier flows. | 55 |

List of tables

| | |
|--|----|
| Table 1: An overview of selected models for modeling occupancy behavior..... | 36 |
| Table 2: Overview of the developed framework modules. | 40 |
| Table 3: Extensions of the municipal energy system optimization model RE ³ ASON. | 46 |

Part I

Overview

1 Introduction

The German residential sector accounted for 28% of the total final energy demand in 2021 and was responsible for 24% of the caused greenhouse gas emissions¹. 45% of the residential sector-related emissions were generated directly through the combustion of fossil fuels to provide heat within buildings. The remaining emissions originated outside the building boundary in the energy carrier supply chains. These emissions must be cut to achieve climate neutrality in Germany by 2045 (Bundesregierung 2021).

The development of pathways to achieve a greenhouse gas-neutral energy system is a highly complex task that requires the consideration of a multitude of interests among stakeholders and is subject to many uncertainties. Specifically, in the residential sector, the increasing diffusion of novel technologies for the generation, storage, and conversion of electricity and heat, along with the growing popularity of electromobility, creates interfaces between sectors that were previously analyzed independently. In recent studies, sector-coupling measures in the building sector are often underrepresented, with a greater emphasis on reducing direct emissions through efficiency measures and low-carbon heat provision technologies (SKN et al. 2022). Studies focussing on sector-coupling within residential buildings or between the residential building stock and the overarching energy system highlight the importance of integrated approaches, especially for the evaluation of sector-coupling technologies like heat pumps, co-generation units, and photovoltaic systems (Kotzur 2018; Zeyen et al. 2021).

To examine sector-coupled residential building energy systems with an integrated consideration of the demand for thermal comfort, electric devices, and mobility, fundamental dependencies that shape the timing of energy demand need to be understood. Over the last years, a variety of bottom-up models have been published to simulate household energy demand based on occupant behavior (Proedrou 2021). While these models can represent aggregate energy demand fluctuations of multiple households, individual demand profiles are of low quality, often due to a poor representation of the underlying occupant behavior. Therefore, models capable of representing complex dependencies in occupant activity and mobility data are needed to provide a basis for consistent electricity, heat, and mobility demand profiles.

Based on a fundamental understanding of the timing of household energy demand, investments in residential renewable energy supply and storage technologies can be evaluated. While investments in energy retrofits and renewable energy technologies are mainly motivated by financial benefits, recent empirical studies indicate that building owners are willing to pay extra for high degrees of self-sufficiency (Acht-
nicht and Madlener 2014; Balcombe et al. 2014; Ecker et al. 2018). To anticipate the possibility of

¹ Calculated according to the polluter principle, see Figure 1 for more information.

residential buildings leaving the grid, temporal highly resolved models are needed that are capable of evaluating innovative technologies under varying climatic and techno-economic conditions from the perspective of building owners.

In addition to approaches for examining cost-minimal building energy systems from a microeconomic perspective, macroeconomic approaches are needed to evaluate building stock transformations from the viewpoint of a central planner to identify optimal transformation strategies. The transformation of the residential building stock should not be examined in isolation from the transformation of the surrounding energy system but instead embedded in municipal and national transformation strategies. Therefore, tools are needed to support local planners in determining optimal energy system transformations. These tools should account for national objectives like renewable expansion targets but also for local conditions such as renewable potentials and local building stock properties.

To overcome the above needs, this thesis contributes to existing research by developing a neural network-based approach to better represent occupant behavior in bottom-up household energy demand models (Paper A). Further, a bottom-up framework is presented for determining cost-minimal energy systems for residential buildings within the European building stock under current and future techno-economic conditions (Paper B). Finally, the municipal energy system optimization model RE³ASON (Mainzer 2019; Weinand 2020) is extended to analyze municipal energy system transformations in line with national greenhouse gas reduction strategies while accounting for temporal dynamic changes and the heterogeneity of the residential building stock (Paper C). Thereby, the following research questions are answered:

- How can long-term dependencies in occupancy behavior be adequately represented in bottom-up household energy demand models to provide a basis for consistent electricity, heat, and mobility demand profiles? (Paper A)
- What is the potential for self-sufficient residential building energy supply under current and future (2050) techno-economic framework conditions in Europe? (Paper B)
- How can temporally dynamic developments in the residential building stock be represented within a municipal energy system transformation in line with national greenhouse gas reduction strategies? (Paper C)

This thesis is organized in two parts. Part I provides the framework of the three papers included in the thesis. Part II contains the manuscript versions of Papers A-C.

Part I is structured as follows. First, Chapter 2 explores the evolution, current status, and future of residential energy systems, covering the dynamics of energy demand, the shift towards local self-supply, and the necessity for integrated building stock transformation approaches within municipal energy sys-

tems. Chapter 3 provides an overview of the used and developed models and highlights the methodological research delta of this thesis. Chapter 4 summarizes the three papers and presents their key findings. Chapter 5 critically reflects the limits of the proposed methods and provides suggestions for further research. Finally, Chapter 6 summarizes the main novelties of this work and derives conclusions.

2 Background

The impacts of human-induced climate change are already visible today through increasing extreme weather events (IPCC 2023). Globally, the energy sector is the main emitter of greenhouse gases, accounting for over 75% of total emissions (IEA 2023). A swift transition from fossil-fuelled power plants to a climate-friendly, renewable energy-based system is essential to reduce greenhouse gas emissions rapidly. Achieving a secure, economic, and environmentally friendly energy system based on 100% renewable energy requires breaking existing paradigms like "demand follows supply". Future energy systems must balance demand and supply spatially through a highly interconnected grid and locally by utilizing demand-side flexibilities. Alongside the industrial, tertiary, and mobility sectors, the residential sector plays a key role in the decarbonization ambitions of several countries, with buildings and households accounting for significant portions of energy demand and associated emissions.

This chapter discusses the current state and future transformation of residential energy systems. Section 2.1 describes the evolution of residential energy demand and discusses the underlying drivers. Section 2.2 analyses the trend towards local residential self-supply by discussing techno-economic framework conditions and non-monetary drivers. Further, a definition of self-sufficient energy systems and a literature review on self-sufficient residential energy supply systems are provided. Due to the interdependencies of the residential building stock and the surrounding energy system, integrated approaches are needed to identify optimal transformation processes. Therefore, Section 2.3 provides the background and discusses the need for integrated building transformation strategies within municipal energy systems.

2.1 Residential energy demand

2.1.1 Residential energy demand composition

The residential sector in Germany consumed 28% of the overall final energy in 2021 and was therefore responsible for 24% of the greenhouse gas emissions (see Figure 1). In the residential sector, the majority of the final energy served the energy service demand for space heating (67%) and domestic hot water (16%) (RWI 2022). The remaining 17% was used to serve the demand for process heating (e.g., cooking and washing - 6%), process cold (e.g., cooling and freezing of food - 5%), and other applications like lighting (2%), and information and communication technologies (3%) (RWI 2022).

The composition of the greenhouse gas emissions shows (see Figure 1) that nearly all of the direct emissions in the residential sector, which are caused by the local combustion of fossil fuels, can be traced back to heat supply applications. Therefore, the contribution of process heating through cooking with gas is negligible compared to the provision of heat for space heating and domestic hot water. The indirect emissions shown in Figure 1 arise in the energy carrier supply chains, e.g., when electricity or heat for district heating is generated in fossil power plants. While these emissions are attributed to the residential sector in Figure 1 (polluter principle), other studies allocate the emissions to the energy sector (source principle) (see, e.g., UBA (2023a)).

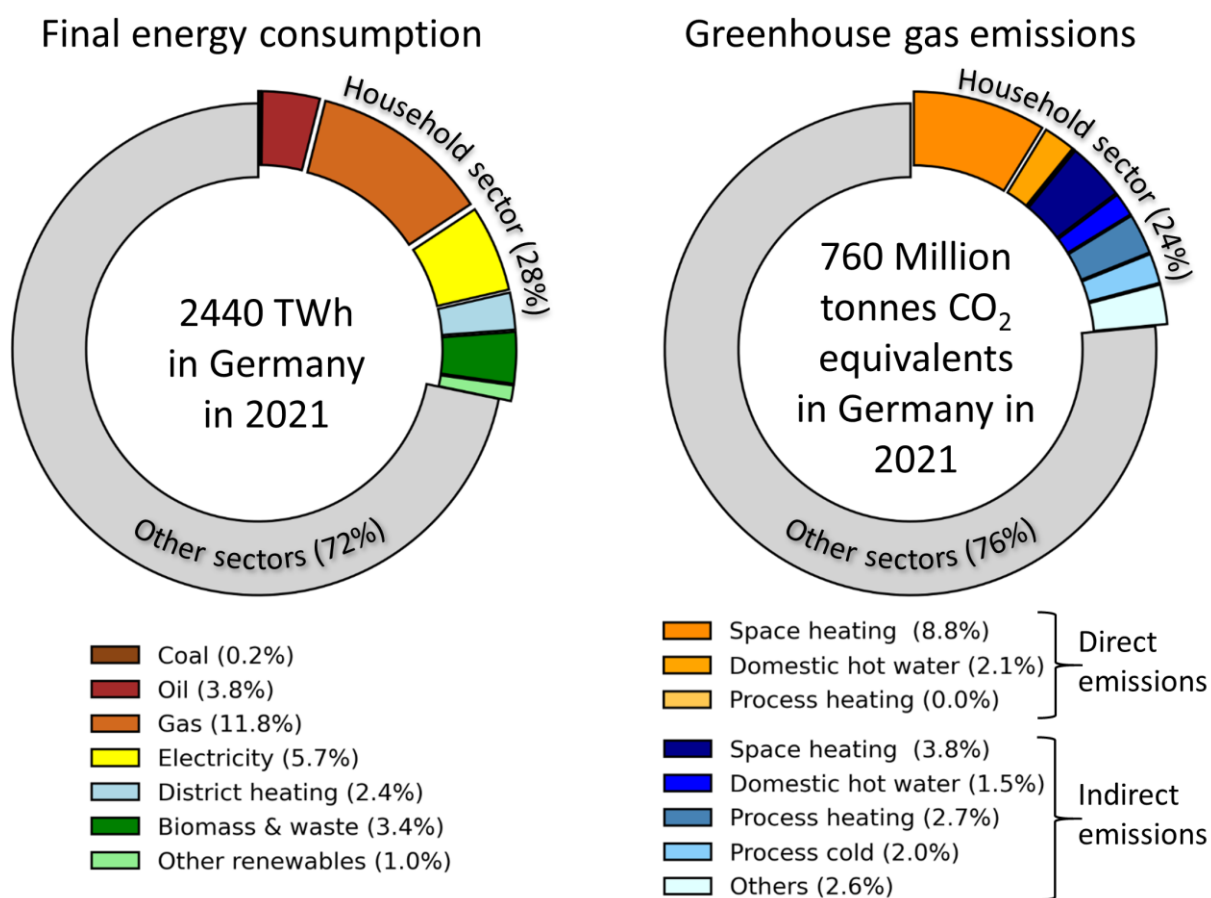


Figure 1: Composition of final energy consumption and greenhouse gas emissions in Germany. Greenhouse gas emissions are differentiated with regard to the energy service application and the location of their origin. Direct CO₂ emissions are caused by burning fossil fuels within the dwelling boundary, while indirect emissions are associated with the energy carrier supply chains. The visualizations are based on own calculations based on data from (AGEB 2023; UBA 2023a, 2023b; RWI 2022; KEA-BW 2023).

2.1.2 Evolution of residential energy demand

Between 1990 and 2021, the final energy demand in the German residential sector increased by 2%, while the living area increased by 39% (AGEB 2022; BMWK 2023a). As a result, the energy intensity, i.e., the total final energy consumption divided by living area, decreased by 26% (BMWK 2023a). The main drivers behind the decrease in energy intensity were higher energy standards for new constructions and retrofit measures for existing buildings. These measures led to a decrease in the energy demand for space heating from above 200 kWh/m² in 1990 to 125 kWh/m² in 2012 (Enerdata 2022; BMWK 2023a). Since then, the energy demand for space heating per living area has remained consistent. Other efficiency measures, such as using more energy-efficient consumer electronics or replacing light bulbs with more modern lighting, have a minor impact on final energy demand reduction. Trends towards more households, more living space, and fewer persons per household have even led to an overall slight increase in final energy demand between 1990 and 2021 (BMWK 2023a).

However, despite the slight increase in final energy demand, CO₂ emissions in the residential sector could be reduced by 40% between 1990 and 2021 (Enerdata 2022). Direct emissions decreased by 36%, mainly due to the shift from coal and heating oil to energy sources with lower carbon emissions, such as gas and renewable energy carriers (AGEB 2022; Enerdata 2022). Indirect emissions were reduced by 44% as a result of the ongoing decarbonization of the German electricity and district heating mix (UBA 2023b; AGEB 2022).

To comply with the objectives of the German Climate Protection Act, greenhouse gas emissions need to be reduced by 65% by 2030 and 88% by 2040 relative to 1990 levels, aiming to achieve greenhouse gas neutrality in Germany by 2045 (Bundesregierung 2021). Therefore, the residential sector has to reduce direct emissions by 40% by 2030 compared to 2022 levels, which means that the emission reduction speed needs to double compared to the last decade (Bundesregierung 2021; UBA 2023a). To accomplish this goal, the renovation rate of residential buildings, which has plateaued at 1% in recent years, must rise to at least 1.6% by 2030 (SKN et al. 2022). In scenarios that are in line with the German Climate Protection Act, the final energy demand for heat in the residential building sector has to be reduced by 15 to 19% by 2030 and by 35 to 47% by 2045 (BCG and BDI 2021; Prognos et al. 2021; Mellwig 2022).

In addition to reducing the final energy demand, transforming the final energy demand composition represents the second important cornerstone for achieving the climate goals. In most scenarios examined, a high degree of electrification of the residential heat demand through heat pumps is expected (SKN et al. 2022). The number of installed heat pumps in Germany is expected to increase from one million heat pumps in 2020 to five to six million in 2030 and 14 to 18 million in 2045 (Mellwig 2022; BCG and BDI 2021; Prognos et al. 2021; Luderer et al. 2021). The remaining heat demand is covered

mainly by district heating networks in areas with high heat densities, with about four to five million connected buildings in 2045 (Mellwig 2022; BCG and BDI 2021; Prognos et al. 2021). Biomass energy and renewable gases play a limited role in high electrification scenarios, primarily used for buildings that are challenging to decarbonize because of factors such as insulation restrictions due to monument protection (Prognos et al. 2021). In other scenarios where an increased prevalence of renewable gases in the building sector is expected by 2045, the primary differences from the high-electrification scenarios occur between 2030 and 2045 (Mellwig 2022; EWI 2021). Up to 2030, limited availability of greenhouse gas-neutral liquid and gaseous energy carriers is assumed, so climate goals are primarily expected to be achieved through efficiency measures and the expansion of heat pumps (ITG 2021). From 2030 onward, higher availability of renewable liquid and gaseous energy carriers is anticipated, which will reduce the pressure on buildings to be renovated and heating system technology to be exchanged (ITG 2021). Mellwig (2022) describes these scenario paths as inconsistent, as a shift towards more heat pumps is initially expected until gas boilers are resurgent.

In addition to the development of energy demand for electrical household appliances and the provision of thermal comfort, the electrification of the mobility sector (excluded in Figure 1) will increasingly influence the electric energy demand in the residential sector. At the beginning of 2023, Germany surpassed the mark of one million purely battery-electric vehicles (Kraftfahrt-Bundesamt 2023). 77% of charging processes occur at home (EUPD Research 2021), resulting in additional electricity demand of 2.2 TWh per year² in the residential sector due to electromobility. By 2045, 35 to 52 million battery-electric passenger cars are expected in Germany (TSO 2023; SKN et al. 2022). With a constant proportion of home chargers, the electrical household demand could increase by 75 to 112 TWh per year², an increase of 54 to 81% compared to the electricity demand of the residential sector in 2021 (AGEB 2023). Finally, it can be concluded that the transformation of the final energy demand of the residential sector can be primarily described by three trends:

- Reduction of energy demand through efficiency measures
- Decarbonization of heat supply through heat pumps and district heating
- Decarbonization of passenger transport through battery-electric vehicles

The effects of the described trends on the transformation of the final energy demand of a representative German household can be seen in Figure 2.

² Based on 14,000 km per year and 20 kWh/100km

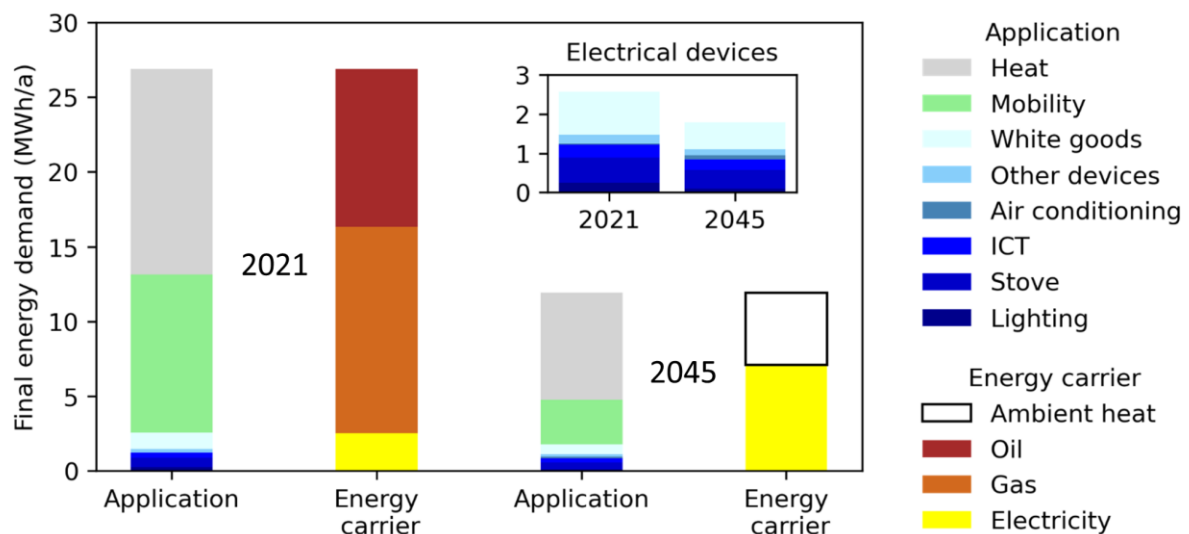


Figure 2: Composition of the final energy demand of a German household in 2021 and 2045. Calculations are conducted for an average German household size of two persons (Statista 2023a, 2023b) and a specific living area of 47 m²/person (Statista 2023c). The development and composition of the energy demand of electrical household appliances is based on the “T45-Strom” scenario presented in Mellwig (2022). For the provision of final energy demand for mobility in passenger cars and the provision of heat, the technology option most widespread in the respective year was chosen. The calculation of energy demand for mobility is based on current and future passenger car kilometers (see SKN et al. (2022)), an average occupancy rate for cars of 1.5 (FIS 2023), and assumptions about the average consumption of direct-electric cars (20 kWh/100km (Galvin 2022; Gaete-Morales et al. 2020)) and cars with combustion engines (7.7 liters of gasoline per 100km (Enerdata 2022)). The final energy demand for heating applications is based on current (140 kWh/m² (Enerdata 2022)) and future projected demands (70 kWh/m² (BCG and BDI 2021)) and an assumed coefficient of performance of the heat pump of 3.1 (Mellwig 2022).

2.1.3 Flexibility and timing of residential energy demand

In addition to decarbonizing household energy demand through efficiency measures and low-carbon technologies, flexible household loads must be identified and utilized in energy systems to help balance the fluctuating generation of renewable supply technologies (Lund et al. 2015). While the principle “supply follows demand” applied in the past, following this principle in the future would lead to oversized capacities in a highly weather-dependent energy system (Müller and Möst 2018). To avoid overcapacities and to reach an efficient future energy system, the electricity demand needs to adapt to demand-side fluctuations. For the integration of an increasing share of intermittent energy supply, models with high temporal and spatial resolution in combination with an appropriate representation of techno-economic flexibility are required (Cruz et al. 2018). An adequate representation of flexibility potentials poses a significant challenge, especially due to the high diversity of potential flexibility providers within and between the different sectors (Kachirayil et al. 2022). This challenge is even intensified by the need to consider non-technical constraints, such as potential limitations in flexibility arising from social acceptance or environmental concerns (Savvidis et al. 2019).

The electricity demand profile of the residential sector is highly correlated with electricity market prices, especially during peak demand (see Figure 3). Therefore, the flexibilization of household demand offers a particularly high potential for achieving a more efficient electricity market. Both electricity demand and market prices peak around 7 pm when people come home from work and the sun goes down. By shifting demand away from peak hours to hours with lower electricity market prices, overall system costs could be reduced (Torrìti 2014). Furthermore, high electricity market prices are correlated with high CO₂ emissions caused by fossil peak-load power plants. Therefore, a less pronounced household demand profile could reduce emissions, especially during peak demand.

In the future, the residential sector's overall and peak electricity demand are expected to increase significantly due to the expected high degree of electrification of heating and mobility demand (Fischer et al. 2020; SKN et al. 2022). Both the supply side of the electricity system and the demand side will become highly dependent on weather-related fluctuations, as seen in Figure 4. Seasonal fluctuations are mainly dominated by the seasonality of heat pump electricity demand for space heating. Without the introduction of demand response countermeasures, peak load demand in the residential sector could increase heavily, especially on cold winter evenings, due to the potential for high simultaneity of electric vehicle charging in combination with high space heating demand and relatively low heat pump efficiencies (Liu 2017; Samweber 2018). In addition to the effects on the electricity market (see above), the described developments could increase the frequency of grid congestion and voltage band violations, especially in low-voltage distribution grids to which residential buildings are typically connected (Stute and Kühnbach 2023).

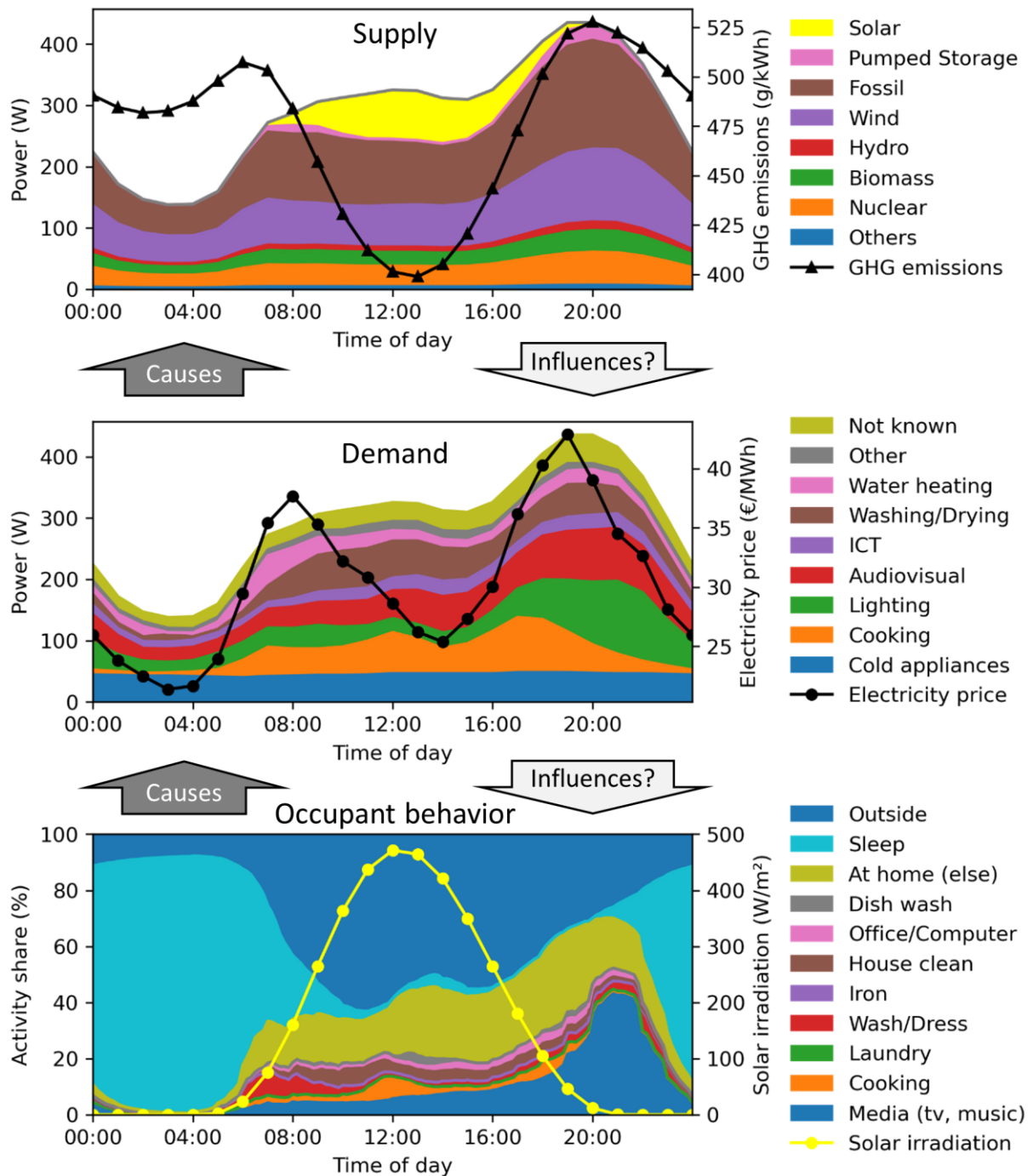


Figure 3: Daily household electricity supply, demand, and activity profiles. The average daily residential sector electricity demand profile was calculated based on smart meter data from Tjaden et al. (2015) and scaled to meet an average German yearly household demand of 2,560 kWh (Sensfuß et al. 2022). Average daily electricity provision by production type and day-ahead market prices are shown for 2020 (BNetzA 2023b; ENTSO-E 2023). The decomposition of the aggregated demand profile to device categories is based on measured data from the UK (Zimmermann et al. 2012). Energy-relevant occupant activity shares were calculated using German time use data (Destatis 2006). The average daily solar irradiation profile for a central German location was calculated based on data provided by Copernicus Climate Change Service (2017). Greenhouse gas (GHG) emissions of the German electricity mix were taken from FFE (2022).

By incentivizing flexible consumption behavior through methods like dynamic electricity price tariffs that reflect the cost of electricity generation and enhance the efficiency of the distribution grid, grid expansion can be delayed or even avoided (Hillemacher 2014; Venkatesan et al. 2011). Dynamic electricity tariffs include pricing based on power demand capacity, real-time pricing, critical peak pricing, and time-of-use (Yunusov and Torriti 2021). At the EU level, regulators have mandated utilities to offer dynamic tariffs to their customers (European Parliament and Council of the European Union 2019). Electricity suppliers in Germany must provide dynamic electricity tariffs from January 1, 2025, for all electricity suppliers according to German law (EnWG §41a). However, a technical prerequisite for the widespread adoption of dynamic electricity price tariffs is the presence of smart meters, which allow for measuring electricity demand with a high temporal granularity. Germany's smart meter roll-out is lagging, with less than 1% of households currently equipped with a smart meter (BNetzA 2022).

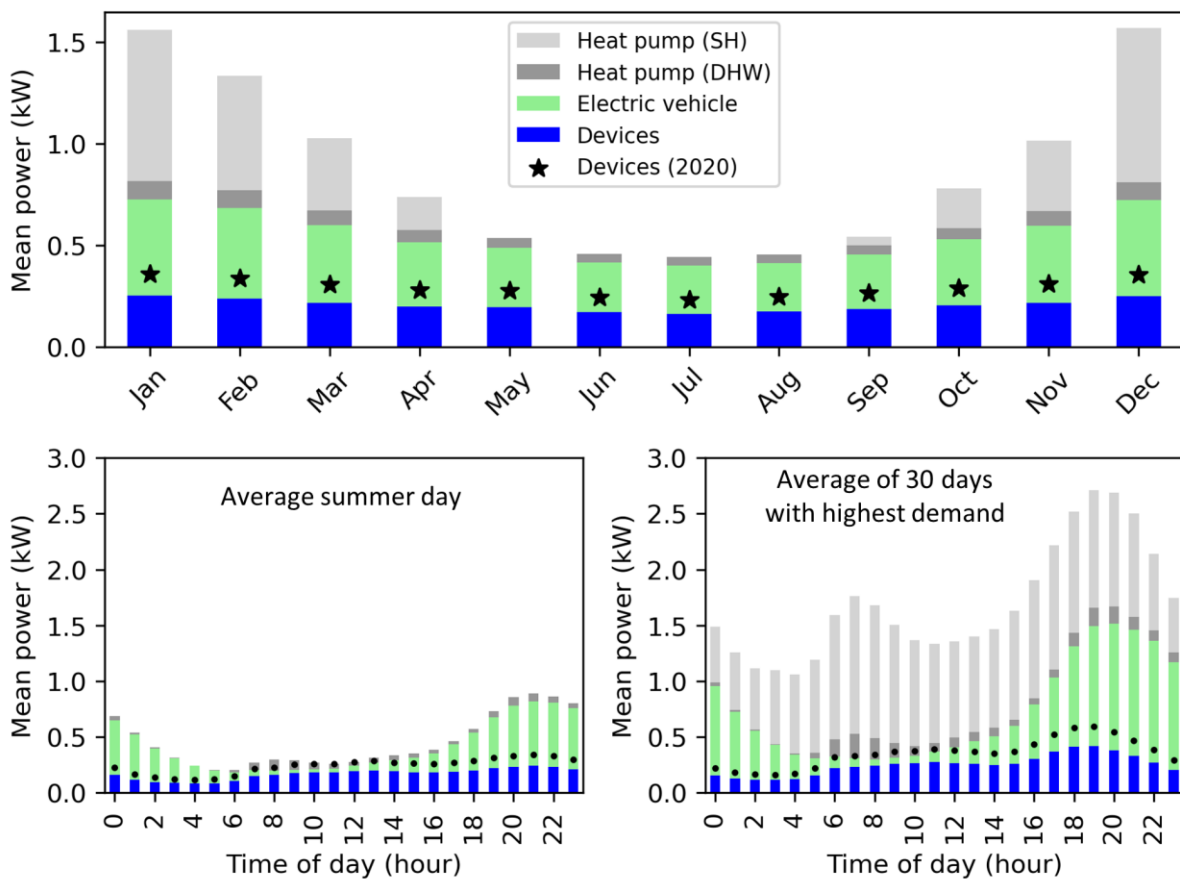


Figure 4: Current and projected (2045) variations in household electricity demand. The demand shapes of electrical household devices were calculated based on 74 yearly demand profiles provided by Tjaden et al. (2015) and scaled to meet an average German annual demand of 2,560 kWh in 2020 and 1,802 kWh in 2045 (Sensfuß et al. 2022). The electric vehicle's home charging electricity demand profile is based on the residential L1 and L2 profiles (50%/50%) presented by the California Energy Commission (2018). Temperature dependency of electric vehicle demand is considered according to Al-Wreikat et al. (2022). Further, 10,790 km per person per year (SKN et al. 2022), 1.5 people per car (infas et al. 2019), and an average household

size of two are assumed for 2045. Domestic hot water (DHW) demand is modeled according to Fischer et al. (2016), assuming a daily hot water use of 45 liters per person per day and system losses of 20% (Fuentes et al. 2018). Electricity demand profiles of the heat pump for space heating (SH) were calculated according to Ruhnau et al. (2023) based on German weather data and assumptions for the start and the end of the heating period (threshold temperature 12 °C for at least three consecutive days). The overall yearly heat demand is finally scaled to match 70 kWh per m² for space heating and domestic hot water (BCG and BDI 2021).

2.1.4 Discussion and research needs

An accurate representation of energy demand is an essential component in modeling the operation and design of building energy systems. While fluctuations on the energy supply side are mostly understood, a fundamental understanding of the underlying drivers that shape the dynamics of residential energy demand is missing. A methodology developed in 1999 for calculating the H0 standard load profile (SLP) for household customers is still used today in research (Camargo et al. 2019) and by energy utilities (Stromnetz Berlin 2023), even outside of Germany (E-Control 2023), without any major modifications (VDEW 1999). One reason for this is the low availability of energy consumption data on the residential level, which is hard to obtain, especially in combination with rich metadata (Anvari et al. 2022; Proedrou 2021).

Anvari et al. (2022) have shown that modern residential electricity load profiles strongly differ from the H0 SLP and provide a data-driven approach to extract trends and fluctuations based on smart-meter data to resolve issues related to the SLP. However, even if a substantial amount of historical smart-meter data were available to train such models, these data typically contain only aggregated information regarding energy demand (usually at the household level), obscuring the underlying devices and energy-related activities that cause the consumption. Therefore, purely data-driven approaches based on smart-meter data are suitable for representing historical or near-present trends and fluctuations in energy demand. However, they won't be helpful for predicting long-term changes that might be caused by fundamental shifts in energy-related activities, for example, through the introduction of dynamic electricity price tariffs or new technologies.

For the development of effective demand management and intelligent control systems, a detailed understanding of the diversity of energy requirements and energy-related behaviors plays a major role. Activity data-driven models offer the opportunity to explore the dependencies between household activities and the associated energy demand loads (see Figure 3) (Yamaguchi et al. 2018; Proedrou 2021). By putting individual occupants at the core of the modeling efforts, activity data-driven models are capable of representing the underlying connections between energy-related activities (e.g., cooking), energy service demand (e.g., 100°C hot water), household technologies (e.g., a stove), and the resulting energy demand (e.g., 1 kW of electricity). Only based on an understanding of these relationships that form

residential energy demand will we be able to fully assess the flexibility potential of the residential sector in a future low-carbon energy system.

An overview of existing activity data-driven models can be found in Yamaguchi et al. (2018) and Proedrou (2021). The applications of the presented models are diverse and range from forecasts of energy demand (Muratori 2018; Fischer et al. 2020), energy system analyses of residential buildings (Kotzur 2018), demand side management (Ramirez-Mendiola et al. 2022) to the evaluation of distributional effects of dynamic electricity price tariffs (Yunusov and Torriti 2021).

Most of the foundational activity models described in the literature, which serve as the basis for energy demand modeling, utilize time-use survey data and Markov chains. Time-use survey data provide information on the temporal course of occupant activities over single days and are available for various countries (Eurostat 2024). Due to the nature of the time-use survey data (only single days are recorded) and the Markov property, which refers to the memorylessness of a stochastic process, it is not possible to consider long-term dependencies over several days with existing occupant behavior models. However, an accurate mapping of long-term dependencies in behavior is of increasing interest, especially for the representation of mobility patterns, which play an important role in the derivation of charging flexibility potentials (Fischer et al. 2019). To accurately represent mobility patterns in activity data-driven models, approaches are needed that are capable of capturing complex long-term dependencies in occupant behavior. Furthermore, time-use survey datasets need to be augmented by mobility data that provide additional information on mobility patterns over multiple days.

Ultimately, future foundational activity models must be able to accurately represent the stability in individuals' or households' behaviors (high fidelity (Alaa et al. 2021)). This is essential to assess the potential for energy demand flexibility and to make informed investment decisions on the single-building level. At the same time, future models need to account for the diverse behaviors observed across different individuals or households (high diversity (Alaa et al. 2021)). This ensures a proper evaluation of potential system impacts of low-carbon technologies, such as the widespread dissemination of electric vehicles and heat pumps. By producing high-quality activity data, these foundational activity models lay the groundwork for an in-depth analysis of the primary factors influencing household energy demand in a sector-coupled energy system.

2.2 Residential energy system design

Besides the trend toward decarbonized residential heat supply, there is a growing interest in local residential energy supply systems motivated by rising energy procurement prices (Eurostat 2023a, 2023c), decreasing costs for renewable technologies (Way et al. 2022; Xiao et al. 2021) and other non-monetary criteria (Engelken et al. 2018). Photovoltaic (PV) systems are the key technology for the local provision of electricity in residential buildings. In 2022, the 27 EU Member States connected over 41 GW of PV capacity to the grid, which resulted in an increase of 47% compared to 2021 and led to a cumulative installed capacity of 209 GW (SolarPower Europe 2022b). The share of PV systems with a capacity of lower than 20 kW, which corresponds to the size of residential PV systems, accounted for 20% in 2020 (Eurostat 2023b).

Figure 5 presents the development of small-scale PV systems (< 20 kW) and residential battery storage systems in the EU27 and Norway. The inability of PV support schemes in some of the EU Member States to react fast enough to extremely rapid growth rates lead to a sharp increase in annual installed capacity till 2011 (Lacal Arantegui and Jäger-Waldau 2018). Subsequent sudden and unpredictable policy shifts dampened investment confidence, leading to a decline in annual installation rates till 2016. Since 2013, particularly in Germany, declining PV electricity remuneration payments combined with relatively high household electricity prices and subsidy programs for residential battery storage systems led to an increase in residential battery storage installations (see Figure 5) (Figgenger et al. 2020). Supported by the recent growth of the European residential solar market, which builds the foundation for a growing residential battery storage market, the average attachment rate between residential battery storage and PV systems has grown to 27% in 2021 (SolarPower Europe 2022a).

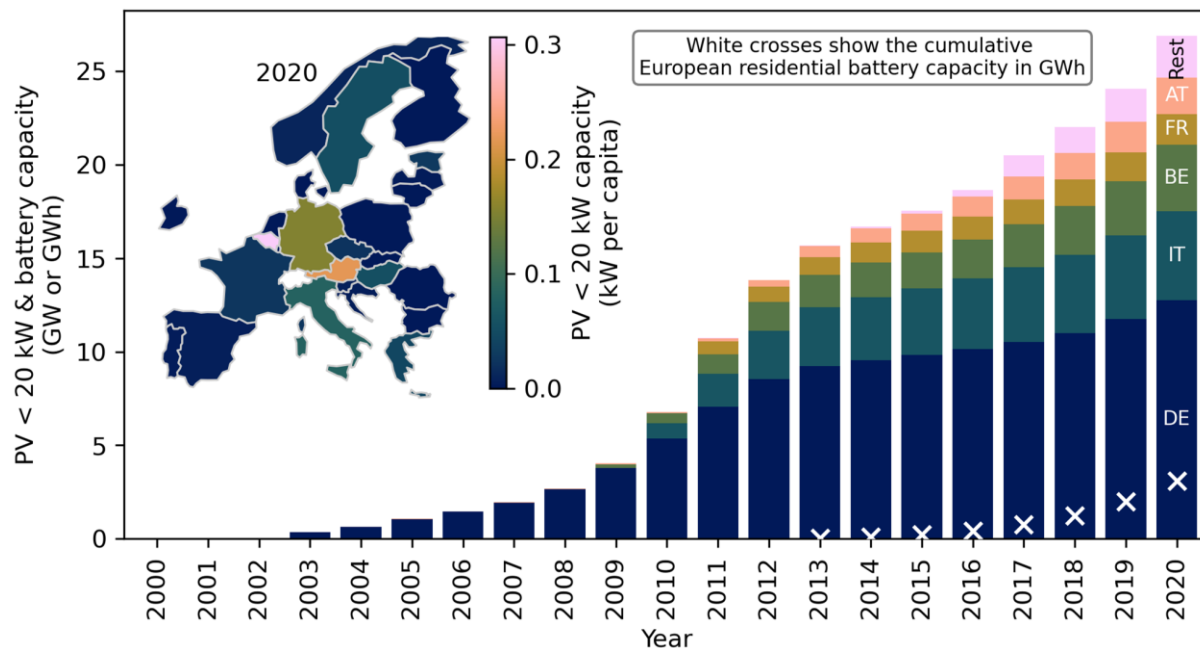


Figure 5: European small-scale photovoltaic and residential battery storage capacity. Visualized data for PV capacity development and per capita capacity are shown for the EU27 plus Norway (Eurostat 2023b, 2023d). Visualized data for residential battery capacity relate to the overall European market, with Germany (59%) and Italy (14%) as the largest sales markets in 2021 (SolarPower Europe 2022a).

2.2.1 Economic framework conditions

To better understand historical developments and to predict future dissemination of low-carbon technologies in the residential building sector, the fundamental motives on the basis of which investments in renewable technologies are made by building owners need to be understood. Profitability plays a key role in the decision whether to invest in a PV battery system (Alipour et al. 2022; Kairies et al. 2019; Engelken et al. 2018). Key factors that have an influence on the profitability of local building energy systems are energy carrier prices, technology costs, and the design of remuneration tariffs and other subsidies. In Figure 6, the development of these key factors over time can be seen for residential PV battery systems in Germany, the country with the highest number of installed residential battery storage systems in Europe (SolarPower Europe 2022a).

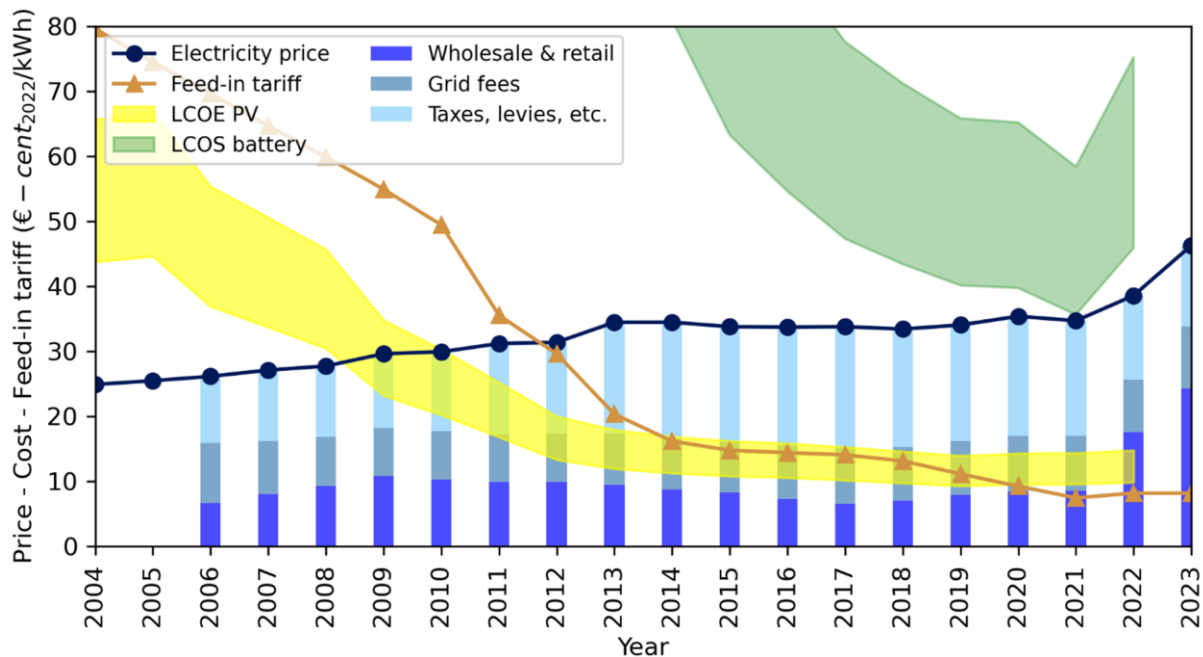


Figure 6: German economic framework conditions for PV-battery systems. German household electricity price, PV feed-in tariff (< 10 kWp), and levelized cost of electricity/storage (LCOE, LCOS) for residential PV and battery systems. The household electricity prices (BDEW 2023) and feed-in tariffs (BNetzA 2023a) shown are average yearly values. The LCOE and LCOS ranges are calculated based on residential PV and battery system prices without value added taxes (capex) (Kraschewski et al. 2023; Jaeger-Waldau 2016; Figgener et al. 2022) and further technical assumptions (PV (ISE 2021)→ lifetime (T): 25 years, annual degradation (ad): 0.25%, operational expenditures (opex): 26 €/kWp, output (E₀): 800-1200 kWh/kWp/year; battery (Schmidt et al. 2017)→ T: 10-20 years, ad: 0.5%, opex: 0 €, depth of discharge (dod): 80%, full charging cycles (cycles): 250 per year; real interest rate (i): 4%/year).

Germany has one of the highest household electricity prices in Europe (Eurostat 2023a). Since 2004, household electricity prices have experienced an inflation-adjusted average annual growth of 3.4% (2% until 2021). Before the recent energy crisis, grid fees, taxes, and levies constituted the main components of the electricity price. Since 2022, the increased costs of electricity procurement on the wholesale market have become the primary factor, which led to a significant overall household electricity price increase, even despite the elimination of the EEG (the German Renewable Energy Act) levy (BDEW 2023). In 2023, prices on the electricity wholesale market decreased again in comparison to the price peak of 2022. These price developments are not yet reflected in the procurement share of the average German household electricity price (see Figure 6). However, wholesale market prices are expected to remain at a higher average level in the coming years compared to the years before 2021 (EWI 2022; BNetzA 2023b). Electricity rates in Germany typically consist of two parts: a fixed monthly fee and a volume-based unit charge (in €/kWh) (Hinterstocker and Roon 2017). High volume-based charges serve as an incentive for self-consumption of locally generated electricity (Schill et al. 2017).

In 2000, feed-in tariffs for PV generation were introduced by the Renewable Energy Act. These tariffs guarantee a fixed remuneration over 20 years per kWh of PV electricity fed into the grid. The rate of the feed-in tariff depends on the system size and installation date. Over time, the feed-in tariff decreased in tandem with the falling costs of PV systems, which are reflected by the LCOE shown in Figure 6. The LCOEs of PV systems and LCOS of battery storage systems are calculated according to Equation 1 (Ahangharnejhad et al. 2022) and Equation 2 (Schmidt et al. 2017). Costs for the provision of electricity are not included in the LCOS.

$$\text{LCOE} = \frac{\text{capex} + \sum_{t=1}^T \frac{\text{opex}_t}{(1+i)^t}}{\sum_{t=1}^T \frac{E_0 \cdot (1-\text{ad})^t}{(1+i)^t}} \quad \text{Equation 1}$$

$$\text{LCOS} = \frac{\text{capex} + \sum_{t=1}^T \frac{\text{opex}_t}{(1+i)^t}}{\text{cycles} \cdot \text{dod} \cdot \sum_{t=1}^T \frac{(1-\text{ad} \cdot t)}{(1+i)^t}} \quad \text{Equation 2}$$

The decline in PV system prices has led to grid parity in many European countries (Bódis et al. 2019; Breyer and Gerlach 2013; Karneyeva and Wüstenhagen 2017), which refers to the point at which the cost of producing electricity is less than or equal to the cost of purchasing electricity from the grid. According to Figure 6, this point was reached in Germany around 2009. Since around 2012, the feed-in tariff for small PV systems (< 10 kWp) in Germany has fallen below the price for grid electricity. Since then, the self-consumption of PV electricity has been economically advantageous to feeding the electricity to the grid. It should be noted that this setting is mainly created by the volumetric charging of levies, taxes, and grid fees.

Due to the decline of the LCOE and LCOS of PV battery systems and the persistently high level of household electricity prices, investing in electricity storage has become increasingly interesting over the last years. However, in 2022, the cost of generating and storing one kWh of electricity still exceeded the cost of obtaining one kWh from the grid³ minus the revenues for the electricity feed-in (LCOS = 46/75 €-cent (lower/upper limit w.r.t. Figure 6) > $P_{\text{el}} - P_{\text{feed-in}} = 25$ €-cent).

In addition to the support already mentioned for local electricity generation and storage, facilitated through high volumetrically billed electricity charges and feed-in tariffs, investments in PV and battery systems received and receive further support. Support measures include a premium for self-consumed electricity (2009 to 2012), low-interest loans and subsidies for residential battery storage systems (2013

³ The volume-based charge is assumed to be 85% of the average yearly electricity price shown in Figure 6, based on a market analysis (Verivox 2023).

to 2018), and exemptions from value-added taxes (since 2023) (Schill et al. 2017; Kairies et al. 2015; § 12 UStG).

2.2.2 Investment motives

In addition to expected economic benefits, non-monetary criteria such as environmental awareness, increased self-sufficiency through independence from rising energy carrier prices, and technology affinity, among others, play an important role when investing in PV battery systems (Engelken et al. 2018; Ecker et al. 2018; Römer et al. 2015). Kairies et al. (2019) show, based on a survey conducted between 2013 and 2017 among German home storage operators, that the main drivers for investing in battery storage systems were hedging against future increases in electricity prices and the wish to proactively participate in the transition towards renewable energies (important for over 80% of participants). Additional drivers were a general interest in the technology (55%) and protection against power failures (25%). Engelken et al. (2018) investigate the motivational factors of private households in Germany to purchase renewable energy system components with the objective of partial energy self-supply. They found that perceived financial advantages and self-sufficiency benefits are the primary attitudinal factors influencing the intention to purchase renewable energy technologies. Römer et al. (2015) confirm that social norms, affinity toward autarky, and concerns about the security of supply influence the adoption of residential storage systems. Based on their previous findings, that independence of supply (autarky) and the ability to control one's own energy supply (autonomy) are the key drivers for the adoption of residential battery storage systems (Ecker et al. 2017), Ecker et al. (2018) further investigate the relative strength of the two factors for investment decisions in the realm of decentralized renewable energy system. By sketching diverse future decentralized energy scenarios, they examined homeowners' willingness to pay extra and experimentally varied the individual autarky and autonomy attained in the scenarios. They show that only autarky has a significant effect on homeowners' willingness to pay extra. In contrast to previous studies, Alipour et al. (2022) examine adoption motivations as well as barriers and show that in the mature PV market in Australia, high system costs are the main barrier to the adoption of solar PV and battery storage.

2.2.3 The definition of self-sufficiency

The expanding body of research on self-sufficient energy systems employs various terms to define the concept, including “energy autarky”, “energy autonomy”, or “off-grid”, “stand-alone”, and “island energy systems”, among others (Weinand et al. 2020b). These differing terms reflect the concept's diverse interpretations in the literature. While Ecker et al. (2018), e.g., distinguish between the terms “energy autarky” and “energy autonomy” (see Section 2.2.2), many others use the terms synonymously (Weinand et al. 2020b). The terms “energy self-sufficiency”, “energy autonomy”, and “energy autarky” are

used as synonyms from here on and refer to the independence of external energy supply. McKenna et al. (2015b) review multiple definitions of the concept of energy autonomy, highlight the most important elements, and derive a working definition. In addition to the spatial system boundary and the types of energy considered, McKenna et al. (2015b) emphasize the degree of self-sufficiency (DSS) as a crucial factor in discussions about self-sufficient energy systems. Many residential building studies calculate the DSS according to Equation 3 (see Schreiber and Hochloff (2013), Weniger et al. (2014), Widén (2014), Luthander et al. (2015), Quoilin et al. (2016), McKenna et al. (2017), Schmid and Behrendt (2022)).

$$\text{DSS} = \frac{\text{self-consumption}}{\text{demand}} = 1 - \frac{\text{import}}{\text{demand}} \quad \text{Equation 3}$$

The DSS is defined as the share of energy demand that is covered by self-consumption of locally supplied energy. Since electricity and heat are different forms of energy, assumptions regarding the energetic value of these energy forms are necessary for calculating the DSS in an integrated energy system analysis, such as employing weighting based on exergy content. From the mentioned studies that calculate the DSS according to Equation 3, only McKenna et al. (2017) and Schmid and Behrendt (2022) consider the building energy demand for heating. While McKenna et al. (2017) avoid making assumptions by only calculating the degree of electrical self-sufficiency, Schmid and Behrendt (2022) consider the heating demand indirectly by including the electricity demand of the heat pump. However, heat is also provided by the electrolyzer and the fuel cell, which is not considered when calculating the DSS.

To avoid making assumptions about the energetic values of electricity and heat in integrated energy system analysis, the DSS in this study is defined based on the system boundary depicted in Figure 7 and can be calculated using Equation 4. The central requirement of the building energy system is to cover the energy service demand of the household(s) under consideration. Based on this requirement, multiple energy systems with different equipment of energy technologies, household devices, and retrofit levels can be compared. For the calculation of the DSS, a reference system needs to be defined in advance. In Kleinebrahm et al. (2023b), e.g., the reference system is defined to be the system with maximum grid dependency, which would be the lowest cost building energy system in a theoretical world with very low energy carrier prices (energy carrier prices $\rightarrow 0$ €/kWh).

$$\text{DSS} = 1 - \frac{\text{import}}{\text{import}^{\text{reference}}} = 1 - \frac{\sum_{\text{ec}}^{\text{EC}} w_{\text{ec}} \int_t^T \text{import}_{\text{ec}}(t) dt}{\sum_{\text{ec}}^{\text{EC}} w_{\text{ec}} \int_t^T \text{import}_{\text{ec}}^{\text{reference}}(t) dt} \quad \text{Equation 4}$$

If the energy import for the building energy system under consideration is zero, the DSS reaches 100%, indicating that the energy service demand is covered completely independent of external infrastructures. Equation 4 explicitly considers varying time dimensions (T) and types of energy carriers (EC), for which

weighting factors (w_{ec}) must be defined. In contrast to the definition of the DSS by Equation 3, fewer energy imports always lead to higher DSS.

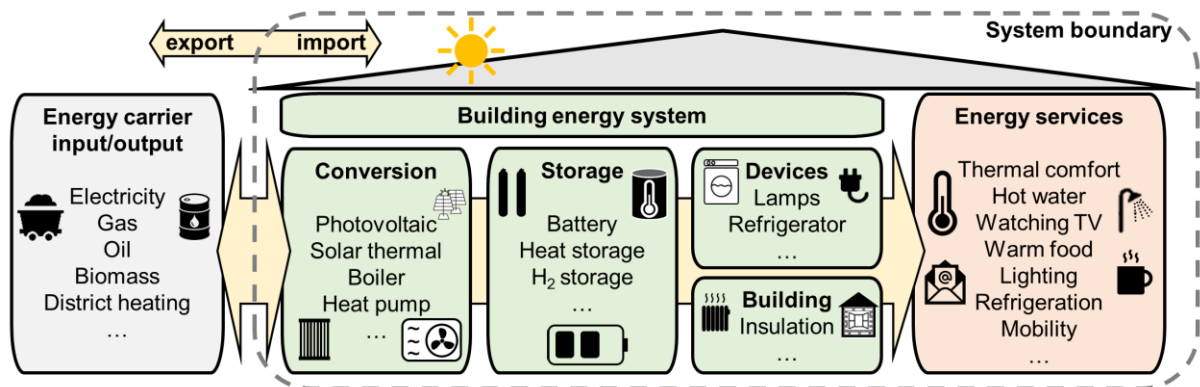


Figure 7: Definition of the system boundary of a residential building energy system.

McKenna et al. (2015b) categorize three types of self-sufficient energy systems: completely self-sufficient systems ($DSS = 100\%$), systems with balanced self-sufficiency ($export \geq import$), and systems with a tendency towards self-sufficiency ($export < import$, $self-generation > 0$). Rae and Bradley (2012) further derive three basic criteria a self-sufficient system must exhibit:

- Energy supply \geq energy demand
- Temporal energy shifting possibilities to compensate for supply/demand mismatch
- Capability to operate off-grid (for example, frequency maintenance)

These three criteria form the foundation for defining a self-sufficient building in this study. Buildings that meet only, for example, the criteria for balanced self-sufficiency are classified as partially self-sufficient buildings from now on.

2.2.4 Self-sufficient residential energy supply

Over the last decades, multiple studies have analyzed the economics of (partly) self-sufficient residential building energy systems under varying geographical, technical, and economic framework conditions.

Many of these studies limit their investigations to the self-supply of electrical demand with PV-battery systems, whereby demand-side management measures are sometimes considered (see, e.g., Widén (2014)). With a photovoltaic system alone and without behavioral interventions, an average European household can cover about a third of its electricity demand on its own (Quoilin et al. 2016; Luthander et al. 2015). Based on the presented residential battery system price developments (see Section 2.2.1) multiple studies analyzed the possibility of leaving the grid based on PV-battery systems (Sabadini and Madlener 2021; Gorman et al. 2020; Liu et al. 2019; Ramirez Camargo et al. 2018; Quoilin et al. 2016; Khalilpour and Vassallo 2015; Bianchi et al. 2014; Goldsworthy and Sethuvenkatraman 2018). Most of

the studies conducted for European residential buildings conclude that PV-battery systems must be drastically oversized to reach degrees of electrical self-sufficiency above 80% (see also Figure 8) (Quoilin et al. 2016; Khalilpour and Vassallo 2015; Sabadini and Madlener 2021; Vögele et al. 2022). A Study analyzing US households also finds that the current grid defection potential is low but could increase with utilities shifting to increased fixed charges in order to cover their non-variable costs (Gorman et al. 2020). In regions with good solar resources and high utility costs, regulators and utilities should be mindful of the scope of significant grid defection. Goldsworthy and Sethuvenkatraman (2018) analyze 28 Australian households and show that demand-side adjustments can significantly improve the economics of self-sufficient building energy systems. Even at current prices, off-grid PV-battery supply systems may be economical for some Australian households if the occupants are willing to adjust their consumption patterns in order to coincide with peak irradiance. Therefore, the authors conclude that although households disconnecting from the electricity grid might not be ideal from a macroeconomic perspective, this trend could become more prevalent.

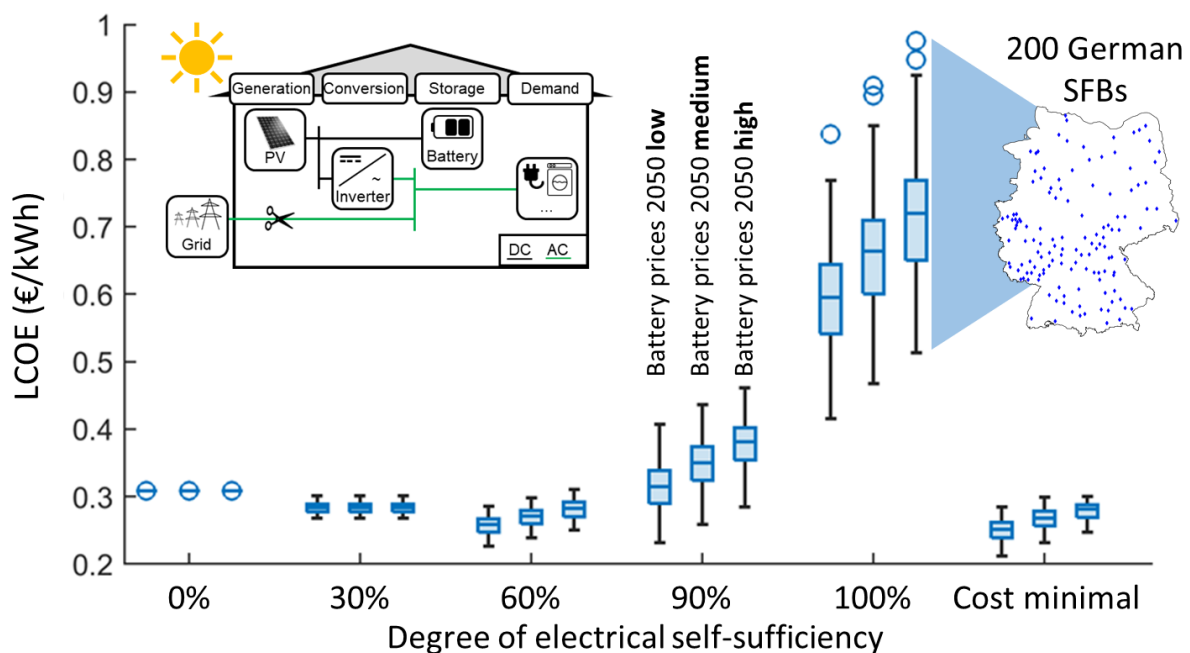


Figure 8: Levelized Cost of Electricity of PV-battery systems in Germany in 2050. Levelized Cost of Electricity (LCOE) for PV-battery systems in single-family buildings (SFBs) in Germany by 2050, varying with the degree of electrical self-sufficiency. The three battery price scenarios are outlined in Vögele et al. (2022). The LCOE variations within the degree of electrical self-sufficiency categories reflect analysis from 200 representative single-family buildings in Germany. Own figure similar to Vögele et al. (2022).

A more holistic form of local energy supply is a self-sufficient building energy system, which supplies the electricity and thermal demand 100% independent from external infrastructures. While the above studies focus exclusively on electrical self-sufficiency, the definition of self-sufficiency is extended to

include the entire residential energy demand for electrical appliances, domestic hot water, and space heating in the following (see Figure 7).

Figure 9A shows that taking thermal energy demand into account increases the seasonal mismatch between energy supply and demand. Furthermore, as depicted in Figure 9B, even without considering the limited rooftop potential for PV, it is evident that even large PV-battery systems (40 kW_p + 40 kWh) can only meet 93% of the electricity demand for household devices and electrified heating of the average German household under consideration. Additionally, over 90% of the generated PV electricity is fed back into the power grid. Due to the relatively high capacity-specific costs of battery storage and the strong seasonal fluctuations in photovoltaic feed-in, alternative storage technologies, such as seasonal thermal or hydrogen storage systems, and electricity generation technologies, such as small wind turbines, are being investigated in the literature. Lacko et al. (2014) analyze an isolated residential building in Slovenia's coastal region and compare alternative supply systems to cover heat and electricity supply. In addition to the PV system, a small wind turbine is used as a second electricity source, together with a hybrid storage system composed of a battery, seasonal thermal storage, and a hydrogen storage system. The authors conclude that 100% renewable supply systems are technically feasible and can be cost-competitive to fossil fuel-based off-grid energy supply systems. Knosala et al. (2021) compare self-sufficient energy supply systems with grid-connected systems for a single-family building in Germany. They focus on different hydrogen storage concepts and show that a reversible solid oxygen cell combined with a liquid organic hydrogen carrier system together with advanced heat integration can reduce system cost by 80% in comparison to a PV-battery-based system in 2030. However, the system cost of a 100% grid-dependent system is still 33% lower. Gstöhl and Pfenninger (2020) analyze 16 residential buildings in Switzerland for techno-economic conditions in 2050 and find that self-sufficient residential buildings may be economically viable in temperate climates, depending on storage and fossil fuel costs and available PV potential. Single-family buildings with low electricity use and urban mobility patterns are more likely to achieve self-sufficiency, while multi-family buildings with high demand and rural mobility patterns face greater challenges in grid disconnection.

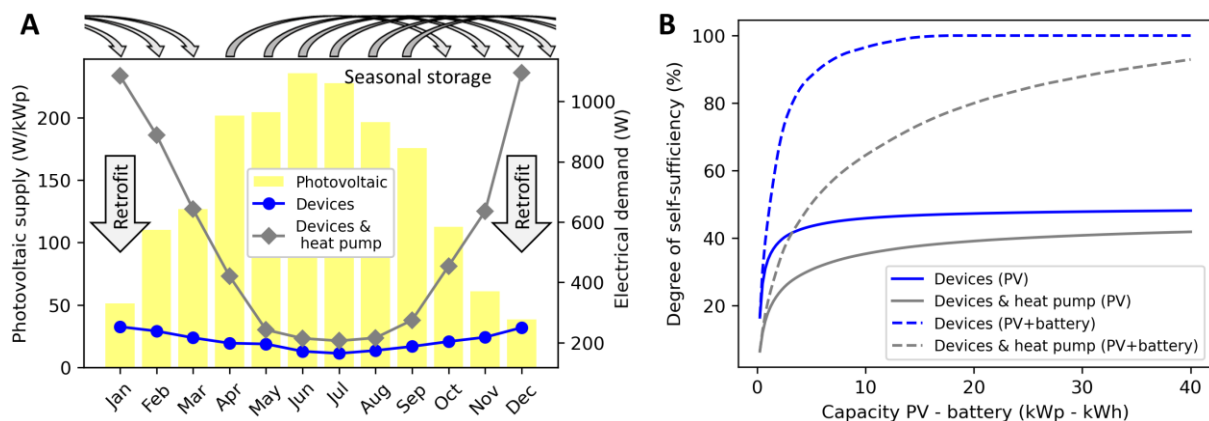


Figure 9: Photovoltaic supply, electricity demand, and the degree of self-sufficiency. Seasonal mismatch between photovoltaic supply and electricity demand (A). Degree of self-sufficiency dependent on PV-battery system size (B). The presented PV feed-in profile is calculated for a central German location based on historical weather data from 2019 and an assumed tilt (35°) and azimuth (180°) (Staffell and Pfenninger 2016). Information about the composition of the demand can be found in the caption of Figure 4. (BS: battery system).

In practice, alongside scientific research, there are already implemented concepts for energy-self-sufficient residential buildings and scalable energy systems that enable existing buildings to operate independently from the electricity grid. Prominent examples of energy-self-sufficient residential buildings include the "Solar House Freiburg" in Germany (Voss et al. 1996) and the "first energy self-sufficient multi-family house" in Switzerland (UAS 2023). Both buildings were equipped with PV and an energy storage system consisting of a battery and hydrogen storage. The building concept 'VitalSonnenhausPro' does not rely on hydrogen storage. It optimizes the use of photovoltaic and solar thermal potential in combination with a large thermal storage system and a battery (Leitl 2016). Home Power Solutions in Germany and Nilsson Energy in Sweden offer hybrid long-term storage solutions for residential buildings, specifically hydrogen/battery systems (Home Power Solution 2022; Nilsson Energy 2022). As of 2022, 80 PICEA units by Home Power Solutions have been installed, with an additional 300 units ordered in Germany (VDI 2022). For a comprehensive overview of scientific studies and practical examples of self-sufficient residential buildings, please refer to the Supplemental Information in Kleinebrahm et al. (2023b).

2.2.5 Discussion and research needs

In light of decreasing costs of renewable technologies and increasing household electricity prices over the last years, an increasing number of studies analyze the economics of (partly) self-sufficient residential energy supply systems. Despite the temporary spike in battery system costs in 2022, long-term projections indicate further decreasing costs for renewable technologies (Few et al. 2018; Schmidt et al. 2017; Schmidt et al. 2019). Additionally, empirical investigations show that homeowners' main non-

monetary motivation for investing in renewable energy supply systems is the desire for self-sufficiency, which motivates homeowners to pay extra (Engelken et al. 2018; Ecker et al. 2018). Given these developments, investigating the possibility of larger-scale dissemination of self-sufficient residential buildings becomes important in order to be able to counteract potentially suboptimal developments from a macroeconomic perspective at an early stage. Existing studies on self-sufficient residential buildings are limited in scope, focusing either on individual buildings at specific locations or only taking into account PV-battery systems when looking at a larger scale. Therefore, a large-scale study based on a unified model approach and a unified set of techno-economic assumptions is needed to analyze the current and future techno-economic potential of self-sufficient buildings, considering the diversity among building stocks of different countries, climates, building types, and household consumption characteristics.

2.3 Municipal energy system transformation

The Paris Agreement, signed in 2015, aims to reduce greenhouse gas emissions from human activities as soon as possible. Its goal is to limit global warming to well below 2°C, preferably to 1.5°C, compared to pre-industrial levels, by the end of the 21st century (UNFCCC 2015). To reach this objective, climate change mitigation strategies and energy political framework conditions with expansion targets for renewable energy sources are defined at the continental and national levels (Section 2.3.1). Due to the characteristics of renewable energy sources, their expansion is mostly decentralized. Cities, municipalities, and local stakeholders have a great interest in climate protection and sustainability, which is reflected in a multitude of initiatives at the regional and municipal level (see, e.g., Wierling et al. (2023) and Mainzer (2019)). However, small municipalities with great potential for the expansion of renewable energies often have little resources and expertise for developing energy system concepts that are in line with overarching climate protection strategies. Therefore, there is a need for automated tools to support local actors in the design process of municipal energy systems (Section 2.3.2).

2.3.1 Energy political framework conditions

Since 1990, the European Union (EU) has steadily decreased its greenhouse gas emissions, reaching a 32.5% reduction in 2022 (see Figure 10). However, to align with the legally binding targets of the EU Green Deal, which aim to reduce net greenhouse gas emissions by at least 55% by 2030 compared to 1990 levels and to achieve climate neutrality by 2050, there is a need to accelerate the pace of emissions reduction (European Parliament 2021). The goal of the “Fit for 55” legislative package is to revise and update EU legislation to align with the EU’s enhanced climate targets.

Key instruments for achieving these targets are the EU Emissions Trading System (EU ETS) and the Effort Sharing Regulation (ESR). The EU ETS covers around 36% of the EU’s total greenhouse gas

emissions in the sectors energy, industry, and aviation (European Commission 2023). The ESR, on the other hand, targets emissions reductions in the sectors transport, buildings, agriculture, small industries, and waste, collectively accounting for 60% of the EU's total greenhouse gas emissions (European Commission 2023). The ESR is implemented in the form of binding national targets. These instruments are complemented by additional directives, such as the Renewable Energy Directive and the Energy Efficiency Directive, which mandate increased utilization of renewable energy and enhanced energy efficiency measures. However, even though the EU is at the forefront of global climate protection with these instruments, Figure 10 indicates that the combined emissions of the individual EU member states, even when considering planned future measures, are currently not in line with the goals of the EU Green Deal.

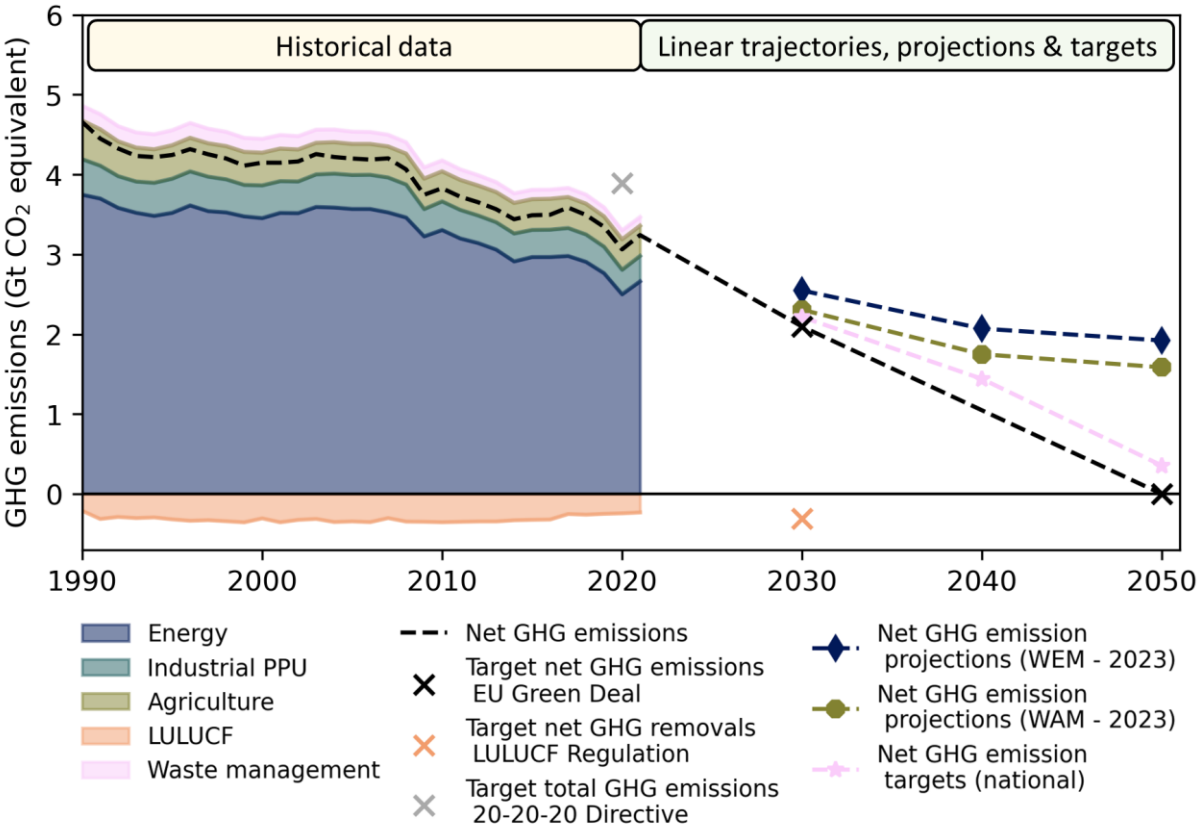


Figure 10: Development of greenhouse gas emissions in the EU-27 member states. Greenhouse gas emissions (excluding international aviation) and removals, linear trajectories to EU targets, and greenhouse gas emission projections from the EU-27 member states. Historical data on sector-specific greenhouse gas emissions were taken from (EEA 2023). Future trajectories, targets, and projections were taken from (European Commission 2023). Own illustration based on (European Commission 2023). (GHG, greenhouse gas; PPU, processes and product use; LULUCF, land use, land-use change and forestry; WEM, with existing measures; WAM, with additional planned measures).

The implementation of concrete measures and the development of long-term strategies for greenhouse gas reduction is the responsibility of the individual member states. In the German Climate Protection

Act, Germany has committed to reducing its greenhouse gas emissions by 65% by 2030 and 88% by 2040, relative to 1990 levels, with the goal of achieving greenhouse gas neutrality by 2045 (Bundesregierung 2021). With the objective of complying with these goals, the German government implemented multiple measures across the transport, energy, building, industry, and agriculture sectors (Bundesregierung 2023). One of these measures was the amendment of the EEG in January 2023, which lays the foundation for the expansion of renewable energies (see Figure 11). By 2030, over 80 percent of Germany's electricity consumption is expected to come from renewable energy sources (§ 1 EEG 2023). This means almost a doubling of the share in total electricity consumption. In order to keep up with the expansion rates, a land area target of 2% for onshore wind energy and specific area targets for federal states were legally established, minimum distance regulations were relaxed, and measures to accelerate the planning of PV and wind energy projects were implemented (Bundesregierung 2023).

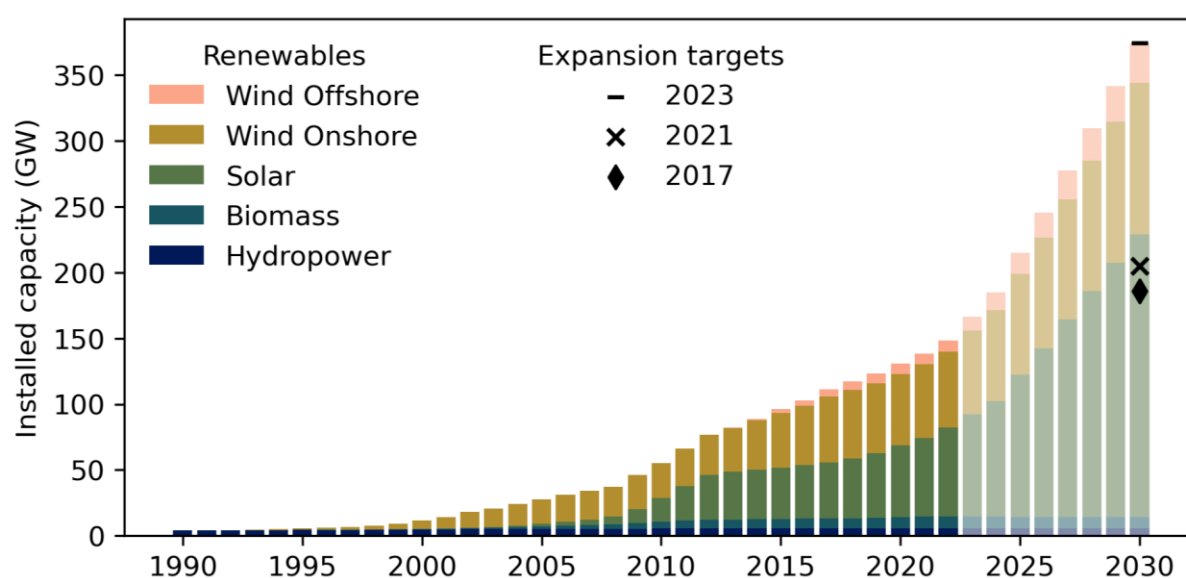


Figure 11: Historical and future targeted renewable capacity expansion in Germany. Own illustration based on historical data from the BMWK (2023b) and expansion targets from § 4 EEG (2017, 2021, 2023) and § 1 WindSeeG (2021, 2023).

In the building sector, around 80% of the heat demand in buildings is currently covered by the use of fossil fuels such as gas and oil (DENA 2023). Through the implementation of the measures from the Building Energy Act (GEG), the federal funding for efficient buildings (BEG), and the introduction of a national emission trading system in the Fuel Emissions Trading Act (BEHG), the goal is to decarbonize 50% of building heat supply by 2030. Additionally, a rapid and significant increase in renovation dynamics and depth must be achieved to reduce overall heat demand.

Particularly in the design of heating supply concepts, the most suitable and cost-effective local approach to a climate-friendly heating supply should be adopted, taking into account local waste heat and renewable energy potentials. Therefore, each planning authority should strategically plan how different areas

are to be supplied with heat, such as through decentralized or grid-connected technologies. To ensure the development of local heat supply concepts, the Heat Planning Act should be passed by the Bundestag in January 2024 (BMWSB 2023). The core of the Heat Planning Act is the obligation for states to ensure that municipalities create heat plans with the aim of improving planning and investment security for local actors.

However, although Figure 11 shows that the German government's new targets (2023) are significantly more ambitious compared to the old ones (2021), it must be noted, even with all currently planned measures taken into account, it is anticipated that Germany will fall short of its greenhouse gas reduction targets by a cumulative total of 200 million tons of CO₂ equivalents till 2030 (Bundesregierung 2023). Therefore, future adjustments to the currently planned measures are needed.

2.3.2 Discussion and research needs

In the planning of municipal heating supply concepts and the expansion of renewable energies, local conditions in the form of renewable and waste heat potentials, local infrastructures, and local energy demand structures of buildings, industry, mobility, and the tertiary sector must be considered in an integrated manner. Section 2.3.1 shows that local planning authorities – often municipalities – are progressively involved in the planning of local energy systems, even at the legislative level. However, particularly small municipalities, which often have a high potential for renewable energies (see Mainzer et al. (2014)) and are mandated to develop heating supply concepts by 2028 (BMWSB 2023), often lack the expertise to design coherent energy supply concepts. On the other hand, local actors show great interest in participating in the local energy transition, which becomes evident by the fact that the majority of renewable energy plants in Germany are owned and operated by private individuals, farmers, and communities (Bringault et al. 2017). Further, studies show that cities and municipalities are especially successful in engaging private building owners at the local level, using regional ties and educational events to influence their investment decisions (Wagner and Sager 2015). Consequently, transferable tools are needed to support local actors in planning energy systems and enable citizens to actively participate in the planning process (McKenna et al. 2018).

3 Methodology

Section 3 provides an overview of the methodological approaches used and developed in this thesis. First, in Section 3.1, approaches for residential energy demand modeling are discussed. It is shown that an adequate representation of household behavior builds the foundation for consistent bottom-up energy demand modeling. In Section 3.2, shortcomings of existing occupancy and mobility simulation models are identified. A neural network-based approach is introduced to overcome these shortcomings. In Section 3.3, a framework for bottom-up residential energy system design for buildings within the European building stock is developed. Finally, Section 3.4 introduces a municipal energy system optimization model, which is extended in this thesis to analyze the residential building stock transformation of a municipality within the context of national greenhouse gas reduction strategies.

3.1 Residential energy demand modeling

Residential energy demand models enable the study, understanding, and forecasting of the dependencies between socio-demographic household determinants, technical and environmental parameters, occupant behavior, and the associated energy demands. Models can be divided into two categories: bottom-up and top-down models (Swan and Ugursal 2009). Bottom-up models calculate the individual dwellings' energy consumption based on all energy consumption devices of the household (see Figure 12). Top-down models, on the other hand, use macro-economic indicators, such as gross domestic product or construction rates, to describe long-term changes in energy consumption on an aggregate level and break it down to the level of individual dwellings based on the structural characteristics of these dwellings (Swan and Ugursal 2009; Proedrou 2021). Top-down models are helpful in evaluating the impact of a changing economy on energy demand on a regional or national level (Swan and Ugursal 2009). However, since top-down models heavily rely on historical energy consumption data, they are not well-suited to function effectively in discontinuous settings, such as those involving disruptive events that lead to structural changes. For example, a technological breakthrough can be regarded as such a disruptive event. Proedrou (2021) further introduces the category of hybrid models. This category includes models that combine bottom-up and top-down approaches. The extent to which the respective approach characteristics are adopted depends on the application.

This thesis focuses on bottom-up models with the objective of better understanding the effects and interactions of technologies in residential energy systems under various techno-economic conditions. Challenges associated with bottom-up models are their high computational complexity and demand for

data due to the high level of detail. However, the growing interest in residential energy demand has driven the development of a number of bottom-up models that try to represent the temporal variations in energy demand for electric household devices, domestic hot water, space heating, and mobility (Proedrou 2021; Yamaguchi et al. 2018; Grandjean et al. 2012). Proedrou (2021) reviews 32 residential electricity load profile models based on their general approach (bottom-up, top-down, hybrid), the sampling rate of the output (one second to one hour), application (demand side management; planning, control, and design of energy systems) and their main statistical methods. To simulate the stochasticity in device starts and occupancy behavior, Markov chain models, non-Markov probabilistic models, and Monte Carlo methods are used as statistical methods. Yamaguchi et al. (2018) further review appliance modeling methods within bottom-up models and distinguish between approaches based on time-use data and those solely based on empirically measured device-specific load profiles. In the latter, time-dependent switch-on probabilities are derived from power demand measurements. Time use data, on the other hand, provide nationally representative information on individuals' daily routines with high temporal resolution and also contain rich information on socio-demographic characteristics (Eurostat 2024). Therefore, this thesis adopts a time-use data-based approach, on the basis of which consistent demand profiles for thermal comfort, mobility, and other energy services can be derived. The general structure of time use data-based load profile models can be seen in Figure 12. Research shows that especially under rising building performance standards, the influence of occupant behavior on building performance increases, and occupant behavior is acknowledged as a main source of discrepancy between predicted and actual performance (Gaetani et al. 2016; Jia et al. 2017; Yoshino et al. 2017). Therefore, a sophisticated representation of occupant behavior is of great importance, not only for thermal demand models but especially for integrated modeling approaches (as can be seen in Figure 12). A detailed overview of modeling approaches for the representation of residential activity patterns in building energy system models is given in Section 3.2.

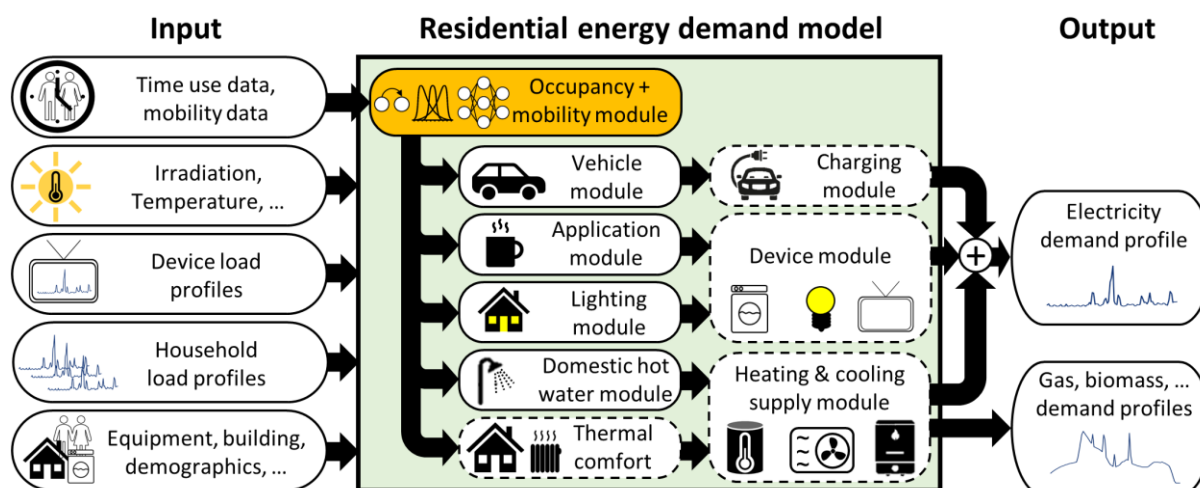


Figure 12: Bottom-up residential energy demand modeling framework. The occupancy + mobility module – highlighted in orange – is discussed in detail in Section 3.2. The modules surrounded by a dashed line are represented as flexibility options in the energy system optimization model, as presented in Section 3.3.2 (in detail: (Kleinebrahm et al. 2018) and (Kleinebrahm et al. 2023b)). The flexible operation of white goods is considered in (Kleinebrahm et al. 2018). Flexible electric vehicle charging strategies are analyzed within a multi-family house setting (Braeuer et al. 2022). The flexible provision of thermal comfort, taking into account the thermal inertia of the building, is represented as analogous to (Schütz et al. 2017a) in the building energy system optimization used in (Kleinebrahm et al. 2023b).

3.2 Residential activity modeling

Over the last years, various approaches have been developed to better understand and simulate occupant behavior and its impact on energy consumption (Osman and Ouf 2021; Gaetani et al. 2016). Initially, models like the one developed by Capasso et al. (1994) employed simplistic two-state (available, unavailable) simulations using Monte Carlo methods. In recent years, advancements have shifted towards more sophisticated techniques, including the use of empirical data from time-use and mobility surveys, where participants log their daily activities over several days. Time-use surveys, conducted every 5 to 10 years in over 100 countries worldwide, have been utilized in 93 research studies for building energy and occupancy analysis (Osman and Ouf 2021). In this thesis, the German part of the Harmonized European Time Use Survey is used, which provides detailed information on the activities of individual persons over three days (Destatis 2006; Eurostat 2024). Mobility surveys, on the other hand, provide information on daily or weekly mobility patterns and are used to analyze electricity demand associated with electric vehicle transport (Fischer et al. 2019; Kaschub et al. 2016). Exemplary artificial individual activity and mobility schedules can be seen in Figure 13.

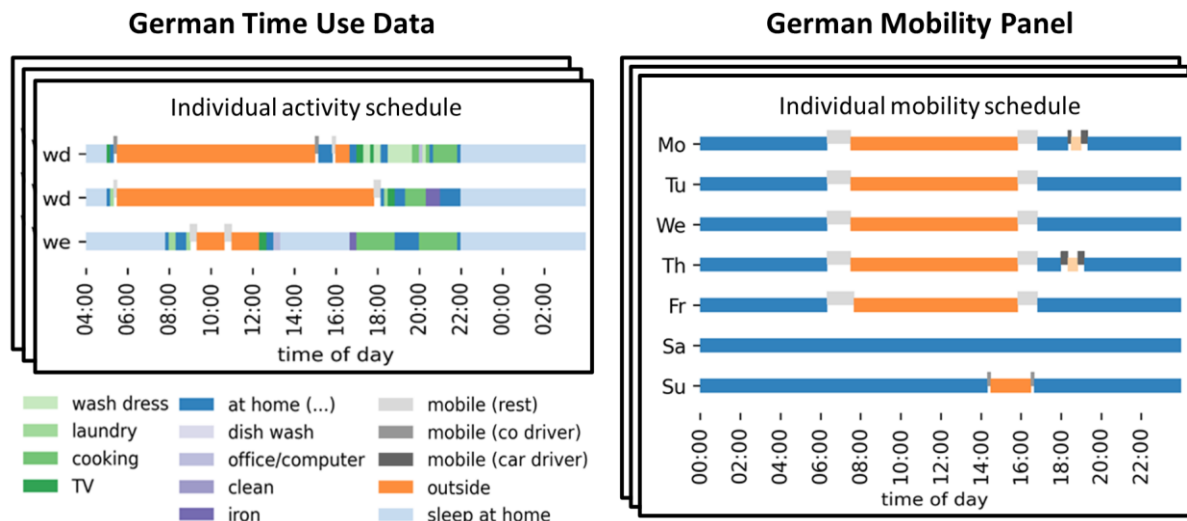


Figure 13: Activity and mobility schedules from time use survey and mobility panel data. Exemplary artificial individual diary entries are based on the structure of the German TUS (Destatis 2006) and the German mobility panel (MOP) (Weiss et al. 2016).

Since time-use and mobility survey data are often subject to strict privacy guidelines, generative models that can learn the distribution of the original data and generate synthetic data with the same characteristics are needed. The trained models, or the synthetic data they generate, can further be used as a basis for open-source models.

When choosing a model, it is important to ensure that the model can capture the complexity in the data while also preventing overfitting, which occurs when a model excessively learns the specifics of the dataset rather than generalize from it. Alaa et al. (2021) propose the usage of three criteria for the evaluation of synthetic data: fidelity, diversity, and generalization. Fidelity refers to the quality of individual samples, while diversity relates to the extent to which these samples cover the full variability of the original data. Further, generalization evaluates the extent to which a model overfits. In the following, an overview of existing methods for residential activity modeling and their shortcomings is provided. Subsequently, the methodological approach developed as part of this work is presented.

3.2.1 Markov chain approach

Markov chains have become the most common approach for modeling the evolution of daily activity sequences. They abstract the way people go about their lives as transitioning from one activity state into another (Ramírez-Mendiola et al. 2019). The Markov chain is thereby defined by a state space, the set of all possible states, and the transition probabilities between the states. Thereby, the transition probability between states depends on the current state (first-order Markov chain) or the current and past states (higher-order Markov chain).

Multiple studies use first-order Markov chains with time-inhomogeneous transition probabilities to describe the behavior of individuals or whole households throughout the day (see Table 1). These approaches produce low-fidelity activity sequences since first-order Markov chains are constrained by the Markov property, which refers to the memorylessness of a stochastic process. Memorylessness is characterized by the fact that the transition probability of the current state to the subsequent state is only conditioned on the current state, while previously observed states are neglected. Since activity schedules of occupants are subject to more complex processes, a variety of more complex Markov models have been proposed over the last years, including semi-Markov chains, higher-order Markov chains, and Markov chains with variable memory length (see Table 1). An abstract representation of the activity sequence generation processes of the respective models can be found in Figure 14. Although the more complex Markov models have partly overcome the memorylessness problem, their effectiveness in capturing complex long-term dependencies remains constrained. This limitation arises because higher-order Markov models are hindered by an exponential increase in their number of free parameters as the model's order increases. This complexity restricts the practical use of past observations for predictions of future states.

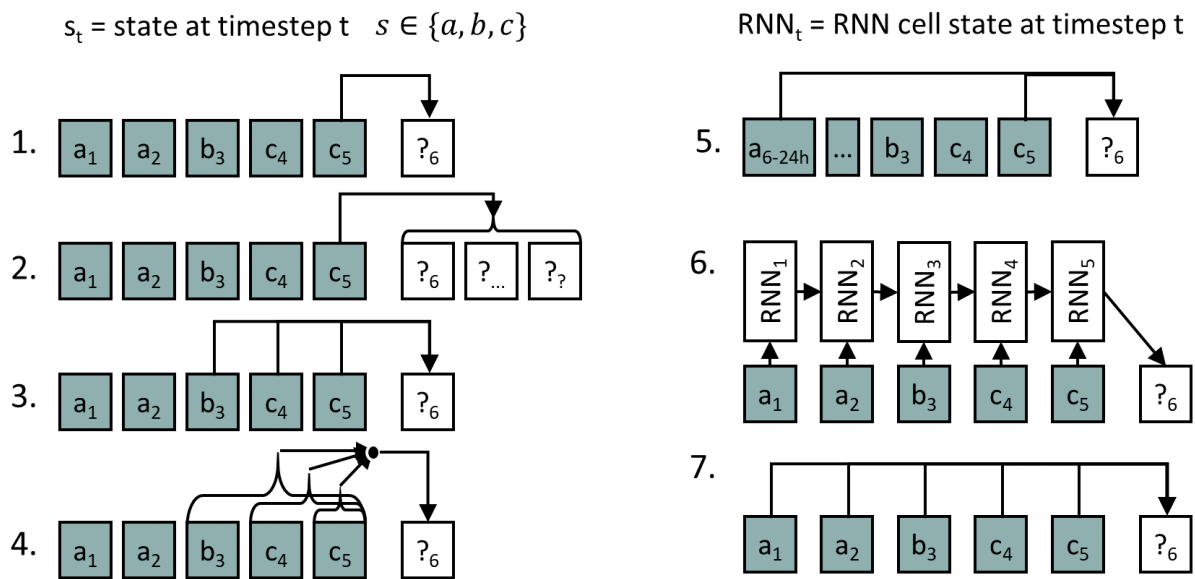


Figure 14: Representation of the sequence generation process with different model approaches. 1. First order Markov chain, 2. Semi-Markov chain, 3. Higher order Markov chain, 4. Markov chain with variable memory length, 5. First order Markov chain with 24h correlation, 6. Recurrent neural network, 7. Transformer neural network.

3.2.2 Hierarchical regression approach

An alternative to a Markov chain approach is provided by Hilgert et al. (2017), who present a utility-based stepwise hierarchical regression approach to generate mobility schedules for travel demand models. While the approaches presented in Section 3.2.1 are solely based on time-use survey data, Hilgert et al. (2017) use weekly mobility data (see Figure 13) and try to represent higher-level mobility patterns instead of detailed household activities. The proposed approach differs fundamentally from the previously discussed Markov models, primarily due to its one-week observation period, which necessitates a more comprehensive representation of mobility sequences, capturing both the day-to-day stability and variability of personal behavior. Rather than evolving activity sequences over time, the mobility schedule generation process is split into smaller decisions due to the high complexity of constructing the entire schedule at once (Bowman 1998). For each of the small decision problems, a logistic regression model is fitted. Due to the high number of sequential decisions and the associated large number of assumptions, the proposed model has a high assumption bias and cannot easily be transferred to other domains.

Table 1: An overview of selected models for modeling occupancy behavior.

| Study | Database | Approach | Object |
|----------------------------------|---------------------|---------------------------------------|-------------------|
| (Richardson et al. 2008) | TUS (UK) | Markov - 1 st order | Household |
| (McKenna et al. 2015a) | TUS (UK) | Markov - 1 st order | Household |
| (Widén and Wäckelgård 2010) | TUS (SE) | Markov - 1 st order | Individual |
| (Santiago et al. 2014) | TUS (ES) | Markov - 1 st order | Individual |
| (Wilke 2013) | TUS (FR) | Markov - semi | Individual |
| (Bottaccioli et al. 2019) | TUS (IT) | Markov - semi | Individual |
| (Aerts et al. 2014) | TUS (BE) | Markov - semi | Individual |
| (Nijhuis et al. 2016) | TUS (NL) | Markov - 1 st order (+24h) | Individual |
| (Flett and Kelly 2016) | TUS (UK) | Markov - higher order | Individuals |
| (Ramírez-Mendiola et al. 2019) | TUS (UK) | Markov - variable length | Individual |
| (Hilgert 2019) | MOP (DE) | Hierarchical regression | Individual |
| (Osman et al. 2023) | TUS (CA) | Markov - semi | Individual |
| (Kleinebrahm et al. 2021) | MOP+TUS (DE) | Deep neural networks | Individual |

3.2.3 Neural network approach

Shove et al. (2012) and Torriti (2017) advocate for more holistic examination approaches of activity schedules to better understand higher-level patterns. Having this in mind, the method developed in this thesis has the objective of not only describing the behavior of a person more holistically within the

temporal dimension but also capturing higher-level patterns that shape the structure of people's activity schedules.

Deep neural networks, which built the basis for the latest breakthroughs in natural language processing (OpenAI 2023a), image recognition (Krizhevsky et al. 2012), and protein folding (Jumper et al. 2021), among others, are capable of learning complex patterns and higher-level concepts from data. Since both activity schedules and natural language can be interpreted as categorical sequences, the same approaches that are successfully used to generate natural language are applied in this thesis to generate residential activity schedules. To process text or activity schedules with neural networks, the input must first be tokenized. In natural language processing, tokenization refers to the process of splitting up a text into words, subwords, or characters, which then are converted to numbers (IDs) through a look-up table. For example, the language models GPT-4 and Llama use subword tokenization, with Llama featuring a vocabulary size of 32k tokens (OpenAI 2023b; Touvron et al. 2023). In this thesis, the chosen activity state space is significantly smaller when generating mobility (6 states) and activity sequences (14 states).

The tokenized sequences are used as input for the neural network. In the first layer, the tokens are converted into embeddings, which are dense vector-space representations learned during the training process of the neural network (Mikolov et al. 2013). The basic concept of embeddings is shown in Figure 15 for an exemplary use case with four aggregate activity states and an embedding space of dimension two. Large language models currently use significantly larger embedding spaces, with up to 8192 dimensions (Touvron et al. 2023).

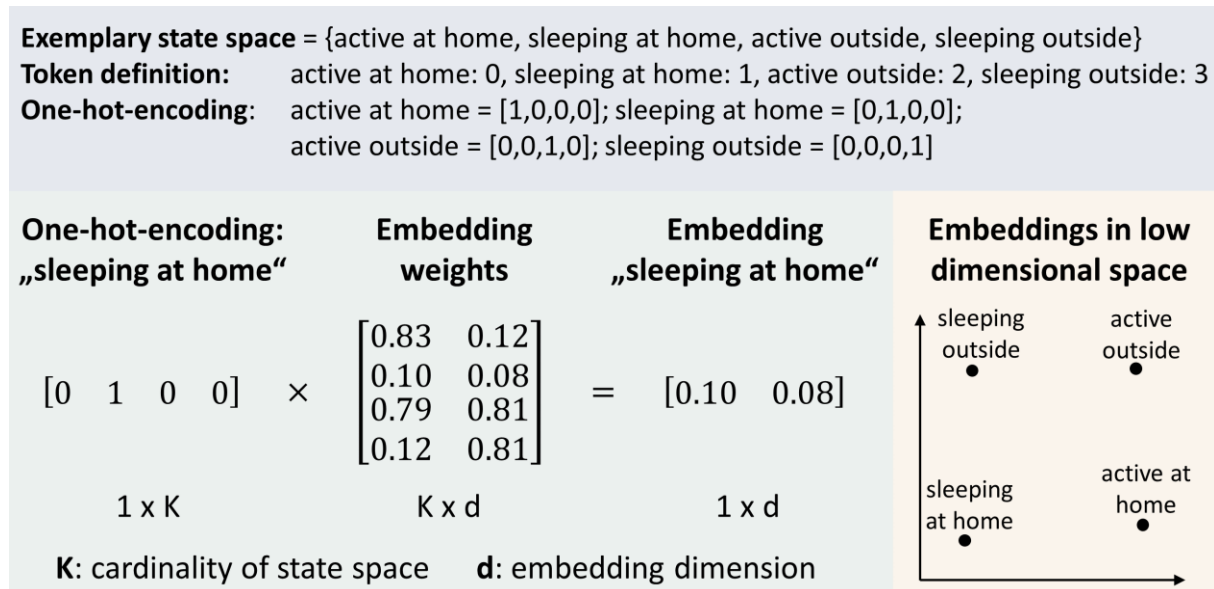


Figure 15: Explanation of the concept of an embedding layer. In the bottom left part of the figure, the embedding layer is described as a linear layer that takes a one-hot encoded vector as input. However, in practice, embedding layers are implemented as look-up tables for efficiency reasons since one-hot encoded vectors

are sparse and high-dimensional, leading to inefficient computations. The embedding weights represent the state-specific embeddings. Own illustration based on Kuhlmann (2021).

In this work, two kinds of neural network architectures are considered: recurrent neural networks and transformer-based neural networks (Hochreiter and Schmidhuber 1997; Vaswani et al. 2017). A recurrent neural network processes each token at a time and thereby inherently learns the sequential structure of the input (see Figure 14). The transformer, on the other hand, which is currently the most widespread neural network architecture for large language models, is based on the attention mechanism (Vaswani et al. 2017). In contrast to recurrent neural networks, the attention mechanism allows the processing of all information within its attention span at once when predicting the next token. This is beneficial for parallelization, but since the transformer processes every step of the sequence independently, the information on the order of the sequence gets lost. Therefore, positional information in the form of positional encodings, which provide context information, is added to the embeddings. Subsequently, dependencies between the states within a sequence are learned by layer one through N of the neural network. The layers are implemented as Long Short-Term Memory (LSTM) layers or transformer layers (Hochreiter and Schmidhuber 1997; Vaswani et al. 2017). The general architecture of the described neural network can be seen in Figure 16.

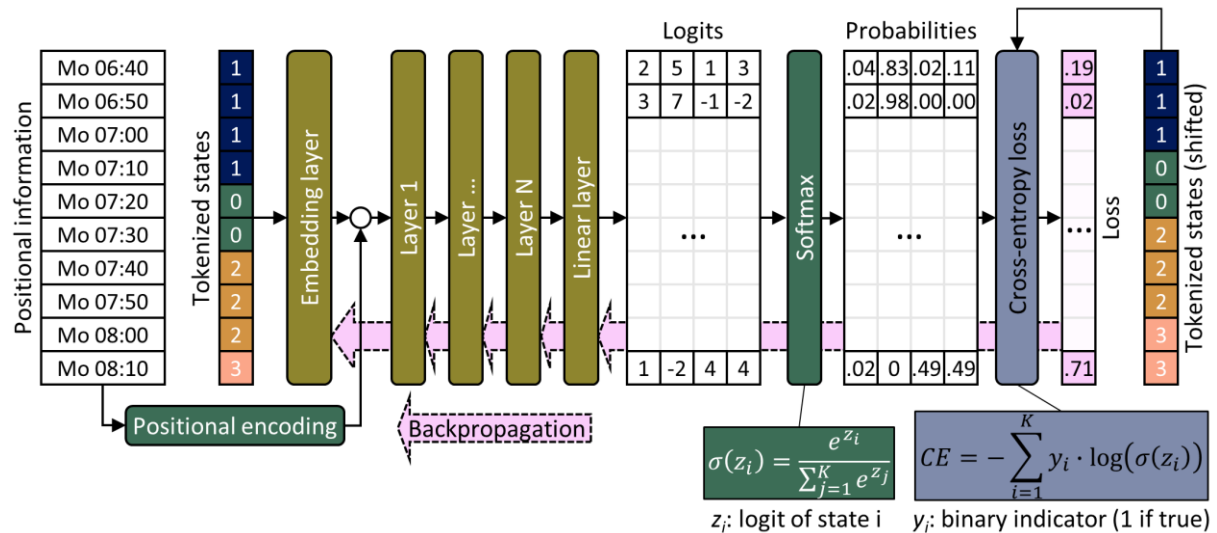


Figure 16: Neural network architecture and the information flow during training process. Black arrows indicate the forward pass of information through the neural network, while the pink arrow indicates the backward pass of information for the update of the weights through backpropagation.

When training autoregressive models to generate activity or mobility sequences, future states are predicted exclusively based on previously observed states. Further, imputation models are developed in this thesis to enrich aggregated mobility schedules with more granular activity information from time-use surveys. For further information on the architecture of the imputation models, please refer to Kleinbrahm et al. (2021).

After the information has been processed in layer one through N , probabilities for the individual states are calculated for each step using a linear layer and the softmax function. To do this, the linear layer first projects the output of layer N into a K -dimensional vector space, where K corresponds to the cardinality of the state space (in the above example, $K = 4$). Further, the unscaled output of the linear layer, called logits, is transferred to probabilities using the softmax function. The cross-entropy loss is calculated based on the calculated probabilities for the occurrence of the respective states and the actual occurring states (ground truth). Based on calculated loss, the weights of the layers are updated using back-propagation.

By using neural networks in combination with mobility and behavioral data, in contrast to the Markov approaches presented, complex long-term time dependencies in the behavior of individuals can be captured, and thus, the problem of memorylessness can be overcome. At the same time, compared to the approach of Hilgert et al. (2017), significantly fewer domain-specific assumptions need to be made, which increases the transferability and quality of the approach presented. Further, the presented approach enables the generation of synthetic behavioral data with high fidelity and diversity and, therefore, builds a promising basis for the application in building energy demand simulations.

3.3 Residential building stock energy system optimization

The complexity of designing future renewable-based building energy systems is vastly increasing due to the growing number of investment options in generation, conversion, storage, and retrofit technologies. Further, the fluctuating supply of renewable energy technologies necessitates modeling with the increased temporal resolution, which directly impacts the size of the optimization problem. Therefore, advanced mathematical models are needed since traditional analytical solving is, in many cases, not possible anymore (Baños et al. 2011).

Investments in energy retrofits and renewable energy technologies for residential buildings are mainly motivated by financial benefits (Achtnicht and Madlener 2014; Balcombe et al. 2014; Kairies et al. 2019). Consequently, in this thesis, a framework is developed on the basis of which techno-economic optimal renewable-based energy systems for residential buildings can be determined, taking into account various technology options and efficiency measures. To be able to infer techno-economic potentials for entire building stocks from results for individual buildings, a dynamic approach is developed for identifying representative buildings, which is based on a synthetic representation of building stocks. Core indicators of the energy system analyses of the representative buildings are ultimately transferred to all examined buildings of the synthetic building stock by using a surrogate model without excessive use of computational resources. The proposed framework builds upon and extends existing literature (see Table 2).

Table 2: Overview of the developed framework modules.

| Framework modules | Main foundational methodological studies | Main research contributions |
|--|--|---|
| 1. Data collection | | Combination of data sources and data imputation for EU27, NO, UK. |
| 2. Synthetic building stock | (Huang and Elsland 2019) | Development of a spatial microsimulation approach for the derivation of local synthetic building stocks at the NUTS3 level. |
| 3. Representative buildings | (Kotzur et al. 2019) | k-means clustering to determine representative buildings based on building energy system relevant features. |
| 4. Energy system model formulation | (Kotzur 2018) (Kaschub 2017) | Technology set expansion to account for, e.g., small wind turbines, flexible operation of demand-side technologies, like white goods, and the renewal of the heat distribution system. Implementation of the Tenant-landlord perspective according to the German tenant electricity law (see Braeuer et al. (2022)). |
| 4.1 Occupancy simulation | (Richardson et al. 2008) | Integration of German behavioral data for occupancy modeling. |
| 4.2 Solar radiation simulation | (Andrews et al. 2014) | |
| 4.3 Electric appliance simulation | (Richardson et al. 2010) | Metaheuristic for time series aggregation for trade-off aggregation error vs. computation time. |
| 4.4 Domestic hot water simulation | (Richardson et al. 2010) | |
| 4.5 Optimization integrated thermal 5RIC model | (Schütz et al. 2017a) | Robust energy system design through a multi-step optimization against 30 historical weather years. |
| 4.6 Time series aggregation | (Kotzur et al. 2018b) | |
| 4.7 Robust energy system design | | |
| 4.8 Solution algorithm | (Kotzur 2018) | |
| 5. Surrogate model | (Weinand et al. 2020a) | Development of a regression/classification-based approach to transfer individual building results to building stocks to derive large-scale techno-economic potentials from bottom-up models. |

In this thesis, the framework is used to calculate the techno-economic potential for a self-sufficient residential energy supply of 41 million freestanding single-family buildings within the European building stock. Beyond the utilization in this thesis, the developed framework is applied in multiple other publications, demonstrating its wider transferability. Kleinebrahm et al. (2018) designed optimal renewable energy-based systems for the self-sufficient energy supply of a residential building in Germany, accounting for the flexible operation of demand-side technologies and flexible electric vehicle charging.

In Vögele et al. (2022), the framework was used to calculate the techno-economic potential of PV-battery systems in the German residential sector up to 2050. In Braeuer et al. (2022), optimal energy systems for energy communities in multi-family buildings were designed under the consideration of the German tenant electricity law. A visualization of the proposed framework can be seen in Figure 17. The individual components of the framework are briefly presented in the following sections. A more detailed description can be found in Kleinebrahm et al. (2023b).

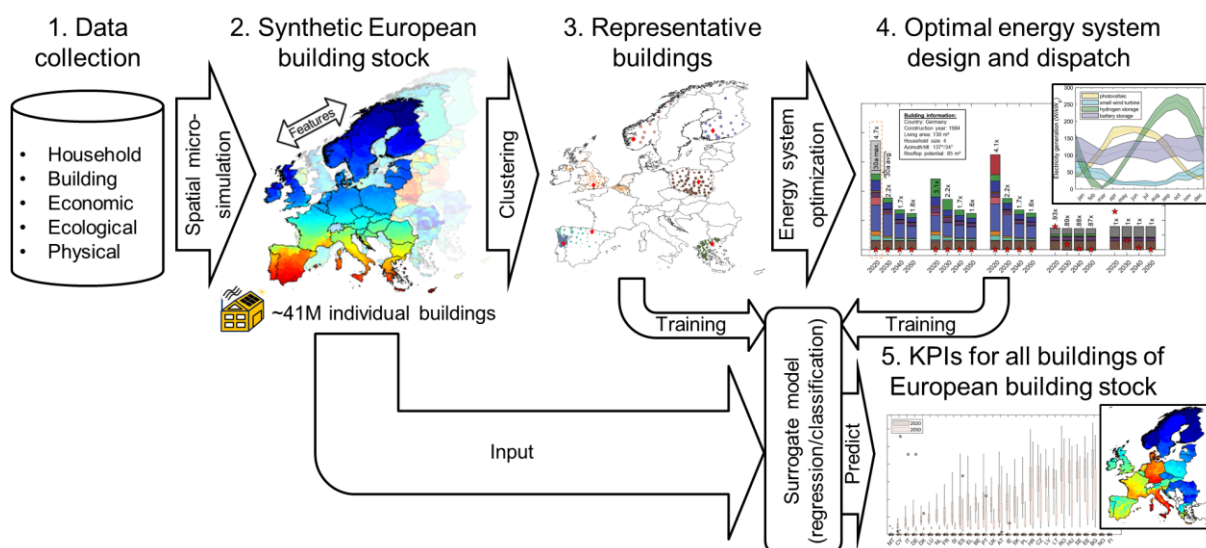


Figure 17: A framework for the evaluation of residential energy systems. The framework is based on a database, which combines spatially resolved building stock data with building energy system-relevant attributes. In the first step, spatial microsimulation is conducted to integrate the building attributes into a synthetic representation of the building stock. A k-means clustering approach is further utilized to identify representative buildings. Subsequently, building energy systems are computed with an optimization model using a high-performance computing cluster. Finally, the findings from these energy system optimizations are extrapolated to the entire synthetic European building stock using a surrogate model. Own visualization published in Kleinebrahm et al. (2023b).

3.3.1 Synthetic building stock

Spatially resolved data for individual buildings are needed for the analysis of building energy systems. For building age, building living area, and household size, only one-dimensional distributions are provided at the NUTS3 level. To address the limitations of aggregated one-dimensional data, spatial microsimulation is used to generate synthetic building stocks for each European NUTS3 region. Therefore, household data from the Socio-Economic Panel are used as individual-level microdata and combined with the aggregated one-dimensional distributions using iterative proportional fitting (Liebig et al. 2019; Blocker 2022). The generated synthetic building stock provides spatial microdata (i.e., empirically-based combinations of the one-dimensional data) while preserving the spatially aggregated statistics for each NUTS3 region. In further steps, the synthetic building stock is enhanced by integrating additional

information relevant to the design of building energy systems. For example, information on weather, building geometry, U-values, and energy carrier prices.

3.3.2 Energy system design

An integrated heat and electricity building energy system optimization approach is developed for the determination of the techno-economically optimal design of building energy systems under varying framework conditions in Europe. To account for weather and country-dependent variations of renewable energy feed-in, conversion efficiencies, solar heat gains, thermal heat losses, lighting, and domestic hot water demand, multiple existing tool chains have been combined to provide input for the building energy system optimization (see Table 2). Further, adjustments were made to account for, e.g., country-specific household appliance equipment or annual appliance and domestic hot water demand.

Based on the available temporally resolved and time-invariant inputs, a model class was selected that is capable of representing the complexity of a highly renewable-based building energy system and is solvable in a feasible time. Kotzur (2018) and Schütz et al. (2017a) show that mixed integer linear programming (MILP) approaches can adequately represent renewable energy supply and demand fluctuations, multiple investment options in building envelope and energy system technologies, thermal building inertia and can be solved within a reasonable timeframe when designing building energy systems. Therefore, a MILP optimization approach is chosen for the determination of cost-minimal building energy system design and operation while accounting for all investment options shown in Figure 18. More details on the model can be found in Kleinebrahm et al. (2018), Kleinebrahm et al. (2023b), and Braeuer et al. (2022).

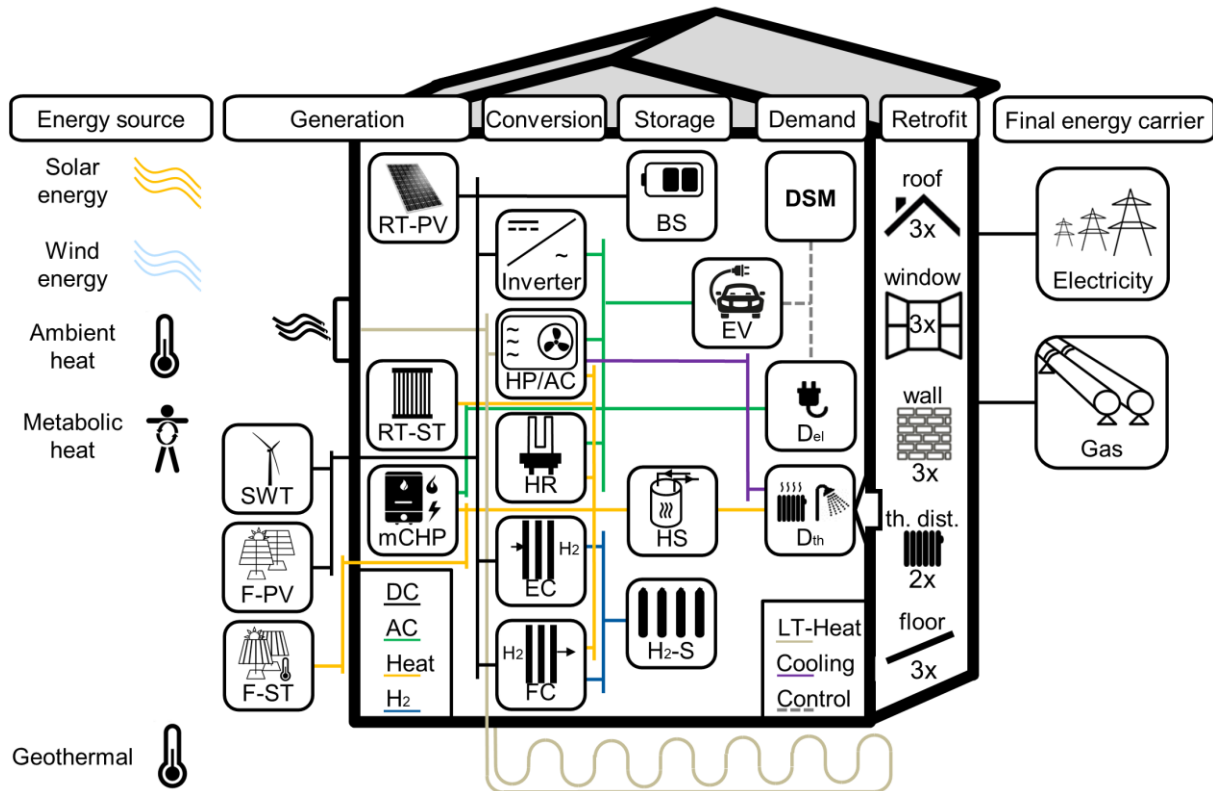


Figure 18: Overview of the energy system components represented in the optimization model. (F/RT-PV, free-standing/rooftop photovoltaic; SWT, small wind turbine; F/RT-ST, free-standing/ rooftop solar thermal; mCHP, micro-combined heat and power; BS, battery storage; HP, heat pump; AC, air conditioner; HR, heating rod; EC, electrolyzer; FC, fuel cell; H₂-S, hydrogen storage; HS, heat storage; EV, electric vehicle; DSM, demand-side management; D_{el}, electrical demand; D_{th}, thermal demand; th. dist., thermal distribution; LT, low temperature).

3.3.3 Complexity reduction

A key challenge in energy system modeling is to find a good compromise between model scope, resolution, and computational feasibility. The computational complexity of the MILP optimization problem leads to long model runtimes due to multiple time-coupling constraints and binary decision variables. For example, the optimization problem presented in Kleinebrahm et al. (2023b) for self-sufficient residential buildings cannot be solved in reasonable time using the full-time series over one year in hourly resolution (for one building and MIP Gaps <1% the model needs >24 hours).

Therefore, three measures are introduced to reduce the complexity of the underlying problem, with the aim of deriving general statements for building stocks within a reasonable timeframe and with adequate accuracy. In the first step, building archetypes that best represent the diversity of the synthetic building stock are derived. In the second step, the building optimization problem is decomposed into a multi-step optimization to reduce complexity and allocate computational resources as efficiently as possible. After

cost-minimal energy systems for all archetype buildings have been calculated, a surrogate model is parameterized to transfer the results of the individual energy system optimizations to all buildings of the examined building stock.

Archetype building derivation. It is not practicable to calculate building energy systems for all buildings of a national or even continental building stock due to computational restrictions and time constraints. Therefore, the problem size is reduced by the determination of representative archetype buildings based on building features that are relevant to the design of the energy system.

The k-means clustering approach is used for the identification of representative buildings due to the feasible time complexity and high computing efficiency (Xu and Tian 2015). An additional benefit of the k-means algorithm lies in its requirement to predefine the number of clusters tailored to the computing resources available for the energy system optimization model. Once the cluster centroids are identified, the nearest building to each centroid within the synthetic building stock is selected, for which optimal energy systems are subsequently determined.

In contrast to the approach presented by Kotzur et al. (2019), who directly derive archetype buildings from spatially aggregated one-dimensional data, the approach presented in this thesis enables the consideration of correlations between building features, such as between household size and residential building area. A comprehensive overview of methods for archetype building selection and building stock synthesis can be found in the supplementary material of Kleinebrahm et al. (2023b).

Multi-step optimization. To reduce the problem size of the building energy system design optimization, a multi-step optimization approach is introduced based on the work presented by Kotzur et al. (2018b), Kotzur et al. (2018a), and Bahl et al. (2017). In the first step, a time series aggregation approach based on typical days is used to reduce the complexity of the optimization problem (Kotzur et al. 2018b). Further, the reduced problem is solved by determining the technology components of the energy system. In the second step, binary decision variables are predetermined based on the results of the first step, and the energy system components are scaled considering the full-time series over the entire year (Bahl et al. 2017). Finally, in the third step, the energy system is optimized against multiple historical weather years to ensure a robust energy system design.

A metaheuristic is introduced to keep the time series aggregation-induced error low and to use the computing capacity as efficiently as possible. The metaheuristic identifies trade-offs between calculation time and optimization error based on hyper-parameters, such as the number of typical days or the deviation between the objective function value of the reduced and full optimization problem. Hyper-parameters are derived on the basis of a micro synthetic building stock (in Kleinebrahm et al. (2023b), 347 buildings). Based on the derived settings, the mean calculation time per building can be used to define the number of archetype buildings to be analyzed with regard to the available computational resources

(in Kleinebrahm et al. (2023b), 4,000 buildings). The identification of an optimal trade-off between computing time and optimization error enables the generation of a large data set of high-quality individual samples. Details of the metaheuristic can be found in the supplementary material of Kleinebrahm et al. (2023b).

Surrogate model. Finally, a surrogate model is employed to approximate key indicators for all buildings in the synthetic building stock. The objective of the surrogate model is to establish a functional relationship between the inputs of the energy system optimization and key output parameters. The derived model can be used to extrapolate the results of the energy system optimizations to the entire synthetic building stock while using significantly fewer computational resources compared with optimizing the energy system of each individual building. Depending on the kind of key indicator to be estimated, a regression or classification approach is utilized.

3.4 Municipal energy system transformation

To analyze the transformation of the residential building stock energy supply within the overarching municipal and national energy system transformation, the *Renewable Energies and Energy Efficiency Analysis and System OptimizatioN* model (RE³ASON, cf. Mainzer (2019) and Weinand (2020)) was used and extended.

The RE³ASON model consists of two parts, “input data determination” and “energy system optimization”. The development of the first part (“input data determination”) was motivated by the large amount of data required to model municipal energy systems, such as renewable potentials and information on the local building stock. Since local municipal energy planners often lack the expertise and financial resources to acquire these data, RE³ASON minimizes the effort involved in data collection. Based on the name of the municipality, local weather data, spatially resolved population, building stock information, and land use potentials for renewable energy sources are gathered and further processed to derive local energy demand and technology-specific available capacities and potentials. All necessary data sources are publicly available, which makes the RE³ASON model easily transferable to all German municipalities. Based on the gathered data, a municipal energy system optimization model was developed as the second part of the RE³ASON model. The objective of the optimization model is to minimize the total discounted system cost from a macroeconomic municipality planner perspective to identify cost-minimal energy system transformation strategies. Within this macroeconomic perspective, taxes, subsidies, and Levies are not considered. The model is implemented in the form of a MILP optimization problem and calculates optimal investments and dispatch for energy system technologies. Thereby, the model considers multiple investment options in energy supply technologies at the municipal level (see Table 3) and at the residential building level (e.g., investments in insulation, heating technologies, or

efficient appliances). In this thesis, long-term municipal energy system transformations are analyzed from 2020 to 2050, whereby each 10th year is modeled.

In this thesis, the RE³ASON model is further extended to be able to optimize the local municipal energy system transformation while considering the transformation of final energy demand in the industry, tertiary, transport, and residential sectors in line with national greenhouse gas reduction strategies. A stochastic, spatially resolved building stock simulation is introduced to consider temporal dynamic changes and the heterogeneity in the municipal residential building stock within the energy system optimization. To maintain realistic growth rates for renewable technologies, local maximum annual expansion rates are set in line with national trends. The range of energy supply technologies in the model is broadened to encompass all significant options found in national energy transformation scenarios. An overview of the model extensions made in this thesis can be found in Table 3. In the following section, the adjustments made to the objective function of the optimization model (Section 3.4.1) and the developed stochastic building stock simulation model (Section 3.4.2) are presented.

Table 3: Extensions of the municipal energy system optimization model RE³ASON.

| RE ³ ASON | RE ³ ASON + model extensions in this thesis |
|--|---|
| Aggregated building stock representation by archetype buildings, no consideration of temporal inertia | Multiple stochastic building stock scenario simulations as binary decision variables in energy system optimization |
| Constant tertiary, industry, and transport sector energy demand | Integration of transport, tertiary, and industry sector energy demand transformation |
| Existing supply side technologies: Wind turbines, rooftop PV, biomass plants, and geothermal plants (see Mainzer (2019) and Weinand et al. (2021)) | Existing technologies + freestanding PV&ST, H ₂ infrastructure, CO ₂ -flows and CO ₂ mitigation technologies + consideration of technology expansion rates |
| One-step optimization based on four typical weeks per year | Two-step optimization solving approach taking into account hourly resolution |

3.4.1 Municipal energy system optimization

The different cost components of the objective function of the MILP optimization problem are highlighted in Figure 19. Energy system technology investments $x_{i,j}^{inv}$ are made between the representative years of consideration $a \in A$ in the intervals $i \in Int$. The expansion costs $c_{i,j}^{inv}$ and costs for operation and maintenance $c_{a,j}^{op}$ are highlighted by the blue and green areas. The connections in orange and grey to the national energy system represent energy carrier and CO₂ flows. The extend of exchange with the national energy system depends on the long-term price projections for energy carriers $c_{a,t,j}^{el}$ and CO₂

emissions $c_{a,j}^{em}$, which are derived from overarching national scenarios. The red area represents the residential building stock transformation scenarios, which are calculated in a stochastic upstream simulation model. Within the energy system optimization, one scenario is chosen by a discrete decision variable x_h^{scen} . The costs connected to the respective scenario c_h^{scen} are also calculated in the upstream simulation model. Thereby, in this thesis, investment decisions regarding heat supply technologies and retrofit measures are made at the level of individual residential buildings outside the optimization model. This allows for the consideration of the high heterogeneity of the residential building stock without making the model intractable. Furthermore, this approach facilitates a detailed analysis of the building stock's dynamics, considering aspects such as the rate and depth of retrofits, modernization rates for heating technologies, and the integration of technologies like heat recovery units and air conditioners.

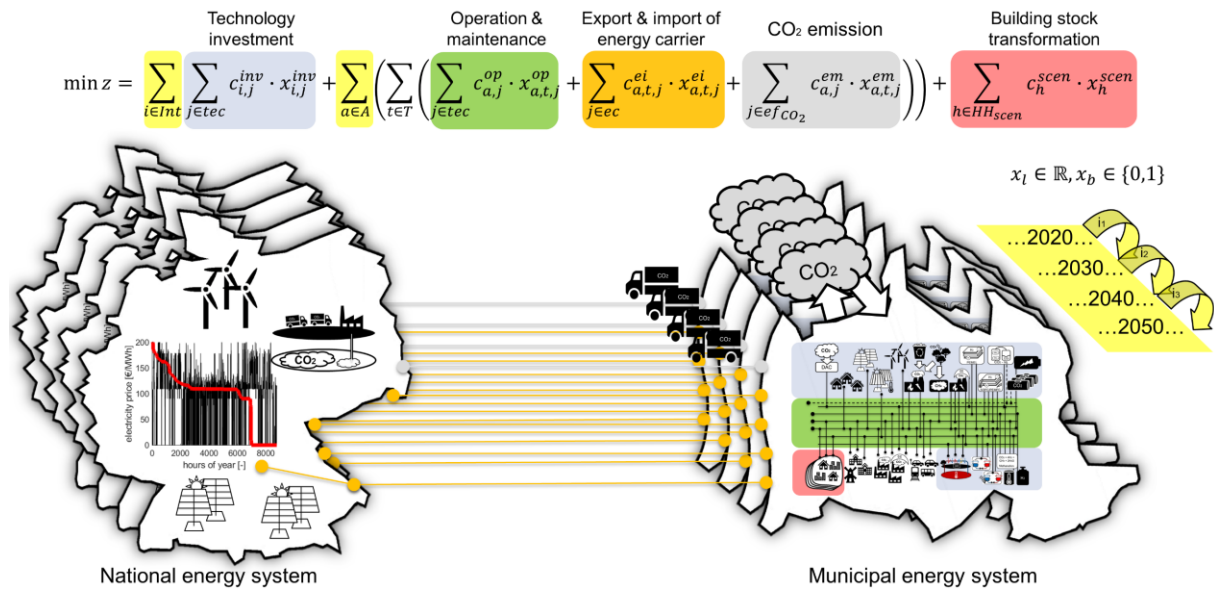


Figure 19: Composition of the municipal energy system optimization objective function. Own visualization published in Kleinebrahm et al. (2023a).

3.4.2 Residential building stock transformation

Multiple existing studies only consider an aggregated final energy demand of the residential building sector (Thellufsen et al. 2020; Thellufsen and Lund 2016; Østergaard and Lund 2011) or use a small number of representative archetype buildings (Weinand et al. 2019c). In Weinand et al. (2019c), already a small number of archetype buildings (~10) lead to long runtimes of the optimization model. As a result, the model was unable to fully represent the diversity of the building stock, and no constraints on maximum rates of retrofit and achievable rates of technology modernization were imposed. This approach allowed for optimal investment decisions at the building level but neglected to consider temporal constraints related to the dynamics of the building stock. This thesis addresses this limitation by introducing

a stochastic model for the building stock transformation (see Figure 20), which is linked with the municipal energy system optimization. By considering each residential building individually, this approach captures the diversity of the residential building stock. Furthermore, the building stock model accounts for the temporal dynamics of building stock transformation by incorporating trends with regard to retrofit rates⁴, retrofit depth, technology modernization, and expansion rates.

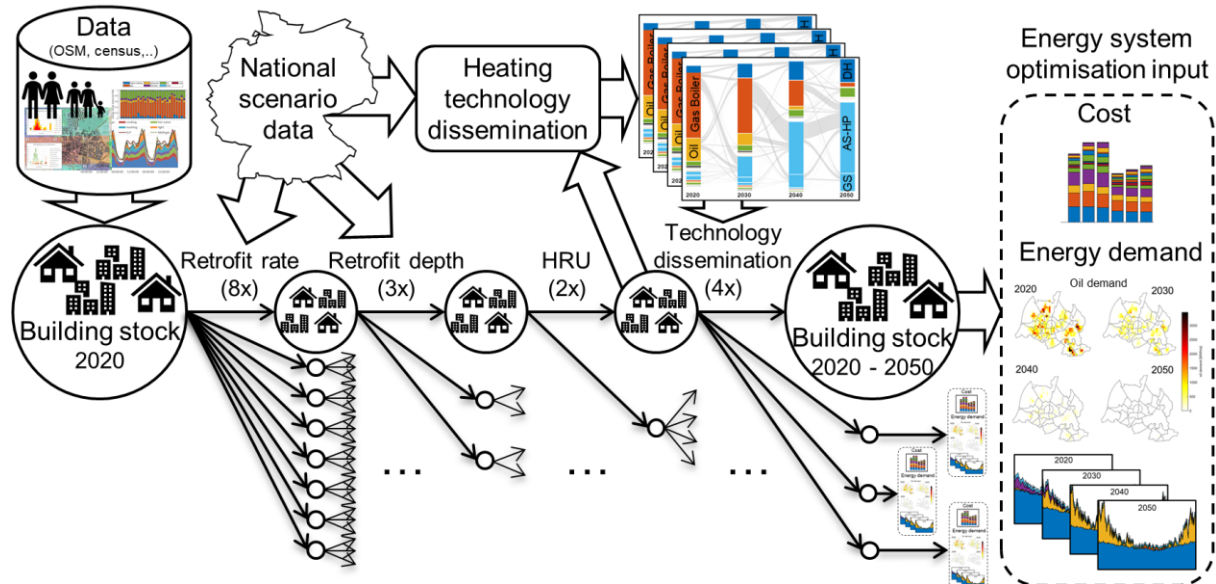


Figure 20: Stochastic process for the generation of residential building transformation scenarios. Own visualization published in Kleinebrahm et al. (2023a).

⁴ Defined as full retrofit equivalents according to Cischinsky and Diefenbach 2018.

4 Summaries of papers and results

This chapter summarizes each of the three papers of this cumulative dissertation in a separate section. More specifically, the study context and the scientific contribution of the articles are presented first, followed by the results and their discussion. The corresponding research papers are included in Part II of the dissertation.

4.1 Paper A: Using neural networks to model long-term dependencies in occupancy behavior

The following subsections refer to the article “Using neural networks to model long-term dependencies in occupancy behavior”, co-authored with Jacopo Torriti, Russell McKenna, Armin Ardone, and Wolf Fichtner. The article was published in the journal *Energy & Buildings* and is cited in this thesis by Kleinebrahm et al. (2021). The graphical abstract of the article is presented in Figure 21.

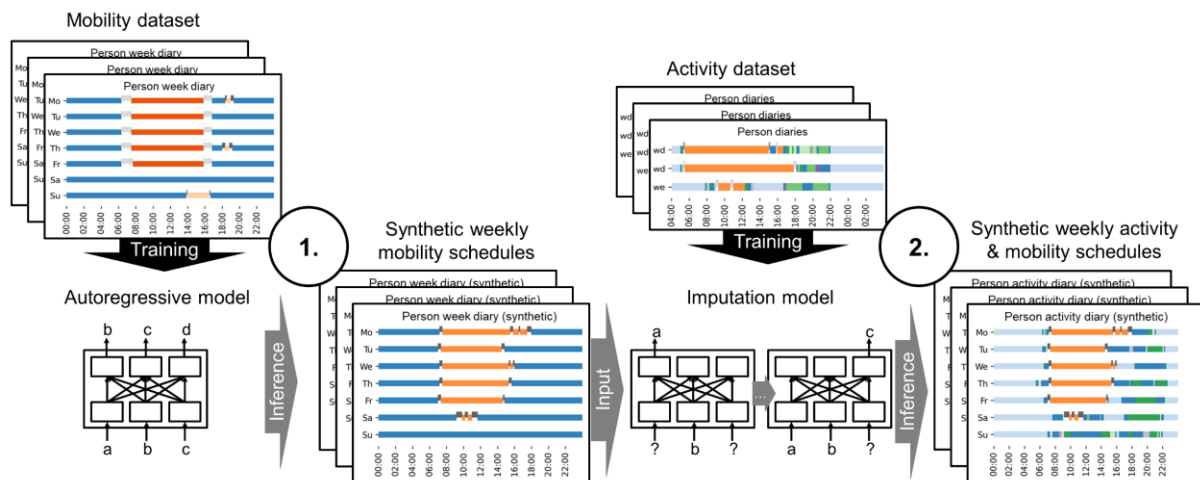


Figure 21: Two-step approach for the generation of weekly activity schedules. Own visualization published in Kleinebrahm et al. (2021).

Study context and contributions.

Section 2.1.2 showed that most future energy system scenarios anticipate a significant shift towards electrified heat generation to decarbonize residential heat supply. This trend is already evident, as heat pumps have become increasingly popular, demonstrated by a 34% market growth and over two million sold units in 2021 in the EU-27 (Rosenow et al. 2022). Further, from 2019 to 2022, the share of new registrations of electric cars in the EU-27 increased from 3% to 22%, which is reflected in over one million cars sold in 2022 (EEA 2023). These trends, which are expected to accelerate in the future, will

fundamentally change the characteristics of the course of electricity demand in the residential sector. Furthermore, different types of storage technologies will enable shifting energy over periods of single days and, therefore, open up flexibility potentials. In order to use these flexibilities, fundamental dependencies that shape household energy demand need to be understood. Occupant behavior has already been identified to have a significant impact on household energy demand and is regarded to be the main source of discrepancy between predicted and actual demand (Gaetani et al. 2016; Yoshino et al. 2017). With rising building performance standards and the growing demand for electric mobility, the impact of household behavior is even expected to become more pronounced in the future. Therefore, in this article, a neural network-based two-step approach for a better representation of occupant and mobility behavior in bottom-up household energy demand models is proposed.

4.1.1 Objective and significance

Over the last years, there has been a growing research interest in behavioral modeling with the objective of better representing the dynamics in residential energy demand through energy-related activities (Torriti 2017, 2014). The majority of models discussed in the literature rely on time-use survey data and Markov chains (see Table 1). However, due to the characteristics of the time use survey data and the inherent limitations of the Markov property, these models are not capable to account for long-term dependencies in behavior that span over multiple days. Therefore, while existing models are capable of simulating the stochastic nature of aggregate residential sector energy demand, they fall short in accurately representing the characteristics of individual households. Accurately capturing long-term behavioral dependencies is becoming increasingly important, particularly for evaluating investment options in renewable technologies or assessing the flexibility potential of individual households. In order to overcome the shortcomings of existing approaches, the objective of this article is to develop a model that combines highly detailed activity information of time use survey data with information on weekly mobility patterns provided by the German mobility panel. Thereby, the presented methodology not only tries to capture the stochasticity in behavior on an aggregate level but also to generate high-quality weekly activity data at the individual level.

4.1.2 Methodology

The developed two-step approach for the generation of weekly activity schedules is shown in Figure 21. In the first step, an autoregressive model is presented, which generates synthetic weekly mobility schedules of individuals and thereby captures long-term dependencies in mobility behavior. The developed autoregressive model is implemented as a deep neural network and compared against a first-order Markov chain model. Due to the parallels in the foundational problem, the choice of models employed is based on the models that define the state of the art in the field of natural language processing. Two kinds

of deep neural networks are proposed: a long, short-term memory-based model and an attention-based transformer model.

In the second step, an imputation model augments the weekly mobility schedules with detailed information about energy relevant 'at home' activities learned from time-use survey data. Two imputation models are compared: a bidirectional LSTM-based neural network and a neural network with a transformer architecture. In the prediction process, the synthetically created weekly mobility schedules serve as input for the imputation model, wherein the 'at home' state is enriched with energy-related activities. In contrast to the autoregressive model of the first step, the imputation model takes into account future state changes from the mobility schedule when predicting 'at home' activities. In this way, the proposed model combines the advantages of the mobility data set, stability in day-to-day mobility patterns, with the advantages of time use survey data and temporally highly detailed information on a diverse set of at-home information in one synthetic dataset.

4.1.3 Key findings and discussion

The presented article shows that current Markov chain models in the field of behavioral modeling are not able to record long-term dependencies in activity patterns and are, therefore, not capable of adequately representing occupancy behavior on an individual level. The proposed neural network-based approach can generate synthetic weekly activity schedules that have stochastic properties similar to the empirically collected data on both the individual and the aggregated levels. The generated data builds the basis for a consistent simulation of energy demand profiles from electric mobility, household devices, space heating, and domestic hot water. By conditioning the developed models on the socio-demographic information of the two basic data sets, activity schedules could be generated representative of different socio-demographic groups. Further, it was shown that the developed approach did not overfit the raw data but learned the general stochastic relationships in human behavior. Further work is needed to train the developed models in a differentially private way in order to be able to provide them publicly available to the scientific community without publishing private information about the underlying datasets.

4.2 Paper B: Two million European single-family homes could abandon the grid by 2050

The following subsections refer to the article “Two million European single-family homes could abandon the grid by 2050”, co-authored with Jann Weinand, Elias Naber, Russell McKenna, Armin Ardone, and Wolf Fichtner. The article was published in the journal *Joule* and is cited in this thesis as Kleinbrahm et al. (2023b).

Study context and contributions

The concept that large, highly interconnected energy systems are the most cost-effective is driven by the principles of economies of scale and the effects of temporal smoothing. However, the impact of economies of scale is less prominent with renewable technologies. Further, heat is typically not transported over long distances, and the regulatory and organizational complexity grows with system size. Having this in mind, this article analyzes the technical and economic potential of 41 million freestanding single-family homes in Europe for off-grid energy self-sufficiency under current and future (2050) conditions.

4.2.1 Objective and significance

Declining capital costs for renewable energy technologies, together with rising energy procurement costs, have stimulated recent trends toward individual and independent energy supply systems across the residential sector. Besides the perceived financial benefits, the desire for self-sufficiency is the main driver behind households' intentions to purchase renewable energy technologies (see Section 2.2.2). Further falling prices of PV and battery systems could lead to a multitude of consumers covering most or all of their energy demand on their own, using the grid only as a backup. However, McKenna et al. (2017) show that partially self-sufficient buildings can put an even greater strain on the electrical grid than traditional end-of-pipe customers. 100% self-sufficient systems, on the other hand, could reduce the need for centralized generation and transmission capacity but currently come with high costs and low stability (McKenna 2018; Tröndle et al. 2020; Tröndle et al. 2019; Khalilpour and Vassallo 2015).

Evidence from practical use cases and scientific case studies suggests that achieving energy self-sufficiency in residential buildings is technically possible, even in conditions that are not ideal for renewable energy sources (Leonard and Michaelides 2018; Knosala et al. 2021; Gstöhl and Pfenninger 2020; Goldsworthy and Sethuvenkatraman 2018; Lacko et al. 2014). Under current energy-political framework conditions, the decreasing marginal utility at very high degrees of self-sufficiency hinders the economical operation of 100% off-grid systems in central Europe. However, considering future decreasing prices of small-scale hydrogen storage systems, efficiency measures, and further demand side flexibility could lower the exponential increase in cost at high degrees of self-sufficiency (Knosala et al. 2021; Leonard and Michaelides 2018; Gstöhl and Pfenninger 2020). Existing studies on 100% self-sufficient residential energy supply only focus on PV-battery systems to cover electrical demand and thereby disregard the synergies of an integrated analysis of electrical and thermal energy demand or are limited to individual buildings and are therefore not able to derive representative statements. Consequently, a large-scale analysis is needed to provide comprehensive insights and comparability across the building stocks of different countries, climates, building types, and household consumption characteristics. Therefore, this article explores the techno-economic potential of 41 million freestanding single-

family buildings in the EU-27, United Kingdom (UK), and Norway (NO) for off-grid energy self-sufficiency.

4.2.2 Methodology

The framework presented in Section 3.3 is used for the analysis of the energy systems of the 41 million single-family buildings in this article (see Figure 17). Based on these 41 million buildings, over 4000 representative building archetypes were identified on the basis of which self-sufficient robust energy systems were designed in parallel in individual energy system optimizations on high-performance computing clusters for 30 historical weather years. The results of the energy system optimizations were used to train surrogate models with the objective of approximating the function between the aggregate energy system optimization input and key output parameters. In the final step, the neural network-based surrogate models were used to calculate the technical and economic potential for the entire synthetic building stock.

A building is regarded to have a technical potential for self-sufficiency if the entire energy demand for electrical appliances, domestic hot water, and space heating can be covered at every hour of the year by only using the local rooftop renewable potential as an energy source. Further, a building is regarded to have an economic potential for self-sufficiency if the total annual system cost (TAC) of a 100% off-grid energy system (NoGridref) is lower than the total annual system cost of an optimized reference system with grid connection and without local self-generation (Grid_{ref}).

4.2.3 Key findings and discussion

The findings of this article show that a cost-minimal PV-based system for achieving residential building energy self-sufficiency in Central Europe should include both short-term battery storage and long-term seasonal hydrogen storage. Even under suboptimal conditions in Finland, individual buildings are capable of supplying all of their energy demand on their own. These results support the findings of previous studies on individual energy self-sufficient residential buildings (Knosala et al. 2021; Gstöhl and Pfenniger 2020; Lacko et al. 2014; Puranen et al. 2021; Schmid and Behrendt 2022).

However, while previous studies only focus on individual buildings, no other article was found that covers a similar level of scale at the spatial dimension and with regard to the complexity of the building energy system. The developed methodology makes it possible for the first time to identify whole regions or climate and economic framework conditions that have a particular potential for self-sufficiency at the individual building level.

Thereby, the results of this article show that even though it is possible for individual buildings to reach 100% energy self-sufficiency in northern regions of Europe, the overall techno-economic potential of

100% self-sufficient buildings is low, even under assumed future techno-economic conditions of 2050. Regions characterized by low seasonal variations (such as Spain, Italy, Portugal, and Cyprus) and with high electricity prices (like Germany) show a pronounced potential for self-sufficient buildings. Under current conditions, 53% of the examined 41 million buildings can technically cover their energy demand on their own by only using local rooftop solar irradiation, and this share could increase to 75% by 2050. If building owners are willing to pay a premium of up to 50% compared with grid-dependent systems with electrified heat supplies, over two million buildings could abandon the grid by 2050.

Given the findings of this article, alongside rising retail energy prices, concerns about energy supply stability, the shift towards local energy sourcing, and technological progress, it's likely that self-sufficient residential buildings will see increased popularity in the future. While this article investigated the technological and economic feasibility from the perspective of building owners, future research should examine system impacts under the consideration of increased dissemination of self-sufficient residential buildings.

4.3 Paper C: Analysing municipal energy system transformations in line with national greenhouse gas reduction strategies

The following subsections refer to the article “Analysing municipal energy system transformations in line with national greenhouse gas reduction strategies”, co-authored with Jann Weinand, Elias Naber, Russell McKenna, and Armin Ardone. The article was published in the journal *Applied Energy* and is cited in this thesis as Kleinebrahm et al. (2023a). The graphical abstract of the article is presented in Figure 22.

Study context and contributions

Strategies for mitigating climate change with expansion targets for renewable energy technologies are often formulated at the national level. However, due to the decentralized character of renewable energy sources, their expansion happens mostly in local communities. Further, the implementation of energy efficiency measures, like building insulation, requires individual decisions. While some local initiatives exist, like the Covenant of Mayors, where local authorities voluntarily commit to renewable energy deployment targets, these local targets may not always align with broader national strategies. Due to the heterogeneity of municipalities in renewable energy potential, energy demand, and size, a direct transfer of national strategies to the local level is not easily possible (Weinand et al. 2019b; Weinand et al. 2019a). Having all of this in mind, aligning local emission reduction strategies with national objectives demands significant coordination, and transferable tools are needed to support local actors in the planning of municipal energy system transformations.

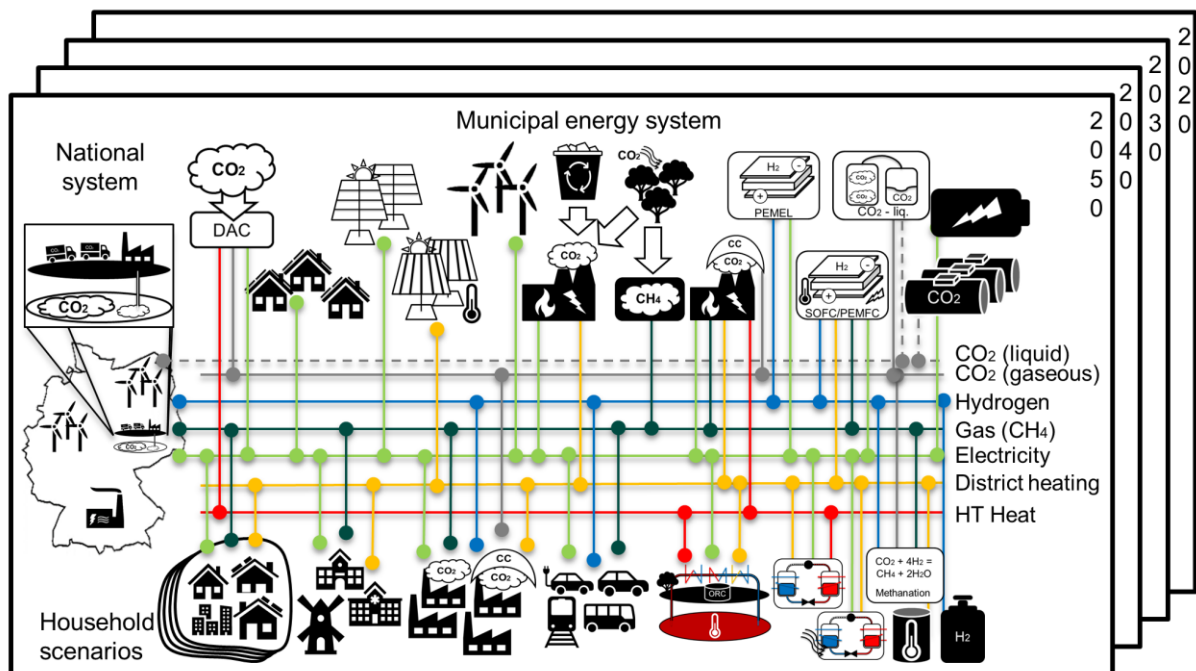


Figure 22: Municipal energy system components and energy carrier flows. Own visualization published in Kleinebrahm et al. (2023a).

4.3.1 Objective and significance

In this article, the municipal energy system model RE³ASON is extended to account for temporally dynamic transformation processes of the local energy system supply and demand side in line with national energy system transformation strategies. Most previous studies on municipal energy systems use an overnight transformation approach, which defines the final state of the desired energy system but does not provide information in terms of how and when to reach this state. Therefore, there is a demand for models that, starting from a predefined energy system, outline a transformation path towards a greenhouse gas-neutral energy system, consisting of specific energy system expansion and efficiency measures. While the original RE³ASON model took into account temporal changes with regard to energy carrier and technology prices, temporal dynamic developments in the form of expansion rates of renewable energy technologies and efficiency measures like building retrofits were not explicitly constrained. This leads to an overly rapid adoption of measures relative to the national system's transformation once they become economically viable, as observed in studies like Weinand et al. (2021). An unrealistically fast implementation of, e.g., residential building retrofit measures is especially favored by an aggregated representation of the building stock.

4.3.2 Methodology

To overcome the identified issues, this article links a stochastic building stock simulation approach with an energy system optimization model to better represent the heterogeneity and temporal inertia of local building stock transformations. By incorporating overarching framework parameters from national scenarios and the initial conditions of local building stocks, multiple household transformation scenarios can be generated ahead of the municipal energy system optimization. The generated scenarios are further represented as binary decision variables associated with their final energy demands and cost in the optimization model. To comprehensively account for the transformation of local energy demand, RE³ASON is further expanded to consider final energy demand transformations across the industrial, tertiary, and transport sectors. Additionally, the portfolio of energy system supply technologies is expanded to consider all relevant technology options represented in the respective national energy system transformation scenarios. Finally, a two-step optimization approach is proposed to solve the municipal energy system optimization problem with reasonable time and accuracy (similar to the approach presented in Section 3.3.3).

4.3.3 Key findings and discussion

To demonstrate the extensions of the presented methodology, an exemplary case study was conducted for the Central European city of Karlsruhe in Germany. 192 building stock transformation scenarios were simulated, which differ in terms of the retrofit rate (8x), the level of the target U-values of retrofit measures (3x), the dissemination of heat recovery units (2x), and the dissemination of the heating system technologies (4x). The results of the building stock transformation show that substantial electrification of the heat supply with a high share of heat pumps and an annual retrofit rate of 2% per year, together with less ambitious U-value requirements, leads to the lowest total discounted system cost and CO₂ emissions. Scenarios with high U-value requirements and high proportions of heat recovery units lead to higher total discounted system costs. This could be explained by the high marginal cost of saving the last few kilowatt-hours in comparison to the cost per kilowatt-hour of heat supplied. The results of the municipal energy system transformation indicate that an accelerated expansion of photovoltaics compared to the national expansion rates can be economically advantageous and lead to lower overall CO₂ emissions. By taking into account anticipated transformations, e.g., the discontinuation of local waste heat sources, it was shown that available biomass and geothermal potentials are used to cover the base load of district heating demand, while large-scale heat pumps and gas boilers are used during peak times. It should be considered that this article does not explore the impact of local energy system transformations on the broader national energy system, and as a result, the simulated exchange with the overarching energy system has no influence on market pricing. However, if many municipalities decide to

accelerate renewable energy expansion, this will impact market prices and could lower the market value of renewable feed-in, possibly influencing future investment choices.

5 Critical reflection

Models are only capable of representing reality to a limited extent. Therefore, it is crucial to approach these representations with a clear awareness of their limitations and the assumptions they embody. This critical reflection chapter aims to illustrate the inherent constraints, simplifications, and necessary trade-offs within the models developed in this thesis. Additionally, for each aspect discussed, insights into potential promising avenues for future research are provided. For more detailed insights into critical aspects, please refer to the discussion sections of each respective paper.

Individuals vs. Households Paper A of this thesis focuses on the simulation of the behavior of individual occupants instead of whole households (see Table 1). This means that one training sample is defined as one activity sequence plus the socio-demographic meta-information of one occupant. This way, dependencies between socio-demographic parameters and temporal dependencies between activity states can be learned by the model. However, intra-household dependencies in the behavior between occupants within one household can't be represented in the synthetic data. A holistic simulation of the household, as opposed to individual members, is especially important for adequately representing activities with a high degree of synchronization, such as joint mobility activities. Future experimental setups should consider intra-household dependencies by defining one training sample as one household, which consists of the activity sequences of its occupants plus meta-information. However, using whole households instead of individual occupants does not come without additional challenges. Enough data are needed to sufficiently represent intra-household dependencies in order to train deep neural networks, which at the current stage are very data-hungry (Adadi 2021). Additionally, the complexity and, therefore, memory and time requirements of the attention mechanism in transformer-based neural networks scale quadratically with respect to sequence length. Therefore, accounting for five household members rather than just one leads to a twenty-five-fold increase in complexity. Consequently, more data sources together with more efficient memory mechanisms in neural networks should be considered in future approaches (see, e.g., Dao et al. (2022), Xiong et al. (2021), Schlag et al. (2021)).

Explainability vs. Accuracy vs. Privacy Bottom-up activity data-based energy demand simulations are used as decision support tools. Yunusov and Torriti (2021), for example, identify socio-demographic groups that may be financially advantaged or disadvantaged by the introduction of time-of-use tariffs. Based on their results, time-of-use tariffs could be redesigned. Consequently, it is important that the underlying tools on the basis of which decisions are made are transparent and explainable. In comparison to existing approaches (see Table 1), the learned connection between inputs and outputs of the neural

networks presented in Paper A can't be explained easily. Therefore, procedures must be developed to ensure that the generated synthetic data not only accurately represents the original data but also is subject to high standards with regard to fairness, privacy, accountability, and transparency (Lo Piano 2020). To ensure that no sensitive data about individual samples in the empirical data is leaked, follow-up work could use algorithms from the field of "differential privacy" when training deep neural networks (Dwork and Roth 2014; Abadi et al. 2016). However, training neural networks in a differentially private way is always accompanied by a loss of model accuracy (Dwork et al. 2019).

Historical Data vs. Future Projections Analyzing future developments based on historical data comes with multiple challenges and is often based on a variety of uncertain assumptions. When analyzing the scenarios presented in this thesis, they should be used to better understand isolated causal relationships and should not be seen as a clear picture of the future.

“Probabilities encode our beliefs about a static world, causality tells us whether and how probabilities change when the world changes, be it by intervention or by act of imagination” (Pearl and Mackenzie 2018). In this thesis, neural networks are trained to learn probability distributions, which are encoded within their structures, using historical data on the behavior of individuals. The learned distributions are conditioned on the socio-demographic parameters of the individuals. Therefore, based on the imagination of a future world with a different distribution of socio-demographic parameters, changes in the overall behavior of the population could be analyzed. However, future behavior will not only change due to changing demographics. Recent history has shown that disruptive events, such as the Covid-19 pandemic or the energy crisis, can lead to significant changes in behavior and, therefore, the way energy is consumed (Lorincz et al. 2022; Buechler et al. 2022; Roth and Schmidt 2023). The energy sector has witnessed numerous innovations that have impacted people's behavior in the past, such as the advent of the internal combustion engine in transportation and the rise of information and communication technology. In the future, technological advancements will continue to fundamentally alter energy service demand and impact human behavior, for example, through the introduction of autonomous vehicles and smart home technologies.

Another prominent source of uncertainty is introduced by the use of historical weather data. In Paper B, robust, self-sufficient residential energy systems are designed based on 30 years of historical weather. In Paper C, only one representative weather year is used. The impact of climate change on energy demand, generation, and infrastructure is well-recognized (Spinoni et al. 2018; Perera et al. 2023; Perera et al. 2020). Future research should incorporate the impact of climate change by utilizing high-resolution climate projection datasets, such as those from the EURO-CORDEX project (Bartók et al. 2019). Particularly, high-probability, low-impact conditions should be considered when designing robust future

energy system designs, as they can notably influence the integration of renewable energy and overall system costs (Perera et al. 2020).

Technical Detail vs. Scope In the development of computer models, many assumptions must be made about trade-offs between the level of detail and the scope of representation. Thereby, it must be ensured that the model has the necessary degree of detail with regard to the research question to be analyzed but is still solvable with reasonable time and accuracy.

As written above, the complexity of the attention mechanism scales quadratically with sequence length. Therefore, in Paper A, mobility data were aggregated from a 1-minute to a 10-minute time resolution. While information is lost in this aggregation step, the complexity of the underlying problem is reduced by a factor of 100. The aggregation process might result in the loss of very short mobility activities, leading to unrealistic state changes in the aggregated data. Thus, future research should focus on either employing more efficient algorithms that eliminate the need for data aggregation or, alternatively, carefully consider the information loss in subsequent applications.

In the development of the energy system models presented in Paper B and Paper C, a multitude of assumptions had to be made to achieve a good trade-off between temporal and spatial resolution and the level of detail with regard to the technologies and operation strategies considered. In both studies, an hourly temporal resolution is used, which could be particularly critical in the analysis of 100% self-sufficient energy systems as short-term power peaks get smoothed out. Therefore, future work should further focus on the impact of short-term power peaks on the design of off-grid energy systems (see, e.g., Omoyele et al. (2024)). In addition to the possibility of covering the power peaks, the potential for demand-side reduction should also be examined. Since there were almost no economic incentives in the past due to mainly volumetric electricity pricing, it can be assumed that there is a certain potential for peak power reduction, for instance, through smart control of consumer devices (Hinterstocker and Roon 2017). Furthermore, the inclusion of part-load efficiencies for inverters, generators, electrolyzers, or fuel cells, such as through nonlinear performance functions, was omitted in the analyses to avoid substantially increasing the complexity of the optimization problem. Others, such as Schütz et al. (2017b), Goderbauer et al. (2016), and Milan et al. (2015), approximate these nonlinear functions by using piecewise linearization or iterative approaches. However, these measures also rapidly increase the complexity of the problem and quickly lead to long model runtimes, even for small systems. Further, the problem of perfect foresight in closed-form energy system optimization models leads to an underestimation of the uncertainty in future developments. In Paper B, dispatchable technologies in the form of hybrid storage systems and power-to-heat technologies are operated with certainty about future weather and energy demand developments, which in reality can only be predicted with uncertainty. Future studies could use the proposed system configurations of this thesis and further develop operation strategies

using, e.g., a rolling horizon stochastic optimization approach to account for uncertainties (Hou et al. 2020). Since it is unlikely that the optimal operation will be perfectly approximated, the energy system components would subsequently need to be rescaled using a heuristic approach until a certain level of supply security can be ensured. In Paper C, investments can be made at multiple stages during the transformation process. Therefore, not only are short-term uncertainties underestimated, but also longer-term uncertainties in, e.g., technological and climate parameters. Thus, the optimizer's reliance on anticipated future developments, which are based on assumptions with significant uncertainty, can lead to less climate action at earlier stages. Technologies that are still under development, like direct air capture, should not be used as a justification for increasing emissions today with the expectation of offsetting them in the future.

Macro- vs. Microeconomic Perspective In Paper C, municipal energy systems are calculated from the perspective of a public welfare-oriented central planner. In this macroeconomic approach, no taxes and levies are considered in order to ensure technology neutrality. Since the perspectives of individual stakeholders are not taken into account, a direct implementation of the determined measures is difficult to achieve in reality. In Paper B and in Braeuer et al. (2022), the proposed framework in Section 3.3 is used to determine cost-minimal residential energy systems, taking into account different microeconomic perspectives. By considering taxes and levies on energy procurement, as well as feed-in tariffs, different framework conditions arise, which lead to a different assessment of investment measures in comparison to macroeconomic assessments. Therefore, the design of taxes, levies, and further subsidies constantly needs to ensure a just transformation process to a greenhouse gas-neutral energy system.

Techno-economic Modeling vs. Socio-technical Realities In this thesis, two techno-economic modeling approaches are proposed with the objective of identifying technically feasible, cost-minimal energy systems. However, energy systems can be regarded as complex socio-technical constructs, possibly consisting of different decision-making entities and technological artifacts governed in a multi-level institutional space (Koirala et al. 2016). Research on the energy-efficiency gap reveals that although technologies have the potential to lower financial expenses and environmental damages linked to energy use, they are not being adopted to the extent that would be justified, even from a strictly financial perspective (Gerarden et al. 2017). To better predict the dissemination of local technologies, social relationships among stakeholders need to be considered since they represent major drivers or barriers to adoption (Rae and Bradley 2012). Understanding adoption behavior is valuable for identifying the barriers to new technologies and determining which policies are crucial for enhancing their diffusion. Consequently, the spread of low-carbon technologies in residential buildings is not just a matter of technical feasibility but also a matter of individual behavior and group dynamics. Future approaches should, therefore, try to better account for factors influencing individual adoption behavior and group dynamics, e.g.,

by considering social factors influencing the acceptance of technologies in energy system models (Weinand et al. 2021).

6 Summary, conclusion, and outlook

While in the past, the electrical energy demand for household devices was mainly provided by the electricity grid, and the heat was primarily generated with fossil fuels, future residential buildings will be mostly electrified. The buildings will contribute to integrating fluctuating renewable energies by installing small-scale photovoltaics and providing flexibility to the overall energy system. Further, integrating the electricity, heat, and transport sectors within residential buildings will fundamentally change the characteristics of residential energy demand. A comprehensive understanding of these changes is essential to design future energy systems efficiently. Thus, this thesis follows the objective of developing novel methods for the technical, economic, and environmental evaluation of sector-coupled residential building energy systems, taking a diverse set of perspectives.

In this thesis, neural network-based approaches from the field of natural language processing were introduced to the field of behavioral modeling to better understand the fundamental connections that shape the structure of future residential energy demand. By combining mobility and activity data to generate high-quality occupant activity schedules, the presented approach accurately represents long-term dependencies in occupant behavior and, therefore, builds the basis for a consistent simulation of residential electricity, heat, and mobility demand. In addition, based on the detailed understanding of the drivers of residential energy demand, a bottom-up framework for determining the cost-minimal design and operation of residential energy systems was proposed for analyzing 41 million European single-family buildings under diverse framework conditions. Finally, to extend the microeconomic perspective of a building owner, a macroeconomic perspective of a central planner was taken to comprehensively consider the transformation of the residential building stock within the transformation of the overarching energy system.

To overcome the shortcomings of previous approaches that aim to capture relationships in activity patterns to explain residential energy demand, a two-step neural network-based approach was presented to combine the advantages of German weekly mobility data and time-use survey data. While previous approaches are not capable of representing long-term dependencies in occupant behavior and, therefore, fail to generate high-quality individual occupant schedules, the proposed approach is capable of representing complex dependencies in mobility and activity patterns and, at the same time, adequately captures the diversity in behavior across the entire population. By combining an autoregressive generative model with an imputation model, synthetic occupant activity schedules are generated, which build the basis for the simulation of residential energy demand and the examination of flexibility potentials needed

for the integration of volatile renewable energy sources. Future studies should consider whole households as input data in contrast to individual occupants. Thereby, intra-household dependencies, which are important for synchronizing occupant activities within households, could be represented in the synthetic data.

Furthermore, in light of diminishing capital costs for renewable energies and rising energy procurement expenses, the developed bottom-up framework was utilized to investigate the viability of energy self-sufficiency for all owner-occupied freestanding single-family buildings in the EU-27, United Kingdom, and Norway. By combining spatial microsimulation, advanced spatial and temporal complexity reduction techniques, building energy system optimization, and neural network-based surrogate models, climate and economic framework conditions that are especially suitable for self-sufficiency were identified. A pronounced potential for self-sufficient buildings was apparent in regions with low seasonality, such as Spain, and high household electricity prices, such as Germany. Under current technological conditions, 53% of the 41 million buildings can technically supply themselves independently from external infrastructures by only using local rooftop solar irradiation. In 2050, this proportion could increase to 75%. Due to the high marginal costs to achieve the final degrees of self-sufficiency, an energy-self-sufficient building is not an optimal economic option, particularly as long as no fixed grid charges are introduced. However, if building owners are willing to pay a premium of up to 50% compared with grid-dependent systems with electrified heat supplies, over two million buildings could abandon the grid by 2050. While this thesis analyzes the technological and economic feasibility of self-sufficiency from the microeconomic perspective of building owners, future studies could examine system impacts and transformations considering increased dissemination of self-sufficient buildings.

In a third study, a municipal energy system model was developed to investigate the residential building stock transformation within a municipal energy system, in line with national greenhouse gas reduction strategies. Existing shortcomings of a highly aggregated building stock representation were overcome by the development of a stochastic building stock model to better capture the temporal inertia and the high heterogeneity of residential buildings in the transformation process. Based on superordinate parameters such as retrofit rates and heating technology diffusion, the stochastic model generates multiple informative building stock scenarios used as input in municipal energy system optimization. 192 residential building stock transformation scenarios were calculated for the exemplary case study of the German city of Karlsruhe. The results showed that an increase in the retrofit rate to 2% per year, together with a substantial electrification of the heat supply in the building sector, is economically and environmentally beneficial.

The developed approaches in this thesis have been validated where possible and checked for plausibility at multiple stages. Furthermore, extensive sensitivity analyses are provided with regard to relevant exogenous assumed parameters to ensure the robustness of the results. The transferability of the developed bottom-up framework presented in Paper B has already been further demonstrated by its use in multiple other studies (see, e.g., Vögele et al. (2022), Braeuer et al. (2022), Kleinebrahm et al. (2018)).

However, while the proposed models already provide important results, there is still space for methodological extensions to increase their usability for practical use cases. The neural network-based approach presented in Paper A currently provides a promising proof of concept and, therefore, should be extended in future studies by incorporating further data sources and differential private training methods to finally provide a synthetic open access dataset of residential occupancy and mobility behavior. Due to the scope of the proposed bottom-up framework utilized in Paper B, multiple assumptions had to be made to calculate the techno-economic potential of self-sufficient residential buildings in the European building stock. For example, archetypal buildings were used with basic assumptions regarding azimuth, tilt, and utilization factors for solar systems. Future studies could include satellite image-based analyses to account for physical obstructions. Furthermore, the willingness to pay extra for a self-sufficient residential energy supply could be investigated in empirical studies to better predict the dissemination of off-grid buildings. Finally, the methodology presented in Paper C could be further extended to account for the preferences of local stakeholders in the modeling process. Thus, the social acceptance of novel technologies, such as wind power plants, open-space photovoltaic, and geothermal plants, could already be taken into account during the planning process of the municipal energy system.

7 References

§ 12 UStG: Umsatzsteuergesetz. Available online at https://www.gesetze-im-internet.de/ustg_1980/___12.html.

- Abadi, Martin; Chu, Andy; Goodfellow, Ian; McMahan, H. Brendan; Mironov, Ilya; Talwar, Kunal; Zhang, Li (2016): Deep Learning with Differential Privacy. In *CCS '16: Proceedings of the 2016 ACM SIGSAC Conference on Computer and Communications Security*, pp. 308–318. DOI: 10.1145/2976749.2978318.
- Achtnicht, Martin; Madlener, Reinhard (2014): Factors influencing German house owners' preferences on energy retrofits. In *Energy Policy* 68, pp. 254–263. DOI: 10.1016/j.enpol.2014.01.006.
- Adadi, Amina (2021): A survey on data-efficient algorithms in big data era. In *J Big Data* 8 (1). DOI: 10.1186/s40537-021-00419-9.
- Aerts, D.; Minnen, J.; Glorieux, I.; Wouters, I.; Descamps, F. (2014): A method for the identification and modelling of realistic domestic occupancy sequences for building energy demand simulations and peer comparison. In *Building and Environment* 75, pp. 67–78. DOI: 10.1016/j.buildenv.2014.01.021.
- AGEB (2022): Energiebilanzen, verschiedene Jahrgänge. Available online at <https://ag-energiebilanzen.de/daten-und-fakten/bilanzen-1990-bis-2020/?wpv-jahresbereich-bilanz=2011-2020>, checked on 1/10/2023.
- AGEB (2023): Energiebilanz der Bundesrepublik 2021. Available online at <https://ag-energiebilanzen.de/wp-content/uploads/2023/03/Bilanz-2021.xlsx>, checked on 8/25/2023.
- Ahanghamejhad, Ramez Hosseinian; Phillips, Adam B.; Song, Zhaoning; Celik, Ilke; Ghimire, Kiran; Koirala, Prakash et al. (2022): Impact of lifetime on the levelized cost of electricity from perovskite single junction and tandem solar cells. In *Sustainable Energy Fuels* 6 (11), pp. 2718–2726. DOI: 10.1039/D2SE00029F.
- Alaa, Ahmed M.; van Breugel, Boris; Saveliev, Evgeny; van der Schaar, Mihaela (2021): How Faithful is your Synthetic Data? Sample-level Metrics for Evaluating and Auditing Generative Models. Available online at <http://arxiv.org/pdf/2102.08921v1>, checked on 2/17/2021.
- Alipour, M.; Irannezhad, Elnaz; Stewart, Rodney A.; Sahin, Oz (2022): Exploring residential solar PV and battery energy storage adoption motivations and barriers in a mature PV market. In *Renewable Energy* 190, pp. 684–698. DOI: 10.1016/j.renene.2022.03.040.
- Al-Wreikat, Yazan; Serrano, Clara; Sodré, José Ricardo (2022): Effects of ambient temperature and trip characteristics on the energy consumption of an electric vehicle. In *Energy* 238, Article 122028. DOI: 10.1016/j.energy.2021.122028.
- Andrews, Robert W.; Stein, Joshua S.; Hansen, Clifford; Riley, Daniel (2014): Introduction to the open source PV LIB for python Photovoltaic system modelling package. In : 2014 IEEE 40th Photovoltaic Specialist Conference (PVSC). 2014 IEEE 40th Photovoltaic Specialists Conference (PVSC). Denver, CO, USA, 08.06.2014 - 13.06.2014: IEEE, pp. 170–174.
- Anvari, Mehrnaz; Proedrou, Elisavet; Schäfer, Benjamin; Beck, Christian; Kantz, Holger; Timme, Marc (2022): Data-driven load profiles and the dynamics of residential electricity consumption. In *Nature communications* 13 (1), Article 4593. DOI: 10.1038/s41467-022-31942-9.
- Bahl, Björn; Kümpel, Alexander; Seele, Hagen; Lampe, Matthias; Bardow, André (2017): Time-series aggregation for synthesis problems by bounding error in the objective function. In *Energy* 135, pp. 900–912. DOI: 10.1016/j.energy.2017.06.082.
- Balcombe, Paul; Rigby, Dan; Azapagic, Adisa (2014): Investigating the importance of motivations and barriers related to microgeneration uptake in the UK. In *Applied Energy* 130, pp. 403–418. DOI: 10.1016/j.apenergy.2014.05.047.
- Baños, R.; Manzano-Agugliaro, F.; Montoya, F. G.; Gil, C.; Alcayde, A.; Gómez, J. (2011): Optimization methods applied to renewable and sustainable energy: A review. In *Renewable and Sustainable Energy Reviews* 15 (4), pp. 1753–1766. DOI: 10.1016/j.rser.2010.12.008.
- Bartók, Blanka; Tobin, Isabelle; Vautard, Robert; Vrac, Mathieu; Jin, Xia; Levvasseur, Guillaume et al. (2019): A climate projection dataset tailored for the European energy sector. In *Climate Services* 16, p. 100138. DOI: 10.1016/j.cliser.2019.100138.

References

- BCG; BDI (2021): Klimapfade 2.0 - Ein Wirtschaftsprogramm für Klima und Zukunft. Available online at https://issuu.com/bdi-berlin/docs/211021_bdi_klimapfade_2.0_-_gesamtstudie_-_vorabve, checked on 10/1/2023.
- BDEW (2023): BDEW-Strompreisanalyse Juli 2023. Haushalte und Industrie. Available online at https://www.bdew.de/media/documents/BDEW-Strompreisanalyse_o_dw_halbjahrlich_Ba_online_24072023.pdf, updated on 7/24/2023, checked on 10/1/2023.
- Bianchi, M.; Branchini, L.; Ferrari, C.; Melino, F. (2014): Optimal sizing of grid-independent hybrid photovoltaic–battery power systems for household sector. In *Applied Energy* 136, pp. 805–816. DOI: 10.1016/j.apenergy.2014.07.058.
- Blocker, Alexander W. (2022): Fast Implementation of the Iterative Proportional Fitting Procedure in C. A fast (C) implementation of the iterative proportional fitting procedure. Available online at <https://github.com/awblocker/ipfp>, checked on 5/18/2022.
- BMWK (2023a): Energieeffizienz in Zahlen 2022. Entwicklungen und Trends in Deutschland 2022. Edited by Bundesministerium für Wirtschaft und Klimaschutz (BMWK). Available online at [https://www.bmwk.de/Redaktion/DE/Publikationen/Energie/energieeffizienz-in-zahlen-2022.pdf?__blob=publicationFile&v=3#:~:text=Die%20Arbeitsgemein%20schaft%20Energiebilanzen%20\(AGEB,zum%20Vorjahr%20\(AGEB%202022e\).,](https://www.bmwk.de/Redaktion/DE/Publikationen/Energie/energieeffizienz-in-zahlen-2022.pdf?__blob=publicationFile&v=3#:~:text=Die%20Arbeitsgemein%20schaft%20Energiebilanzen%20(AGEB,zum%20Vorjahr%20(AGEB%202022e).,) checked on 12/1/2023.
- BMWK (2023b): Time series for the development of renewable energy sources in Germany. Available online at https://www.erneuerbare-energien.de/EE/Navigation/DE/Service/Erneuerbare_Energien_in_Zahlen/Zeitreihen/zeitreihen.html, updated on 09.2023, checked on 12/1/2023.
- BMWSB (2023): Weg frei für eine klimafreundliche und bezahlbare Wärmeversorgung. Available online at <https://www.bmwsb.bund.de/SharedDocs/pressemitteilungen/Webs/BMWSB/DE/2023/11/wpg.html>, checked on 12/1/2023.
- BNetzA (2022): Monitoringbericht 2022. Available online at https://www.bundesnetzagentur.de/SharedDocs/Mediathek/Monitoringberichte/MonitoringberichtEnergie2022.pdf?__blob=publicationFile&v=3, checked on 12/1/2023.
- BNetzA (2023a): Archivierte EEG-Ver-gü-tungs-sät-ze und Daten-meldungen. Available online at https://www.bundesnetzagentur.de/DE/Fachthemen/ElektrizitaetundGas/ErneuerbareEnergien/ZahlenDatenInformationen/EEG_Registerdaten/ArchivDaten-Meldgn/artikel.html, checked on 11/8/2023.
- BNetzA (2023b): SMARD Strommarktdaten. Available online at [SMARD.de](https://www.smard.de), checked on 4/20/2023.
- Bódis, Katalin; Kougias, Ioannis; Jäger-Waldau, Arnulf; Taylor, Nigel; Szabó, Sándor (2019): A high-resolution geospatial assessment of the rooftop solar photovoltaic potential in the European Union. In *Renewable and Sustainable Energy Reviews* 114, Article 109309. DOI: 10.1016/j.rser.2019.109309.
- Bottaccioli, Lorenzo; Di Cataldo, Santa; Acquaviva, Andrea; Patti, Edoardo (2019): Realistic Multi-Scale Modeling of Household Electricity Behaviors. In *IEEE Access* 7, pp. 2467–2489. DOI: 10.1109/ACCESS.2018.2886201.
- Bowman, John (1998): The Day Activity Schedule Approach to Travel Demand Analysis. Dissertation. Cambridge, Massachusetts.
- Brauer, Fritz; Kleinebrahm, Max; Naber, Elias; Scheller, Fabian; McKenna, Russell (2022): Optimal system design for energy communities in multi-family buildings: the case of the German Tenant Electricity Law. In *Applied Energy* 305, Article 117884. DOI: 10.1016/j.apenergy.2021.117884.
- Breyer, Christian; Gerlach, Alexander (2013): Global overview on grid-parity. In *Prog. Photovolt: Res. Appl.* 21 (1), pp. 121–136. DOI: 10.1002/pip.1254.
- Bringault, A.; Eisermann, M.; Lacassagne, S. (2017): Cities Heading towards 100% Renewable Energy. Available online at <https://energy-cities.eu/wp-content/uploads/2018/11/publi100percentfinal-weben.pdf>, checked on 12/5/2023.
- Buechler, Elizabeth; Powell, Siobhan; Sun, Tao; Astier, Nicolas; Zanolto, Chad; Bolorinos, Jose et al. (2022): Global changes in electricity consumption during COVID-19. In *iScience* 25 (1), Article 103568. DOI: 10.1016/j.isci.2021.103568.
- Bundesregierung (2021): Klimaschutzgesetz 2021. Generationenvertrag für das Klima. Available online at <https://www.bundesregierung.de/breg-de/themen/klimaschutz/klimaschutzgesetz-2021-1913672>, checked on 12/1/2023.

- Bundesregierung (2023): Klimaschutzprogramm 2023 der Bundesregierung. Available online at https://www.bmwk.de/Redaktion/DE/Downloads/klimaschutz/20231004-klimaschutzprogramm-der-bundesregierung.pdf?__blob=publicationFile&v=4, checked on 12/1/2023.
- California Energy Commission (2018): California Plug-In Electric Vehicle Infrastructure Projections: 2017–2025. Future Infrastructure Needs for Reaching the State’s Zero-Emission-Vehicle Deployment Goal. Available online at <https://www.nrel.gov/docs/fy18osti/70893.pdf>, checked on 10/9/2023.
- Camargo, Luis Ramirez; Gruber, Katharina; Nitsch, Felix; Dörner, Wolfgang (2019): Hybrid renewable energy systems to supply electricity self-sufficient residential buildings in Central Europe. In *Energy Procedia* 158, pp. 321–326. DOI: 10.1016/j.egypro.2019.01.096.
- Capasso, A.; Grattieri, W.; Lamedica, R.; Prudenzi, A. (1994): A bottom-up approach to residential load modeling. In *IEEE Trans. Power Syst.* 9 (2), pp. 957–964. DOI: 10.1109/59.317650.
- Cischinsky, Holger; Diefenbach, Nikolaus (2018): Datenerhebung Wohngebäudebestand 2016. Datenerhebung zu den energetischen Merkmalen und Modernisierungsraten im deutschen und hessischen Wohngebäudebestand. Stuttgart: Fraunhofer IRB Verlag (Forschungsinitiative Zukunft Bau, F 3080).
- Copernicus Climate Change Service (2017): ERA5: Fifth generation of ECMWF atmospheric reanalyses of the global climate. Copernicus Climate Change Service Climate Data Store (CDS). Available online at <https://cds.climate.copernicus.eu/cdsapp>, checked on 12/1/2023.
- Cruz, Marco R.M.; Fitiwi, Desta Z.; Santos, Sérgio F.; Catalão, João P.S. (2018): A comprehensive survey of flexibility options for supporting the low-carbon energy future. In *Renewable and Sustainable Energy Reviews* 97, pp. 338–353. DOI: 10.1016/j.rser.2018.08.028.
- Dao, Tri; Fu, Daniel Y.; Ermon, Stefano; Rudra, Atri; Ré, Christopher (2022): FlashAttention: Fast and Memory-Efficient Exact Attention with IO-Awareness. Available online at <http://arxiv.org/pdf/2205.14135v2>, checked on 12/1/2023.
- DENA (2023): DENA-Gebäudereport 2024. Available online at https://www.dena.de/fileadmin/dena/Publikationen/PDFs/2023/dena-Gebae-dereport_2024.pdf, checked on 1/1/2024.
- Destatis (2006): Zeitbudgeterhebung: Aktivitäten in Stunden und Minuten nach Geschlecht, Alter und Haushaltstyp. Zeitbudgets - Tabellenband I. 2001/2002. Wiesbaden. Available online at https://www.statistischebibliothek.de/mir/receive/DEMografie_mods_00003054, checked on 12/1/2023.
- Dwork, Cynthia; Kohli, Nitin; Mulligan, Deirdre (2019): Differential Privacy in Practice: Expose your Epsilons! In *JPC* 9 (2). DOI: 10.29012/jpc.689.
- Dwork, Cynthia; Roth, Aaron (2014): The Algorithmic Foundations of Differential Privacy. In *FNT in Theoretical Computer Science* 9 (3–4), pp. 211–407. DOI: 10.1561/04000000042.
- Ecker, Franz; Hahnel, Ulf J. J.; Spada, Hans (2017): Promoting Decentralized Sustainable Energy Systems in Different Supply Scenarios: The Role of Autarky Aspiration. In *Front. Energy Res.* 5, Article 14. DOI: 10.3389/fenrg.2017.00014.
- Ecker, Franz; Spada, Hans; Hahnel, Ulf J.J. (2018): Independence without control. Autarky outperforms autonomy benefits in the adoption of private energy storage systems. In *Energy Policy* 122, pp. 214–228. DOI: 10.1016/j.enpol.2018.07.028.
- E-Control (2023): Sonstige MarktregelnStrom Kapitel 6 Zählwerte, Datenformate undstandardisierte Lastprofile. Tech. Rep. Energie-Control Austria für die Regulierung der Elektrizitäts- und Erdgaswirtschaft, Rudolfspl. 13A, 1010 Wien, Austria. Wien, Austria. Available online at <https://www.e-control.at/recht/marktregeln/sonstige-marktregeln-strom>, checked on 10/25/2023.
- EEA (2023): EEA greenhouse gases — data viewer. Edited by European Environment Agency. Available online at https://www.eea.europa.eu/ds_resolveuid/5e8d1c3335a342b1822a39b5eb964715, checked on 1/1/2024.
- Enerdata (Ed.) (2022): Odyssee Database on the Energy Consumption Drivers by End-use, Energy Efficiency and CO 2 Related Indicators. Available online at <https://odyssee.enerdata.net/database/>, checked on 4/19/2022.
- Engelken, Maximilian; Römer, Benedikt; Drescher, Marcus; Welpke, Isabell (2018): Why homeowners strive for energy self-supply and how policy makers can influence them. In *Energy Policy* 117, pp. 423–433. DOI: 10.1016/j.enpol.2018.02.026.

References

- ENTSO-E (2023): TransparencyPlatform. Available online at <https://transparency.entsoe.eu/>, checked on 10/24/2023.
- EUPD Research (2021): EndkundenMonitor11.0. Der deutsche PV Markt aus der Perspektive des Endkunden: Umfrage unter 2.000 PV Besitzern und Planern. Fokus: Elektromobilität und Energiemanagement. Available online at https://www.eupd-research.com/wp-content/uploads/EUPD_Research_EndkundenMonitor_11.pdf, checked on 1/1/2024.
- European Commission (2023): Climate Action Progress Report 2023. Shifting gears: Increasing the pace of progress towards a green and prosperous future. Available online at https://climate.ec.europa.eu/document/download/60a04592-cf1f-4e31-865b-2b5b51b9d09f_en, checked on 1/1/2024.
- European Parliament (2021): European Climate Law, revised Regulation (EU) 2021/1119 of the European Parliament and of the Council of 6/30/2021 establishing the framework for achieving climate neutrality and amending Regulations (EC) No 401/2009 and (EU) 2018/1999 ('European Climate Law'). Available online at <http://data.europa.eu/eli/reg/2021/1119/oj>.
- European Parliament and Council of the European Union (2019): Directive (EU) 2019/944 of the European Parliament and of the Council of 5 June 2019 on common rules for the internal market for electricity and amending Directive 2012/27/EU. EU Official Journal of the European Union. Available online at <http://data.europa.eu/eli/dir/2019/944/oj>, checked on 12/1/2023.
- Eurostat (2023a): Electricity prices for household consumers - bi-annual data (from 2007 onwards). Edited by Eurostat. Available online at https://ec.europa.eu/eurostat/databrowser/view/nrg_pc_204/default/map?lang=de, updated on 18.10.23, checked on 18.10.23.
- Eurostat (2023b): Electricity production capacities for renewables and wastes. Available online at https://ec.europa.eu/eurostat/databrowser/view/nrg_inf_epcrw__custom_8253461/default/table?lang=en, updated on 3/31/2023, checked on 12/1/2023.
- Eurostat (2023c): Gas prices for household consumers - bi-annual data (from 2007 onwards). Edited by Eurostat. Available online at https://ec.europa.eu/eurostat/databrowser/view/NRG_PC_202/default/table?lang=de&category=nrg.nrg_price.nrg_pc, updated on 1/14/2023, checked on 12/14/2023.
- Eurostat (2023d): Population change - Demographic balance and crude rates at national level. Available online at https://ec.europa.eu/eurostat/databrowser/view/DEMO_GIND__custom_8246121/default/table?lang=en, updated on 9/25/2023, checked on 12/1/2023.
- Eurostat (2024): Harmonized European Time of Use Surveys. Available online at <https://ec.europa.eu/eurostat/web/microdata/harmonised-european-time-use-surveys#:~:text=The%20harmonised%20European%20time%20use,life%2C%20travel%2C%20and%20leisure,> checked on 1/1/2024.
- EWI (2021): dena-Leitstudie Aufbruch Klimaneutralität. Klimaneutralität 2045 - Transformation der Verbrauchssektoren und des Energiesystems. Herausgegeben von der Deutschen Energie-Agentur GmbH (dena). Available online at https://www.ewi.uni-koeln.de/cms/wp-content/uploads/2021/10/211005_EWI-Gutachterbericht_dena-Leitstudie-Aufbruch-Klimaneutralitaet.pdf, checked on 12/1/2023.
- EWI (2022): Scenarios for the Price Development of Energy Commodities. Institute of Energy Economics at the University of Cologne. Available online at https://www.ewi.uni-koeln.de/cms/wp-content/uploads/2022/09/EWI-Study-Scenarios-for-the-price-development-of-energy-commodities_English-Summary.pdf, checked on 12/1/2023.
- Few, Sheridan; Schmidt, Oliver; Offer, Gregory J.; Brandon, Nigel; Nelson, Jenny; Gambhir, Ajay (2018): Prospective improvements in cost and cycle life of off-grid lithium-ion battery packs. An analysis informed by expert elicitations. In *Energy Policy* 114, pp. 578–590. DOI: 10.1016/j.enpol.2017.12.033.
- FFE (2022): Daily updated specific Greenhouse Gas Emissions of the German Electricity Mix. Available online at <https://www.ffe.de/en/publications/tagesaktuelle-spezifische-thg-emissionen/>, checked on 12/1/2023.
- Figgenger, Jan; Hecht, Christopher; Haberschusz, David; Bors, Jakob; Spreuer, Kai Gerd; Kairies, Kai-Philipp et al. (2022): The development of battery storage systems in Germany: A market review (status 2023). Available online at <http://arxiv.org/pdf/2203.06762v3>, checked on 12/1/2023.
- Figgenger, Jan; Stenzel, Peter; Kairies, Kai-Philipp; Linßen, Jochen; Haberschusz, David; Wessels, Oliver et al. (2020): The development of stationary battery storage systems in Germany – A market review. In *Journal of Energy Storage* 29, p. 101153. DOI: 10.1016/j.est.2019.101153.

- FIS (2023): Pkw-Besetzungsgrad bei der privaten Autonutzung. Edited by Forschungsinformationssystem. Available online at <https://www.forschungsinformationssystem.de/servlet/is/79638/>, checked on 9/28/2023.
- Fischer, David; Harbrecht, Alexander; Surmann, Arne; McKenna, Russell (2019): Electric vehicles' impacts on residential electric local profiles – A stochastic modelling approach considering socio-economic, behavioural and spatial factors. In *Applied Energy* 233-234, pp. 644–658. DOI: 10.1016/j.apenergy.2018.10.010.
- Fischer, David; Surmann, Arne; Lindberg, Karen Byskov (2020): Impact of emerging technologies on the electricity load profile of residential areas. In *Energy and Buildings* 208, p. 109614. DOI: 10.1016/j.enbuild.2019.109614.
- Fischer, David; Wolf, Tobias; Scherer, Johannes; Wille-Haussmann, Bernhard (2016): A stochastic bottom-up model for space heating and domestic hot water load profiles for German households. In *Energy and Buildings* 124, pp. 120–128. DOI: 10.1016/j.enbuild.2016.04.069.
- Flett, Graeme; Kelly, Nick (2016): An occupant-differentiated, higher-order Markov Chain method for prediction of domestic occupancy. In *Energy and Buildings* 125, pp. 219–230. DOI: 10.1016/j.enbuild.2016.05.015.
- Fuentes, E.; Arce, L.; Salom, J. (2018): A review of domestic hot water consumption profiles for application in systems and buildings energy performance analysis. In *Renewable and Sustainable Energy Reviews* 81, pp. 1530–1547. DOI: 10.1016/j.rser.2017.05.229.
- Gaetani, Isabella; Hoes, Pieter-Jan; Hensen, Jan L.M. (2016): Occupant behavior in building energy simulation: Towards a fit-for-purpose modeling strategy. In *Energy and Buildings* 121, pp. 188–204. DOI: 10.1016/j.enbuild.2016.03.038.
- Gaete-Morales, Carlos; Kramer, Hendrik; Schill, Wolf-Peter; Zerrahn, Alexander (2020): An open tool for creating battery-electric vehicle time series from empirical data: emobpy. Available online at <http://arxiv.org/pdf/2005.02765v1>, checked on 12/1/2023.
- Galvin, Ray (2022): Are electric vehicles getting too big and heavy? Modelling future vehicle journeying demand on a decarbonized US electricity grid. In *Energy Policy* 161, p. 112746. DOI: 10.1016/j.enpol.2021.112746.
- Gerarden, Todd D.; Newell, Richard G.; Stavins, Robert N. (2017): Assessing the Energy-Efficiency Gap. In *Journal of Economic Literature* 55 (4), pp. 1486–1525. DOI: 10.1257/jel.20161360.
- Goderbauer, Sebastian; Bahl, Björn; Voll, Philip; Lübbecke, Marco E.; Bardow, André; Koster, Arie M.C.A. (2016): An adaptive discretization MINLP algorithm for optimal synthesis of decentralized energy supply systems. In *Computers & Chemical Engineering* 95, pp. 38–48. DOI: 10.1016/j.compchemeng.2016.09.008.
- Goldsworthy, M. J.; Sethuvenkatraman, S. (2018): The off-grid PV-battery powered home revisited; the effects of high efficiency air-conditioning and load shifting. In *Solar Energy*. DOI: 10.1016/j.solener.2018.02.051.
- Gorman, Will; Jarvis, Stephen; Callaway, Duncan (2020): Should I Stay Or Should I Go? The importance of electricity rate design for household defection from the power grid. In *Applied Energy* 262, p. 114494. DOI: 10.1016/j.apenergy.2020.114494.
- Grandjean, A.; Adnot, J.; Binet, G. (2012): A review and an analysis of the residential electric load curve models. In *Renewable and Sustainable Energy Reviews* 16 (9), pp. 6539–6565. DOI: 10.1016/j.rser.2012.08.013.
- Gstöhl, Ursin; Pfenninger, Stefan (2020): Energy self-sufficient households with photovoltaics and electric vehicles are feasible in temperate climate. In *PloS one* 15 (3), e0227368. DOI: 10.1371/journal.pone.0227368.
- Hilgert, Tim (2019): Erstellung von Wochenaktivitätenplänen für Verkehrsnachfragemodelle. Available online at <https://publikationen.bibliothek.kit.edu/1000097893/46739012>, checked on 10/22/2019.
- Hilgert, Tim; Heilig, Michael; Kagerbauer, Martin; Vortisch, Peter (2017): Modeling Week Activity Schedules for Travel Demand Models. In *Transportation Research Record* 2666 (1), pp. 69–77. DOI: 10.3141/2666-08.
- Hillemacher, Lutz (2014): Lastmanagement mittels dynamischer Strompreissignale bei Haushaltskunden. Dissertation. Karlsruhe Institut für Technologie. Available online at <https://d-nb.info/106400301X/34>.

References

- Hinterstocker, Michael; Roon, Serafin von (2017): Implementation of Variable Retail Electricity Rates in the German System of Taxes, Fees and Levies. Available online at https://www.eeg.tuwien.ac.at/conference/iaee2017/files/paper/652_Hinterstocker_fullpaper_2017-09-07_15-39.pdf, checked on 12/1/2023.
- Hochreiter, S.; Schmidhuber, J. (1997): Long Short-Term Memory. Available online at <https://www.mitpressjournals.org/doi/10.1162/neco.1997.9.8.1735>, checked on 8/13/2020.
- Home Power Solution (Ed.) (2022). Available online at www.homepowersolution.de, checked on 8/31/2022.
- Hou, Weilin; Liu, Zhaoxi; Ma, Li; Wang, Lingfeng (2020): A Real-Time Rolling Horizon Chance Constrained Optimization Model for Energy Hub Scheduling. In *Sustainable Cities and Society* 62, p. 102417. DOI: 10.1016/j.scs.2020.102417.
- Huang, Charlotte; Elsland, Rainer (2019): A survey-based approach to estimate residential electricity consumption at municipal level in Germany. Available online at <https://www.econstor.eu/bitstream/10419/209625/1/1685814336.pdf>, checked on 10/1/2020.
- IEA (2023): Greenhouse Gas Emissions from Energy Data Explorer. IEA. Available online at <https://www.iea.org/data-and-statistics/data-tools/greenhouse-gas-emissions-from-energy-data-explorer>, checked on 12/1/2023.
- infas; DLR; IVT; infas 360 (2019): Mobilität in Deutschland (im Auftrag des BMVI). - MiD Kurzreport Verkehrsaufkommen - Struktur - Trends. BMVI, infas, DLR, IVT, infas 360. Bonn, Berlin. Edited by infas. Available online at https://www.mobilitaet-in-deutschland.de/archive/pdf/infas_Mobilitaet_in_Deutschland_2017_Kurzreport_DS.pdf, checked on 10/20/2023.
- IPCC (2023): Weather and Climate Extreme Events in a Changing Climate, pp. 1513–1766. DOI: 10.1017/9781009157896.013.
- ISE (2021): Studie: Stromgestehungskosten erneuerbare Energien. Edited by Fraunhofer ISE. Available online at https://www.ise.fraunhofer.de/content/dam/ise/de/documents/publications/studies/DE2021_ISE_Studie_Stromgestehungskosten_Erneuerbare_Energien.pdf, checked on 12/1/2023.
- ITG, F. I.W. (2021): Klimaneutralität 2045 - Transformation des Gebäudesektors. Gebäudespezifische Modellierung und Begleitung des Studienprozesses. Edited by DENA. Available online at https://www.dena.de/fileadmin/dena/Dokumente/Landingpages/Leitstudie_II/Gutachten/211005_DLS_Gutachten_ITG_FIW_final.pdf, checked on 1/1/2023.
- Jaeger-Waldau, Arnulf (2016): Costs and Economics of Electricity from Residential PV Systems in Europe. Available online at <http://www.europeanenergyinnovation.eu/Articles/Winter-2016/Costs-and-Economics-of-Electricity-from-Residential-PV-Systems-in-Europe>, checked on 12/1/2023.
- Jia, Mengda; Srinivasan, Ravi S.; Raheem, Adeeba A. (2017): From occupancy to occupant behavior: An analytical survey of data acquisition technologies, modeling methodologies and simulation coupling mechanisms for building energy efficiency. In *Renewable and Sustainable Energy Reviews* 68, pp. 525–540. DOI: 10.1016/j.rser.2016.10.011.
- Jumper, John; Evans, Richard; Pritzel, Alexander; Green, Tim; Figurnov, Michael; Ronneberger, Olaf et al. (2021): Highly accurate protein structure prediction with AlphaFold. In *Nature*. DOI: 10.1038/s41586-021-03819-2.
- Kachirayil, Febin; Weinand, Jann Michael; Scheller, Fabian; McKenna, Russell (2022): Reviewing local and integrated energy system models: insights into flexibility and robustness challenges. In *Applied Energy* 324, Article 119666. DOI: 10.1016/j.apenergy.2022.119666.
- Kairies, Kai-Philipp; Figgenger, Jan; Haberschusz, David; Wessels, Oliver; Tepe, Benedikt; Sauer, Dirk Uwe (2019): Market and technology development of PV home storage systems in Germany. In *Journal of Energy Storage* 23, pp. 416–424. DOI: 10.1016/j.est.2019.02.023.
- Kairies, Kai-Philipp; Magnor, Dirk; Sauer, Dirk Uwe; Badeda, Julia; Leuthold, Matthias; Haberschusz, David (2015): Wissenschaftliches Mess- und Evaluierungsprogramm Solarstromspeicher 2015. ISEA. Available online at <https://publications.rwthachen.de/record/750562>, checked on 12/1/2023.
- Karneyeva, Yuliya; Wüstenhagen, Rolf (2017): Solar feed-in tariffs in a post-grid parity world. The role of risk, investor diversity and business models. In *Energy Policy* 106, pp. 445–456. DOI: 10.1016/j.enpol.2017.04.005.
- Kaschub, Thomas (2017): Batteriespeicher in Haushalten unter Berücksichtigung von Photovoltaik, Elektrofahrzeugen und Nachfragesteuerung. Dissertation.

- Kaschub, Thomas; Jochem, Patrick; Fichtner, Wolf (2016): Solar energy storage in German households. Profitability, load changes and flexibility. In *Energy Policy* 98, pp. 520–532. DOI: 10.1016/j.enpol.2016.09.017.
- KEA-BW (2023): Technikatalog zur Kommunalen Wärmeplanung. Edited by Die Landesenergieagentur (KEA-BW). Available online at https://www.kea-bw.de/fileadmin/user_upload/Waermewende/Wissensportal/Technikkatalog_Tabellen_v1.1.zip, checked on 8/25/2023.
- Khalilpour, Rajab; Vassallo, Anthony (2015): Leaving the grid. An ambition or a real choice? In *Energy Policy* 82, pp. 207–221. DOI: 10.1016/j.enpol.2015.03.005.
- Kleinebrahm, Max; Torriti, Jacopo; McKenna, Russell; Ardone, Armin; Fichtner, Wolf (2021): Using neural networks to model long-term dependencies in occupancy behavior. In *Energy and Buildings* 240 (3–4), Article 110879. DOI: 10.1016/j.enbuild.2021.110879.
- Kleinebrahm, Max; Weinand, Jann; Ardone, Armin; McKenna, Russell (2018): Optimal renewable energy based supply systems for self-sufficient residential buildings. In *IBPSA BauSIM2018, 7. Deutsch-Österreichische Konferenz*. DOI: 10.5445/IR/1000085753.
- Kleinebrahm, Max; Weinand, Jann Michael; Naber, Elias; McKenna, Russell; Ardone, Armin (2023a): Analysing municipal energy system transformations in line with national greenhouse gas reduction strategies. In *Applied Energy* 332, Article 120515. DOI: 10.1016/j.apenergy.2022.120515.
- Kleinebrahm, Max; Weinand, Jann Michael; Naber, Elias; McKenna, Russell; Ardone, Armin; Fichtner, Wolf (2023b): Two million European single-family homes could abandon the grid by 2050. In *Joule* 7 (11), pp. 2485–2510. DOI: 10.1016/j.joule.2023.09.012.
- Knosala, Kevin; Kotzur, Leander; Röben, Fritz T.C.; Stenzel, Peter; Blum, Ludger; Robinius, Martin; Stolten, Detlef (2021): Hybrid Hydrogen Home Storage for Decentralized Energy Autonomy. In *International Journal of Hydrogen Energy* 46 (42), pp. 21748–21763. DOI: 10.1016/j.ijhydene.2021.04.036.
- Koirala, Binod Prasad; Koliou, Elta; Friege, Jonas; Hakvoort, Rudi A.; Herder, Paulien M. (2016): Energetic communities for community energy: A review of key issues and trends shaping integrated community energy systems. In *Renewable and Sustainable Energy Reviews* 56, pp. 722–744. DOI: 10.1016/j.rser.2015.11.080.
- Kotzur, Leander (2018): Future Grid Load of the Residential Building Sector. Jülich: Forschungszentrum Jülich GmbH, Zentralbibliothek, Verlag (Schriften des Forschungszentrums Jülich. Reihe Energie & Umwelt, Band/volume 442). Available online at <https://juser.fz-juelich.de/record/858675>, checked on 4/4/2022.
- Kotzur, Leander; Markewitz, Peter; Robinius, Martin; Cardoso, Gonçalo; Stenzel, Peter; Heleno, Miguel; Stolten, Detlef (2019): Bottom-up energy supply optimization of a national building stock. In *Energy and Buildings*, p. 109667. DOI: 10.1016/j.enbuild.2019.109667.
- Kotzur, Leander; Markewitz, Peter; Robinius, Martin; Stolten, Detlef (2018a): Impact of different time series aggregation methods on optimal energy system design. In *Renewable Energy* 117, pp. 474–487. DOI: 10.1016/j.renene.2017.10.017.
- Kotzur, Leander; Markewitz, Peter; Robinius, Martin; Stolten, Detlef (2018b): Time series aggregation for energy system design. Modeling seasonal storage. In *Applied Energy* 213, pp. 123–135. DOI: 10.1016/j.apenergy.2018.01.023.
- Kraftfahrt-Bundesamt (Ed.) (2023): Jahresbilanz 2023. Zahlen, Daten, Fakten. Available online at https://www.kba.de/DE/Statistik/Fahrzeuge/Bestand/Jahresbilanz_Bestand/fz_b_jahresbilanz_node.html?yearFilter=2023.
- Kraschewski, Tobias; Brauner, Tim; Heumann, Maximilian; Breitner, Michael H. (2023): Disentangle the price dispersion of residential solar photovoltaic systems: Evidence from Germany. In *Energy Economics* 121, p. 106649. DOI: 10.1016/j.eneco.2023.106649.
- Krizhevsky, Alex; Sutskever, Ilya; E. Hinton, Geoffrey (2012): ImageNet Classification with Deep Convolutional Neural Networks. In *Advances in neural information processing systems* (25). Available online at <https://proceedings.neurips.cc/paper/2012/file/c399862d3b9d6b76c8436e924a68c45b-Paper.pdf>.
- Kuhlmann, Marco (2021): Learning word embeddings with neural networks. Natural Language Processing. Department of Computer and Information Science, Linköping University. Available online at <https://www.ida.liu.se/~TDDE09/commons/NLP-2021-13.pdf>, checked on 12/12/2023.

References

- Lacal Arantegui, Roberto; Jäger-Waldau, Arnulf (2018): Photovoltaics and wind status in the European Union after the Paris Agreement. In *Renewable and Sustainable Energy Reviews* 81, pp. 2460–2471. DOI: 10.1016/j.rser.2017.06.052.
- Lacko, R.; Drobníč, B.; Mori, M.; Sekavčnik, M.; Vidmar, M. (2014): Stand-alone renewable combined heat and power system with hydrogen technologies for household application. In *Energy* 77, pp. 164–170. DOI: 10.1016/j.energy.2014.05.110.
- Leitl (Ed.) (2016): VitalSonnenHausPro. Building Report 2016. Available online at https://www.vitalsonnenhauspro.at/wp-content/uploads/2016/10/LA_Leitl_Sonnenhauspro_Baureport_A4_EN_161013.pdf, checked on 8/31/2022.
- Leonard, Matthew D.; Michaelides, Efstathios E. (2018): Grid-independent residential buildings with renewable energy sources. In *Energy* 148, pp. 448–460. DOI: 10.1016/j.energy.2018.01.168.
- Liebig, Stefan; Goebel, Jan; Schröder, Carsten; Grabka, Markus; Richter, David; Schupp, Jürgen et al. (2019): Sozio-oekonomisches Panel (SOEP), Daten der Jahre 1984-2018. DOI: 10.5684/soep-core.v35.
- Liu, Hangyue; Azuatalam, Donald; Chapman, Archie C.; Verbič, Gregor (2019): Techno-economic feasibility assessment of grid-defection. In *International Journal of Electrical Power & Energy Systems* 109, pp. 403–412. DOI: 10.1016/j.ijepes.2019.01.045.
- Liu, Lan (2017): Einfluss der privaten Elektrofahrzeuge auf Mittel- und Niederspannungsnetze. Dissertation. Technische Universität Darmstadt. Available online at https://tuprints.ulb.tu-darmstadt.de/7171/1/Liu_Diss_2018e.pdf, checked on 10/24/2023.
- Lo Piano, Samuele (2020): Ethical principles in machine learning and artificial intelligence: cases from the field and possible ways forward. In *Humanit Soc Sci Commun* 7 (1), p. 973. DOI: 10.1057/s41599-020-0501-9.
- Lorincz, Mate Janos; Ramírez-Mendiola, José Luis; Torriti, Jacopo (2022): COVID-19 lockdowns in the United Kingdom: Exploring the links between changes in time use, work patterns and energy-relevant activities. In *ECEEE Summer Study*. Available online at <https://centaur.reading.ac.uk/105689/>.
- Luderer, Gunnar; Kost, Christoph; Sörgel, Dominika (2021): Deutschland auf dem Weg zur Klimaneutralität 2045 - Szenarien und Pfade im Modellvergleich. Available online at <https://ariadneprojekt.de/publikation/deutschland-auf-dem-weg-zur-klimaneutralitat-2045-szenarienreport/>, checked on 1/1/2023.
- Lund, Peter D.; Lindgren, Juuso; Mikkola, Jani; Salpakari, Jyri (2015): Review of energy system flexibility measures to enable high levels of variable renewable electricity. In *Renewable and Sustainable Energy Reviews* 45, pp. 785–807. DOI: 10.1016/j.rser.2015.01.057.
- Luthander, Rasmus; Widén, Joakim; Nilsson, Daniel; Palm, Jenny (2015): Photovoltaic self-consumption in buildings. A review. In *Applied Energy* 142, pp. 80–94. DOI: 10.1016/j.apenergy.2014.12.028.
- Mainzer, Kai (2019): Analyse und Optimierung urbaner Energiesysteme - Entwicklung und Anwendung eines übertragbaren Modellierungswerkzeugs zur nachhaltigen Systemgestaltung, checked on 4/23/2019.
- Mainzer, Kai; Fath, Karoline; McKenna, Russell; Stengel, Julian; Fichtner, Wolf; Schultmann, Frank (2014): A high-resolution determination of the technical potential for residential-roof-mounted photovoltaic systems in Germany. In *Solar Energy* 105, pp. 715–731. DOI: 10.1016/j.solener.2014.04.015.
- McKenna, Eoghan; Krawczynski, Michal; Thomson, Murray (2015a): Four-state domestic building occupancy model for energy demand simulations. In *Energy and Buildings* 96, pp. 30–39. DOI: 10.1016/j.enbuild.2015.03.013.
- McKenna, R.; Bertsch, V.; Mainzer, K.; Fichtner, W. (2018): Combining local preferences with multi-criteria decision analysis and linear optimization to develop feasible energy concepts in small communities. In *European Journal of Operational Research* 268 (3), pp. 1092–1110. DOI: 10.1016/j.ejor.2018.01.036.
- McKenna, Russell (2018): The double-edged sword of decentralized energy autonomy. In *Energy Policy* 113, pp. 747–750. DOI: 10.1016/j.enpol.2017.11.033.
- McKenna, Russell; Herbes, Carsten; Fichtner, Wolf (2015b): Energieautarkie: Vorschlag einer Arbeitsdefinition als Grundlage für die Bewertung konkreter Projekte und Szenarien. In *Z Energiewirtschaft* 39 (4), pp. 235–252. DOI: 10.1007/s12398-015-0164-1.

- McKenna, Russell; Merkel, Erik; Fichtner, Wolf (2017): Energy autonomy in residential buildings. A techno-economic model-based analysis of the scale effects. In *Applied Energy* 189, pp. 800–815. DOI: 10.1016/j.apenergy.2016.03.062.
- Mellwig, Peter (2022): Langfristszenarien für die Transformation des Energiesystems in Deutschland. Energienachfrage Gebäudesektor. Available online at https://langfristszenarien.de/enertile-explorer-wAssets/docs/20221117_LFS3_Webinar_Gebaeude_Geraete_PHH_GHD.pdf, checked on 12/1/2023.
- Mikolov, Tomas; Chen, Kai; Corrado, Greg; Dean, Jeffrey (2013): Efficient Estimation of Word Representations in Vector Space. Available online at <http://arxiv.org/pdf/1301.3781v3>, checked on 12/1/2023.
- Milan, Christian; Stadler, Michael; Cardoso, Gonçalo; Mashayekh, Salman (2015): Modeling of non-linear CHP efficiency curves in distributed energy systems. In *Applied Energy* 148, pp. 334–347. DOI: 10.1016/j.apenergy.2015.03.053.
- Müller, Theresa; Möst, Dominik (2018): Demand Response Potential: Available when Needed? In *Energy Policy* 115, pp. 181–198. DOI: 10.1016/j.enpol.2017.12.025.
- Muratori, Matteo (2018): Impact of uncoordinated plug-in electric vehicle charging on residential power demand. In *Nat Energy* 3 (3), pp. 193–201. DOI: 10.1038/s41560-017-0074-z.
- Nijhuis, M.; Gibescu, M.; Cobben, J.F.G. (2016): Bottom-up Markov Chain Monte Carlo approach for scenario based residential load modeling with publicly available data. In *Energy and Buildings* 112, pp. 121–129. DOI: 10.1016/j.enbuild.2015.12.004.
- Nilsson Energy (Ed.) (2022): Nilsson Energy. Available online at <https://nilssonenergy.com>, checked on 8/31/2022.
- Omoyele, Olalekan; Hoffmann, Maximilian; Koivisto, Matti; Larrañeta, Miguel; Weinand, Jann Michael; Linßen, Jochen; Stolten, Detlef (2024): Increasing the resolution of solar and wind time series for energy system modeling: A review. In *Renewable and Sustainable Energy Reviews* 189, p. 113792. DOI: 10.1016/j.rser.2023.113792.
- OpenAI (2023a): ChatGPT Version 4.0. Available online at <https://openai.com/chatgpt>, checked on 12/1/2023.
- OpenAI (2023b): Tokenizer. Learn about language model tokenization. Available online at <https://platform.openai.com/tokenizer>, updated on 12/11/2023.
- Osman, Mohamed; Ouf, Mohamed (2021): A comprehensive review of time use surveys in modelling occupant presence and behavior: Data, methods, and applications. In *Building and Environment* 196, p. 107785. DOI: 10.1016/j.buildenv.2021.107785.
- Osman, Mohamed; Ouf, Mohamed; Azar, Elie; Dong, Bing (2023): Stochastic bottom-up load profile generator for Canadian households' electricity demand. In *Building and Environment* 241, p. 110490. DOI: 10.1016/j.buildenv.2023.110490.
- Østergaard, Poul Alberg; Lund, Henrik (2011): A renewable energy system in Frederikshavn using low-temperature geothermal energy for district heating. In *Applied Energy* 88 (2), pp. 479–487. DOI: 10.1016/j.apenergy.2010.03.018.
- Pearl, Judea; Mackenzie, Dana (2018): The book of why. The new science of cause and effect. First edition. New York: Basic Books.
- Perera, A. T. D.; Javanroodi, Kavan; Mauree, Dasaraden; Nik, Vahid M.; Florio, Pietro; Hong, Tianzhen; Chen, Deliang (2023): Challenges resulting from urban density and climate change for the EU energy transition. In *Nat. Energy* 8 (4), pp. 397–412. DOI: 10.1038/s41560-023-01232-9.
- Perera, A. T. D.; Nik, Vahid M.; Chen, Deliang; Scartezzini, Jean-Louis; Hong, Tianzhen (2020): Quantifying the impacts of climate change and extreme climate events on energy systems. In *Nat Energy* 5 (2), pp. 150–159. DOI: 10.1038/s41560-020-0558-0.
- Proedrou, Elisavet (2021): A Comprehensive Review of Residential Electricity Load Profile Models. In *IEEE Access* 9, pp. 12114–12133. DOI: 10.1109/ACCESS.2021.3050074.
- Prognos; Öko-Institut; Wuppertal-Institut (2021): Klimaneutrales Deutschland 2045. Wie Deutschland seine Klimaziele schon vor 2050 erreichen kann. Langfassung im Auftrag von Stiftung Klimaneutralität, Agora Energiewende und Agora Verkehrswende. Available online at https://www.agora-verkehrswende.de/fileadmin/Projekte/2021/KNDE_2045_Langfassung/Klimaneutrales_Deutschland_2045_Langfassung.pdf, checked on 1/1/2024.

References

- Puranen, Pietari; Kosonen, Antti; Ahola, Jero (2021): Technical feasibility evaluation of a solar PV based off-grid domestic energy system with battery and hydrogen energy storage in northern climates. In *Solar Energy* 213, pp. 246–259. DOI: 10.1016/j.solener.2020.10.089.
- Quoilin, Sylvain; Kavvadias, Konstantinos; Mercier, Arnaud; Pappone, Irene; Zucker, Andreas (2016): Quantifying self-consumption linked to solar home battery systems. Statistical analysis and economic assessment. In *Applied Energy* 182, pp. 58–67. DOI: 10.1016/j.apenergy.2016.08.077.
- Rae, Callum; Bradley, Fiona (2012): Energy autonomy in sustainable communities—A review of key issues. In *Renewable and Sustainable Energy Reviews* 16 (9), pp. 6497–6506. DOI: 10.1016/j.rser.2012.08.002.
- Ramirez Camargo, Luis; Nitsch, Felix; Gruber, Katharina; Dorner, Wolfgang (2018): Electricity self-sufficiency of single-family houses in Germany and the Czech Republic. In *Applied Energy* 228, pp. 902–915. DOI: 10.1016/j.apenergy.2018.06.118.
- Ramirez-Mendiola, Jose Luis; Mattioli, Giulio; Anable, Jillian; Torriti, Jacopo (2022): I'm coming home (to charge): The relation between commuting practices and peak energy demand in the United Kingdom. In *Energy Research & Social Science* 88, p. 102502. DOI: 10.1016/j.erss.2022.102502.
- Ramírez-Mendiola, José Luis; Grünewald, Philipp; Eyre, Nick (2019): Residential activity pattern modelling through stochastic chains of variable memory length. In *Applied Energy* 237, pp. 417–430. DOI: 10.1016/j.apenergy.2019.01.019.
- Richardson, Ian; Thomson, Murray; Infield, David (2008): A high-resolution domestic building occupancy model for energy demand simulations. In *Energy and Buildings* 40 (8), pp. 1560–1566. DOI: 10.1016/j.enbuild.2008.02.006.
- Richardson, Ian; Thomson, Murray; Infield, David; Clifford, Conor (2010): Domestic electricity use. A high-resolution energy demand model. In *Energy and Buildings* 42 (10), pp. 1878–1887. DOI: 10.1016/j.enbuild.2010.05.023.
- Römer, Benedikt; Reichhart, Philipp; Picot, Arnold (2015): Smart energy for Robinson Crusoe: an empirical analysis of the adoption of IS-enhanced electricity storage systems. In *Electron Markets* 25 (1), pp. 47–60. DOI: 10.1007/s12525-014-0167-5.
- Rosenow, Jan; Gibb, Duncan; Nowak, Thomas; Lowes, Richard (2022): Heating up the global heat pump market. In *Nat Energy* 7 (10), pp. 901–904. DOI: 10.1038/s41560-022-01104-8.
- Roth, Alexander; Schmidt, Felix (2023): Not only a mild winter: German consumers change their behavior to save natural gas. In *Joule* 7 (6), pp. 1081–1086. DOI: 10.1016/j.joule.2023.05.001.
- Ruhnau, Oliver; Lundström, Lukas; Dürr, Linus; Hunecke, Florian (2023): Empirical weather dependency of heat pump load: Disentangling the effects of heat demand and efficiency. In : 2023 19th International Conference on the European Energy Market (EEM). 2023 19th International Conference on the European Energy Market (EEM). Lappeenranta, Finland, 06.06.2023 - 08.06.2023: IEEE, pp. 1–5.
- RWI (2022): Erstellung der Anwendungsbilanzen 2021 für den Sektor der Privaten Haushalte und den Verkehrssektor in Deutschland. Edited by RWI – Leibniz-Institut für Wirtschaftsforschung. Available online at https://ag-energiebilanzen.de/wp-content/uploads/2021/02/AGEB-AnwBil-2021-priv.-HH-und-Verkehr_vorl._EB-09-2022.pdf, checked on 12/1/2023.
- Sabadini, Felipe; Madlener, Reinhard (2021): The economic potential of grid defection of energy prosumer households in Germany. In *Advances in Applied Energy* 4, p. 100075. DOI: 10.1016/j.adapen.2021.100075.
- Samweber, Florian (2018): Systematischer Vergleich Netzoptimierender Maßnahmen zur Integration elektrischer Wärmeerzeuger und Fahrzeuge in Niederspannungsnetze. Dissertation. Technische Universität München. Available online at <https://mediatum.ub.tum.de/download/1379767/1379767.pdf>, checked on 10/24/2023.
- Santiago, I.; Lopez-Rodriguez, M. A.; Trillo-Montero, D.; Torriti, J.; Moreno-Munoz, A. (2014): Activities related with electricity consumption in the Spanish residential sector: Variations between days of the week, Autonomous Communities and size of towns. In *Energy and Buildings* 79, pp. 84–97. DOI: 10.1016/j.enbuild.2014.04.055.
- Savvidis, Georgios; Siala, Kais; Weissbart, Christoph; Schmidt, Lukas; Borggreffe, Frieder; Kumar, Subhash et al. (2019): The gap between energy policy challenges and model capabilities. In *Energy Policy* 125, pp. 503–520. DOI: 10.1016/j.enpol.2018.10.033.

- Schill, Wolf-Peter; Zerrahn, Alexander; Kunz, Friedrich (2017): Prosumage of solar electricity: pros, cons, and the system perspective. In *EEEP* 6 (1). DOI: 10.5547/2160-5890.6.1.wsch.
- Schlag, Imanol; Irie, Kazuki; Schmidhuber, Jürgen (2021): Linear Transformers Are Secretly Fast Weight Memory Systems. Available online at <http://arxiv.org/pdf/2102.11174v2>, checked on 12/1/2023.
- Schmid, Fabian; Behrendt, Frank (2022): Genetic sizing optimization of residential multi-carrier energy systems: The aim of energy autarky and its cost. In *Energy*, p. 125421. DOI: 10.1016/j.energy.2022.125421.
- Schmidt, O.; Hawkes, A.; Gambhir, A.; Staffell, I. (2017): The future cost of electrical energy storage based on experience rates. In *Nat. Energy* 2 (8), p. 17110. DOI: 10.1038/nenergy.2017.110.
- Schmidt, Oliver; Melchior, Sylvain; Hawkes, Adam; Staffell, Iain (2019): Projecting the Future Levelized Cost of Electricity Storage Technologies. In *Joule* 3 (1), pp. 81–100. DOI: 10.1016/j.joule.2018.12.008.
- Schreiber, Michael; Hochloff, Patrick (2013): Capacity-dependent tariffs and residential energy management for photovoltaic storage systems. In *2013 IEEE Power & Energy Society General Meeting*, pp. 1–5. DOI: 10.1109/PESMG.2013.6672200.
- Schütz, Thomas; Schiffer, Lutz; Harb, Hassan; Fuchs, Marcus; Müller, Dirk (2017a): Optimal design of energy conversion units and envelopes for residential building retrofits using a comprehensive MILP model. In *Applied Energy* 185, pp. 1–15. DOI: 10.1016/j.apenergy.2016.10.049.
- Schütz, Thomas; Schraven, Markus Hans; Remy, Sebastian; Granacher, Julia; Kemetmüller, Dominik; Fuchs, Marcus; Müller, Dirk (2017b): Optimal design of energy conversion units for residential buildings considering German market conditions. In *Energy* 139, pp. 895–915. DOI: 10.1016/j.energy.2017.08.024.
- Sensfuß, Frank; Lux, Benjamin; Bernath, Christiane; Kiefer, Christoph; Pfluger, Benjamin; Kleinschmitt, Christoph et al. (2022): Langfrist-szenarien für die Transformation des Energiesystems in Deutschland. T45 Hauptszenarien. Available online at https://langfristszenarien.de/enertile-explorer-wAssets/docs/LFS3_T45_Szenarien_15_11_2022_final.pdf, checked on 12/1/2023.
- Shove, Elizabeth; Pantzar, Mika; Watson, Matt (2012): *The Dynamics of Social Practice: Everyday Life and How it Changes*: SAGE Publications Ltd.
- SKN; Agora; BDI; DENA; BMWK; Kopernikus (2022): Vergleich der „Big 5“ Klimaneutralitätsszenarien. Available online at https://www.dena.de/fileadmin/dena/Publikationen/PDFs/2022/Vergleich_der_Big_5_Klimaneutralitaetsszenarien.pdf, checked on 12/1/2023.
- SolarPower Europe (2022a): European Market Outlook for Residential Battery Storage 2022-2026. Available online at <https://www.solarpowereurope.org/insights/thematic-reports/european-market-outlook-for-residential-battery-storage-1>, checked on 12/1/2023.
- SolarPower Europe (2022b): European Market Outlook for Solar Power 2022-2026. Available online at https://api.solarpowereurope.org/uploads/5222_SPE_EMO_2022_full_report_ver_03_1_319d70ca42.pdf?updated_at=2022-12-19T08:21:34.541Z, checked on 12/1/2023.
- Spinoni, Jonathan; Vogt, Jürgen V.; Barbosa, Paulo; Dosio, Alessandro; McCormick, Niall; Bigano, Andrea; Füssel, Hans-Martin (2018): Changes of heating and cooling degree-days in Europe from 1981 to 2100. In *Int. J. Climatol* 38, e191-e208. DOI: 10.1002/joc.5362.
- Staffell, Iain; Pfenninger, Stefan (2016): Using bias-corrected reanalysis to simulate current and future wind power output. In *Energy* 114, pp. 1224–1239. DOI: 10.1016/j.energy.2016.08.068.
- Statista (2023a): Anzahl der Privathaushalte in Deutschland von 1991 bis 2022. Available online at <https://de.statista.com/statistik/daten/studie/156950/umfrage/anzahl-der-privathaushalte-in-deutschland-seit-1991/>, checked on 9/28/2023.
- Statista (2023b): Bevölkerung - Einwohnerzahl von Deutschland von 1990 bis 2022. Available online at <https://de.statista.com/statistik/daten/studie/2861/umfrage/entwicklung-der-gesamtbevoelkerung-deutschlands/>, checked on 9/28/2023.
- Statista (2023c): Wohnfläche je Einwohner in Wohnungen in Deutschland von 1991 bis 2022. Available online at <https://de.statista.com/statistik/daten/studie/36495/umfrage/wohnflaeche-je-einwohner-in-deutschland-von-1989-bis-2004/>, checked on 9/28/2023.

References

- Stromnetz Berlin (Ed.) (2023): Informationen zu Standardlastprofilen für 2024. Available online at <https://www.stromnetz.berlin/netz-nutzen/netznutzer/>, checked on 10/25/2023.
- Stute, Judith; Kühnbach, Matthias (2023): Dynamic pricing and the flexible consumer – Investigating grid and financial implications: A case study for Germany. In *Energy Strategy Reviews* 45, p. 100987. DOI: 10.1016/j.esr.2022.100987.
- Swan, Lukas G.; Ugursal, V. Ismet (2009): Modeling of end-use energy consumption in the residential sector: A review of modeling techniques. In *Renewable and Sustainable Energy Reviews* 13 (8), pp. 1819–1835. DOI: 10.1016/j.rser.2008.09.033.
- Theellufsen, J. Z.; Lund, H.; Sorknæs, P.; Østergaard, P. A.; Chang, M.; Drysdale, D. et al. (2020): Smart energy cities in a 100% renewable energy context. In *Renewable and Sustainable Energy Reviews* 129, p. 109922. DOI: 10.1016/j.rser.2020.109922.
- Theellufsen, Jakob Zinck; Lund, Henrik (2016): Roles of local and national energy systems in the integration of renewable energy. In *Applied Energy* 183, pp. 419–429. DOI: 10.1016/j.apenergy.2016.09.005.
- Tjaden, Tjarko; Bergner, Joseph; Weniger, Johannes; Quaschnig, Volker (2015): Repräsentative elektrische Lastprofile für Wohngebäude in Deutschland auf 1-sekündiger Datenbasis. Available online at <https://solar.htw-berlin.de/elektrische-lastprofile-fuer-wohnbaeude/>, checked on 7/21/2023.
- Torriti, Jacopo (2014): A review of time use models of residential electricity demand. In *Renewable and Sustainable Energy Reviews* 37, pp. 265–272. DOI: 10.1016/j.rser.2014.05.034.
- Torriti, Jacopo (2017): Understanding the timing of energy demand through time use data. Time of the day dependence of social practices. In *Energy Research & Social Science* 25, pp. 37–47. DOI: 10.1016/j.erss.2016.12.004.
- Touvron, Hugo; Lavril, Thibaut; Izacard, Gautier; Martinet, Xavier; Lachaux, Marie-Anne; Lacroix, Timothée et al. (2023): LLaMA: Open and Efficient Foundation Language Models. Available online at <http://arxiv.org/pdf/2302.13971v1>, checked on 12/1/2023.
- Tröndle, Tim; Lilliestam, Johan; Marelli, Stefano; Pfenninger, Stefan (2020): Trade-Offs between Geographic Scale, Cost, and Infrastructure Requirements for Fully Renewable Electricity in Europe. In *Joule* 4 (9), pp. 1929–1948. DOI: 10.1016/j.joule.2020.07.018.
- Tröndle, Tim; Pfenninger, Stefan; Lilliestam, Johan (2019): Home-made or imported: On the possibility for renewable electricity autarky on all scales in Europe. In *Energy Strategy Reviews* 26, p. 100388. DOI: 10.1016/j.esr.2019.100388.
- TSO (2023): Netzentwicklungsplan Strom 2037/2045, zweiter Entwurf. Edited by Transmission system operators. Available online at https://www.netzentwicklungsplan.de/sites/default/files/2023-07/NEP_2037_2045_V2023_2_Entwurf_Teil1.pdf, checked on 12/1/2023.
- UAS (2023): Erstes energieautarkes Mehrfamilienhaus in Brütten. Edited by Umwelt Arena Schweiz. Available online at <https://www.umweltarena.ch/ueber-uns/architektur-und-bauprojekte/>, checked on 12/1/2023.
- UBA (2023a): Emissionsübersichten nach Sektoren des Bundesklimaschutzgesetzes 1990 - 2022. Edited by Umweltbundesamt (UBA). Available online at https://www.umweltbundesamt.de/sites/default/files/medien/361/dokumente/2023_03_15_em_entwicklung_in_d_ksg-sektoren_pm.xlsx, checked on 8/25/2023.
- UBA (2023b): Entwicklung der spezifischen Treibhausgas-Emissionen des deutschen Strommix in den Jahren 1990 - 2022. Edited by Umweltbundesamt (UBA). Available online at https://www.umweltbundesamt.de/sites/default/files/medien/1410/publikationen/2023_05_23_climate_change_20-2023_strommix_bf.pdf, checked on 8/25/2023.
- UNFCCC (2015): Paris Agreement to the United Nations Framework Convention on Climate Change. Edited by United Nations Framework Convention on Climate Change. Available online at https://unfccc.int/sites/default/files/english_paris_agreement.pdf, checked on 12/1/2023.
- Vaswani, Ashish; Shazeer, Noam; Parmar, Niki; Uszkoreit, Jakob; Jones, Llion; Gomez, Aidan N. et al. (2017): Attention Is All You Need. Available online at <http://arxiv.org/pdf/1706.03762v5>.

- VDEW (1999): Repräsentative VDEW Lastprofile Aktionsplan Wettbewerb, M-32/99. With assistance of R. Bitterer, B. Schieferdecker. Frankfurt, Germany. Available online at https://www.bdew.de/media/documents/1999_Repraesentative-VDEW-Lastprofile.pdf, checked on 12/1/2023.
- VDI (2022): CO₂-freier Strom fürs Eigenheim. In *VDI 2022*, 8/26/2022 (17), p. 25, checked on 12/1/2023.
- Venkatesan, Naveen; Solanki, Jignesh; Solanki, Sarika Khushalani (2011): Demand response model and its effects on voltage profile of a distribution system. In *2011 IEEE Power and Energy Society General Meeting*, pp. 1–7. DOI: 10.1109/PES.2011.6039760.
- Verivox (2023): Electricity tariff comparison. Available online at <https://www.verivox.de/>, checked on 12/1/2023.
- Vögele, Stefan; Pogonietz, Witold-Roger; Kleinebrahm, Max; Weimer-Jehle, Wolfgang; Bernhard, Jesse; Kuckshinrichs, Wilhelm; Weiss, Annika (2022): Dissemination of PV-Battery systems in the German residential sector up to 2050: Technological diffusion from multidisciplinary perspectives. In *Energy* 248, Article 123477. DOI: 10.1016/j.energy.2022.123477.
- Voss, K.; Goetzberger, A.; Bopp, G.; Häberle, A.; Heinzel, A.; Lehmborg, H. (1996): The self-sufficient solar house in Freiburg—Results of 3 years of operation. In *Solar Energy* 58 (1-3), pp. 17–23. DOI: 10.1016/0038-092X(96)00046-1.
- Wagner, Hermann-Josef; Sager, Christine (Eds.) (2015): Kommunikation und Partizipation. Kommunikation und Partizipation. With assistance of Hermann-Josef Wagner, Christine Sager. Berlin, Münster: LIT (Energie und Nachhaltigkeit, Bd. 19).
- Way, Rupert; Ives, Matthew C.; Mealy, Penny; Farmer, J. Doyné (2022): Empirically grounded technology forecasts and the energy transition. In *Joule*. DOI: 10.1016/j.joule.2022.08.009.
- Weinand, J. M.; McKenna, R.; Fichtner, W. (2019a): Developing a municipality typology for modelling decentralised energy systems. In *Utilities Policy* 57, pp. 75–96. DOI: 10.1016/j.jup.2019.02.003.
- Weinand, Jann M.; McKenna, Russell; Kleinebrahm, Max; Scheller, Fabian; Fichtner, Wolf (2021): The impact of public acceptance on cost efficiency and environmental sustainability in decentralized energy systems. In *Patterns (New York, N.Y.)* 2 (7), Article 100301. DOI: 10.1016/j.patter.2021.100301.
- Weinand, Jann M.; McKenna, Russell; Mainzer, Kai (2019b): Spatial high-resolution socio-energetic data for municipal energy system analyses. In *Scientific data* 6 (1), p. 243. DOI: 10.1038/s41597-019-0233-0.
- Weinand, Jann Michael (2020): Energy system analysis of energy autonomous municipalities. Available online at <https://publikationen.bibliothek.kit.edu/1000124837/90337876>, checked on 12/1/2023.
- Weinand, Jann Michael; McKenna, Russell; Kleinebrahm, Max; Mainzer, Kai (2019c): Assessing the contribution of simultaneous heat and power generation from geothermal plants in off-grid municipalities. In *Applied Energy* 255, p. 113824. DOI: 10.1016/j.apenergy.2019.113824.
- Weinand, Jann Michael; Ried, Sabrina; Kleinebrahm, Max; McKenna, Russell; Fichtner, Wolf (2020a): Identification of Potential Off-Grid Municipalities with 100% Renewable Energy Supply for Future Design of Power Grids. In *IEEE Trans. Power Syst.*, p. 1. DOI: 10.1109/TPWRS.2020.3033747.
- Weinand, Jann Michael; Scheller, Fabian; McKenna, Russell (2020b): Reviewing energy system modelling of decentralized energy autonomy. In *Energy* 203, p. 117817. DOI: 10.1016/j.energy.2020.117817.
- Weiss, C.; Chlond, B.; Hilgert, T.; Vortisch, P. (2016): Deutsches Mobilitätspanel (MOP). Wissenschaftliche Begleitung und Auswertungen Bericht 2014/2015, Alltagsmobilität und Fahrleistung. Available online at https://bmdv.bund.de/SharedDocs/DE/Anlage/G/mop-jahresbericht-2014-15.pdf?__blob=publicationFile, checked on 1/10/2024.
- Weniger, Johannes; Tjaden, Tjarko; Quaschnig, Volker (2014): Sizing of Residential PV Battery Systems. In *Energy Procedia* 46, pp. 78–87. DOI: 10.1016/j.egypro.2014.01.160.
- Widén, Joakim (2014): Improved photovoltaic self-consumption with appliance scheduling in 200 single-family buildings. In *Applied Energy* 126, pp. 199–212. DOI: 10.1016/j.apenergy.2014.04.008.

References

- Widén, Joakim; Wäckelgård, Ewa (2010): A high-resolution stochastic model of domestic activity patterns and electricity demand. In *Applied Energy* 87 (6), pp. 1880–1892. DOI: 10.1016/j.apenergy.2009.11.006.
- Wierling, August; Schwanitz, Valeria Jana; Zeiss, Jan Pedro; Beck, Constantin von; Paudler, Heather Arghandeh; Koren, Ingrid Knutsdotter et al. (2023): A Europe-wide inventory of citizen-led energy action with data from 29 countries and over 10000 initiatives. In *Scientific data* 10 (1), p. 9. DOI: 10.1038/s41597-022-01902-5.
- Wilke, Urs (2013): Probabilistic Bottom-up Modelling of Occupancy and Activities to Predict Electricity Demand in Residential Buildings. PHD Thesis.
- Xiao, Mengzhu; Junne, Tobias; Haas, Jannik; Klein, Martin (2021): Plummeting costs of renewables - Are energy scenarios lagging? In *Energy Strategy Reviews* 2021, p. 100636. DOI: 10.1016/j.esr.2021.100636.
- Xiong, Yunyang; Zeng, Zhanpeng; Chakraborty, Rudransis; Tan, Mingxing; Fung, Glenn; Li, Yin; Singh, Vikas (2021): Nyströmformer: A Nyström-Based Algorithm for Approximating Self-Attention. Available online at <http://arxiv.org/pdf/2102.03902v1>, checked on 12/1/2023.
- Xu, Dongkuan; Tian, Yingjie (2015): A Comprehensive Survey of Clustering Algorithms. In *Ann. Data. Sci.* 2 (2), pp. 165–193. DOI: 10.1007/s40745-015-0040-1.
- Yamaguchi, Y.; Yilmaz, S.; Prakash, N.; Firth, S. K.; Shimoda, Y. (2018): A cross analysis of existing methods for modelling household appliance use. In *Journal of Building Performance Simulation* 12 (2), pp. 160–179. DOI: 10.1080/19401493.2018.1497087.
- Yoshino, Hiroshi; Hong, Tianzhen; Nord, Natasa (2017): IEA EBC annex 53: Total energy use in buildings—Analysis and evaluation methods. In *Energy and Buildings* 152, pp. 124–136. DOI: 10.1016/j.enbuild.2017.07.038.
- Yunusov, Timur; Torriti, Jacopo (2021): Distributional effects of Time of Use tariffs based on electricity demand and time use. In *Energy Policy* 156, p. 112412. DOI: 10.1016/j.enpol.2021.112412.
- Zeyen, Elisabeth; Hagenmeyer, Veit; Brown, Tom (2021): Mitigating heat demand peaks in buildings in a highly renewable European energy system. In *Energy* 231, p. 120784. DOI: 10.1016/j.energy.2021.120784.
- Zimmermann, Jean-Paul; Evans, Matt; Griggs, Jonathan; King, Nicola; Harding, Les; Roberts, Penelope; Evans, Chris. (2012): Household Electricity Survey A study of domestic electrical product usage. Available online at https://assets.publishing.service.gov.uk/government/uploads/system/uploads/attachment_data/file/208097/10043_R66141HouseholdElectricitySurveyFinalReportissue4.pdf, checked on 3/16/2019.

Part II

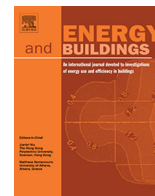
Research Papers

Paper A

Using neural networks to model long-term dependencies in occupancy behavior

Reference

Kleinebrahm, Max; Torriti, Jacopo; McKenna, Russell; Ardone, Armin; Fichtner, Wolf (2021): Using neural networks to model long-term dependencies in occupancy behavior. In Energy and Buildings 240 (3–4), Article 110879. DOI: [10.1016/j.enbuild.2021.110879](https://doi.org/10.1016/j.enbuild.2021.110879).



Using neural networks to model long-term dependencies in occupancy behavior



Max Kleinebrahm^{a,*}, Jacopo Torriti^b, Russell McKenna^{c,d}, Armin Ardone^a, Wolf Fichtner^a

^a Chair of Energy Economics, Karlsruhe Institute for Technology, Hertzstraße 16, 76187 Karlsruhe, Germany

^b School of the Built Environment, University of Reading, Whiteknights, PO Box 219, Reading RG6 6AY, United Kingdom

^c DTU Management, Technical University of Denmark, 2800 Kgs. Lyngby, Denmark

^d Chair of Energy Transition, School of Engineering, University of Aberdeen, Aberdeen AB24 3FX, United Kingdom

ARTICLE INFO

Article history:

Received 13 November 2020

Revised 14 January 2021

Accepted 1 March 2021

Available online 9 March 2021

Keywords:

Activity modelling

Mobility behavior

Neural networks

Synthetic data

ABSTRACT

Models simulating household energy demand based on different occupant and household types and their behavioral patterns have received increasing attention over the last years due the need to better understand fundamental characteristics that shape the demand side. Most of the models described in the literature are based on Time Use Survey data and Markov chains. Due to the nature of the underlying data and the Markov property, it is not sufficiently possible to consider long-term dependencies over several days in occupant behavior. An accurate mapping of long-term dependencies in behavior is of increasing importance, e.g. for the determination of flexibility potentials of individual households urgently needed to compensate supply-side fluctuations of renewable based energy systems. The aim of this study is to bridge the gap between social practice theory, energy related activity modelling and novel machine learning approaches. The weaknesses of existing approaches are addressed by combining time use survey data with mobility data, which provide information about individual mobility behavior over periods of one week. In social practice theory, emphasis is placed on the sequencing and repetition of practices over time. This suggests that practices have a memory. Transformer models based on the attention mechanism and Long short-term memory (LSTM) based neural networks define the state of the art in the field of natural language processing (NLP) and are for the first time introduced in this paper for the generation of weekly activity profiles. In a first step an autoregressive model is presented, which generates synthetic weekly mobility schedules of individual occupants and thereby captures long-term dependencies in mobility behavior. In a second step, an imputation model enriches the weekly mobility schedules with detailed information about energy relevant *at home* activities. The weekly activity profiles build the basis for multiple use cases one of which is modelling consistent electricity, heat and mobility demand profiles of households. The approach developed provides the basis for making high-quality weekly activity data available to the general public without having to carry out complex application procedures.

© 2021 Elsevier B.V. All rights reserved.

1. Introduction

In the course of the decarbonisation of domestic heat demand, it is expected that a large part of the heat will be generated by electricity (e.g. through heat pumps) Paardekooper and Lund [26]. In order to decarbonise the mobility sector, the aim is to increase the amount of electric vehicles in the European union from 1.3 million in 2020 to at least 33 million by 2030 [38]. Due to the expected developments, fundamental characteristics will change in the course of energy demand in the household sector. Furthermore, the introduction of stationary and mobile electricity storage sys-

tems as well as stationary heat storage systems enable the storage of energy over periods of single days and therefore open up flexibility potentials in the residential sector, which can support the integration of fluctuating renewable energies. To evaluate these flexibility potentials, fundamental relationships that shape household energy demand must be understood.

Occupant behavior has been identified as having a significant impact on household energy demand [32]. Therefore, there has been an increasing research interest in the field of behavioral modelling over the last years with the aim to explain dynamics in residential energy demand based on energy related activities [36,37]. A large number of studies focus on the modelling of activity sequences of single households or individuals with the objective to describe occupant behavior on an aggregated level for socio-

* Corresponding author.

E-mail address: max.kleinebrahm@kit.edu (M. Kleinebrahm).

demographic differentiated groups [2,17,29,42]. Time use data (TUD) are used as a data basis, which provide information on the temporal course of occupant activities over single days and are available for various countries in the form of population representative samples [15]. Based on occupant behavior, different approaches were developed that connect occupant activities with electrical household appliances and thus generate synthetic electricity demand profiles Yamaguchi et al. [46]. The aim of these studies is to gain a deeper understanding of household electricity demand in order to e.g. be able to evaluate device-specific efficiency measures, time-dependent electricity tariffs or load shift potentials.

However, TUD only provide information on activity patterns of individual days, therefore longer-term dependencies in mobility behavior and energy relevant *at home* activities that extend over several days are not captured in existing TUD based models. Fig. 1 compares the autocorrelation of power consumption data generated on the basis of TUD with measured power consumption data. The autocorrelation in the generated data is underestimated. Especially, dependencies between subsequent days (48 lags) are not properly reproduced by the examined models.

Models based on device-specific power consumption data available over periods longer than one day are able to account for day-to-day variability in electricity demand [47]. However, due to the data underpinning these approaches, not much is known about the occupants and their behavior, therefore it is not (easily) possible to calculate consistent heat and mobility demand profiles matching the electricity demand. One possible way to infer the occupancy behavior would be to use non-intrusive occupancy monitoring methods in order to calculate internal heat gains (metabolic gains and device-specific heat losses) [9]. However, integrating demand through electrical vehicles would be another challenge.

The objective of this study is to develop a methodology that enables the generation of synthetic weekly activity schedules in which long-term dependencies in mobility behavior and energy relevant *at home* activities are captured on an individual level. These schedules can be used as a basis for generating consistent energy service demand profiles, taking into account heating, mobility and device specific energy service demand. In order to identify trends and potentials at the individual household level, like flexible charging behavior of electric vehicles, day-to-day variability in mobility patterns needs to be captured in the proposed approach. Therefore, novel machine learning based algorithms from the field of natural language processing (NLP) which are capable of capturing long-term dependencies in time series are trans-

ferred to the field of activity modelling. To answer the research question to what extent these algorithms are able to capture long-term dependencies in individual energy related occupancy patterns while maintaining the diversity of occupancy behavior on an individual and aggregated level, two behavioral data sets are combined in a two-step approach. Mobility data are used which provide information about weekly mobility patterns and combined with time use survey data which provide detailed information about daily activities (sleeping, cooking, eating, ...).

The two-step approach enables to combine the advantages of mobility data (long-term dependencies in mobility behavior) with the advantages of TUD (detailed information about activities) and generates high quality weekly activity schedules. Novel machine learning algorithms which are used in the area of NLP are used for the first time to model occupancy behavior. These models have fundamental advantages over Markov chains, because they provide the capability to learn long term dependencies in time series. In comparison to existing approaches which were developed to reproduce aggregated occupancy behavior the proposed approach reproduces aggregated occupancy behavior and at the same time provides high quality individual activity schedules. Therefore, the synthetic activity schedules can be used to analyse trends in the household sector on an individual level and to examine their impact on an aggregated level at the same time. Due to the rich socio-demographic information in the underlying data sets, differences in behavior between socio-demographic groups can be analysed based on the synthetic activity schedules.

The paper is structured as follows. Section 2 presents an overview about current approaches to activity based residential demand modelling and gives a short introduction to the field of social practice theory. Furthermore, the latest developments in the field of NLP are summarized. Section 3 presents the mobility and activity data used in this work. Subsequently, two autoregressive models are presented for the generation of weekly mobility schedules and two imputation models are presented for enriching the synthetic mobility schedules with energy related activity information. The section concludes with a presentation of the metrics used to evaluate the activity plans. In Section 4 the generated activity schedules are evaluated. Finally, the results are discussed and an outlook on future work is given in Section 5 before conclusions are drawn in Section 6.

2. Introducing NLP to activity modelling

The majority of studies in the residential energy demand modelling literature simulate residential energy demand based on activity patterns. The most important data basis for modelling activity sequences is TUD. TUD are large-scale surveys which provide detailed information about how people spend their time. The mean of data collection is the time-diary instrument in which the respondents enter their activities in regular time steps. These so-called time-diaries contain activity sequences for the period of usually one single day. When selecting households for the study, care is taken to select a sample of households representative of the population. Time diaries are collected for all persons in the households except for young children for usually one weekday and one weekend day to capture the differences between the days. Since TUD are collected in a harmonised procedure in most countries in Europe, these data provide a good basis for a variety of similar models for modelling activity sequences. In the following, different model approaches are presented which generate activity sequences based on TUD and similar activity-based data sets. Furthermore, the weaknesses of the models reviewed in the literature is described and a short insight into social practice theory is given.

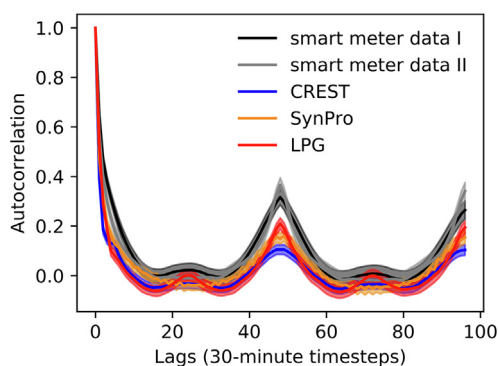


Fig. 1. Mean autocorrelation and 95% confidence interval of electricity consumption profiles of the three load profile generators (LPG [27], CREST [30], SynPro [16]) and empirical smart meter data (I: HTW [35], II: (described in [23])).

Finally, the field of NLP is briefly introduced due to similarities in modelling human behavior and language.

2.1. Markov chain based approaches

One of the most commonly used approaches to map activity sequences is to describe them as Markov chains. A Markov chain is a stochastic process that describes a sequence of possible states in which the probability of each state depends only on the previous states. The state space of a Markov chain describes the set of possible states and their corresponding state transition probabilities. The abstract idea behind the modelling of activity sequences that describe the behavior of individuals is that individuals go about their lives by transitioning between different elements of a set of potential states of activity [28]. Richardson et al. have developed an occupancy model which uses a first order Markov chain and distinguishes between the states 'active at home' and 'not active at home' for each person of a household [29]. Based on aggregated household states they calculate transition probabilities in order to model the activity level of the household over the timeframe of one day. By modelling households in an aggregated way instead of individual persons, inter personal relations are better represented than in models where individuals are modelled individually [24]. First order Markov models are adequately suited to describe processes that fulfill the Markov property. The term Markov property refers to the memorylessness of a stochastic process. For a first order Markov model, this means that the transition to a subsequent state depends only on the current state and is independent of previously observed states in the evolution of the process. It is obvious that residential activity schedules represent more complex processes and therefore cannot easily be represented by a first order Markov model. To overcome this problem, a variety of more complex Markov models have been presented in recent years. In contrast to first order Markov models, so-called semi-Markov models determine not only the subsequent state but also the duration of the subsequent state. As this kind of models represent an improvement to first order Markov Chains, due to a better mapping of state durations, they are used in various studies for activity modelling [2,42,5]. Flett et al. [17] present a Markov model for occupancy simulation that uses transition probabilities which are calculated based on the current state and the length of the current state. By considering the state length of the current state, this model represents an improvement over previous models, so that this model cannot be called memoryless. The logical next step would be to develop higher order Markov models, which allow any number of past states to be taken into account when choosing the subsequent state. However, two serious issues can be associated with higher-order Markov chains. On the one hand the number of free parameters in the model increases exponentially with the order of the model and on the other hand the collection of all possible full high-order Markov chain models is limited and completely stratified [28]. Ramírez-Mendiola et al. [28] addressed this issues by presenting a Markov chain model with variable memory length which allows the order of the model to vary during the evolution of the stochastic process. In order to find relevant portions of the past based on the influence on the outcomes of the transition probabilities to subsequent states the authors present a novel algorithm based on the Kullback-Leibler divergence and the log-likelihood test.

A graphical overview of the different Markov chain variations can be seen in Fig. 2. It can be concluded that over the last few years more and more complex models based on Markov chains have been developed, which partly overcome the memorylessness problem. However, due to their structure, Markov models are only able to capture the states of the short-term past in order to predict subsequent states. Long-term relationships in daily schedules cannot be adequately represented by these types of models.

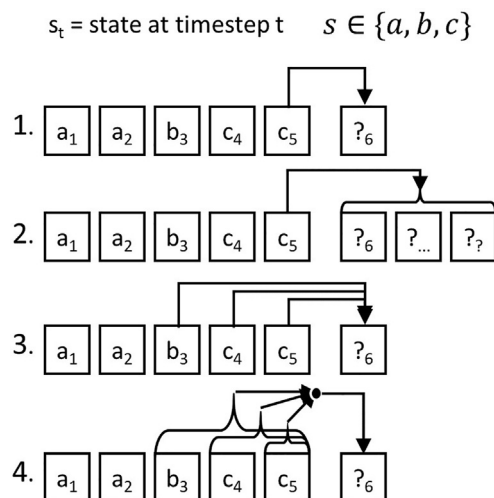


Fig. 2. Graphical representation of the process of sequence generation with different kinds of Markov chains (1. first order Markov chain, 2. semi Markov chain, 3. higher order Markov chain, 4. Markov chain with variable memory length).

2.2. Timing of social practices

Markov chain approaches are based on the assumption that activities develop over time and are only dependent on the evolution of previous states. However, social practice theory literature points out that in order to understand people's daily/weekly schedules these should be treated as a whole [31,37]. While practice theoretical accounts of social life vary, they remain consistent on at least two counts: (1) that practices are shared (socially/as part of the social i.e. performed by more than one person) and, because of that, (2) are repeated (performed more than once). If we also add that practices are connected and depend more and less on each other in being reproduced, it follows that we need to know more about how practices are repeated and with what effect for the relative strengths of their dependencies, connections, and extended relationships. In order to do justice to this statement in the patterning of activities, models must be developed which not only make it possible to capture connections between activities from the short-term past in order to predict the future, but also capture higher-level patterns which shape patterns of people's activities. In other words, models need to understand how temporal dynamics are embedded in the social world in order to understand how activities and thus energy consumption change and vary over time [40]. The majority of people structure their lives in daily rhythms, which are based on regular working hours, meal times and other constraints. These constraints form the basis for a certain degree of synchronization of social activities and thus for demand patterns [40]. Future models should be able to recognize and reproduce logical sequences in activity patterns, so that dependencies in activities are taken into account. For instance, food should first be prepared and then eaten.

Hilgert et al. [19] use a utility-based stepwise regression approach to generate weekly activity schedules for travel demand models. Due to the observation period of one week and the associated extended requirements for the mapping of activity sequences (day to day stability and variability of personal behavior), this approach differs from the approaches presented so far. Compared to Markov chain based approaches, activity sequences do not evolve over time but are the result of regression based utility functions and time budgets. Based on Bowman [6] the construction process of activity schedules is split into smaller decisions due to the high complexity of constructing the entire schedule directly.

These small decisions are then integrated downward vertically in the form of many logistic regression models. Due to the large number of regression models and their integration, many assumptions must be made when creating such a model, which increase the assumption bias. Future approaches should be less assumption driven to be easily transferable to different applications and datasets. To capture the high complexity of a complete activity plan without many intermediate steps, as described by Bowman, data-driven approaches could be used that need less assumptions and can capture complex relationships due to their structure. Table 1 gives an overview of the approaches presented in this section and compares them with the approach presented in this study.

2.3. A brief review of natural language processing

The term natural language processing covers applications such as text classification, text understanding, text generation and text translation. NLP algorithms give machines the ability to read, understand and derive meaning from human languages. Over the last years NLP evolved from the era of punch cards and batch processing, in which the procession of a sentence could take up to 7 min, to the era of Transformer based model architectures like Googles BERT or OpenAIs GPT-3 with models up to 175 Billion parameters which are trained on large web corpora like Wikipedia and are able to generate articles which human evaluators have difficulty distinguishing from articles written by humans [48,7,12].

The first neural language model was based on a feed-forward neural network [4]. Vector representations of the n previous words are taken from a table and used as input in order to predict the probabilities of the following words. Nowadays dense vector representations of words or word embeddings are trained in an efficient way while training the neural network and are capable of capturing the context of words in a document [25].

From 2013 on neural network models in the form of recurrent neural networks (RNN), convolutional neural networks (CNN), and recursive neural networks got adopted in the field of NLP [33,22]. RNNs are the obvious choice to deal with dynamic word sequences as they process the sequences from left-to-right or right-to-left and provide some kind of memory in the form of the hidden state [14]. RNNs in the form of long-short term memory networks (LSTM) proved to be more resilient to the vanishing gradient problem and therefore be able to better represent long-term dependencies in time series [20]. The in 2014 presented sequence-to-sequence approach builds the basis for multiple machine translation applications. First, an LSTM-based encoder is used to compress an input sequence into a vector representation and then a decoder network, also based on LSTMs, predicts the target sequence step by step [34]. The main shortcoming of the sequence-to-sequence approach is that the input sequence needs to be compressed into a fixed-size vector. The Attention mechanism tackles this shortcoming by allowing the decoder to look back at the input sequence hidden states, which are provided as additional input to the decoder [3]. A rare feature of the Attention

mechanism is, that it provides superficial insides about the learning process by providing information, through the attention weights, about which parts of the input are relevant for particular parts of the output. In 2016 Google presented their neural machine translation system which consisted of a deep LSTM network combining multiple encoder and decoder layers using residual connections and the attention mechanism [45]. However, in 2017 the paper "Attention is all you need" was presented, which builds the basis for numerous transformer architectures which work on the principle of self-attention and define the state of the art in multiple NLP tasks [39,7]. It was shown that the sequential nature can be captured by only using attention mechanisms and positional encodings without the use of RNNs. Due to the fundamental constraint of sequential computation of RNNs, it is not possible to parallelize training, therefore it is hard to learn on long sequences. Transformer models are fully based on fully connected layers and can be easily parallelized. Since 2017 multiple different transformer based architectures were introduced, consisting of multiple encoder and/or decoder blocks and an increasing number of trainable parameters [44]. In Fig. 3 the model architecture of a sequence to sequence RNN based model is compared to the model structure of an attention based transformer, consisting of an encoder and decoder block.

Adversarial learning methods have gained increased intention especially in the area of image processing/generation and have also been used in different forms in NLP over the last years. Generative adversarial networks (GANs) for example are able to generate synthetic data with similar statistical properties as real data by using two neural networks, a generator and a discriminator [18]. The generator produces synthetic data and the discriminator classifies generated data as fake and real data as real. Both networks are trained in an iterative way while trying to minimize the reverse Kullback-Leibler divergence. Therefore, in comparison to the previously presented model architectures, GANs are not trained by maximum likelihood estimation (MLE) and thus are said to be less vulnerable to suffer from the exposure bias in the inference stage: the model generates a sequence iteratively and predicts next token conditioned on its previously predicted ones that may be never seen in the training data [49]. With that in mind many GAN based architectures were developed for natural language generation based on the approach presented in [49] which combines GANs with a reinforcement learning policy in order to deal with the differentiability problem. However, it was shown that MLE based approaches still dominate GANs when quality and diversity metrics are taken into account [8]. Therefore, GAN architectures are not considered further in this work, even if they form a promising basis for future work.

3. Data and methodology

The German Mobility Panel (MOP) and German Time Use Data are used as an exemplary data source for analysing activity patterns in this study. In Section 3.1 the data preparation of the two

Table 1
An overview of selected models for modelling occupancy behavior.

| Study | Database | Approach | Object of consideration | Country |
|------------|-----------|--------------------------|-------------------------|---------|
| [29] | TUD | Markov – 1st order | Household | UK |
| [42] | TUD | Markov – semi | Individual | FR |
| [5] | TUD | Markov – semi | Individual | IT |
| [2] | TUD | Markov – semi | Individual | BE |
| [17] | TUD | Markov – higher order | Individuals | UK |
| [28] | TUD | Markov – variable length | Individual | UK |
| [19] | MOP | Regression | Individual | DE |
| This study | MOP + TUD | Neural networks | Individual | DE |

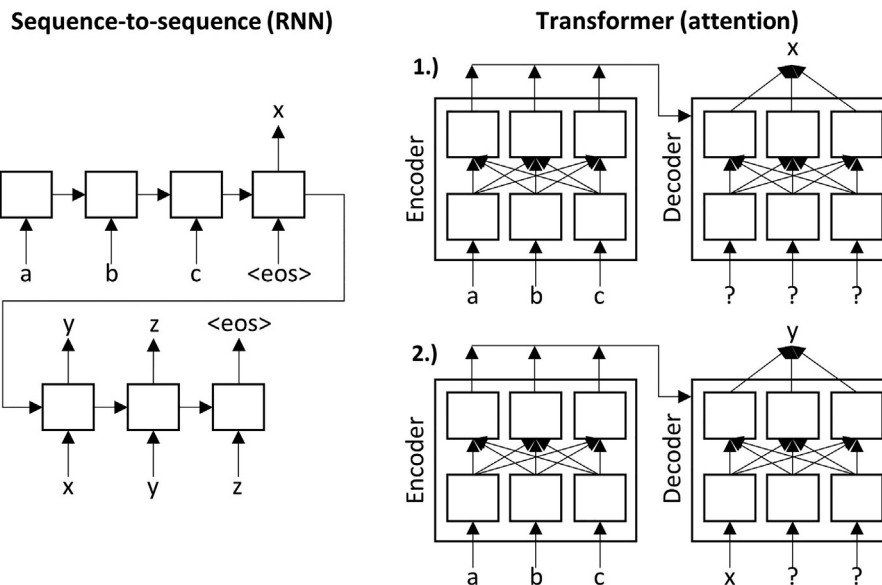


Fig. 3. Abstract graphical representation of the RNN based sequence-to-sequence architecture (left) [34] and an encoder/decoder based transformer architecture on the right [39].

data sets is described and the processed data is visualized. Further on, Section 3.2 presents the methodology developed to generate weekly activity schedules. Finally, Section 3.3 describes the metrics that are used to evaluate the activity plans.

3.1. Data

3.1.1. German mobility panel

The MOP collects information on the mobility behavior of the German population every year since 1994. About 1500 to 3100 persons (10 years and older), who make up about 900–1900 households, fill out travel diaries over a period of one week. The travel diaries contain information about all trips during the week (start and arrival time, distance, modes used, purpose). In addition, socio-demographic information and information on refuelling behavior are recorded in the form of personal, household and fuel diaries. The survey is conducted every year in autumn to avoid distortions caused by holidays. The data is representative of the travel behavior of the German population. The Institute for Transport Studies at the Karlsruhe Institute of Technology is responsible for the implementation and design of the survey [41,50]. Due to changes in the survey design, data from the surveys from 2001 to 2017 are used in this study.

3.1.2. German time use survey

For the analysis of energy relevant activities, the German part of the Harmonized European Time Use Survey, supplied by the German Statistic Office, was used [11,15]. Since the current version of 12/13 incorrectly recorded the location of the people, this data is not used. The data set contains activity diaries and socio-demographic information for 11,921 individual persons (age >10 years) out of 5443 households. Most of the participants provided diaries on two weekdays and one weekend-day in a 10-minute resolution. In this study time dependent data about primary activities and location as well as socio-demographic information are used.

3.1.3. Data preparation

In general, neural networks based machine learning methods have good adaptive feature learning ability. But in the present

study the employed datasets are of a very different format, therefore they need to be aligned before the training. In order to create activity plans from the travel diaries, the basic dataset consisting of 833,986 travel entries for 35,014 person-weeks is converted into weekly activity plans with a time resolution of 10 min. The generation of activity plans is inspired by Hilgert et al. [19]. In a first step, person weeks with missing or unrealistic entries are eliminated so that finally 26,610 person-weeks can be used for further analysis. Based on the travel entries and their purpose, states are determined for each time interval of the week. The choice of the initial state is based on the final state of the time series. Subsequently, the data are aggregated from a 1-minute resolution to 10-minute resolution, assuming the state that is most frequently taken in the respective 10-minute interval. The reason for the reduction of the temporal resolution of the data is, on the one hand, the increased information density, since machine learning algorithms have problems with sparse data. On the other hand, TUD data are also recorded in 10-minute resolution.

The diary entries in the German TUD consist of >200 activity codes describing activities in the everyday life of human beings. Before the diary data is used as input for further processing, these activities are aggregated to activities relevant for household energy demand. The choice of activities is based on similar studies [16,30]. The aggregated activities are visualized in Fig. 4. In the upper two figures, the time course of the aggregated state probabilities of the two data sets is provided over a week. The lower two partial figures show example artificial activity plans for individual persons. Inter-day dependencies in behavior from Monday to Friday can be easily recognized from the visualization of the mobility schedule. The example activity plan, on the other hand, provides detailed daily information on energy-related home, sleep and mobility activities. Further comparative analyses based on socio-demographic characteristics of the data sets can be found in Section 5 and in the appendix.

3.2. Methodology

The approach for the generation of weekly activity schedules with a time resolution of 10 min is presented in Fig. 5. In the first step, weekly mobility schedules of individual persons from the

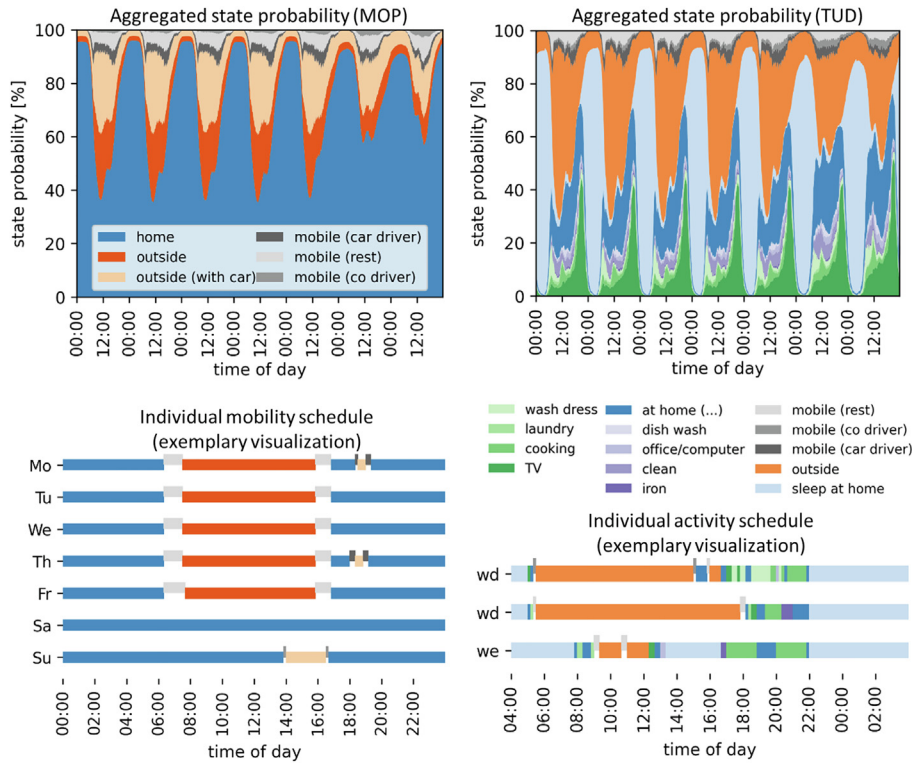


Fig. 4. Visualization of aggregated state probabilities and exemplary artificial individual diary entries based on the MOP [41] and the TUD [11].

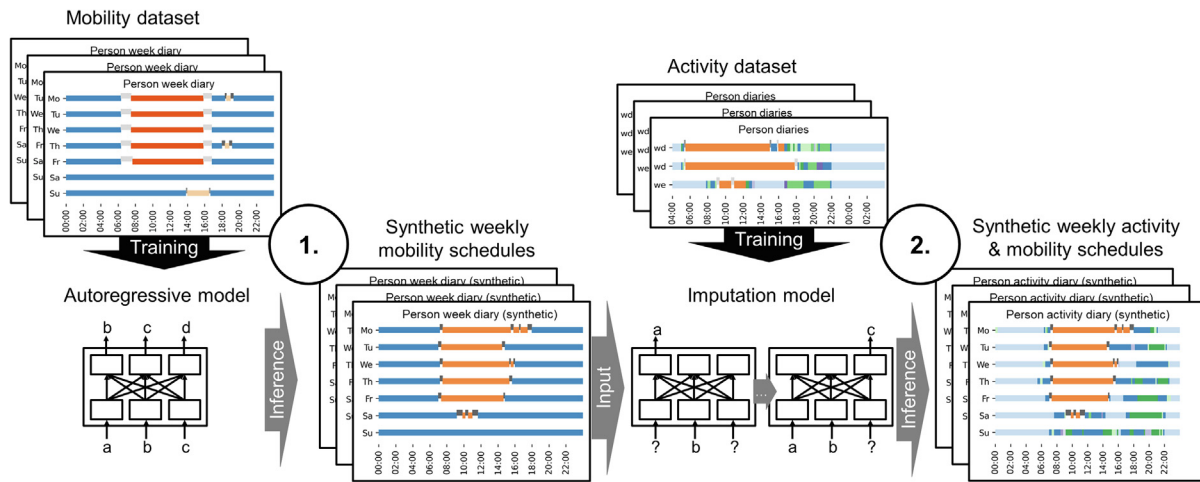


Fig. 5. Two-step model approach for generating weekly activity schedules.

German Mobility Panel are used as input data. The objective of the first step is to generate synthetic mobility schedules with statistical properties similar to the empirical schedules. The developed approaches are autoregressive. This means that it is assumed that the choice of the next mobility state ms_{t+1} only depends on all the states $ms_{0..t}$ that have already been observed. In Section 3.2.1, an LSTM-based and an attention-based approach for sequence generation of mobility states are presented. Due to the similarity of the underlying problem, the selection of the methods used in this paper is based on the models that define the state of the art in the field of NLP. These are currently attention-based transformer architectures. Before that, LSTM based neural networks were used as described in Section 2.3.

The objective of the second model step is to enrich the synthetic mobility plans with energy-related *at home* activities. For this pur-

pose, two imputation models are presented in Section 3.2.2. Bidirectional LSTM model architectures are compared with attention-based architectures. Time Use Survey data from individuals are used to train the models. During the prediction process, the synthetically generated weekly mobility schedules are fed into the imputation model as input and the *at home* state is replaced by energy-relevant activities. A graphic representation of the step by step procedure of the autoregressive and imputation models can be found in Fig. 7a.

3.2.1. Autoregressive models for weekly mobility schedule generation

To generate high-quality mobility plans on an individual level and at the same time representative mobility plans on an aggregated level that adequately describe the diversity of human behavior, approaches are required that capture the complex

relationships in human behavior. In contrast to the Markov-based approaches used in the majority of the studies described in Section 2.1, LSTM and attention-based approaches can take into account longer-term time dependencies in the timing of individual activities due to their different memorisation mechanisms. While in Markov models probabilities are assigned to individual activity sequences and thus the number of free parameters increases exponentially with the order of the model, these kind of models are not suitable to take into account long-term dependencies in behavior between single days [28].

LSTM based models process time series sequentially and take as input the current state vector $x_t \in \mathbb{R}^d$ the hidden state vector $h_{t-1} \in \mathbb{R}^h$ and the cell state vector $c_{t-1} \in \mathbb{R}^h$. The dimension of the hidden state and the cell state vector h is the number of LSTM units which define the memory capacity of the LSTM cell. The cell states are adjusted every timestep using different gating mechanisms (input gate, output gate, forget gate) and activation functions. Due to the additive structure of the LSTM cells they partly solve the vanishing gradient problem and therefore are able to capture long-term dependencies in time series [20].

Attention based models do not process time series sequentially and therefore are suitable to better parallelize the learning process. The time dependencies between individual time steps are learned from scratch. To make this easier, positional encodings are added to the individual states in this study, which provide information about the relative position of the state in the time series. To calculate the masked dot product attention matrix, the matrices $Q, K, V \in \mathbb{R}^{T \times d}$ (query, key, value) and the mask $M \in \mathbb{R}^{T \times T}$ are required as input according to Fig. 6. In the case of self-attention Q, K, V are the same. The mask shown in Fig. 6 is a look ahead mask. The masked (black) cells contain high negative values and are added to the scaled result of the matrix multiplication of Q and K . The subsequent use of the softmax function prevents to put attention on dependencies between already observed and future states. The Softmax function transforms a T -dimensional vector with real components into a T -dimensional vector $\sigma(z)$ also as a vector of real components in the value range $[0,1]$, where the components add up to 1.

$$\sigma(z)_t = \frac{e^{z_t}}{\sum_{t=0}^T e^{z_t}} \quad t = 1, \dots, T \quad (1)$$

Before the dependencies between individual states can be learned in the LSTM/attention layers, layers must be introduced that use all the available information of a single state as input and learn its state representation in a multidimensional space.

Fig. 7b./c. show the different kinds of input provided to the autoregressive and imputation models and their first layers. Input to the autoregressive model is provided in the form of the mobility state $ms_{p,t}$, the time of the day/week τ_t , the day of the week d_t of person p at timestep t and as socio-demographic information $sd_{i,p}$. The time of the day/week is translated into a sinusoidal posi-

tional encoding using periods of one day/week. This is a typical approach to provide information about cyclical characteristics in time series (e.g. daily/weekly patterns) to the model. All other model inputs ($ms_{p,t}$, $d_t, sd_{i,p}$) are categorical and are therefore inserted into an embedding layer. Through the embedding layer the categorical information is mapped into a m -dimensional continuous space. The weights of the embedding layer and therefore the way the categorical variables are represented in the m -dimensional space are learned during the training process of the model. Further on, all the time step specific information are concatenated. The input time series is shifted one time step to the right ($t = 0 \dots T - 1$) and starts with a dummy time step at $t = 0$, which is composed of a start token consisting of the start time and day and socio demographic information of the specific person. This training method is called teacher forcing [43].

Fig. 8a. describes the central components of the LSTM based autoregressive model. After concatenating the time specific information, the vector state representations are fed into a linear dense layer before the state representations are inserted into a sequence to sequence LSTM layer. The final dense layer contains $|ms| = 6$ neurons which represent the probabilities (logits) of each mobility state $ms_{p,t}(t = 1 \dots T)$.

Fig. 9 describes the architecture of the attention based transformer model. The transformer layer consists out of three linear dense layers for Q, K, V , the attention layer consisting of the scaled dot-product attention and two feed forward dense layers with dropout similar to [39]. Both models are trained by minimizing the cross entropy loss between the ground truth and the predicted probabilities.

3.2.2. Energy related activity imputation / enrichment

In the second model step, the generated weekly mobility plans are enriched with energy-related activities. A bidirectional LSTM model (Fig. 8b.) is compared with an attention-based transformer model (Fig. 9b.). In contrast to the first model step, information about individual mobility behavior over the entire week is already available when the first ‘‘at home’’ activity is estimated, this information has an impact on the activity choice. The procedure of the prediction process of the imputation model can be found in Fig. 7a.

As input data during the training process, the model is provided with activity time series of individual persons over 3 days ($2 \times$ weekday, $1 \times$ weekend), the time and day of the week as well as socio-demographic parameters (job, age). The time step specific input processing can be seen in Fig. 7c. In contrast to the autoregressive models, the imputation models do not necessarily receive consecutive days as input, as this is not possible due to the structure of the time use survey. The connection between the three respective days is learned in the training process and applied to a whole week in the imputation process. In contrast to Fig. 8a., it can be seen in Fig. 8b. that the bidirectional LSTM architecture also takes future states into account when predicting the current state.

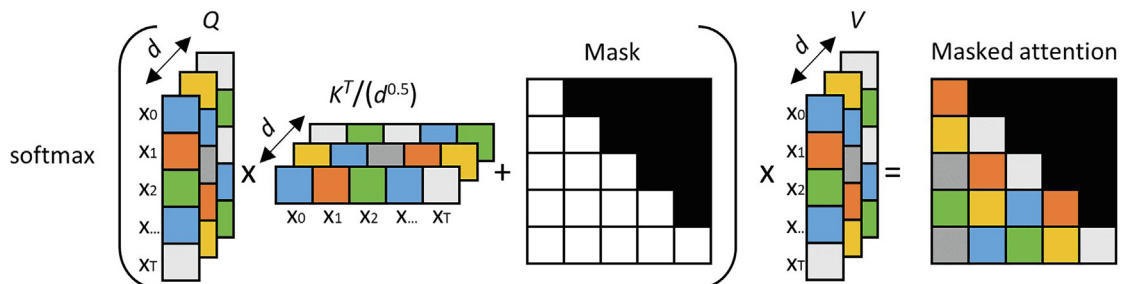


Fig. 6. Illustration of the masked scaled dot product self-attention mechanism of an autoregressive model based on [39].

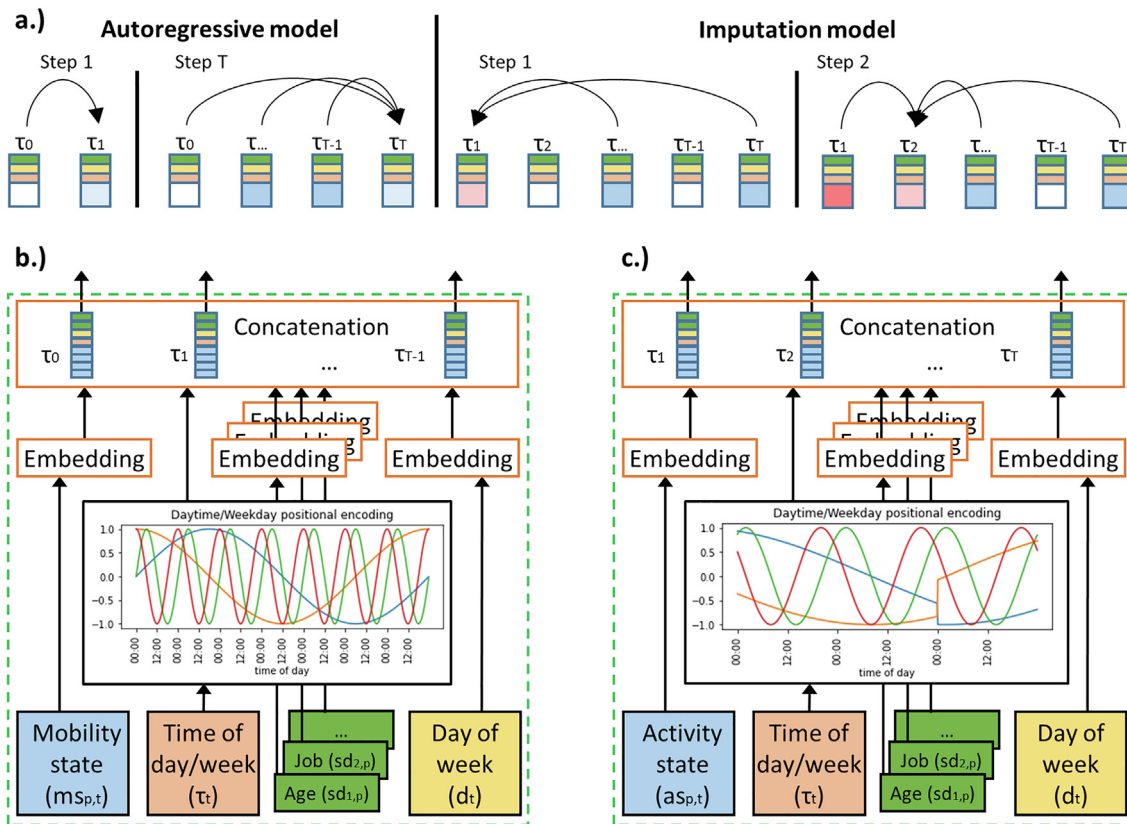


Fig. 7. a.) Illustration of the relevant time step specific dependencies in the autoregressive and imputation models, b./c.) training input of the autoregressive/imputation (b./c.) models and visualization of their first layers.

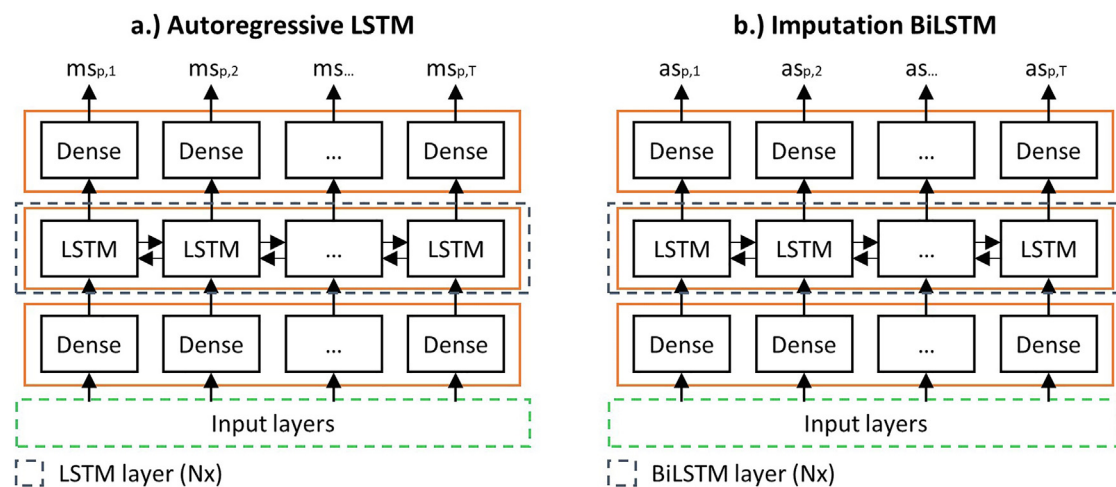


Fig. 8. a.) LSTM based autoregressive model architecture and b.) BiLSTM based imputation model architecture.

In contrast to the autoregressive transformer model, the imputation transformer does not use self-attention. The query vector Q of the first transformer layer contains the information about the unknown home states (unknown state, time, day, socio-demographic information). The key and value vector are identical and contain information about the mobility states of the three days (during training) or the week (during prediction). During the training process, *at home* activities of the TUD are masked and fed to the model as input. In all of the following Transformer layers, the output of the previous Transformer layer represents the query vector Q . The imputation models are trained using the cross entropy loss function.

3.3. Metrics

To evaluate the models presented, metrics must be introduced on the basis of which the model output can be assessed on an individual and aggregated level. The metrics presented below are generated and visualized at constant intervals during the training process.

The model-specific metrics are the cross entropy loss, which is minimized during the training process, and the model accuracy which provides information about how well the model predicts the next state. For the evaluation of the generated activity schedules, metrics are used to assess whether the proposed models

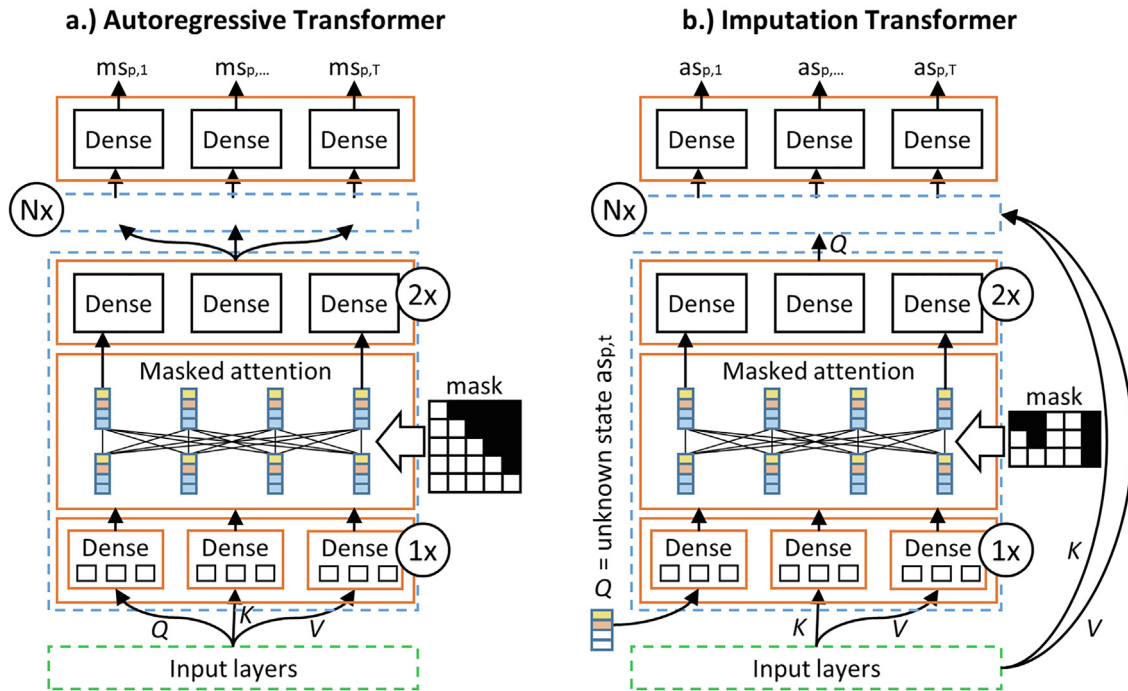


Fig. 9. a.) Transformer based autoregressive model architecture and b.) Transformer based imputation model architecture (residual connections are not visualized).

reflect the variability in human behavior. Furthermore, metrics describing the variability of intrapersonal behavior are used to assess the consistency within a person’s activity plan.

The aggregated state probability (sp) describes the aggregated probability $sp_{s,t}$ of a state $s \in S$ at time step $t \in T$ over a sample with the sample size N .

$$sp_{s,t} = \frac{\sum_{i=1}^N x_{i,s,t}}{N} \forall s \in S, t \in T \quad (2)$$

State durations (sd) are calculated for all states $s \in S$ and are visualized by their cumulative distributions. The distribution of the duration of states can be used as a first indicator to evaluate the models with regard to the consideration of long-term time dependencies. For the evaluation of the intrapersonal variability within an activity schedule, the number of activities per week (na), the autocorrelation (ac) and the Hamming distance (hd) are calculated for each activity schedule of a sample. The autocorrelation is calculated for each activity state and each individual and is used to obtain information about the regularity of activities. The Hamming distance is calculated between all working days $d \in \{1 \dots 5\}$ of the week and thus provides information about the similarity of the daily behavior of individuals.

$$hd_n = \sum_{d_1=1}^5 \sum_{d_2=1}^5 |\{t \in \{1, \dots, T_d\} | s_{d_1,t} \neq s_{d_2,t}\}| \forall n \in N \quad (3)$$

From the variability of these metrics (na, ac, hd), information about the diversity in behavior can be obtained.

4. Results

The results presented below were calculated with an XLA compiler and a “Tesla V100-SXM2-16 GB” GPU in Tensorflow 2.3. To provide the models from overfitting, the data sets are randomly split up into training data (9-fold cross validation → 80% training, 10% validation) and test data (10%).

4.1. Mobility schedule generation

As a reference model for the presented autoregressive models, a time-inhomogeneous first order Markov model is used. The first order Markov model characteristics are representative for the models presented in Section 2.1, since marginal changes in the metrics can be achieved by using more complex Markov chains, but the basic problems remain (no long-term memory). The introduced metrics are visualized in Fig. 10. All metrics shown are calculated based on a sample size of $N = 2000$ unless explicitly stated otherwise. The course of the aggregated state probability of the state *outside* deviates only slightly from the empirical course. The averaged root mean square error (rmse) over all states of the aggregated state probability is 0.53% and tends towards zero with increasing sample size. From the course of the cumulative state durations of the state *mobile (car driver)* and the other states shown in Fig. 16 it can be observed that the state durations of the schedules produced by the first order Markov model partly deviate from the empirical data. Furthermore, the distribution of the Hamming distance and the autocorrelation clearly differ between the data generated by the Markov model and the empirical data, which is reflected in large deviations in the rmse of the autocorrelation and the mean absolute error of the Hamming distance. The peak in the autocorrelation in mobility behavior after 144 lags (one day) describes daily mobility patterns in the mobility behavior of individual persons. This peak, which can be clearly identified in the empirical data, is not represented in the synthetic mobility schedules of the Markov model. Compared to the empirical distribution, the distribution of the Hamming distances is shifted to the right, towards higher distances. Consequently, subsequent days of single individuals differ more from one another than in the empirical data. The distribution of number of activities per week indicates that the Markov model matches the empirical data well on average, but the boxplot indicates that the diversity in behavior deviates from the one observed in the empirical data.

The autoregressive models presented in Section 3.2.1 are trained to predict the multinomial state distribution of the subse-

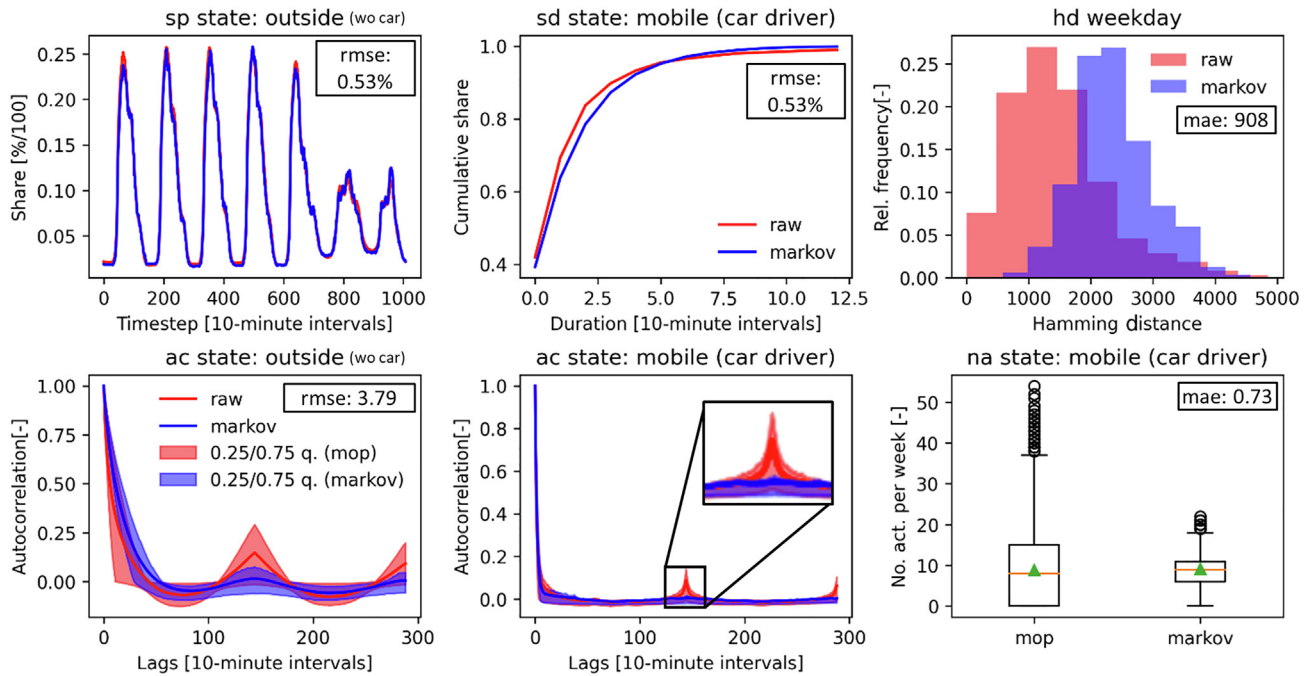


Fig. 10. Visualization of the metrics for empirical MOP data (N = 26,610) and data generated with a first order Markov model (N = 2000) (blue). The shown state dependent errors are calculated over all states and the mean is presented. (For interpretation of the references to colour in this figure legend, the reader is referred to the web version of this article.)

quent state. To achieve this, the cross entropy loss is minimized. **Fig. 11** and **12** describe the course of the cross entropy loss during the training process. An epoch is defined as one training step of the nine-fold cross validation. After nine epochs, the training and validation data set are reshuffled and divided into nine new participations. During the training of the attention-based models, the loss function converges continuously for the training and test dataset. In the LSTM-based model, however, it can be seen that the course of the loss and accuracy function of the test data set diverges from the course of the training and validation data after around 14 epochs. From this point on, the model overfits on the training data and the training process can be stopped. In order not to use over-trained models, the weights of the model are saved at constant intervals during the training process. Furthermore, the development of the model accuracy during the training process is shown. This converges to a value of approx. 96.3%. This means that 96.3% of the time the correct value is predicted in the training process. Of course, the prediction is easier during the night when people are asleep than, for example, in the afternoon when there are many

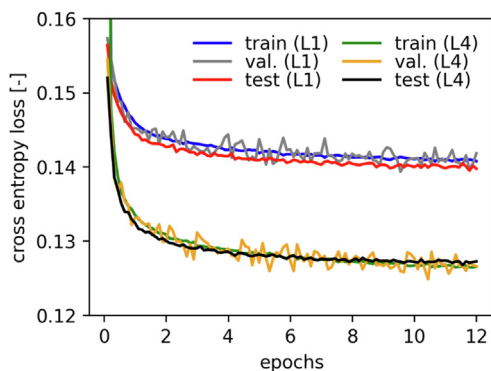


Fig. 11. Loss development during training of the autoregressive transformer (L1/L4: 1/4 transformer layers).

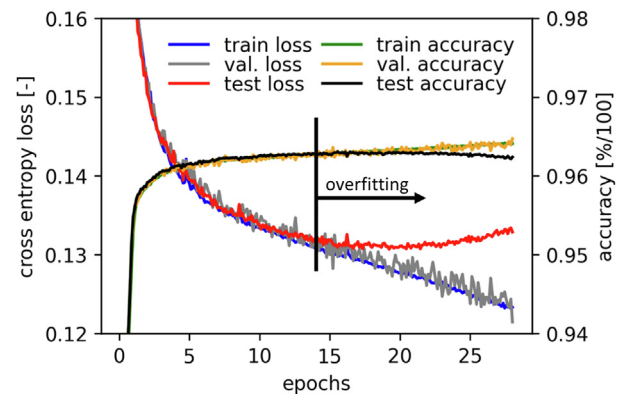


Fig. 12. Loss and accuracy development during LSTM training.

changes in activity. **Fig. 11** shows the course of the cross entropy loss for two model configurations, with one transformer layer and with four transformer layers. By increasing the depth of the neural network, the model can better map the complexity of mobility behavior. However, only marginal improvements can be achieved by further increasing the number of transformer layers from four to eight (**Table 3**). Since the performance of the models presented depends heavily on the choice of hyperparameters, various parameter settings were tested during the training phase for the LSTM and the attention based models. The parameter settings varied during the training process and the corresponding metrics can be found in **Tables 2** and **3**. In addition to the learning rate and the batch size, the number of LSTM units was varied, which limits the complexity of the internal state of the LSTM and is therefore important to capture temporal dependencies in behavior. The number of dense neurons (LSTM) or the model dimension (transformer) was varied to ensure that state-specific information is appropriately represented. Furthermore, the depth of the neural networks was varied, as this enables the neural network to learn

higher level representations in human behavior. The results of the parameter variations show that the attention-based models are slightly superior to the LSTM-based models in most metrics, consequently, the attention-based model no. 3 from Table 3 is used for the presentation of the mobility schedule specific metrics.

Selected mobility schedule specific metrics for the attention based autoregressive model described in Table 3 (model no. 3) are presented in Fig. 13. A holistic overview of all metrics for all states can be found in the appendix (Fig. 16). In contrast to the first order Markov model, the aggregated state probability is represented slightly worse by the attention based model. The rmse of the state probability averaged over all states and time steps is higher than the error of the first-order Markov model for all the models shown in Table 2 and 3 in the appendix. The Markov error corresponds to the standard error that arises with a sample size of 2000. The standard error was calculated by randomly sampling 2000 samples 30 times from the entire population and calculating their deviation from the metrics of the entire population (N = 26,610). The mean value of the error of the 30 samples is called the standard error. The mean absolute error of the number of weekly activities in the attention-based model is also higher than that of the Markov model (3.6 > 0.73). The diversity of the number of weekly activities is, however, recorded much more accurately by the attention-based model, which is shown in the lower right illustration in Fig. 13 for the state *mobile (car driver)* and in Fig. 16 for all other states. While the machine learning models presented in this work have slight deviations in the description of the averaged behavior and therefore perform slightly less accurately than Markov models, the mobility schedules generated differ fundamentally on the individual level, which is shown by the distribution of the cumulative state durations, the Hamming distance between weekdays and the autocorrelation of the individual states. Using the Hamming distance and the autocorrelation, it can be clearly seen that day-to-day dependencies in behavior are very accurately taken into account by the models presented in this work. In order to be able

to adequately capture daily rhythms in mobility behavior, it is very important that the peak in the autocorrelation graph is captured well after 24 h (144 10-minute time steps), which can be seen in the bottom center graph in Fig. 13. From the course of the mean values and the ranges of the 25%/75% quantile, it becomes clear that both these dependencies in the mean and in the spread are well represented across the entire population. These visual findings are also reflected in the significantly lower rmse of the autocorrelation compared to the Markov model (0.54 < 3.79).

The difference between LSTM-based models and attention-based models is particularly evident from the autocorrelation peak in mobility behavior after 24 h. LSTM models are also able to recognize relationships over such long periods of time, but in this work it was not possible to reproduce the peak as well with LSTM-based models as it can be seen in Fig. 13 (bottom center) with the attention-based model. In addition to the low deviation of the mean error in the distribution of the Hamming distance (5 < 908), it can also be clearly recognized from the form of the distribution that the diversity in the profiles generated matches the real distributions much better than that of the Markov models, in which individual weekdays of a person do not have the similarities found in the empirical data.

4.2. Energy-related activity imputation

Since the model approach presented in this paper (step-by-step simulation of mobility behavior and subsequent enrichment of the results with energy-related activities based on different data sets) is new and no classical comparable applications in the field of behavioral modeling are known, only the results of the imputation models presented in Section 3.2.2 are benchmarked against each other in this section. As with the autoregressive models, the model performance of the imputation models is strongly dependent on the choice of hyperparameters. The parameters of the BiLSTM-based and the attention-based imputation model that were varied during the training process

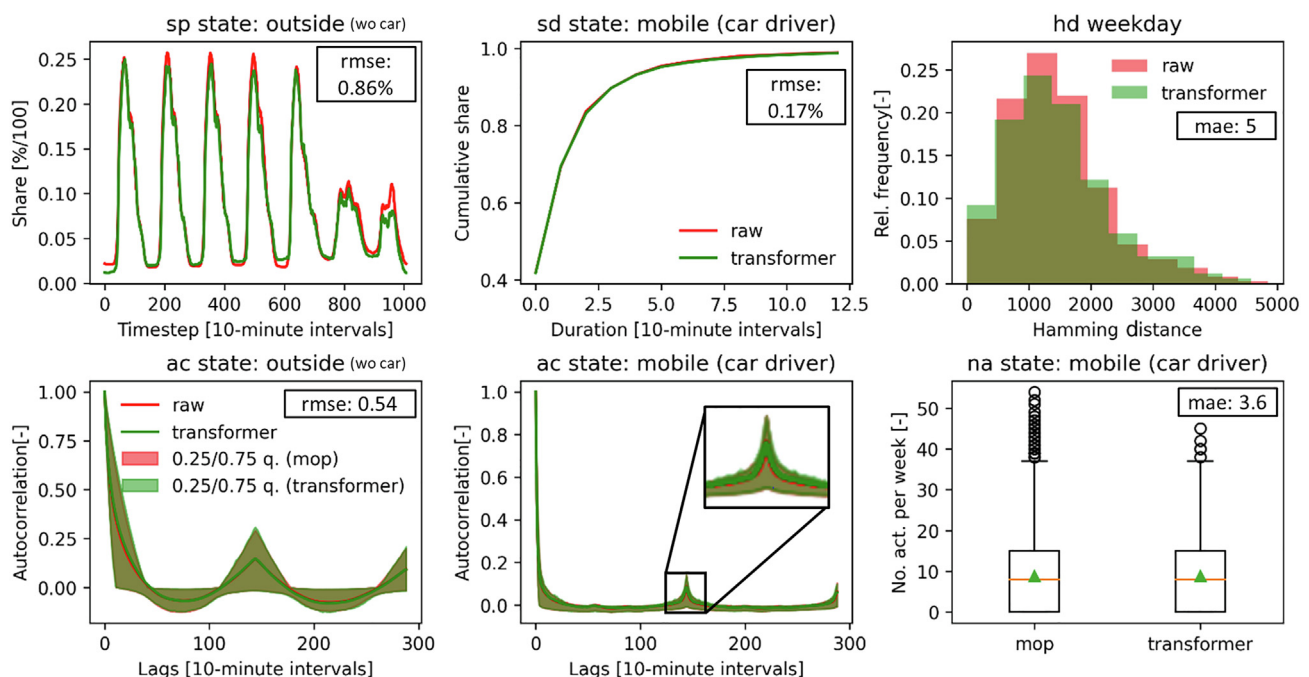


Fig. 13. Visualization of the metrics for empirical MOP data (N = 26,610) and data generated with an attention based model (N = 2000) (green). Model parameters can be seen in Table 3 (no. 3). The shown state dependent errors are calculated over all states and the mean is presented. The overlapping green and red ranges in the left-bottom and center-bottom graph describe the 25%/75% quantiles. (For interpretation of the references to colour in this figure legend, the reader is referred to the web version of this article.)

can be found in Tables 4 and 5 in the appendix. To ensure that dependencies between time steps can be adequately captured by the model, sufficient amounts of LSTM units and attention layers must be provided. The dimension of the model must be chosen so that all time-step-specific information can be mapped well. In the following, the activity schedule-specific metrics for the attention-based model no. 6 from Table 5 are compared with the empirically collected TUD data. The metrics are visualized for specific states in Fig. 14. A holistic overview of all metrics for all states and the development of the model loss and accuracy can be found in the appendix (Fig. 17/ Fig. 18).

Similar to the autoregressive models, it can be seen from the course and the rmse of the aggregated state probability that this differs slightly from the empirically collected data. The averaged errors over all states and time steps can be taken from Fig. 14, Table 4 and 5 for the various model variants. The error in the simulation of the state durations, on the other hand, is smaller than that which occurs when modelling activities with a first-order Markov chain (no imputation model). Since the German TUD data set contains diary entries for three days of the week, the model can also learn day-to-day dependencies between energy-relevant activities. The autocorrelation graphs in Fig. 18 show that the imputation model is able to recognize and reproduce these dependencies. For example, daily sleep rhythms can be reproduced in the synthetic data, which is another unique selling point of this work.

When comparing the metrics shown in Table 4 and 5, it is noticeable that the attention-based models perform slightly better in representing the aggregated state probability, while the BiLSTM-based models tend to map the duration of states and autocorrelation better. This could be attributed to the fact that when representing energy-relevant activities, short-term temporal dependencies between individual states are of higher importance than the one seen in the mobility schedules and the sequential character of the BiLSTM depicts these dependencies well, while

attention-based models tend to capture individual states and their time-dependent probability of occurrence more strongly than short-term sequential dependencies.

4.3. Generation of weekly activity schedules

After the training processes of the autoregressive models and the imputation models have been described and evaluated in Sections 4.1 and 4.2, synthetic weekly activity plans are now generated for various socio-demographic groups and compared with empirical data. Table 6 in the appendix gives an overview of the socio-demographic composition of the empirical data. The age distribution of the MOP data shows that older population groups are overrepresented in contrast to the TUD data. Younger groups of the population such as students and part-time workers, on the other hand, are under-represented. Due to the consideration of socio-demographic factors when coupling the data sets in the approach presented, a different distribution of the socio-demographic groups in the individual data sets is not problematic. When considering the sample sizes of the MOP and TUD data, it must be taken into account that the TUD samples, in contrast to the MOP samples, only consist of two to three days. The MOP data set with 10-minute time resolution has more than five times as many data points as the TUD data set. From the rmse of the aggregated state probabilities for the different socio-demographic groups, it can be seen that the data sets differ in some cases more strongly (rmse (age < 18): 4.0%). In the synthetic profiles, the mobility behavior is generated on the basis of the MOP data, consequently, when looking at the rmse, fewer errors can be found between the synthetically generated data and the MOP data, both when looking at the socio-demographic groups in a differentiated manner and when looking at the aggregate as a whole dataset.

Finally, Fig. 15 shows the course of the aggregated state probabilities over a week and two exemplary activity plans of syntheti-

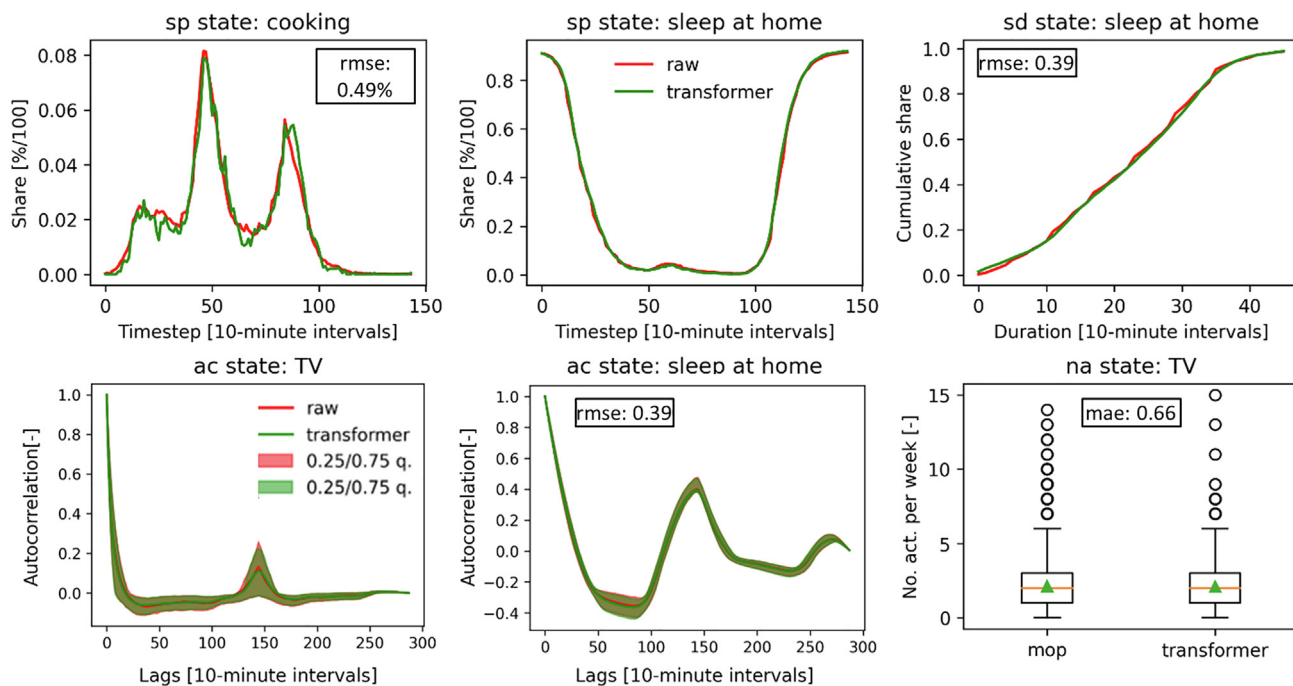


Fig. 14. Visualization of the metrics for empirical TUD data (N = 35,691 diary days) and data generated with an attention based model (N = 2000 diary days) (green). Model parameters can be seen in Table 5 (model no. 6). The shown state dependent errors are calculated over all states and the mean is presented. The overlapping green and red ranges in the left-bottom and center-bottom graph describe the 25%/75% quantiles. The autocorrelation graphs were calculated based on the two work days over 288 10-minute timesteps. (For interpretation of the references to colour in this figure legend, the reader is referred to the web version of this article.)

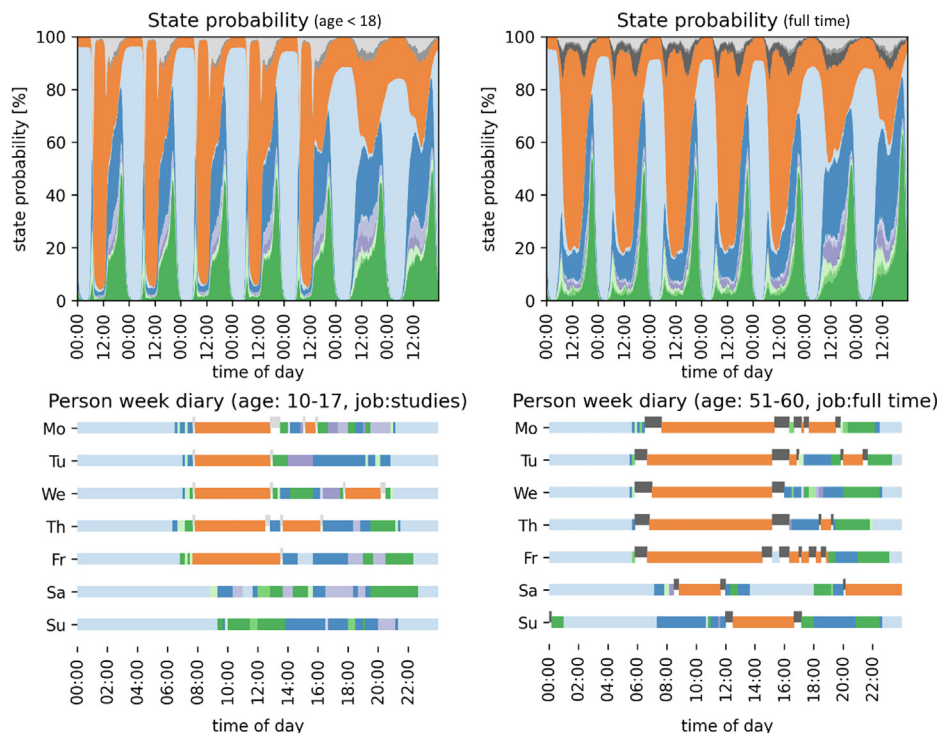


Fig. 15. The top two figures represent the course of the aggregated state probability for 1,500 generated activity plans for persons under 18 years of age and for full time employees. The lower two representations are two exemplary activity plans for a person under the age of 18 and a full-time employee (A legend can be found in Fig. 4).

cally generated schedules for two socio-demographic groups (age < 18, full time employees). From the visualization of the aggregated state probabilities it can be seen that children under the age of 18 are mainly out of the home in the mornings and have two pronounced mobility peaks at around 8 am and 1 pm, while full-time employees are mainly outside during the day. Rhythmic behavior within the working days can be seen in the exemplary individual profiles. In the activity plan of the student on Friday morning, the student changes from an *at home* state to an *outside* state without a mobility activity in between. At first glance, this seems unrealistic, but these transitions can also be found in the empirical data due to the temporal aggregation of the mobility data over 10 min.

5. Discussion

The results of Section 4.1 show that the Markov model used as a reference model is not able to record long-term dependencies in activity patterns and, due to the structure of the approach, is not able to adequately record the diversity in occupancy behavior. Consequently, synthetic activity schedules generated with Markov chains cannot be used to analyse occupancy behavior on an individual level and are only suitable for studies on an aggregated level. The approach presented in this paper combines weekly mobility data with a large sample size with high-resolution activity data with the help of new machine learning algorithms. The approach creates a new data basis which can be used for further analyses of home occupancy and mobility behavior. The profiles generated have similar stochastic properties as the empirically collected data on both the individual and the aggregated level.

By adequately capturing long-term dependencies in people’s activities, the behavior of individual people can be reproduced. As a result, the data generated represent the basis for a variety of potential applications, one of which is the examination of potential charging

periods of people with electric vehicles, assuming that electric mobility does not change mobility behavior. By combining the detailed mobility data with high-resolution activity data, a unique data basis is created which offers the possibility of consistently simulating the energy demand from personal mobility, the electrical demand for household devices and the heat demand for space heating and domestic hot water. Therefore, simultaneity effects in energy demand can be analysed based on one fundamental data set.

When analyzing such future developments, it should be taken into account that the data sets on which this work is based describe historical behavior (MOP: 2001–2017, TUD: 2001/02). Not taking into account the dynamics in people’s behavioral habits could lead to significant errors, depending on the application. The energy sector includes many examples of innovations that have changed people’s behavior for example, the internal combustion engine for transport and the development of ICT in recent decades. Hence groundbreaking/disruptive technologies could change the nature of the energy service demand itself (e.g. autonomous electric vehicles and smart home applications). In order to take into account temporal changes in behavior in the data set, the survey year of the respective sample could be provided as additional information in future studies. Furthermore, the data sets used differ in their temporal resolution, while the mobility data (MOP) are available in minute resolution, activities in the TUD are recorded in ten-minute resolution. The aggregation of the mobility data to a temporal resolution of 10 min can lead to distortions in short mobility states.

Through the use of machine learning approaches the assumption bias in the presented approach is low in comparison to e.g. utility-based stepwise regression approaches [19], therefore the developed approach is highly transferable. TUD data are collected uniformly in several European countries, but there are some differences in the design of the surveys. Some countries only provide activity time series for one weekday and one weekend day, which makes it harder to capture interday dependencies in activities.

Longitudinal surveys of mobility behavior are not carried out in a harmonized way at the European level. However, similar mobility studies are available, for example in the UK and the Netherlands, which examine the mobility behavior over a whole week of a sample that is representative of the nation [10,21]. The approach presented could therefore easily be applied to behavioral data in the UK and the Netherlands. Instead of training individual models for different countries, it would make more sense to implement the country information as a socio-demographic parameter in a transnational model in order to learn country-specific behavior and at the same time provide the model with a larger database for learning general behavioral relationships.

In this work, the focus was placed on the mapping of the mobility and activity behavior of individual persons and therefore no interpersonal relationships in the behavior of several individuals in a household were taken into account. However, the presented approach can and will be extended to represent household behavior in order to capture interpersonal relationships. Furthermore, only socio-demographic behavioral differences based on age and employment are currently taken into account in the model. Since the underlying data sets contain significantly more socio-demographic differentiations, an extension to include further socio-demographic characteristics is possible.

Since the training process is stopped before the presented models overfit, it can be stated that the models have learned the general stochastic relationships in human behavior and not simply learned the raw data sets by heart. This statement is supported by Fig. 18 in the appendix, which describes the distribution of the minimum distances of a sample of data set a with all samples of data set b. The distribution of the minimum distances between the synthetic mobility schedules and the raw data is similar to the distribution of the minimum distances within the empirically collected data. However, even if the raw data used in this paper are already provided in anonymized form, it must be ensured that no information about individual samples in the empirical data is revealed by the synthetic data sets. Consequently, in follow-up work, prior to making the models presented in this paper available to the general public, algorithms from the field of “differential privacy” must be used to ensure that no information about individual samples is provided [13]. Algorithms that ensure the privacy of individuals have been developed in recent years for deep learning applications [1]. Ensuring differential privacy is always accompanied by a loss of quality in the model, whereby this trade-off between quality and privacy can be clearly quantified by the so-called privacy budget.

6. Conclusion and outlook

Over the past few years, many models have been published that aim to capture relationships in activity patterns to explain residential energy demand. Most of these models are different Markov variants or regression models that have a strong assumption bias and are therefore unable to capture complex long-term dependencies and the diversity in occupancy behavior. In this work it was shown that machine learning models from the field of natural language processing are able to capture long-term dependencies in mobility and activity patterns and at the same time adequately depict the diversity in behavior across the entire population. In a

first step, two autoregressive models are presented which are able to recognize and reproduce weekly mobility patterns. In a second step, two imputation models are trained with time use data, which, based on the mobility information of individual people, enrich them with energy-related activities. Finally, the two models are combined to generate weekly activity plans. By combining an autoregressive generative model with an imputation model, the advantages of two data sets are combined and new data are generated which are beneficial for multiple use cases. One of which is the examination of flexibility potentials of individual households which is urgently needed for the integration of volatile renewable energy sources. Furthermore, metrics were introduced that enable activity profiles to be investigated in terms of intrapersonal and interpersonal variability. Based on these metrics, it is shown that the synthetically generated activity plans represent weekly mobility patterns and day-to-day dependencies of the energy-relevant activities with a high quality on an individual and aggregated level. The evaluation metrics show that LSTM and attention-based neural networks outperform existing approaches on an individual level by a large margin and at the same time have only slight deviations in the aggregated behavior.

Due to the availability of rich socio-demographic information in the two basic data sets, activity plans can be generated for different socio-demographic groups and can be used in future work to simulate consistent energy demand profiles from electric mobility, household devices and space heating. The approach developed provides the basis for making high-quality weekly activity data available to the general public without having to carry out complex application procedures. It was shown that the presented approach does not learn the training data by heart, however, it must be ensured that no private information about individuals is revealed by the model before the synthetic data can be provided to the community, which cannot be ensured at the current time. Therefore, in further work the model will be trained in a differential private way. Furthermore, the presented methodology can be trained with behavioral data from different European countries in order to develop a transnational model. Instead of individual behavior, household behavior could be learned to take interpersonal dependencies into account.

Declaration of Competing Interest

The authors declare that they have no known competing financial interests or personal relationships that could have appeared to influence the work reported in this paper.

Acknowledgements

This work was supported by the Helmholtz Association under the Joint Initiative “Energy Systems Integration” (funding reference: ZT-0002) and was done during a research stay funded by the Centre for Research into Energy Demand Solutions (CREDS) at the University of Reading (UK). This work was supported by UKRI [grant numbers EP/R000735/1, EP/R035288/1 and EP/P000630/1].

Appendix

Figs. 16–19 and Tables 2–6

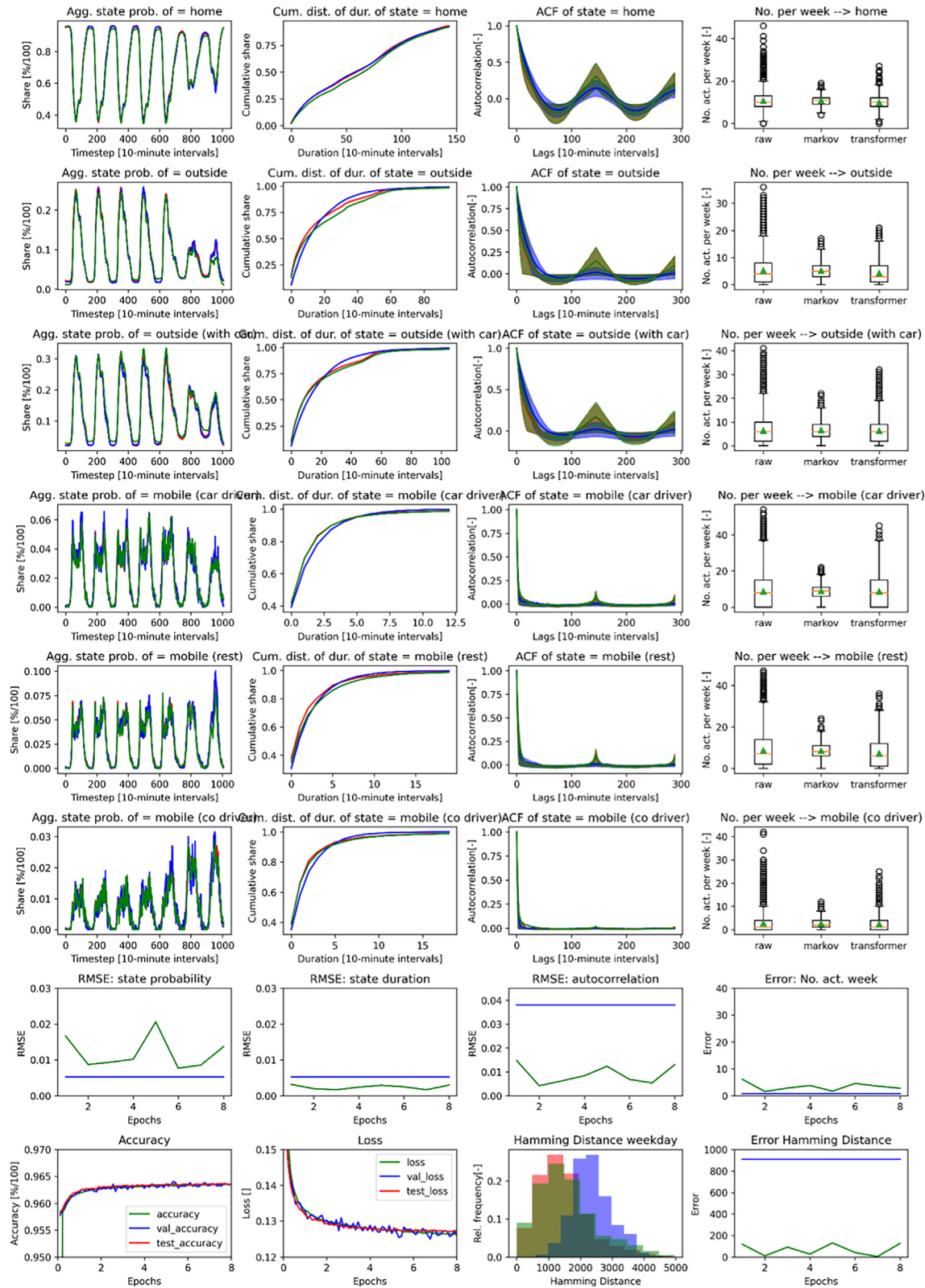


Fig. 16. Comparison of all metrics and all states for the mop data (red), the attention based autoregressive model described in Table 3 (no. 3) (green) and a first order Markov model (blue). The mobility schedule specific metrics of the attention based model are calculated based on the model weights after epoch 7. (For interpretation of the references to colour in this figure legend, the reader is referred to the web version of this article.)

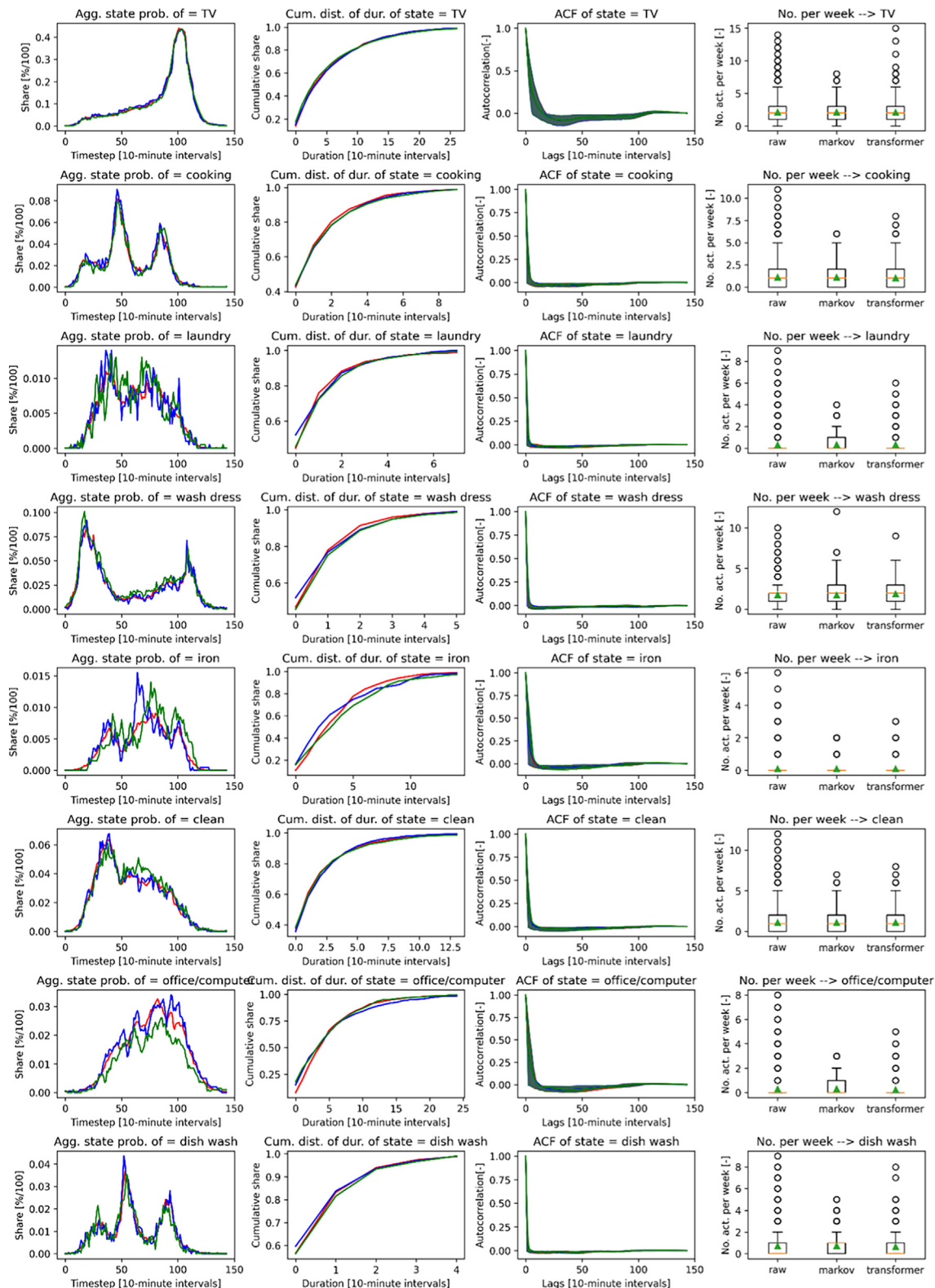


Fig. 17. Part a: Comparison of all metrics and all states for the TUD data (red), the attention based imputation model described in Table 5 (model no. 6) (green) and a first order Markov model (blue – no imputation model). The mobility schedule specific metrics of the attention based model are calculated based on the model weights after epoch 37. The autocorrelation graphs were calculated based on single days. (For interpretation of the references to colour in this figure legend, the reader is referred to the web version of this article.)

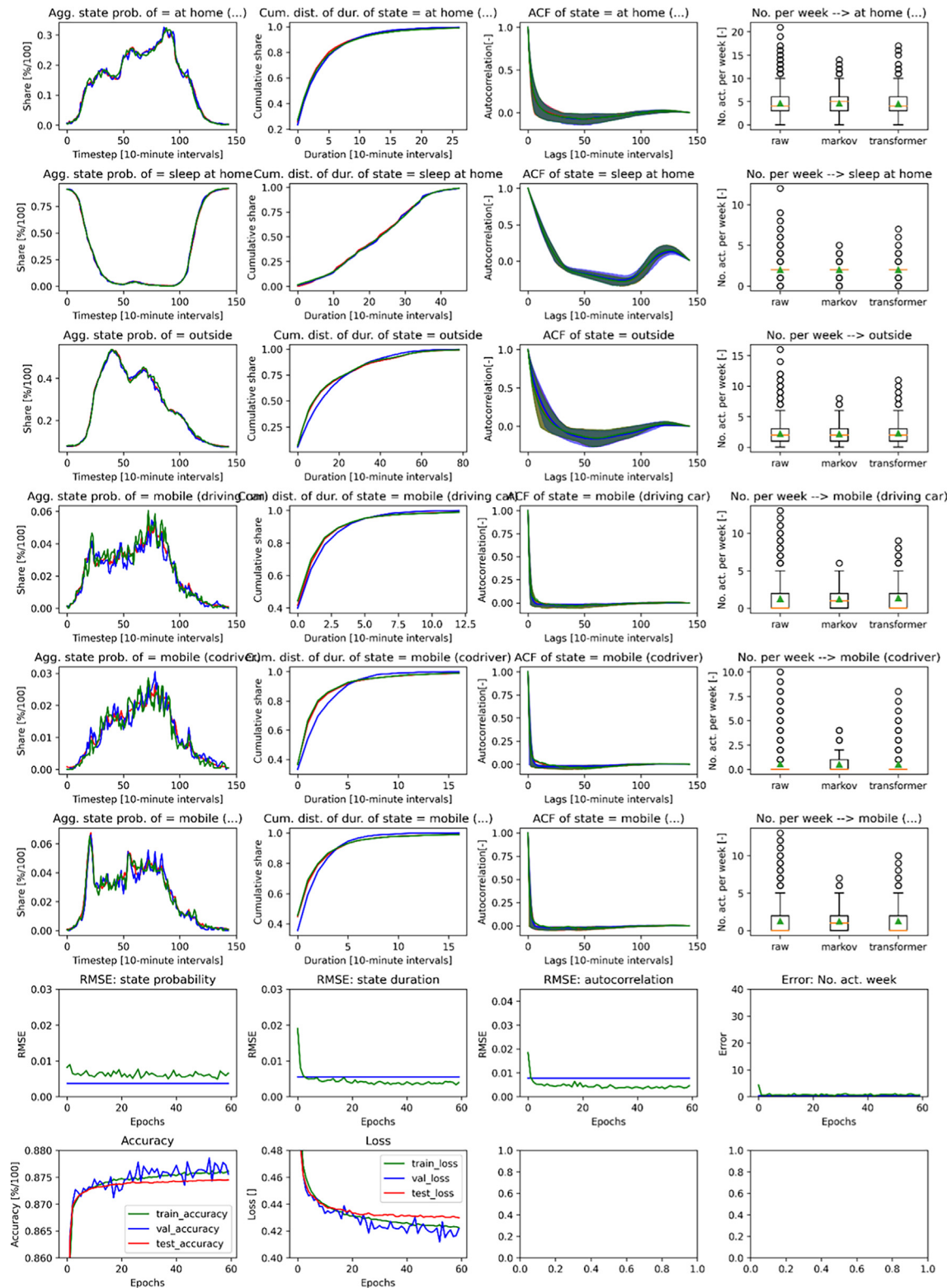


Fig. 18. Part b: Comparison of all metrics and all states for the TUD data (red), the attention based imputation model described in Table 5 (model no. 6) (green) and a first order Markov model (blue – no imputation model). The mobility schedule specific metrics of the attention based model are calculated based on the model weights after epoch 37. The autocorrelation graphs were calculated based on single days. Furthermore, the course of the model loss and accuracy is visualized. (For interpretation of the references to colour in this figure legend, the reader is referred to the web version of this article.)

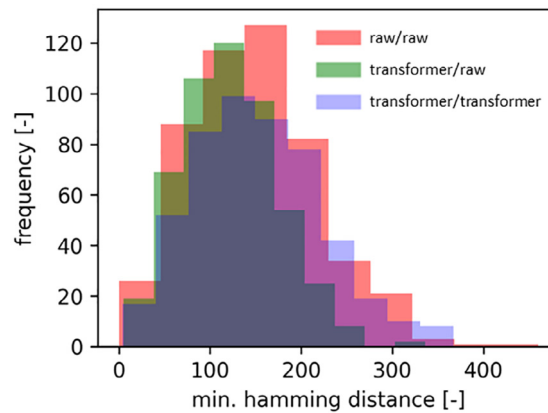


Fig. 19. Distribution of the minimum Hamming distances of the samples from dataset a (sample size N = 500) to the samples in dataset b (dataset a/ dataset b).

Table 2

Hyperparameter configurations and model metrics for the LSTM based autoregressive model. Metrics were calculated based on a sample size of N = 2000. Furthermore, a mean standard error due to the sample size of 2000 is given.

| No. | LSTM units/Learning rate/Batch size/Dense neurons | Sp rmse [%] | Sd rmse [%] | Ac rmse [%] | Na mae [l] | Hd mae [l] | Cross-entropy Loss | Accuracy [%] | CV Epochs |
|---------------------------|---|-------------|-------------|-------------|------------|------------|--------------------|--------------|-----------|
| 1 | 512/0.0005/512/32 | 0.99 | 0.13 | 0.71 | 1.11 | 144 | 0.133 | 96.27 | 14 |
| 2 | 128/0.0005/512/32 | 1.03 | 0.17 | 1.65 | 1.57 | 423 | 0.142 | 96.12 | 8 |
| 3 | 512/0.001/512/32 | 1.05 | 0.18 | 0.66 | 3.04 | 235 | 0.131 | 96.30 | 11 |
| 4 | 512/0.0005/64/32 | 1.27 | 0.22 | 0.89 | 3.39 | 114 | 0.134 | 96.26 | 3 |
| 5 | 512/0.0005/512/64 | 0.90 | 0.18 | 0.80 | 0.67 | 98 | 0.131 | 96.29 | 17 |
| 6 | 512/0.0005/256/32 | 0.90 | 0.13 | 0.60 | 1.85 | 83 | 0.131 | 96.29 | 11 |
| 7 | 2x256/0.001/512/32 | 0.69 | 0.14 | 0.95 | 2.08 | 120 | 0.131 | 96.29 | 12 |
| 8 | 2x256/0.0005/256/32 | 0.97 | 0.19 | 0.63 | 3.61 | 1.5 | 0.132 | 96.28 | 10 |
| Standard error (N = 2000) | | 0.52 | 0.09 | 0.24 | 0.6 | 13 | - | - | - |

Table 3

Hyperparameter configurations and model metrics for the attention based autoregressive model. 2xh means that two attention heads are used (see [39]). Results in this work are generated with model configuration no. 3.

| No. | Transformer layers/D_model/Learning rate/Batch size | Sp | Sd rmse | Ac rmse | Na mae | Hd mae | Cross-entropy Loss | Accuracy | CV Epochs |
|----------------------------|---|-------------|-------------|-------------|------------|----------|--------------------|--------------|-----------|
| 1 | 1/64/0.001/64 | 0.83 | 0.31 | 1.32 | 2.96 | 244 | 0.14 | 95.95 | 9 |
| 2 | 4/64/0.001/64 | 0.91 | 0.16 | 0.70 | 2.53 | 33 | 0.128 | 96.34 | 15 |
| 3 | 8/64/0.001/64 | 0.86 | 0.17 | 0.54 | 3.6 | 5 | 0.127 | 96.36 | 7 |
| 4 | 4/64/0.001/128 | 0.95 | 0.22 | 0.54 | 3.28 | 44 | 0.130 | 96.29 | 3 |
| 5 | 4/128/0.001/128 | 0.89 | 0.24 | 0.59 | 3.60 | 9 | 0.128 | 96.33 | 6 |
| 6 | 4/64/0.0005/64 | 0.86 | 0.18 | 0.48 | 4.78 | 6 | 0.128 | 96.33 | 20 |
| 7 | 2(2xh)/64/0.001/64 | 0.97 | 0.22 | 0.60 | 6.33 | 74 | 0.129 | 96.31 | 11 |
| 8 | 4(2xh)/64/0.001/64 | 1.20 | 0.20 | 0.42 | 4.52 | 126 | 0.127 | 96.35 | 8 |
| Standard errors (N = 2000) | | 0.52 | 0.09 | 0.24 | 0.6 | 13 | - | - | - |

Table 4

Hyperparameter configurations and model metrics for the BiLSTM based imputation model. Metrics were calculated based on a sample size of N = 2000 diary days. Furthermore, a mean standard error due to the sample size of 2000 diary days is given.

| No. | LSTM units/D_model/Learning rate/Batch size | Sp rmse | Sd rmse | Ac rmse | Na mae | Cross-entropy Loss | Accuracy | CV Epochs |
|----------------------------|---|---------|---------|---------|--------|--------------------|----------|-----------|
| 1 | 64/32/0.001/64 | 0.70 | 0.27 | 0.36 | 0.88 | 0.434 | 87.48 | 21 |
| 2 | 128/32/0.001/64 | 0.74 | 0.28 | 0.44 | 0.86 | 0.435 | 87.36 | 11 |
| 3 | 256/32/0.001/64 | 0.60 | 0.26 | 0.37 | 0.59 | 0.432 | 87.46 | 9 |
| 4 | 128/64/0.001/128 | 0.75 | 0.26 | 0.42 | 0.96 | 0.432 | 87.54 | 13 |
| 5 | 128/32/0.001/128 | 0.71 | 0.42 | 0.48 | 0.98 | 0.433 | 87.44 | 11 |
| 6 | 128/32/0.0005/128 | 0.64 | 0.28 | 0.43 | 1.27 | 0.434 | 87.48 | 12 |
| 7 | 64/32/0.0005/128 | 0.60 | 0.30 | 0.38 | 0.62 | 0.434 | 87.39 | 33 |
| 8 | 64/32/0.0005/64 | 0.62 | 0.34 | 0.44 | 0.82 | 0.434 | 87.43 | 33 |
| Standard errors (N = 2000) | | 0.40 | 0.19 | 0.24 | 0.33 | - | - | - |

Table 5

Hyperparameter configurations and model metrics for the attention based imputation model. Metrics were calculated based on a sample size of N = 2000 diary days. Furthermore, a mean standard error due to the sample size of 2000 diary days is given. Results in this work are generated with model configuration no. 6.

| No. | Transformer layers/D_model/Learning rate/Batch size | Sp rmse | Sd rmse | Ac rmse | Na mae | Cross-entropy Loss | Accuracy | CV Epochs |
|----------------------------|---|-------------|-------------|-------------|-------------|-----------------------|--------------|--------------|
| 1 | 1/64/0.001/256 | 0.58 | 0.39 | 0.50 | 0.50 | 0.469 | 86.97 | 158 |
| 2 | 4/64/0.001/256 | 0.58 | 0.39 | 0.44 | 0.62 | 0.436 | 87.32 | 22 |
| 3 | 4/64/0.001/64 | 0.57 | 0.38 | 0.36 | 0.90 | 0.436 | 87.35 | 8 |
| 4 | 4/64/0.001/128 | 0.63 | 0.39 | 0.46 | 1.05 | 0.438 | 87.31 | 12 |
| 5 | 4/64/0.0005/64 | 0.59 | 0.36 | 0.39 | 0.72 | 0.435 | 87.35 | 10 |
| 6 | 4/64/0.0005/128 | 0.49 | 0.39 | 0.39 | 0.66 | 0.431 | 87.41 | 37 |
| 7 | 4/14/0.0005/64 | 1.27 | 0.54 | 0.72 | 1.42 | 0.458 | 87.14 | 46 |
| 8 | 4/14/0.0005/128 | 0.84 | 0.60 | 0.61 | 0.65 | 0.459 | 87.14 | 47 |
| Standard errors (N = 2000) | | 0.40 | 0.19 | 0.24 | 0.33 | - | - | - |

Table 6

Comparative presentation of the socio-demographic composition of the MOP and TUD data sets. The calculated rmse of the aggregated state probabilities are calculated on the basis of the five aggregated states (home, outside, mobile (car driver), mobile (co driver), mobile (rest)). For the calculation of the rmse between the synthetic profiles and the MOP and TUD data, synthetic data with the same socio-demographic characteristics as in the comparison data sets were generated.

| Age | <18 | <26 | <36 | <51 | <61 | <71 | ≥71 |
|------------------|--------------|-------------|-------------|--------------|--------------|--------------|--------------|
| Samples MOP | 1971 (7.4%) | 1430 (5.4%) | 2288 (8.6%) | 6107 (22.9%) | 5132 (19.3%) | 5809 (21.8%) | 3873 (14.6%) |
| Samples TUD | 2169 (18.2%) | 1106 (9.3%) | 1140 (9.6%) | 4080 (34.2%) | 1654 (13.9%) | 1167 (9.8%) | 494 (4.1%) |
| rmse sp MOP/TUD | 4.0% | 3.8% | 2.3% | 1.9% | 2.2% | 2.7% | 2.8% |
| rmse sp syn./MOP | 1.7% | 1.6% | 1.3% | 0.9% | 1.1% | 0.7% | 0.9% |
| rmse sp syn./TUD | 3.9% | 4.2% | 2.1% | 1.7% | 1.9% | 2.6% | 2.7% |

| Job | - | Full time | Part time | Students | Training | No job | Pensioner |
|----------------------------------|------------|--------------|--------------|--------------|------------|-------------|--------------|
| Samples MOP | 212 (0.8%) | 8853 (33.3%) | 3627 (13.6%) | 2759 (10.4%) | 489 (1.8%) | 2052 (7.7%) | 8618 (32.4%) |
| Samples TUD | - | 3938 (33.0%) | 2599 (21.8%) | 2214 (18.6%) | 375 (3.1%) | 1184 (9.9%) | 1611 (13.5%) |
| rmse sp MOP/TUD | - | 2.2% | 2.5% | 2.9% | 3.8% | 2.4% | 2.4% |
| rmse sp syn./MOP | 2.8% | 1.1% | 1.1% | 1.3% | 4.0% | 1.0% | 0.7% |
| rmse sp syn./TUD | - | 2.1% | 2.0% | 3.6% | 4.69% | 2.1% | 2.1% |
| rmse sp MOP/TUD (entire sample) | - | - | - | 2.9% | - | - | - |
| rmse sp syn./TUD (entire sample) | - | - | - | 1.8% | - | - | - |
| rmse sp syn./MOP (entire sample) | - | - | - | 0.7% | - | - | - |

References

- [1] Abadi, Martin; Chu, Andy; Goodfellow, Ian; McMahan, H. Brendan; Mironov, Ilya; Talwar, Kunal; Zhang, Li, Deep Learning with Differential Privacy. In CCS '16: Proceedings of the 2016 ACM SIGSAC Conference on Computer and Communications Security, pp. 308–318, 2016. DOI: 10.1145/2976749.2978318.
- [2] D. Aerts, J. Minnen, I. Glorieux, I. Wouters, F. Descamps, A method for the identification and modelling of realistic domestic occupancy sequences for building energy demand simulations and peer comparison, *Build. Environ.* 75 (2014) 67–78, <https://doi.org/10.1016/j.buildenv.2014.01.021>.
- [3] Bahdanau, Dzmitry; Cho, Kyunghyun; Bengio, Yoshua (2015): Neural Machine Translation by Jointly Learning to Align and Translate. In Proceedings of International Conference on Learning Representations. Available online at <http://arxiv.org/pdf/1409.0473v7>.
- [4] Yoshua Bengio, Réjean Ducharme, Pascal Vincent, Christian Jauvin, A neural probabilistic language model, *J. Machine Learning Res.* 3 (2003) 1137–1155.
- [5] Lorenzo Bottaccioli, Santa Di Cataldo, Andrea Acquaviva, Edoardo Patti, Realistic Multi-Scale Modeling of Household Electricity Behaviors, *IEEE Access* 7 (2019) 2467–2489, <https://doi.org/10.1109/ACCESS.2018.2886201>.
- [6] Bowman, John (1998): The Day Activity Schedule Approach to Travel Demand Analysis. Dissertation. Cambridge, Massachusetts.
- [7] Brown, Tom B.; Mann, Benjamin; Ryder, Nick; Subbiah, Melanie; Kaplan, Jared; Dhariwal, Prafulla et al. (2020): Language Models are Few-Shot Learners, 5/28/2020. Available online at <http://arxiv.org/pdf/2005.14165v4>.
- [8] Caccia, Massimo; Caccia, Lucas; Fedus, William; Laroche, Hugo; Pineau, Joelle; Charlin, Laurent (2020): Language GANs Falling Short. In Proceedings of the Seventh International Conference on Learning Representation. Available online at <https://openreview.net/pdf?id=r110gyrKDS>.
- [9] Zhenghua Chen, Chaoyang Jiang, Lihua Xie, Building occupancy estimation and detection. A review, *Energy and Buildings* 169 (2018) 260–270, <https://doi.org/10.1016/j.enbuild.2018.03.084>.
- [10] Department for Transport (2020): 2019 National Travel Survey.
- [11] Destatis (2006): Zeitbudgeterhebung: Aktivitäten in Stunden und Minuten nach Geschlecht, Alter und Haushaltstyp. Zeitbudgets - Tabellenband 1. 2001/2002. Wiesbaden. Available online at https://www.statistischebibliothek.de/mir/receive/DEMonografie_mods_00003054.
- [12] Devlin, Jacob; Chang, Ming-Wei; Lee, Kenton; Toutanova, Kristina (2018): BERT: Pre-training of Deep Bidirectional Transformers for Language Understanding. Available online at <http://arxiv.org/pdf/1810.04805v2>.
- [13] Cynthia Dwork, Aaron Roth, The Algorithmic Foundations of Differential Privacy, *FNT in Theoretical Computer Science* 9 (3–4) (2014) 211–407, <https://doi.org/10.1561/04000000042>.
- [14] Jeffrey L. Elman, *Finding Structure in Time, Cognitive Science* 1990 (14) (1990) 179–211.
- [15] Eurostat (2000): Harmonized European Time of Use Survey.
- [16] David Fischer, Andreas Härtl, Bernhard Wille-Haussmann, Model for electric load profiles with high time resolution for German households, *Energy Build.* 92 (2015) 170–179, <https://doi.org/10.1016/j.enbuild.2015.01.058>.
- [17] Graeme Flett, Nick Kelly, An occupant-differentiated, higher-order Markov Chain method for prediction of domestic occupancy, *Energy Build.* 125 (2016) 219–230, <https://doi.org/10.1016/j.enbuild.2016.05.015>.
- [18] Goodfellow, Ian; Jean Pouget-Abadie; Mehdi Mirza; Bing Xu; David Warde-Farley; Sherjil Ozair et al. (2014): Generative Adversarial Nets. In Advances in neural information processing systems, pp 2672–2680.
- [19] Tim Hilgert, Michael Heilig, Martin Kagerbauer, Peter Vortisch, Modeling Week Activity Schedules for Travel Demand Models, *Transp. Res. Rec.* 2666 (1) (2017) 69–77, <https://doi.org/10.3141/2666-08>.
- [20] Hochreiter, S.; Schmidhuber, J. (1997): Long Short-Term Memory. Available online at <https://www.mitpressjournals.org/doi/10.1162/neco.1997.9.8.1735>, checked on 8/13/2020.136Z.
- [21] Sascha Hoogendoorn-Lanser, Nina T.W. Schaap, Marie-José OldeKalter, The Netherlands Mobility Panel: An Innovative Design Approach for Web-based Longitudinal Travel Data Collection, *Transp. Res. Procedia* 11 (2015) 311–329, <https://doi.org/10.1016/j.trpro.2015.12.027>.
- [22] Kalchbrenner, Nal; Grefenstette, Edward; Blunsom, Phil (2014): A Convolutional Neural Network for Modelling Sentences. Available online at <http://arxiv.org/pdf/1404.2188v1>.
- [23] Thomas Kaschub, *Batteriespeicher in Haushalten unter Berücksichtigung von Photovoltaik, Elektrofahrzeugen und Nachfragesteuerung. Dissertation.* (2017).
- [24] Eoghan McKenna, Michal Krawczynski, Murray Thomson, Four-state domestic building occupancy model for energy demand simulations, *Energy Build.* 96 (2015) 30–39, <https://doi.org/10.1016/j.enbuild.2015.03.013>.
- [25] Mikolov, Tomas; Chen, Kai; Corrado, Greg; Dean, Jeffrey (2013): Efficient Estimation of Word Representations in Vector Space. Available online at <http://arxiv.org/pdf/1301.3781v3>.
- [26] Paardekooper, Susana; Lund, Rasmus Sogaard; Mathiesen, Brian Vad; Chang, Miguel (2018): Heat Roadmap Europe 4. Quantifying the Impact of Low-Carbon Heating and Cooling Roadmaps.

- [27] Noah Daniel Pflugradt, Modellierung von Wasser und Energieverbräuchen in Haushalten, 2016. Available online at <http://nbn-resolving.de/urn:nbn:de:bsz:ch1-qucosa-209036>, checked on 4/12/2018.
- [28] José Luis Ramírez-Mendiola, Philipp Grünewald, Nick Eyre, Residential activity pattern modelling through stochastic chains of variable memory length, *Appl. Energy* 237 (2019) 417–430, <https://doi.org/10.1016/j.apenergy.2019.01.019>.
- [29] Ian Richardson, Murray Thomson, David Infield, A high-resolution domestic building occupancy model for energy demand simulations, *Energy Build.* 40 (8) (2008) 1560–1566, <https://doi.org/10.1016/j.enbuild.2008.02.006>.
- [30] Ian Richardson, Murray Thomson, David Infield, Conor Clifford, Domestic electricity use. A high-resolution energy demand model, *Energy Build.* 42 (10) (2010) 1878–1887, <https://doi.org/10.1016/j.enbuild.2010.05.023>.
- [31] Elizabeth Shove, Miika Pantzar, Matt Watson, *The Dynamics of Social Practice: Everyday Life and How it Changes*, SAGE Publications Ltd., 2012.
- [32] Koen Steemers, Geun Young Yun, Household energy consumption. A study of the role of occupants, *Build. Res. Information* 37 (5–6) (2009) 625–637, <https://doi.org/10.1080/09613210903186661>.
- [33] Ilya Sutskever, Training Recurrent Neural Networks. Dissertation, 2013.
- [34] Ilya Sutskever, Oriol Vinyals, V. Le, Quoc, Sequence to Sequence Learning with Neural Networks, 2014. Available online at <http://arxiv.org/pdf/1409.3215v3>.
- [35] Tjarko Tjaden, Joseph Bergner, Johannes Weniger, Volker Quaschnig, Repräsentative elektrische Lastprofile für Wohngebäude in Deutschland auf 1-sekündiger Datenbasis, 2015.
- [36] Jacopo Torriti, A review of time use models of residential electricity demand, *Renew. Sustain. Energy Rev.* 37 (2014) 265–272, <https://doi.org/10.1016/j.rser.2014.05.034>.
- [37] Jacopo Torriti, Understanding the timing of energy demand through time use data. Time of the day dependence of social practices, *Energy Res. Social Sci.* 25 (2017) 37–47, <https://doi.org/10.1016/j.erss.2016.12.004>.
- [38] Transport & Environment, Recharge EU. How many charge points will Europe and its member states need in the 2020s. With assistance of William Todts, 2020. Available online at <https://www.transportenvironment.org/sites/te/files/publications/01%202020%20Draft%20TE%20Infrastructure%20Report%20Final.pdf>.
- [39] Ashish Vaswani, Noam Shazeer, Niki Parmar, Jakob Uszkoreit, Llion Jones, Aidan N. Gomez, et al., Attention Is All You Need, 2017. Available online at <http://arxiv.org/pdf/1706.03762v5>.
- [40] Gordon Walker, The dynamics of energy demand: Change, rhythm and synchronicity, *Energy Res. Social Sci.* 1 (2014) 49–55, <https://doi.org/10.1016/j.erss.2014.03.012>.
- [41] Weiß, Christine; Chlond, Bastian; Hilgert, Tim; Vortisch, Peter (2016): Deutsches Mobilitätspanel (MOP) - wissenschaftliche Begleitung und Auswertungen, Bericht 2014/2015. Alltagsmobilität und Fahrleistung, checked on 10/22/2019.
- [42] Urs Wilke, Probabilistic Bottom-up Modelling of Occupancy and Activities to Predict Electricity Demand in Residential Buildings, 2013, PHD Thesis.
- [43] Ronald J. Williams, David Zipser, A learning algorithm for continually running fully recurrent neural networks, *Neural Comput.* 1 (2) (1989) 270–280.
- [44] Thomas Wolf, Lysandre Debut, Victor Sanh, Julien Chaumond, Clement Delangue, Anthony Moi, et al. HuggingFace's Transformers: State-of-the-art Natural Language Processing, 2020. Available online at <http://arxiv.org/pdf/1910.03771v5>.
- [45] Yonghui Wu, Mike Schuster, Zhifeng Chen, V. Le, Norouzi Quoc, Macherey Mohammad, Wolfgang et al., Google's Neural Machine Translation System: Bridging the Gap between Human and Machine Translation, 2016. Available online at <http://arxiv.org/pdf/1609.08144v2>.
- [46] Y. Yamaguchi, S. Yilmaz, N. Prakash, S.K. Firth, Y. Shimoda, A cross analysis of existing methods for modelling household appliance use, *J. Build. Perform. Simul.* 12 (2) (2019) 160–179, <https://doi.org/10.1080/19401493.2018.1497087>.
- [47] Selin Yilmaz, Steven K. Firth, David Allinson, Occupant behaviour modelling in domestic buildings: the case of household electrical appliances, *J. Build. Perform. Simul.* 10 (5–6) (2017) 582–600, <https://doi.org/10.1080/19401493.2017.1287775>.
- [48] Tom Young, Devamanyu Hazarika, Soujanya Poria, Erik Cambria, Recent Trends in Deep Learning Based Natural Language Processing, 2017. Available online at <http://arxiv.org/pdf/1708.02709v8>.
- [49] Lantao Yu, Weinan Zhang, Jun Wang, Yong Yu, SeqGAN: Sequence Generative Adversarial Nets with Policy Gradient, 2017, Available online at <https://www.nature.com/articles/nature16961.pdf>.
- [50] D. Zumkeller, B. Chlond, Dynamics of Change: Fifteen-Year German Mobility Panel. Presented at 88th Annual Meeting of the Transportation Research Board. Washington, D.C., 2009.

Paper B

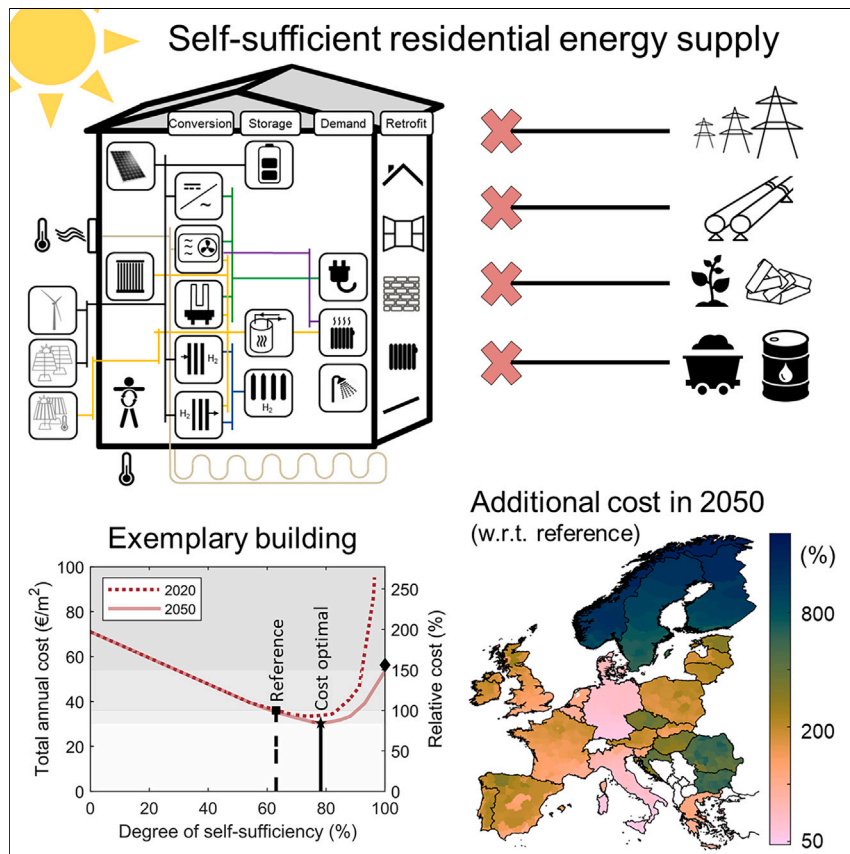
Two million European single-family homes could abandon the grid by 2050

Reference

Kleinebrahm, Max; Weinand, Jann Michael; Naber, Elias; McKenna, Russell; Ardone, Armin; Fichtner, Wolf (2023b): Two million European single-family homes could abandon the grid by 2050. In *Joule* 7 (11), pp. 2485–2510. DOI: [10.1016/j.joule.2023.09.012](https://doi.org/10.1016/j.joule.2023.09.012).

Article

Two million European single-family homes could abandon the grid by 2050



Max Kleinebrahm, Jann Michael Weinand, Elias Naber, Russell McKenna, Armin Ardone, Wolf Fichtner

max.kleinebrahm@kit.edu

Highlights

Evaluation of self-sufficiency potential for 41 million European homes

Large-scale optimization and regression on high-performance computing clusters

Current technical conditions allow 53% of homes to become energy self-sufficient

Two million homes could go off-grid by paying a premium of up to 50% in 2050

In light of diminishing capital costs for renewables and rising energy procurement expenses, we investigate the viability of energy self-sufficiency for 41 million European single-family homes. Our findings spotlight regions with low seasonal variations, such as Spain, and high household electricity prices, such as Germany, as particularly suited for off-grid solutions. Remarkably, with a willingness to pay a premium of up to 50%, two million homes could abandon the grid by 2050, challenging conventional beliefs in large, interconnected energy systems.

Article

Two million European single-family homes could abandon the grid by 2050

Max Kleinebrahm,^{1,5,*} Jann Michael Weinand,² Elias Naber,¹ Russell McKenna,^{3,4} Armin Ardone,¹ and Wolf Fichtner¹

SUMMARY

Rising energy procurement costs and declining capital costs for renewable technologies are provoking interest in self-sufficiency for individual buildings. In this study, we evaluate the potential of self-sufficient energy supply for 41 million freestanding single-family buildings under current and future (2050) conditions. We identify 4,000 representative buildings, calculate weather-robust cost-minimal energy systems, and transfer the optimization results to the entire European building stock. Our analyses show that buildings in regions with low seasonality and high electricity procurement costs have a high potential for self-sufficiency. Under current techno-economic conditions, 53% of the 41 million buildings are technically able to supply themselves independently from external infrastructures by only using local rooftop solar irradiation, and this proportion could increase to 75% by 2050. By paying a premium of up to 50% compared with grid-dependent systems with electrified heat supplies, building owners could make over two million buildings fully energy self-sufficient by 2050.

INTRODUCTION

In Europe, self-sufficient off-grid energy supply is transitioning from a niche concept, mostly reserved for special applications or remote areas, to a potentially mainstream idea. Rising energy procurement costs and decreasing capital costs for renewable energy technologies have fostered recent trends toward individual and independent energy supply systems across the residential sector. In the design of these systems, non-monetary criteria such as high shares of renewables, increased self-control through independence from rising energy carrier prices, or rejection of the use of nuclear and carbon-intensive fossil energy, potentially from regions with questionable governance and values, play an increasingly important role.^{1–3} These priorities could even be reinforced by disruptive events such as the recent energy crisis, with high energy carrier prices due to a lack of fossil fuel supplies, which show that existing energy system structures with a high dependence on imports must be reconsidered.⁴ In addition to the perceived financial benefits, the pursuit of self-sufficiency most influences households' intentions to purchase renewable energy technologies.²

The very strong decline in photovoltaic (PV) system prices has led to grid parity in many European countries,^{5–9} which refers to the point at which the cost of producing electricity from renewable sources is less than or equal to the cost of purchasing electricity from the grid. Furthermore, battery costs are predicted to decrease further in the future, leading to improved economic performance among stationary battery systems.^{10–12} The increasing economic viability of local energy generation

CONTEXT & SCALE

Economies of scale and temporal smoothing effects lead to the belief that widespread, highly interconnected energy systems come with the lowest cost. However, economies of scale are less pronounced with renewable technologies. Organizational and regulatory complexities increase with increasing system size, and heat is typically not transported over long distances.

Having this in mind, we analyze the technical and economic potential of 41 million single-family homes in Europe for off-grid energy self-sufficiency under current and future (2050) conditions. We find a pronounced potential for off-grid buildings in regions with low seasonality (e.g., Spain) and high electricity prices (e.g., Germany). If building owners are willing to pay a premium of up to 50%, two million buildings could abandon the grid by 2050.

will lead to a multitude of consumers meeting most or all of their energy demand on their own and only using the grid as a back-up when local energy supply is not available. However, partially self-sufficient building energy systems put an even greater strain on the electrical grid than traditional end-of-pipe customers.^{13,14} Fully self-sufficient systems, on the other hand, reduce the demand for centralized generation and transmission capacity but currently come with high cost and low stability due to the lack of scaling effects.^{13,15–17} By using cost-effective renewable resources through large centralized power plants (economies of scale) in highly interconnected energy systems, temporal and spatial fluctuations between supply and demand can be balanced without the need for massive dispatchable capacities (smoothing effects).¹⁶ The choice of the optimal degree or scale of self-sufficiency thus represents a complex socio-techno-economic question.¹³ Although trade-offs between geographic scale, cost, and infrastructure requirements for 100% renewable electricity systems in Europe have been discussed on continental, national, and regional scales,¹⁶ this study presents the first large-scale analysis of the European potential for self-sufficiency among all 41 million freestanding single-family buildings (SFBs).

Real-world examples and academic case studies indicate that from a technical point of view, energy self-sufficient residential buildings are feasible even under suboptimal conditions for renewable energy sources.^{18–22} From an economic point of view, the decreasing marginal utility with higher degrees of self-sufficiency precludes the economic operation of energy self-sufficient residential buildings in central Europe under current energy-political framework conditions.^{19,20} However, the use of certain technologies and measures such as hydrogen-storage (H₂-storage) options,¹⁹ efficiency measures,¹⁸ or demand-side adjustments²¹ can reduce the exponentially increasing system costs at high degrees of self-sufficiency. Although self-sufficient residential buildings can already be cost-competitive in Australia if the occupants are willing to make small changes to their consumption patterns, households in temperate climates can become cost-competitive in the future, depending on energy storage and procurement prices.^{20,21}

Multiple studies have analyzed the possibility of “leaving the grid” or “living off-grid” using PV-battery systems.^{17,21,23–28} Research on European residential buildings mostly concludes that PV-battery systems must be drastically oversized to reach degrees of self-sufficiency above 80%, and it is therefore advantageous to preserve grid connections but minimize electricity purchasing and optimize feed-in.^{17,23,27} Similar work on residential buildings in Australia and the United States has shown that grid defection could be economically viable under certain electricity tariff schemes, especially if occupants are willing to adjust their consumption patterns.^{21,24} However, existing studies tend to be limited to PV-battery systems to cover electrical demand and thereby neglect the synergies of an integrated consideration of electrical and thermal energy demands.^{17,21,23–27,29} On the other hand, studies that follow an integrated approach are limited to typical residential buildings and therefore not suitable for deriving representative statements.^{19,20,22,30,31} A large-scale study is required in order to provide comprehensive insights and comparability across the building stocks of different countries, climates, building types, and household consumption characteristics. We therefore explore the techno-economic potential of all 41 million freestanding owner-occupied SFBs in the EU-27, United Kingdom (UK), and Norway (NO) for off-grid energy self-sufficiency under current (2020) and future (2050) techno-economic framework conditions.

As a first step, based on a spatial microsimulation with economic, environmental, and physical data, a synthetic building stock containing about 41 million

¹Institute for Industrial Production (IIP), Karlsruhe Institute of Technology, Karlsruhe, Germany

²Forschungszentrum Jülich GmbH, Institute of Energy and Climate Research – Techno-economic Systems Analysis (IEK-3), Jülich, Germany

³Chair of Energy Systems Analysis, Institute of Energy and Process Engineering, Department of Mechanical and Process Engineering, ETH Zürich, Zürich, Switzerland

⁴Laboratory for Energy Systems Analysis, Paul Scherrer Institute, Villigen, Switzerland

⁵Lead contact

*Correspondence: max.kleinebrahm@kit.edu
<https://doi.org/10.1016/j.joule.2023.09.012>

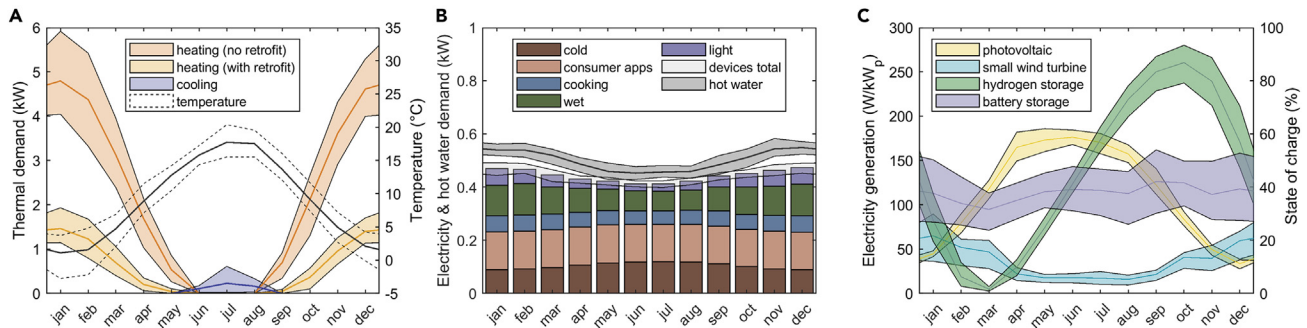


Figure 1. Visualization of the seasonal variation of energy demand and supply of a representative four-person single-family house in Germany

The ranges shown in all figures are based on simulations over 30 historical weather years (1991–2020) and represent the 10%/90% quantile and mean. In (A), the useful energy demand for space heating and cooling is presented, whereby a distinction is made between two typical retrofit states. In (B), the device category-specific electricity and domestic hot water demand is shown. In (C), the normalized PV and small wind turbine power profiles are displayed together with the state of charge of the battery and pressurized hydrogen storage. Although the normalized power profiles are used as inputs for the energy system optimization, the storage levels represent an optimization result.

freestanding owner-occupied SFBs was created. Subsequently, a clustering approach was applied to identify representative SFBs across Europe. Self-sufficient, robust energy systems of up to 4,000 buildings were then designed in parallel in individual energy system optimizations on high-performance computing clusters for multiple weather years. Finally, we combined the results of the previous steps to train a surrogate model to approximate the function between the aggregate energy system optimization input and key output parameters. This enables the results of the energy system optimizations to be transferred to the entire synthetic building stock with a high degree of accuracy and without the use of excessive computational resources.

RESULTS

Toward 100% energy self-sufficient buildings

The energy systems of self-sufficient residential buildings must guarantee supply security at any point in the year. The useful energy demand in residential buildings consists of space heating and cooling, domestic hot water, and energy service demands for lighting, cooking, and other services. Although the ambient temperature correlates positively with electrical demand for cold appliances and the demand for space cooling, there is a negative correlation with space heating, lighting, and domestic hot water demand (Figures 1A and 1B). At an exemplary German location, the seasonal feed-in profiles of PV and small wind turbines complement each other well (Figure 1C). However, a small wind turbine has significantly fewer full load hours compared with a PV system and significantly higher costs per installed unit of capacity. To compensate for the seasonal mismatch between electricity generation from PV systems and energy demand, various investment options, such as retrofitting measures to reduce space heating demand, seasonal hydrogen storage technologies, or complementary generation technologies, can be exploited. The optimal selection and dimensioning of the investment options are performed by minimizing the system's total annual cost (TAC). In order to be able to compare costs between different SFBs, the TAC is normalized with the living area.

At very low energy carrier prices, it is advantageous to import all of the energy required to meet the building energy service demand. Very high energy carrier prices lead to a minimization of energy imports and useful energy demand through efficiency measures and maximization of self-generation. Figure 2 shows the transition

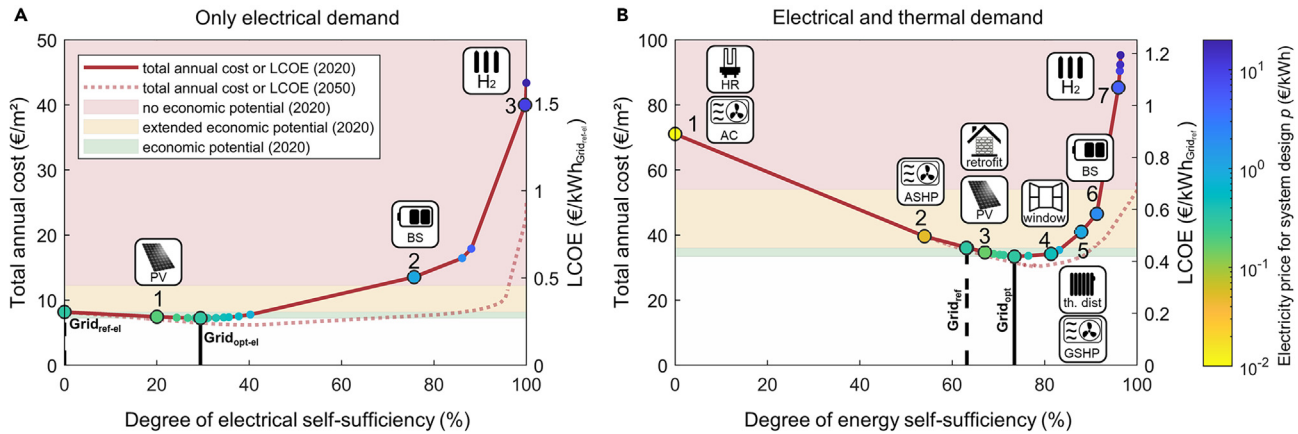


Figure 2. Visualization of the relationship between energy system costs and the degree of self-sufficiency for a representative German building Although in (A), only the demand for electrical appliances is considered, in (B), the demand side is extended by the heating demand for domestic hot water and the space heating demand to maintain an indoor temperature between 20°C and 26°C. Multiple energy system optimizations are carried out in which the electricity price used for the determination of the energy system design is successively increased (from $p = 0.01$ €/kWh to $p = 20$ €/kWh). In (A), a reference system with 100% electricity grid supply is used at $p_{-0} = 0.01$ €/kWh for calculating the degree of self-sufficiency; in (B), an electrical heating rod is installed together with an air conditioner. Each colored point represents the result of an energy system optimization given the electricity purchasing price shown in the color bar. The associated technology choices and sizes of the highlighted optimized systems can be found in Tables S4 and S5. The red lines represent the total annual system costs, which are calculated based on a constant electricity purchasing price of $p_{DE} = 0.3$ €/kWh instead of the electricity price p used in the energy system optimization. Each time the energy system in 2020 is expanded by a technology, the corresponding technology is displayed together with a reference number. Costs are normalized using the building living area or the total annual electricity demand of the Grid_{ref(-el)} system. (PV, photovoltaic; BS, battery storage; H₂, hydrogen system; HR, heating rod; AC, air conditioning; ASHP/GSHP, air/ground source heat pump; th. dist, new thermal distribution system).

between these two extremes for the representative German SFB. The optimal degree of self-sufficiency (DSS) is defined according to Equation 1, in which import_p represents the imported quantity of electricity at a given price p . Only electricity imports are permitted in the energy systems shown in Figure 2, due to the strong electrification trend,³² in order to not have to weigh between energy carriers and for the sake of clarity.

$$\text{DSS}_p = 1 - \frac{\text{import}_p}{\text{import}_{p \rightarrow 0}} \quad (\text{Equation 1})$$

The cost-optimal degrees of self-sufficiency of the examined building in Germany (DE) were 29% in 2020 and 40% in 2050, as long as only the electrical demand for household appliances is considered (Figure 2A). This means that 29% or 40% of the annual electricity demand of the building is supplied by a PV plant, and excess electricity is fed into the grid. Higher degrees of electrical self-sufficiency led to a relatively strong increase in costs in 2020 compared with 2050, which levels off significantly due to the expected increase in the efficiency of battery production. Compared with the energy system without local electricity self-generation, the costs of grid-independent systems were 5.3 times higher in 2020 and could be 3.1 times higher in 2050.

If the thermal demand is also taken into account, the cost-optimal degrees of energy self-sufficiency are 73% in 2020 and 78% in 2050 (see Figure 2B). This is an interesting result, as in most other studies only the electrical demand is considered^{14,17,27} and therefore, in principle, much lower optimal degrees of self-sufficiency are assumed for decentralized energy systems. This implies that the optimal DSS depends strongly on the system under consideration and the definition of the

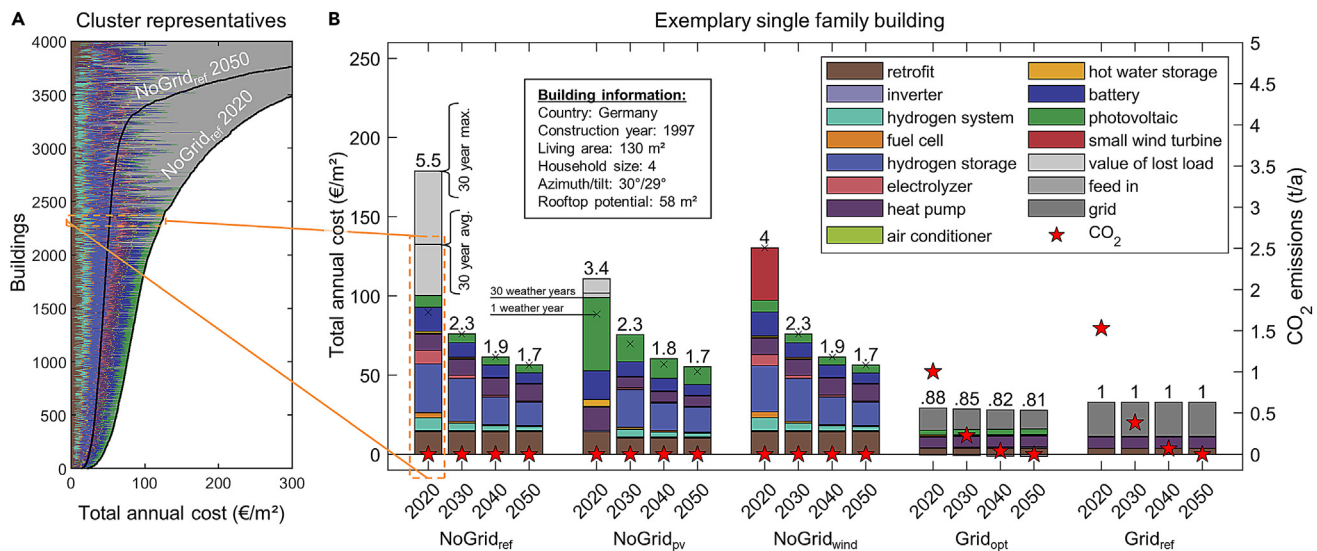


Figure 3. Cost composition of residential energy supply systems

The left-hand panel (A) depicts the energy system cost composition for 4,000 representative single-family buildings in the EU-27, United Kingdom, and Norway for the NoGrid_{ref} scenario. The right-hand panel (B) presents the progression of the energy system cost composition of a representative SFB in Germany over time until 2050 for all scenarios.

Relevant characteristics of the residential building, the composition of the total annual system costs, and energy system-related CO₂ emissions are presented. System costs in the NoGrid scenarios are calculated using 30 years of historical weather, with the black crosses indicating the system costs (value of lost load excluded) if only 1 weather year is used for the system design. Relative cost differences with respect to the Grid_{ref} scenario are shown as numbers above the bars. Under the techno-economic framework conditions in 2020, load is shed in the Grid_{ref} and Grid_{pv} scenarios, thereby a distinction is made between the average (avg.) and maximum (max.) value of lost load over the 30 weather years.

DSS. In this study, the system with maximum dependence on the electricity grid is the energy system that results when the electricity price approaches zero (see Equation 1 and, e.g., Figure 2B, system no. 1). This system has a DSS of 0%, consists of a heating rod and an air conditioner, and is still in the initial state of construction (no retrofit measures). Although this system is anything but cost-optimal, the TAC in 2020 is still lower than that with 100% self-sufficiency. Under rising electricity purchase prices, an air source heat pump is first installed before investments in retrofit measures and technologies such as PV systems and ground-source heat pumps, in conjunction with a renewal of the heat distribution system, become economical. Finally, battery and hydrogen storage systems are built to increase the DSS from 87% to 96% in 2020 and from 85% to 100% in 2050, which is associated with a significant increase in TAC. The less pronounced cost increase in 2050 compared with 2020 can primarily be attributed to the future efficiency developments of hydrogen and battery storage systems. Although battery storage is used primarily as a diurnal storage medium throughout the year to reach a DSS of 91%, the hydrogen system is used for seasonal storage in order to provide energy, mainly in winter for space heating, either directly by using heat from the fuel cell or indirectly by converting electricity into heat in a heat pump. Due to the still low degree of maturity of hydrogen storage systems in 2020 and the associated high costs, a DSS increase from 91.3% to 96.4% (1.4 MWh) results in mean additional costs of 4.5 €/kWh. The described results relate to one representative German SFB (see Figure 3 for more information) and differ from building to building with regard to the skewness of the U-shape (the red line in Figure 2B). Older buildings, for example, tend to have an even more pronounced right skewness of the U-shape to higher optimal degrees of energy self-sufficiency, as a large share of the space heating demand can be saved through retrofit measures at a low cost.

Table 1. Overview of energy system design scenarios and respective energy system technology options

| No. | Scenario | Electrical grid ^a | Freestanding PV and ST | Small wind turbines | Rooftop PV and ST, battery, H ₂ | Retrofit, P2H, heat storage | Diesel generator | Demand |
|----------------|---------------------------|------------------------------|------------------------|---------------------|--|-----------------------------|------------------|----------|
| 1 | NoGrid _{ref} | – | – | – | ✓ | ✓ | – | el., th. |
| 2 ^b | NoGrid _{pv} | – | ✓ | – | ✓ | ✓ | – | el., th. |
| 3 ^b | NoGrid _{wind} | – | – | ✓ | ✓ | ✓ | – | el., th. |
| 4 | Grid _{opt} | ✓ | – | – | ✓ | ✓ | – | el., th. |
| 5 | Grid _{ref} | ✓ | – | – | – | ✓ | – | el., th. |
| 6 | NoGrid _{ref-el} | – | – | – | ✓ | – | – | el. |
| 7 ^b | NoGrid _{pv-el} | – | ✓ | – | ✓ | – | – | el. |
| 8 ^b | NoGrid _{wind-el} | – | – | ✓ | ✓ | – | – | el. |
| 9 | NoGrid _{gen-el} | – | – | – | ✓ | – | ✓ | el. |
| 10 | Grid _{opt-el} | ✓ | – | – | ✓ | – | – | el. |
| 11 | Grid _{ref-el} | ✓ | – | – | – | – | – | el. |

Scenarios 1–3 cover the energy demand completely independently of external energy infrastructures. In scenario 2, freestanding PV and ST can be installed next to buildings, in addition to the restricted rooftop PV and ST potential. Scenario 3 considers the option to install a small wind turbine. In scenario 4, electricity can be purchased and fed back into the grid and investments in local self-generation technologies are considered. Scenario 5 serves as the reference scenario in which all of the electricity demand is covered by the electricity grid and electricity self-generation is excluded. Scenarios 6–11 exclude the thermal energy demand for space heating and domestic hot water and only focus on covering the electricity demand for household appliances and can be found in the [supplemental information](#) (ST, solar thermal; P2H, power-to-heat; el, electricity; th., thermal).

^aElectricity can be obtained for the national household electricity price⁶⁴ and fed into the grid for a feed-in premium of 3 €-cents/kWh (based on PV-weighted mean of wholesale electricity prices¹⁰⁷). A constant household electricity price is assumed between 2020 and 2050.

^bScenarios 2, 3, 7, and 8 are presented to analyze the impact of a restricted rooftop potential—as the only energy source—on the economic potential of self-sufficiency. The potential for freestanding PV and ST and small wind turbines is not restricted by the consideration of local land use conflicts or other site-specific obstructions. Consequently, the results of these scenarios represent an upper potential limit, which would be lower if site-specific restrictions were taken into account.

Even if a 100% self-sufficient system is not cost-optimal, the question arises as to where such systems can be economically achieved, especially considering a willingness to pay for self-sufficiency. Therefore, [Figure 2](#) presents the (extended) economic potential. The economic potential is defined by the Grid_{opt} and Grid_{ref} systems (see [Table 1](#)).

- Grid_{opt}: Cost-optimal energy system taking into account all technology options and electricity grid exchange (lower limit of economic potential).
- Grid_{ref}: Similar to Grid_{opt}, but self-generation of electricity is excluded (upper limit of economic potential).
- NoGrid_{ref}: Similar to Grid_{opt}, but without electricity grid exchange.

An SFB has a technical potential for self-sufficiency if the entire energy demand for electrical appliances, domestic hot water, and space heating for maintaining an indoor temperature between 20°C and 26°C can be covered at every hour of the year by only using the local rooftop renewable potential as an energy source.

Cost-optimal energy system designs for self-sufficient buildings

We investigate energy systems for self-sufficient SFBs across three energy system design scenarios (see scenarios 1–3 in [Table 1](#)) and changing techno-economic framework conditions between 2020 and 2050. All of the following results refer to full self-sufficiency considering electric and thermal demands. For some of the SFBs, it is not possible or very expensive to cover the energy demand for every hour of the year. In order to prevent the energy system model from being infeasible or configuring oversized energy systems, shedding the load for an assumed value of lost load of 10 €/kWh³³ is possible. Intermediate results of the energy system design process, the demonstration of the robustness of the systems against multiple weather years, sensitivity analysis regarding future price, weather, building stock,

and energy demand developments, and detailed results for scenarios 6–11 can be found in the [supplemental information](#).

System costs of self-sufficient residential buildings could approximately halve by 2050 compared with 2020 (Figure 3A). The TAC of a representative self-sufficient German SFB (NoGrid scenarios) exceeds the costs of those systems with electricity grid connections (Grid scenarios) at all times (Figure 3B). However, although the system costs of the NoGrid scenarios decrease over time due to assumed future technology efficiency developments, the costs of the Grid_{ref} scenario remain constant due to an assumed constant electricity purchasing price for household customers and no assumed price changes for construction materials. This leads to relative cost reductions from 5.5 times higher costs in 2020 to only 1.7 times higher costs in 2050.

In all NoGrid scenarios for the representative German SFB, the demand for space heating is maximally reduced by selecting advanced insulation measures. In order to balance the seasonal mismatch between electricity generation from PV and the remaining space heating demand, hydrogen storage systems are installed. Only in the NoGrid_{pv} scenario in 2020, no hydrogen system is used, and over 37 kW_p of freestanding PV is installed next to the SFB. The area consumption of the freestanding PV system would be more than 10 times higher than the building floor area.³⁴ Consequently, the NoGrid_{pv} scenario represents a rather hypothetical scenario that illustrates the relevance of space restrictions for PV systems. Compared with the NoGrid_{pv} and NoGrid_{wind} scenarios, the capacity to generate electricity is limited in the NoGrid_{ref} scenario by the available rooftop potential. Therefore, it is not technically possible to cover the entire energy demand under the techno-economic framework conditions in 2020, and the load is shed with a value of lost load of 10 €/kWh. On average, 3.8% of the total annual electricity demand is shed over the 30 weather years considered (at most 8.3%). Due to assumed technological developments of PV, battery, and hydrogen storage systems, however, it could be possible to cover the entire energy demand in the NoGrid_{ref} scenario from 2030 onward. The projected increase in the PV efficiency means that more electricity can be provided on the same roof area. Furthermore, projected improvements in conversion efficiencies of electrolyzers and fuel cells make long-term energy storage more efficient. In the NoGrid_{pv} scenario, in 2020, it is cheaper to shed the load for 10 €/kWh than to dimension the freestanding PV or battery system larger and thus supply an additional kWh of energy demand. These marginal costs of supplying an additional kWh are significantly lower with a hydrogen-based system since the fixed system costs of the hydrogen system are high compared with the variable capacity-dependent costs. If the building owner had the opportunity of setting up a small wind turbine, all energy demands could already be covered in 2020. If the building is instead still connected to the electricity grid (Grid_{opt}), investments in a PV system and heat pump in conjunction with insulation measures are economically beneficial and can lead to 12%–19% lower costs in comparison to the Grid_{ref} scenario, in which no local self-generation is considered.

Potentials for self-sufficient buildings across Europe

In 2020, 53% of the 41 million examined SFBs in Europe could technically achieve energy self-sufficiency without shedding load, and this share could increase to about 75% by 2050 (NoGrid_{ref} scenario; see Figure 4). Especially in the northern regions of Europe such as Finland (FI), NO, and Sweden (SE), the technical potential is low due to the increased seasonal mismatch of heat demand and solar irradiation. A higher potential exists in regions with high solar irradiation (e.g., Malta [MT], Cyprus [CY],

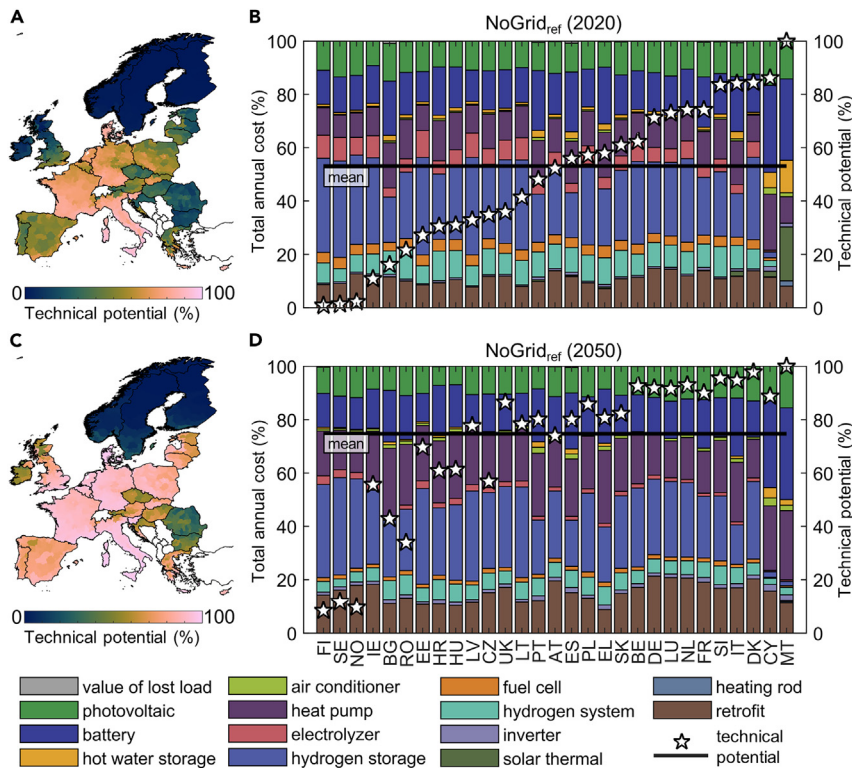


Figure 4. Technical potential for self-sufficient single-family buildings in Europe

Visualization of the share of technically feasible self-sufficient single-family buildings in NUTS3 regions in Europe for 2020 (A) and 2050 (C) for the NoGrid_{ref} scenario. In the right-hand parts of the figure (B) and (D), the building-weighted average composition of the total annual cost by energy system components and value of lost load is shown together with the country-specific technical potential.

Each technically feasible self-sufficient residential building of the synthetic building stock is assigned the TAC composition of the corresponding cluster representative, and based on that, the average composition per country is calculated. Countries are sorted in ascending order of their share of technical potential in 2020.

Italy [IT], Spain [ES]), and/or areas with large rooftop potential for solar rooftop systems (e.g., Denmark [DK], Slovenia [SI], the Netherlands [NL], France [FR], Luxembourg [LU], or DE). The increasing share in 2050 can be attributed to the anticipated increases in PV efficiency, which can lead to higher electricity yields. Improvements in demand-side efficiency are not assumed, and developments in storage technologies have no impact in this instance, although future increases in conversion efficiency are assumed for the hydrogen system. However, these improvements have no impact on the technical potential, as the battery system has a higher round-trip efficiency and is therefore advantageous as long as no economic factors are taken into account. If only the electrical demand for household devices is considered on the demand side (NoGrid_{ref-el}), 94% of the examined SFBs could technically achieve self-sufficiency in 2020, and this share could increase to about 98% in 2050.

The ratio of seasonal hydrogen storage capacity to short-term battery storage capacity in the cost-optimal energy systems of self-sufficient buildings increases with increasing latitude, with buildings in MT and CY requiring mostly short-term battery storage solutions (see Figure 4). The lowest TAC of 14 €/m² in 2020 (10 €/m² in 2050) was achieved for a building with four residents and 220 m² of living

space in MT (see [Figure 3A](#)). With only 174 heating degree days on average between 1991 and 2020 and a yearly global horizontal irradiation (GHI) of 1,830 kWh/m², a PV system (7 kW_p) in combination with a battery (17 kWh), a small heat pump, an air conditioner, and a hot water storage tank are sufficient to provide the thermal and electrical energy supplies of the SFB. The SFB with the highest TAC among the representative buildings that supply themselves without shedding load was a very small SFB (36 m² living space) with two residents located in Romania. The TAC was 205 €/m² in 2020 (89 €/m² in 2050). A hybrid battery and hydrogen storage system (battery: 13 kWh, H₂-storage: 1,800 kWh_{LHV}) in combination with a PV system (7 kW_p), heat pump, and hot water storage tank in conjunction with advanced retrofit measures ensure the provision of electricity and thermal comfort.

The expansion of the energy supply system via freestanding PV and a small wind turbine can significantly reduce the TAC, especially in 2020. Additional space for freestanding PV in the NoGrid_{pV} scenario was used by over 92% of SFBs in 2020 with an average of 18 kW_p (75% in 2050 with 6 kW_p) and could help reduce costs by over 30% (20% in 2050) on average. Although the cost reductions are fairly small in countries such as DE, FR, and IT, higher cost reductions could be achieved in countries with a low technical potential for self-sufficient residential buildings such as NO (see [Figure 4](#)). In the NoGrid_{wind} scenario, the possibility of generating electricity via a small wind turbine is used by 30% of the SFBs in 2020 (12% in 2050) to complement the electricity feed-in from PV. Thereby, costs could be reduced by 18% on average in 2020 (24% in 2050) when installing a small wind turbine compared with the NoGrid_{ref} scenario. In countries with good conditions for small wind turbines, such as the UK, up to 77% of the energy systems in 2020 were equipped with a small wind turbine. The average wind speed at the locations of the SFBs with small wind turbines at 10 m above ground level was 3.6 m/s (in the UK, 4.3 m/s).

Although many European SFBs can technically achieve energy self-sufficiency, the economic feasibility in 2050 is only given for 5% of the buildings considered if the owners are willing to pay a premium compared with the reference system (see [Figure 5](#)). SFBs with a lower TAC than in the Grid_{ref} scenario are considered to have economic potential. Additionally, SFBs with a maximum 50% higher TAC than in the Grid_{ref} scenario are regarded as having an extended economic potential, as building owners could be willing to pay a premium to be self-sufficient from external infrastructures and supply the building energy demand on the basis of renewable energy.² The geospatial distribution of the mean TAC of all SFBs per NUTS3 area for the Grid_{ref} and NoGrid_{ref} scenarios can be found in [Figures 5A](#) and [5B](#).

On average, the TAC in Europe amounts to 27 €/m² in the Grid_{ref} scenario in 2020 and 2050. Due to the low electricity price for household customers in MT (13.5 €-cents/kWh) and the small number of heating degree days, the costs of the reference system are the lowest of all countries considered, with a mean value of 11 €/m². The highest TAC arises in the northern countries of NO, FI, and SE due to the high number of heating degree days (>3,500) in combination with an above-average demand for electricity, followed by the countries with the highest household electricity prices of 28–31 €-cents/kWh of DK, Belgium (BE), and DE.

The mean TAC for the self-sufficient building energy systems in Europe amount to 175 €/m² (2020) and 97 €/m² (2050), respectively, or 84 €/m² (2020) and 48 €/m² (2050) if only buildings are considered that cover 100% of their demand

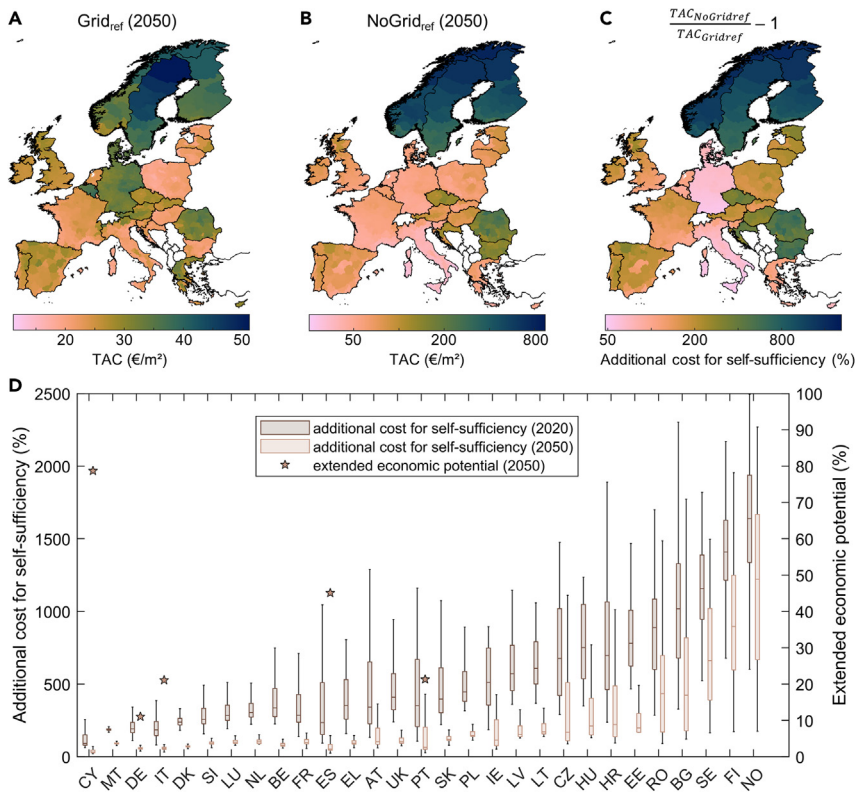


Figure 5. Economic potential and cost of self-sufficient single-family buildings in Europe

(A) and (B) show the geospatial distribution of the mean total annual system cost (TAC) for all NUTS3 regions for the $Grid_{ref}$ (A) and the $NoGrid_{ref}$ (B) scenario. The mean percentage share of additional cost for self-sufficient energy supply per NUTS3 region compared with the $Grid_{ref}$ scenario can be found in (C). In (D), the distributions of the additional cost for self-sufficiency by country for every single SFB are shown for the $NoGrid_{ref}$ scenario in 2020 and 2050. Countries are sorted by mean additional cost. The share of buildings per country with additional cost < 50% is considered extended economic potential and is represented by stars (only shares > 0% are shown).

without shedding load. The cost reduction by 2050 is due to the assumed technological efficiency increases and cost degeneration effects. The system costs are particularly low in the southern regions of Europe that feature high solar irradiation and high PV rooftop potential (e.g., MT, IT, or CY). Although MT has the lowest average costs among all of the countries considered, it has no (extended) economic potential due to the low electricity purchasing price. CY, on the other hand, with slightly higher costs on average, in combination with an electricity price of 22 €-cents/kWh, has the highest country-specific extended economic potential (81% in 2050). Despite the fact that DE has inferior solar irradiation conditions to its southern neighbors, it has a high extended economic potential, which is primarily driven by the relatively high electricity purchasing cost of the reference system and high PV rooftop potential of the detached SFBs analyzed.

The sensitivity analysis (see section sensitivity analysis in the [supplemental information](#)) shows that the extended economic potential presented is heavily dependent on technological developments, especially for small-scale hydrogen systems. Although a 20% cost increase of the hydrogen system in 2050 would lead to a reduction of the extended economic potential to 2%, a 20% cost reduction would lead to an increase of the potential to over 15% of the investigated SFBs.

DISCUSSION

Our results show that a successful, cost-optimal PV-based self-sufficient energy supply system for buildings in central Europe will consist of a combination of short-term battery storage and a long-term seasonal hydrogen storage system. These results are in accordance with previous studies on individual energy self-sufficient residential buildings.^{19,20,22,30,31} Furthermore, the possibility of self-sufficiency under sub-optimal conditions in Finland³⁰ can be confirmed by the results of our study. However, we show that in general, the techno-economic potential of self-sufficient buildings in Finland is low, even under the future techno-economic conditions of 2050. The main reason for the low potential lies in the strong seasonal mismatch between solar irradiation and heat demand, as well as the exclusion of auxiliary heating with, e.g., a wooden stove in our work. Others¹⁹ have shown that for a typical building in Germany, the costs of an energy self-sufficient system with H₂-storage and Li-ion battery systems compared with a grid-connected system are about twice as high in 2030, which also corresponds to our results. Although further costs could be saved by considering liquid organic hydrogen carriers (technology readiness level [TRL]: 5–7³⁵) and reversible solid oxide cell-based (TRL: 4–5^{36,37}) systems,¹⁹ these technologies are not considered in our work, as the current TRL is regarded as being too low for large-scale deployment. Similar to the results reported in another recent article,²⁰ our study confirms that the available roof area potential for solar systems is one of the most important parameters when identifying potentially self-sufficient buildings. Although we can show for individual buildings that our results are in line with those of the existing case studies, no other study covers a similar level of scale, both at the spatial dimension and with regard to the complexity of the individual building energy system (see detailed literature review in [supplemental information](#)). By combining spatial microsimulation, advanced spatial and temporal complexity reduction techniques, building energy system optimization, and neural network-based regression models, we are able to quantify the techno-economic potential for self-sufficiency of SFBs between different regions of Europe. This allows for the first time to identify regions or climate and economic framework conditions that are less or especially suitable for self-sufficiency at the building level. A pronounced potential for self-sufficient buildings is evident in regions with low seasonality (e.g., Spain, Italy, Portugal, and Cyprus) and high electricity prices (e.g., Germany).

A widespread dissemination of fully self-sufficient systems would lower the demand for energy transport infrastructure. On the other hand, widespread dissemination of only partially self-sufficient systems could alter the shape of residual electricity demand to a U-shaped demand curve, limiting the need for base-load power plants and flexibility of the electricity grid.¹⁸ In that case, network expenses would need to be distributed across less energy, and therefore, network charges would keep increasing, which in turn could lead to a self-reinforcing “death spiral,” in which higher degrees of energy self-sufficiency become even more attractive.^{17,38–41} Energy utilities and policymakers could intervene by introducing adjusted network tariffs, with higher fixed charges (back-up fees) or adjusted compensation schemes (feed-in tariff vs. net metering).^{23,38,42} This in turn could be economically favorable for fully self-sufficient off-grid systems against partly self-sufficient systems. Consequently, it is important to gain a deeper understanding of the underlying socio-techno-economic dynamics of residential off-grid systems, especially given the heterogeneity of the building stock^{43,44} (e.g., building type, age, size, and location) and the people living in it^{45–47} (e.g., in terms of age, income, occupation, and attitude). When designing future electricity tariffs, system-supportive behavior should be rewarded through spatially and temporally dynamic price structures combined

with fixed system integration costs, which reflect operational and fixed system costs based on their origin.

Given the high marginal costs to achieve the final degrees of self-sufficiency, it follows that an energy self-sufficient building is not an optimal economic option as long as no fixed grid charges are introduced (which is in line with previous studies²⁴ on PV-battery systems). However, our results also show that even if a self-sufficient system is not the most cost-optimal option, it can be cost-competitive compared with grid-dependent supply systems, especially in 2050, in countries with low seasonality, high solar irradiation, and relatively high electricity procurement costs. Therefore, considering the findings from studies on non-monetary incentives,^{2,3} self-sufficient buildings could spread more quickly in regions where cost-competitive operation is achieved, e.g., in Cyprus, Spain, Portugal, Italy, and Germany, without necessarily being cost-optimal. There is already a growing concern from Australian utilities and governments regarding increasing numbers of households leaving the grid, as a self-sufficient energy supply becomes technically feasible and cost-effective.³ To better understand the possible future diffusion of such systems, analyses from multidisciplinary perspectives are needed on the strength of non-monetary drivers.^{2,3,48} Given that currently not much is known about households living off-grid, Lovell and Watson³ conceptualize them as an instance of scarce data that describe the opposite to the concept of big data and serve as a barrier to effective governance. Previous research provides evidence for high grid connection costs being the main financial motivation for people to live off-grid³ and that grid limits can pose major constraints to the future deployment of local energy systems.⁴⁹ Therefore, local grid access restrictions in the form of high grid connection costs or limited options for the grid integration of decentralized energy systems could increase the motivation for grid defection and should be considered by policymakers and in future research. Consequently, regionally differentiated electricity tariffs and system integration costs should be designed in such a way that the flexibility potential of self-sufficient buildings is available to the higher-level energy system, especially in regions where investments in alternative flexibility options such as smart grids or central storage systems can be replaced.

In larger SFBs with more residents, economies of scale and temporal smoothing promote economic efficiency. Under German economic framework conditions, e.g., scaling effects through the aggregation of over 560 households must be achieved to operate an economically self-sufficient energy system.¹⁴ Other studies analyze and discuss the effects of aggregation across different scales.^{13–16} Research from the macroeconomic perspective on the European electricity system indicates that continent-spanning supply systems result in minimal overall costs by utilizing the best renewable resources and balancing local supply fluctuations with a large grid.^{16,50,51} However, in contrast to large-scale electricity systems, decentralized residential energy systems are more integrated, both vertically from supply to demand and horizontally between energy vectors such as electricity and heat.¹³ As heat is typically not transported over large distances and most building rooftops provide enough space for PV systems to cover 100% of building energy demand (>53% of SFBs in 2020), self-sufficient residential energy systems could avoid transmission network expansion and centralized generation capacity.¹³ Even if economies of scale make larger energy systems economically advantageous, the complexity of energy system planning grows with increasing scale.⁵² Municipal energy system concepts, for example, are difficult to transfer due to their high diversity in terms of renewable potential, existing infrastructure, and energy demand characteristics.^{53,54} Furthermore, resources are needed to integrate and align the

various stakeholder interests of local authorities, citizens, utilities, and companies during the planning and implementation process.⁵⁵ Residential building energy systems, on the other hand, occur in large quantities and are less complex with regard to involved stakeholders and system boundaries. At the same time, the economies of scale of renewable-based supply side technologies are less pronounced. On this basis, companies develop small-scale “one-size-fits-all” solutions and expect to bring down system costs by scaling up production.^{56,57}

In our study, we assumed an interest rate of 4%/a for all households, whereas other studies have employed country-specific weighted average costs of capital of 3.5%–12% for evaluating investments.⁵ However, the use of country-specific weighted average costs of capital is more common for the evaluation of corporate-level investments. Due to the large difference in the timing of the cash flows of a self-sufficient system (high up-front investment) and a grid-connected energy system (constant payments), the discount rate has a major impact on the economic assessment. Higher discount rates (up to 12%, e.g., in eastern Europe) would therefore reduce the profitability of self-sufficient buildings. Other major sources of uncertainty are future price developments of small-scale, low-carbon technologies^{8,58,59} and energy carriers, as well as the impact of behavioral change on the dimensioning of self-sufficient energy systems in residential buildings. Although diurnal shifts in electricity demand only have a minor impact on the dimensioning of self-sufficient buildings,⁶⁰ seasonal behavioral adjustments, such as using dishwashers as luxury items only in the summer,³ could lead to significant cost reductions. By considering innovative construction concepts in conjunction with integrated energy system design and including feedback systems that sensitize users in critical energy system situations with respect to energy demand, further cost-saving potentials could be tapped, which would increase the potential for self-sufficient buildings. Although our study uses 30 years of historical weather data to ensure a robust system design, future studies could analyze the impact of climate change on optimal residential energy systems, as milder winters and warmer summers and an increase in extreme weather conditions will impact the dimensioning of weather-robust self-sufficient systems.^{61–63} Furthermore, we use archetypal buildings for rooftop potential estimations in combination with basic assumptions with regard to azimuth, tilt, and utilization factors for solar systems. Future studies could include more detailed procedures to account for physical obstructions at the individual building level (e.g., with satellite image-based analyses⁵).

This study sheds light on the technical and economic potential of fully energy self-sufficient residential buildings in 2020 and 2050. Of the 41 million European SFBs considered here, 53% or 75% have the technical potential and 0% or 5% have an extended economic potential for energy self-sufficiency between 2020 and 2050, respectively. Through the findings provided in our study and in the face of surging energy retail prices,^{64,65} energy supply insecurity,⁶⁶ the trend of local energy sourcing,^{8,39} and technological advancement,^{8,11,12,58,59} these self-sufficient building configurations could become more popular in the future. Although we demonstrate the technological and economic feasibility of this objective from the perspective of SFB owners, future studies should examine system impacts and transformations considering the increased dissemination of self-sufficient SFBs. The daily demand shape of household electricity demand and electricity prices on the day-ahead market are highly correlated ($R \sim 0.7$; see example for Germany in [Figure S27](#)). Therefore, a less pronounced household demand profile through the large-scale dissemination of self-sufficient SFBs would lead to a more efficient electricity market by reducing the demand for peak load power plants. From the point of view of a grid

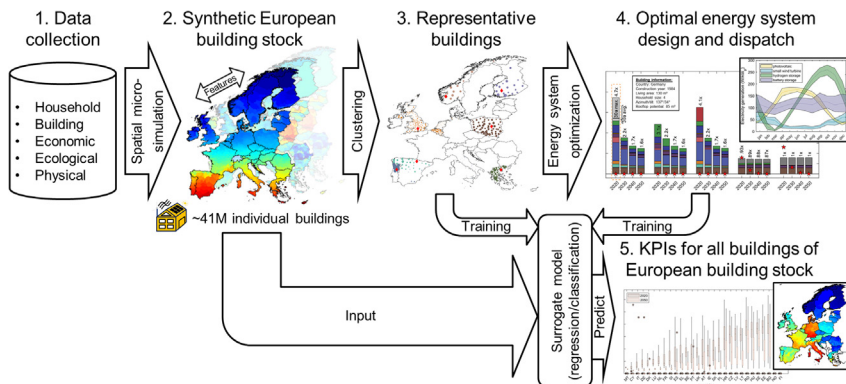


Figure 6. Overview of the framework developed in this study to derive the potential of self-sufficient residential buildings in the EU-27, United Kingdom, and Norway

In a first step, a database was created by collecting spatially resolved information of building stock characteristics and energy system-relevant attributes. Further on, spatial microsimulation was used to integrate the attributes into a synthetic building stock. In a third step, cluster-representative buildings were derived using a k-means clustering approach. Subsequently, weather-robust energy systems for the representative buildings were calculated with a high-performance cluster. Finally, the results of the energy system optimization were transferred to the entire synthetic European building stock using a surrogate model to estimate key performance indicators (KPIs).

operator, partially self-sufficient SFBs with a low DSS interact much more strongly with the electricity grid than 100% grid-dependent or self-sufficient SFBs under current regulation schemes.¹⁴ Policymakers should therefore foster grid-friendly behavior through, for example, dynamic electricity price tariffs and reward SFBs for the provision of system services.

EXPERIMENTAL PROCEDURES

Resource availability

Lead contact

Further information and requests for resources should be directed toward and will be fulfilled by the lead contact, Max Kleinebrahm (max.kleinebrahm@kit.edu).

Materials availability

No materials were used in this study.

Data and code availability

Data will be provided on request.

Methodology and data

First, we describe the spatially resolved building stock information as well as the use of different data sources in a spatial microsimulation to create a synthetic European SFB stock (see Figure 6). Based on this building stock, a cluster approach is employed to reduce the problem's complexity and identify representative SFBs. A multistep optimization model is developed to derive the techno-economically optimal and weather-robust energy system design and dispatch. Finally, a regression model is used as a surrogate for the energy system optimization model to estimate key parameters, e.g., the TAC or levelized cost of energy (LCOE) for all SFBs in the European synthetic building stock.

Synthetic spatially resolved building stock

For the analysis of the energy systems of SFBs in Europe, spatially resolved data are needed, including the geometry and thermal properties of the building envelope,

Table 2. Overview of the spatially resolved attributes required for the building energy system analysis in this study, their degree of spatial resolution, and their data source

| Attributes (set or cardinality) | Data source | Dimension | Spatial resolution |
|--|--|---------------------|--------------------|
| Building type (SFB, MFB), building age (9), household size (6), building area (9) | European Statistical System, ⁶⁷ Entranze, ⁶⁸ and Enerdata ⁶⁹ | building, household | NUTS3, NUTS0 |
| Building ownership (2) | European Statistical System ⁶⁷ | building | NUTS2 |
| Degree of urbanization (3) | Eurostat ⁷¹ | physical | LAU |
| Building type (detached, semi-detached; degree of urbanization) | European Statistical System, ⁶⁷ Eurostat, ⁷⁰ and Eurostat ⁷¹ | building | NUTS0 |
| Building U-values (~building age, type) | EPISCOPE ⁴⁴ and European Commission ⁷² | building | NUTS0 |
| Building geometry (building age/type) | EPISCOPE ⁴⁴ | building | NUTS0 |
| Electricity demand | Enerdata ⁶⁹ | household | NUTS0 |
| Domestic hot water demand | Enerdata ⁶⁹ | household | NUTS0 |
| Energy carrier prices, price level indices, value added tax | Eurostat, ⁶⁴ Eurostat, ⁶⁵ European Commission, ⁷⁴ and European Commission ⁷⁵ | economic | NUTS0 |
| CO ₂ -intensity electricity mix | European Commission ⁷⁶ | environmental | NUTS0 |
| Temperature, irradiation, wind speed, pressure (historical data from 1991 to 2020) | Copernicus Climate Change Service ⁷³ | physical | 31 × 31 km |

The information in parentheses after the attributes indicates the number of categories or the type of further attributes for which the attribute is differentiated.

domestic hot water and electrical appliance demand of households, and the physical, economic, and environmental framework conditions (see Table 2). The various attributes are available in different qualities concerning their disaggregation form. As the primary data sources are spatially resolved in NUTS3 units, data handling and analyses are conducted on this level.

One-dimensional distributions for SFBs are provided for building age, building living area, and household size.⁶⁷ Information on living area distributions is sometimes incomplete for entire countries. By using the average living area for SFBs from alternative sources at the NUTS0 level,^{68,69} similar countries are identified, and incomplete values estimated. The Eurostat data⁶⁷ differentiates the building type into single- and multi-family buildings at the NUTS3 level. To further differentiate SFBs into freestanding and semi-detached buildings, information on the NUTS0 level regarding the shares of detached and semi-detached buildings for areas with different degrees of urbanization⁷⁰ are combined with spatial information about the degree of urbanization at the local administrative unit (LAU) level.⁷¹ The degree of urbanization is first aggregated from the LAU to the NUTS3 levels using the respective LAU population as a weighting factor. Subsequently, NUTS3-specific degrees of urbanization shares are derived, and the proportions of detached and semi-detached buildings estimated.

Building age and type-specific information about the U-values of building components and the buildings' geometries were taken from the Tabula building database⁴⁴ and the EU buildings database.⁷² Missing geometric information was estimated by using information from the neighboring countries. Household-specific information regarding the average yearly demand for domestic hot water and electricity and the percentage share for lighting are available at the NUTS0 level.⁶⁹ Historical weather data with a spatial resolution of about 31 × 31 km⁷³ were used to derive local weather information which was assigned to the respective NUTS3 levels using the area-weighted centroid.

In order to overcome the downside of spatially aggregated one-dimensional data, spatial microsimulation was used to synthesize a representative European building stock (see Figure 7). For this, household data from the socio-economic panel⁷⁷

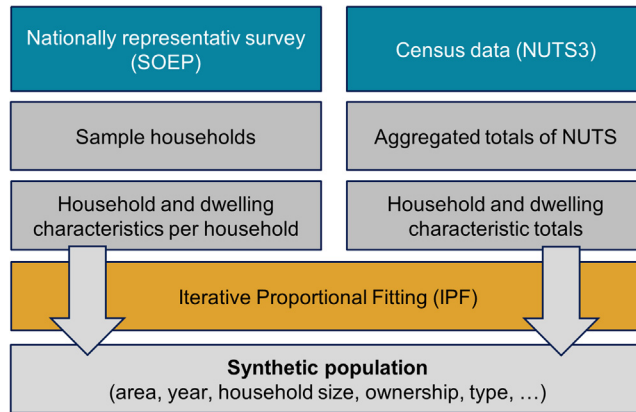


Figure 7. Schematic procedure for deriving the synthetic population

(SOEP) was used as individual-level microdata to generate synthetic buildings for each of the aggregated one-dimensional NUTS3-level target data. This synthetic building stock provides spatial microdata (i.e., empirically based combinations of the one-dimensional data with respect to household size, living area, and construction year of the building) while preserving the spatially aggregated statistics for each NUTS3 unit.

Due to the lack of access to Europe-wide SOEP data, findings from the German SOEP were used to approximate the synthetic building stock. Although this work-around was related to the strong assumption of similar households' and buildings' combinatorial relations across SFBs in the analyzed countries, it was the sole option due to the data available for this study. The individual-level microdata used features are the relations of household size, living area, building age, ownership status, and building type. For the spatial microsimulation, iterative proportional fitting was performed in R with the IPFP Package.⁷⁸ The simulation generated synthetic building stocks for each European NUTS3 region and comprised ~78 million buildings, which were further enriched via relational joins and other location-specific data.

The NUTS3-level microdata are further combined with the geographic information described in Table 2. In order to determine heat gains from solar irradiation as well as potentials for PV and solar thermal systems based on the geometric information about the buildings in downstream steps, the orientation, tilt, and available areas for rooftop systems are needed for each SFB. The geometry of the SFB is derived by scaling the archetype buildings of the Tabula building typology with the respective living areas of the buildings of the synthetic building stock. The estimation of the tilt angle and orientation of the buildings is based on Mainzer et al.⁷⁹ and Kotzur.⁸⁰ The roof azimuth angles are assumed to be evenly distributed (0°–360°). A tilted roof is divided into two opposing roof areas, and the tilt is estimated using a normal distribution with a mean of 37° and a standard deviation of 5°. For flat roofs, it is assumed that the rooftop solar installations are oriented toward the south with a tilt of 30°. For tilted and flat roofs, utilization factors for rooftop systems are assumed to be 75% and 28%, respectively.^{80,81} Household electricity and domestic hot water demand (d_{hh}^{el} , d_{hh}^{dhw}) is calculated based on country-specific average household consumption ($d_{ctr}^{el,avg}$, $d_{ctr}^{dhw,avg}$) and household size (N_{ctr}^{avg}) using a linear relationship as a function of the household size (see Equations 2 and 3).^{82–85} For electricity demand, a household size independent share is taken into account.

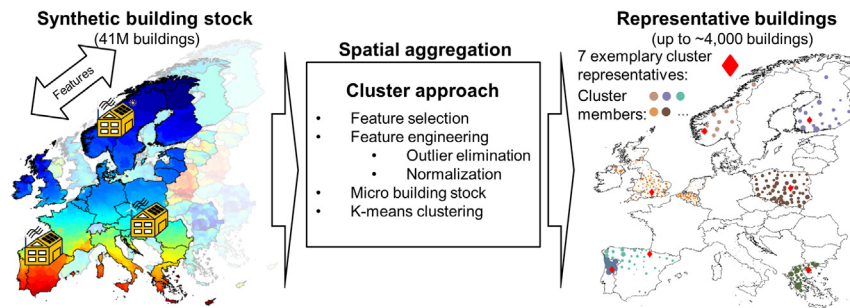


Figure 8. Visualization of the procedure for determining representative single-family buildings for energy system optimization

The European heat maps on the left exemplify the geospatial distribution (averaged at the NUTS3 level) of the building features (top layer: global horizontal irradiation), which are used as inputs for the cluster approach. The map on the right shows the locations of seven (out of 4,000) cluster-representative buildings and the locations and frequency (\sim circle size) of their associated cluster members. The size of the circles represents the number of cluster members located in the respective NUTS3 region.

$$d_{hh}^{el} = \frac{d_{ctr}^{el,avg}}{(N_{ctr}^{avg} + 1)} \cdot (N_{hh} + 1) \quad (\text{Equation 2})$$

$$d_{hh}^{dhw} = \frac{d_{ctr}^{dhw,avg}}{N_{ctr}^{avg}} \cdot N_{hh} \quad (\text{Equation 3})$$

Archetype building derivation

Before deriving the representative buildings, the dataset of 77.6 million SFBs was first reduced by excluding the attached SFBs (semi-detached and terraced) due to inconsistencies in the definitions regarding type of buildings in the different datasets.^{44,67,77} Furthermore, SFBs that are occupied by tenants are excluded (similar to Gorman et al.²⁴), as the divergence of homeowner and occupant leads to additional complexity in the design process for residential energy systems (e.g., via the challenges posed by the principal-agent dilemma⁸⁶). Thus, 41.6 million detached SFBs were considered in this study.

Due to computational restrictions and time constraints, it was not practicable to calculate optimal energy systems for 41.6 million SFBs.⁸⁷ Therefore, representative archetype buildings were determined, taking into account the features relevant to the layout of the energy systems (see Figure 8). For self-sufficient SFBs, these features comprise building living area, building average U value (component area-weighted), building orientation, rooftop tilt, rooftop potential for solar systems, electricity demand, domestic hot water demand, temperature, heating and cooling degree days, GHI, and wind speed. For the weather-dependent features, average values were calculated based on the years 1991–2020.⁷³ The computation of heating and cooling degree days is based on Spinoni et al.⁶² As the features are all continuous, the k-means clustering method was used to identify representative archetype buildings due to the feasible time complexity $O(NKI)$ (only linear increases in time with population size N , number of cluster centers K , and number of iterations I), and high computing efficiency.⁸⁸ Another advantage of the k-means algorithm is that the number of cluster centers must be specified in advance, which in the case of this study was performed with respect to the available computing resources for the energy system optimization model. Due to the higher sensitivity of the k-means algorithm to outliers, these were removed at a 2% percentile before clustering, and the features were normalized to between 0 and 1.⁵³ Depending on the computing

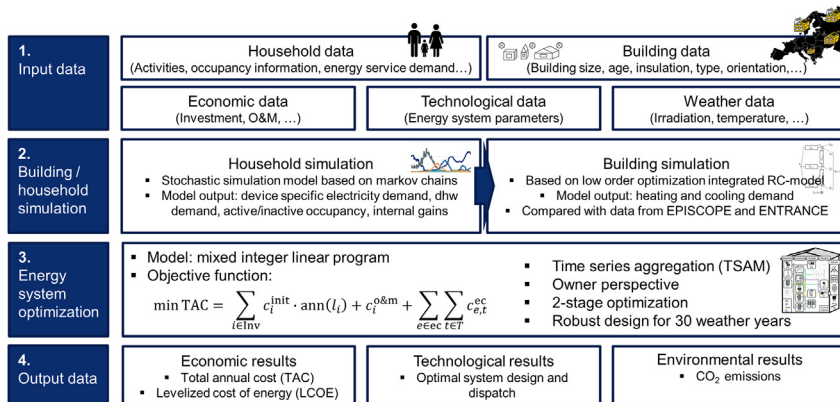


Figure 9. Structural overview of the integrated building simulation and energy system optimization

capacity available, a micro-synthetic building stock was used, as the space complexity of the k-means algorithm increases linearly with the population size N (space complexity: $O(N(F + K))$; F describes the number of features). The micro-building stock was generated by means of random sampling from the original synthetic building stock. After identifying the cluster centroids, for each centroid, the closest SFB in the synthetic building stock was determined. For those SFBs, energy system analyses were carried out (see the next section).

Residential energy system optimization

For the determination of the techno-economically optimal design of the energy systems for the representative SFBs, an integrated building simulation and energy system optimization approach is developed (see Figure 9).

Electricity and thermal demand simulation

To ensure that energy demand and supply are balanced in every hour of the year, time-resolved energy demand profiles of electrical devices and domestic hot water are required as inputs for the energy system optimization. The yearly simulation of electrical devices and domestic hot water demand is based on a stochastic model, which uses first-order Markov chains for the simulation of household occupancy behavior on the basis of which household appliance starts are simulated using start-up probabilities.^{89–91} The Markov chains are parameterized on the basis of German Time Use Survey data.⁹² In addition to household size, the local weather conditions, country-specific household appliance equipment,⁹³ the annual electricity and domestic hot water demand, on the basis of which the start-up probabilities of the devices are calibrated, are used as inputs for the simulation.

The thermal building simulation was based on a 5R1C-model from EN ISO 13790,⁹⁴ which is integrated into the mixed-integer linear energy system optimization model (MILP), analogous to Kotzur et al.⁹⁵ and Schütz et al.⁹⁶ The building simulation uses the internal heat gains from the household simulation (metabolic and device-specific gains), local weather conditions, as well as the thermal properties of the building envelope as inputs.^{44,72} By integrating the thermal building model into the energy system optimization, discrete retrofit options can be considered while taking into account investment options for supply-side technologies. Discrete retrofit options for building components such as the walls, roofs, and floors were derived from the

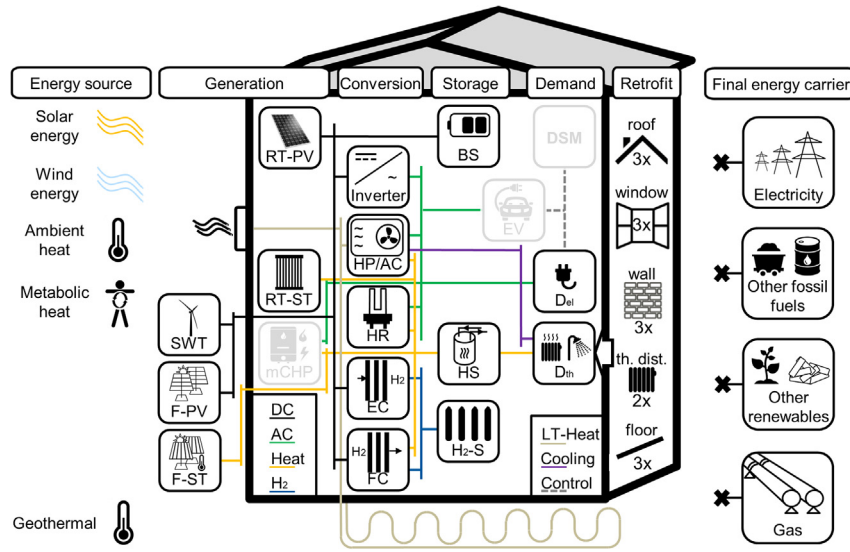


Figure 10. Energy system components considered in the optimization model

Demand side management options⁶⁰ and electricity demand for electric vehicles are included in the model but not analyzed in this study.

F/RT-PV, free-standing/rooftop photovoltaic; SWT, small wind turbine; F/RT-ST, free-standing/rooftop solar thermal; mCHP, micro-combined heat and power; BS, battery storage; HP, heat pump; AC, air conditioner; HR, heating rod; EC, electrolyzer; FC, fuel cell; H₂-S, hydrogen storage; HS, heat storage; EV, electric vehicle; DSM, demand-side management; D_{el}, electrical demand; D_{th}, thermal demand; th. dist, thermal distribution; LT, low temperature.

Tabula building typology,⁴⁴ which provides information about U-values for “usual retrofit” and “advanced retrofit” states. The associated retrofit costs were calculated according to Equation 4 based on the component-specific surface area A_{comp} , U-values u_{comp}^{fs} , component prices p_{comp} , and an assumed heat conductivity λ of 0.035 W/(mK) according to Hinz.⁹⁷ The energy-related component-specific prices were taken from Hinz⁹⁷ and were adjusted with regard to the country-specific construction price index I^{ctr} .⁹⁸ The window retrofit options were taken from Kotzur,⁸⁰ who defines two states with respect to the solar and thermal transmittance of the different window types.

$$c_{comp}^{rm} = \left(\left(\frac{1}{u_{comp}^{rs(rm)}} - \frac{1}{u_{comp}^{rs(existing)}} \right) \cdot \lambda \cdot p_{comp}^{var} + p_{comp}^{fix} \right) \cdot A_{comp} \cdot \frac{I^{ctr}}{pDE} \quad (\text{Equation 4})$$

$$comp \in \{wall, roof, floor\}, \forall rm \in \{usual, advanced\}$$

Supply and conversion technologies

For the simulation of the thermal and electrical energy supply profiles of solar thermal and PV plants, solar irradiation simulations were first carried out with PV-Lib⁹⁹ on the basis of which the energy supply profiles for the different roof orientations were calculated.¹⁰⁰ Furthermore, a small wind turbine was considered in the energy system optimization. The normalized electricity supply profile of the small wind turbine, with a height of 12 m, was calculated analogously to the procedure presented in Kleinebrahm et al.⁶⁰ using local wind speed and an averaged power curve profile, which was based on small wind turbines certified by the Small Wind Certification Council within a rated power range of 1–6 kW. An overview of all modeled supply and demand-side technologies considered in the energy system optimization model can be seen in Figure 10.

Although conversion technologies such as inverters and heating rods are represented with conversion efficiencies that are constant over time, the time step variable coefficients of performance and energy efficiency ratios were determined for the heat pump and air conditioner. The coefficient of performance of the heat pump was calculated analogously to the procedure presented in Ruhnau et al.¹⁰¹ considering building age-specific heat sink temperatures, in accordance with Kotzur.⁸⁰ By investing in a new thermal distribution system, lower heat sink temperatures and therefore better coefficients of performance could be reached. Ambient heat or geothermal heat at a depth of 2 m below the surface can be used as a heat source for the heat pump. The energy efficiency ratio of the air conditioner was calculated by using the empirically derived regression model (model no. 3) in Meissner et al.,¹⁰² assuming a dry bulb set temperature of 26°C.

Energy can be stored in the form of warm water in a hot water storage system, in chemical form in a Li-ion battery, or in a pressurized hydrogen storage tank. The power and capacity components of the Li-ion battery can be independently scaled. Hydrogen can be generated from electricity using a polymer electrolyte membrane (PEM) electrolyzer and subsequently compressed to 160 bar assuming an $H_{2,LHV}/power$ ratio of 22.97.¹⁹ By using a PEM fuel cell, hydrogen can be converted back into electricity with the waste heat released as a by-product. The technology parameters and price developments from 2020 to 2050 of the technologies considered in this work can be found in [Table S6](#).

Optimization objective

The objective of the energy system optimization is to determine a cost-minimal system for providing thermal living comfort as well as the demand for domestic hot water and electrical energy for household appliances. For this purpose, the TAC of the energy system is minimized (see [Equations 5, 6, and 7](#)), with the optimization variables presented in bold>:

$$\min TAC = \sum_{i \in Inv} c_i^{init} \cdot ann(l_i) + c_i^{o\&m} + \sum_{e \in ec} \sum_{t \in T} c_{e,t}^{ec} \quad (\text{Equation 5})$$

$$c_i^{init} = capex^{fix} \cdot x_i^{bi} + capex^{var} \cdot x_i^{size} \quad \forall i \in Inv \quad (\text{Equation 6})$$

$$c_{e,t}^{ec} = x_{e,t}^{import} \cdot p_e^{import} - x_{e,t}^{export} \cdot p_e^{export} \quad \forall e \in ec, \forall t \in T \quad (\text{Equation 7})$$

The TAC comprises the annualized initial costs of the investments in the various technology and retrofit options c_i^{init} , the annual costs for operation and maintenance $c_i^{o\&m}$, as well as the costs and revenues of the energy carrier flows $c_{e,t}^{ec}$. The annuity factor is calculated using the technology lifetime l_i and a real interest rate of 4%/a. To take economies of scale into account, size-independent $capex^{fix}$, and size-dependent $capex^{var}$ cost components were considered for the technology investment options by using a binary x_i^{bi} and a continuous x_i^{size} decision variable. Prices for energy carrier exports p_e^{export} and imports p_e^{import} are calculated for every time step t in T of the year ($x_{e,t}^{export}$, $x_{e,t}^{import}$). However, in the case of full self-sufficiency, energy carrier imports and exports are excluded.

Complexity reduction and robust design

The number of representative SFBs and the computational complexity of the described mixed-integer linear optimization problem leads to long model runtimes due to multiple time-coupling constraints (battery, H_2 -storage, hot water storage, thermal capacity of the SFBs) and binary decision variables. Therefore, time series aggregation is used as a complexity reduction measure to determine the energy

system design of the SFB with reasonable time and accuracy.^{96,103} The optimal design of the energy system is subject to a sequential optimization procedure that ensures that the final configuration meets the weather conditions of 30 weather years (1991–2020). Based on the initially chosen most critical weather year (scenarios 1–3: maximum amount of heating degree days; scenarios 6–8: minimal solar irradiation), the composition of energy system components was determined using an aggregated time series structure, while still maintaining energy storage variables over the entire year.¹⁰³ Typical days were identified with K-medoids clustering based on the hourly electricity demand, domestic hot water demand, GHI, and the temperature time series, using the time series aggregation method presented in Kotzur et al.^{103,104} In a second optimization step, the binary decision variable x_i^{bi} was predetermined and the energy system components scaled $x_{i,n=1}^{size}$ considering the full time series over the entire year.¹⁰⁵ Subsequently, the energy system was optimized for each of the remaining 29 weather years in descending order of heating degree days ($n = 2, \dots, 30$). The technology scaling decision variable $x_{i,n-1}^{size}$ from the previous optimization step was used as a lower bound in the subsequent optimization step n . The resulting energy system design $x_{i,n=30}^{size}$ ensures that demand will be met in all 30 weather years. Further information on optimal trade-offs between calculation time and error can be found in the [supplemental information](#). For the determination of the technical potential for self-sufficiency the optimization model was set up with the most critical weather year and hourly resolution over 8,760 time steps for the NoGrid_{ref(-el)} scenario without the possibility of shedding load. Instead of solving the optimization problem, it was only checked for solvability, as this is the necessary indication for the technical feasibility of self-sufficiency. For the calculation of the optimized energy systems, the CPLEX solver was used with a Linux-based high-performance cluster with up to 180 GB RAM and 40 cores at 2.1 GHz per node. Up to 50 nodes in parallel were used for the model runs.

Surrogate model

To estimate the potential for self-sufficient energy supply systems for all SFBs specified in the synthetic building stock, a regression model was trained as a surrogate for the energy system optimization model. The objective of the surrogate model was to approximate the function between the aggregated energy system optimization input and key output parameters. The derived model is used to transfer the results of the energy system optimizations to the entire synthetic building stock while using significantly less computational power compared with optimizing the energy system of each individual building. The living area normalized TAC and LCOE were used as the dependent variables. The LCOE was calculated according to [Equation 8](#).

$$\text{LCOE} = \frac{\text{TAC}}{\text{TAE}} \quad (\text{Equation 8})$$

$$\text{TAE} = \frac{1}{N} \sum_{n=1}^N \sum_{t=1}^T D_{n,t}^{el} + \frac{D_{n,t}^{th}}{\text{COP}_{n,t}} + \frac{D_{n,t}^c}{\text{EER}_{n,t}} \quad (\text{Equation 9})$$

The mean total annual electricity demand over the considered weather years TAE of the SFB in the existing state (no retrofit measures) was used as a reference, assuming the heating and cooling demands (D^{th}, D^c) were covered by a heat pump and an air conditioner (see [Equation 9](#)).

Up to 12 input features were used as input parameters for the regression model, depending on the scenario considered. These features comprise building living area, average building U value, building orientation, rooftop tilt, rooftop potential for solar systems, household electricity price, yearly electricity demand, yearly domestic

hot water demand, as well as 30-year average temperature, heating and cooling degree days, GHI, and wind speed.

Classification of the technical potential

Over 4,000 cluster-representative SFBs were identified and analyzed for the analysis presented in this article. For the calculation of the technical potential for energy self-sufficiency, a feedforward neural network was used as a classification model to differentiate all SFBs of the synthetic building stock into technically suitable and non-suitable self-sufficient residential buildings. Other classification models like decision trees, support vector machines, and ensemble classifiers were tried as well but achieved worse results. The performance metrics of the used two-layer neural networks used are shown in [Figure S15A](#) for different dataset sizes. The trade-off between computation time and model accuracy was derived on the basis of the diminishing marginal utility with increasing sample size. For each year (2020, 2050), a separate classification model was trained. The neural networks used to generate the presented results are trained on 4,000 SFB samples and achieved an accuracy of 89% and 94% for the years 2020 and 2050 (precision: 91%/95%, recall: 91%/97%).

Regression of system costs

Based on the results of the TAC of the cluster-representative SFBs for the NoGrid_{ref} and Grid_{ref} scenarios, neural networks were trained to estimate the TAC for both system configurations for the years 2020 and 2050 for all SFBs of the synthetic building stock. The performance metrics of the training process can be found in [Figures S15B–S15D](#) for multiple dataset sizes and neural network configurations. The results show that the different neural networks benefit from increasing dataset size while the marginal utility decreases. On the basis of the time aggregated features, a large part of the variance of the TAC can be explained in both scenarios ($R^2 \sim 0.95$). However, the achieved mean percentage error for the NoGrid_{ref} scenario (2020/2050: 12%/13%) compared with the reference system (2020/2050: 4%) is significantly higher due to the more complex energy system design process of a self-sufficient residential energy system, which is highly dependent on the local weather conditions.

Methodological limitations and possible extensions

Inherent limitations of the underlying methodology include the assumption of perfect foresight and the sequential structure for the derivation of the robust energy system design. Perfect foresight allows the energy system model to schedule the operation of dispatchable technologies without considering uncertainties in, e.g., future energy demand or renewable supply. This could lead to unrealistic good solutions. On the other hand, the sequential process to reach a weather-robust energy system design leads to energy system costs probably exceeding those of an integrated 30-year energy system optimization. Through further complexity reduction measures, e.g., the integration of typical periods in addition to typical days, a time series aggregation over a critical number of weather years could make it possible to solve the optimization problem in closed form.¹⁰⁶ Although our study compares different target states for residential building energy systems, future work could use a gray-field approach and consider the initial retrofit state and existing technologies within a transformation process. Furthermore, the database for the generation of the synthetic residential building stock should be continuously adapted and expanded. Currently, e.g., only German time use survey data are employed for the occupancy simulation, which forms the basis for the electrical and thermal demand simulation. The results of this study could be transferred to

regions with similar techno-economic framework conditions using the trained surrogate model.

SUPPLEMENTAL INFORMATION

Supplemental information can be found online at <https://doi.org/10.1016/j.joule.2023.09.012>.

ACKNOWLEDGMENTS

This work was supported by the Helmholtz Association under the Joint Initiative, “Energy Systems Integration” (funding reference: ZT-0002), and the program “Energy System Design”

AUTHOR CONTRIBUTIONS

Conceptualization, M.K.; methodology, M.K., E.N., and J.M.W.; formal analysis, M.K., J.M.W., and E.N.; data curation, M.K. and E.N.; writing – original draft, M.K., J.M.W., and E.N.; writing – review and editing, M.K., J.M.W., R.M., and E.N.; writing – interactive feedback, J.M.W., E.N., R.M., and W.F.; visualization, M.K.; project administration, A.A. and W.F.; funding acquisition, A.A. and W.F.

DECLARATION OF INTERESTS

The authors declare no competing interests.

DECLARATION OF GENERATIVE AI AND AI-ASSISTED TECHNOLOGIES IN THE WRITING PROCESS

During the preparation of this work, the authors used OpenAI’s GPT-4 in order to assist with text editing and refining. After using this tool, the authors reviewed and edited the content as needed and take full responsibility for the content of the publication.

Received: June 9, 2023

Revised: July 28, 2023

Accepted: September 25, 2023

Published: November 2, 2023

REFERENCES

1. Bronski, P., Creyts, J., Guccione, L., Madrazo, M., Mandel, J., Rader, B., Seif, D., Lilienthal, P., Glassmire, J., and Abramowitz, J. (2014). The Economics of Grid Defection: when and where distributed solar generation plus storage competes with traditional utility service. <https://rmi.org/insight/the-economics-of-grid-defection-when-and-where-distributed-solar-generation-plus-storage-competes-with-traditional-utility-service/>.
2. Engelken, M., Römer, B., Drescher, M., and Welpe, I. (2018). Why homeowners strive for energy self-supply and how policy makers can influence them. *Energy Policy* 117, 423–433. <https://doi.org/10.1016/j.enpol.2018.02.026>.
3. Lovell, H., and Watson, P. (2019). Scarce data: off-grid households in Australia. *Energy Policy* 129, 502–510. <https://doi.org/10.1016/j.enpol.2019.02.014>.
4. European Commission (2022). REPowerEU: a plan to rapidly reduce dependence on Russian fossil fuels and fast forward the green transition. https://ec.europa.eu/commission/presscorner/detail/en/IP_22_3131.
5. Bódis, K., Kougias, I., Jäger-Waldau, A., Taylor, N., and Szabó, S. (2019). A high-resolution geospatial assessment of the rooftop solar photovoltaic potential in the European Union. *Renew. Sustain. Energy Rev.* 114, 109309. <https://doi.org/10.1016/j.rser.2019.109309>.
6. Breyer, C., and Gerlach, A. (2013). Global overview on grid-parity. *Prog. Photovolt.: Res. Appl.* 21, 121–136. <https://doi.org/10.1002/pip.1254>.
7. Karneyeva, Y., and Wüstenhagen, R. (2017). Solar feed-in tariffs in a post-grid parity world: the role of risk, investor diversity and business models. *Energy Policy* 106, 445–456. <https://doi.org/10.1016/j.enpol.2017.04.005>.
8. Victoria, M., Haegel, N., Peters, I.M., Sinton, R., Jäger-Waldau, A., del Cañizo, C., Breyer, C., Stocks, M., Blakers, A., Kaizuka, I., et al. (2021). Solar photovoltaics is ready to power a sustainable future. *Joule* 5, 1041–1056. <https://doi.org/10.1016/j.joule.2021.03.005>.
9. Xiao, M., Junne, T., Haas, J., and Klein, M. (2021). Plummeting costs of renewables - are energy scenarios lagging? *Energy Strategy Rev.* 35, 100636. <https://doi.org/10.1016/j.esr.2021.100636>.
10. Few, S., Schmidt, O., Offer, G.J., Brandon, N., Nelson, J., and Gambhir, A. (2018). Prospective improvements in cost and cycle life of off-grid lithium-ion battery packs: an analysis informed by expert elicitations. *Energy Policy* 114, 578–590. <https://doi.org/10.1016/j.enpol.2017.12.033>.
11. Schmidt, O., Hawkes, A., Gambhir, A., and Staffell, I. (2017). The future cost of electrical energy storage based on experience rates. *Nat. Energy* 2, 17110. <https://doi.org/10.1038/nenergy.2017.110>.

12. Schmidt, O., Melchior, S., Hawkes, A., and Staffell, I. (2019). Projecting the future leveled cost of electricity storage technologies. *Joule* 3, 81–100. <https://doi.org/10.1016/j.joule.2018.12.008>.
13. McKenna, R. (2018). The double-edged sword of decentralized energy autonomy. *Energy Policy* 113, 747–750. <https://doi.org/10.1016/j.enpol.2017.11.033>.
14. McKenna, R., Merkel, E., and Fichtner, W. (2017). Energy autonomy in residential buildings: a techno-economic model-based analysis of the scale effects. *Appl. Energy* 189, 800–815. <https://doi.org/10.1016/j.apenergy.2016.03.062>.
15. Tröndle, T., Pfenninger, S., and Lilliestam, J. (2019). Home-made or imported: on the possibility for renewable electricity autarky on all scales in Europe. *Energy Strategy Rev.* 26, 100388. <https://doi.org/10.1016/j.esr.2019.100388>.
16. Tröndle, T., Lilliestam, J., Marelli, S., and Pfenninger, S. (2020). Trade-offs between geographic scale, cost, and infrastructure requirements for fully renewable electricity in Europe. *Joule* 4, 1929–1948. <https://doi.org/10.1016/j.joule.2020.07.018>.
17. Khalilpour, R., and Vassallo, A. (2015). Leaving the grid: an ambition or a real choice? *Energy Policy* 82, 207–221. <https://doi.org/10.1016/j.enpol.2015.03.005>.
18. Leonard, M.D., and Michaelides, E.E. (2018). Grid-independent residential buildings with renewable energy sources. *Energy* 148, 448–460. <https://doi.org/10.1016/j.energy.2018.01.168>.
19. Knosala, K., Kotzur, L., Röben, F.T.C., Stenzel, P., Blum, L., Robinus, M., and Stolten, D. (2021). Hybrid hydrogen home storage for decentralized energy autonomy. *Int. J. Hydrog. Energy* 46, 21748–21763. <https://doi.org/10.1016/j.ijhydene.2021.04.036>.
20. Gstöhl, U., and Pfenninger, S. (2020). Energy self-sufficient households with photovoltaics and electric vehicles are feasible in temperate climate. *PLoS One* 15, e0227368. <https://doi.org/10.1371/journal.pone.0227368>.
21. Goldsworthy, M.J., and Sethuvenkatraman, S. (2018). The off-grid PV-battery powered home revisited; the effects of high efficiency air-conditioning and load shifting. *Sol. Energy* 172, 69–77. <https://doi.org/10.1016/j.solener.2018.02.051>.
22. Lacko, R., Drobnič, B., Mori, M., Sekavčnik, M., and Vidmar, M. (2014). Stand-alone renewable combined heat and power system with hydrogen technologies for household application. *Energy* 77, 164–170. <https://doi.org/10.1016/j.energy.2014.05.110>.
23. Sabadini, F., and Madlener, R. (2021). The economic potential of grid defection of energy prosumer households in Germany. *Adv. Appl. Energy* 4, 100075. <https://doi.org/10.1016/j.adapen.2021.100075>.
24. Gorman, W., Jarvis, S., and Callaway, D. (2020). Should I stay or should I go? The importance of electricity rate design for household defection from the power grid. *Appl. Energy* 262, 114494. <https://doi.org/10.1016/j.apenergy.2020.114494>.
25. Liu, H., Azuatalam, D., Chapman, A.C., and Verbić, G. (2019). Techno-economic feasibility assessment of grid-defection. *Int. J. Electr. Power Energy Syst.* 109, 403–412. <https://doi.org/10.1016/j.ijepes.2019.01.045>.
26. Ramirez Camargo, L., Nitsch, F., Gruber, K., and Dorner, W. (2018). Electricity self-sufficiency of single-family houses in Germany and the Czech Republic. *Appl. Energy* 228, 902–915. <https://doi.org/10.1016/j.apenergy.2018.06.118>.
27. Quoilin, S., Kavvadias, K., Mercier, A., Pappone, I., and Zucker, A. (2016). Quantifying self-consumption linked to solar home battery systems: statistical analysis and economic assessment. *Appl. Energy* 182, 58–67. <https://doi.org/10.1016/j.apenergy.2016.08.077>.
28. Bianchi, M., Branchini, L., Ferrari, C., and Melino, F. (2014). Optimal sizing of grid-independent hybrid photovoltaic–battery power systems for household sector. *Appl. Energy* 136, 805–816. <https://doi.org/10.1016/j.apenergy.2014.07.058>.
29. Ren, Z., Paevere, P., and Chen, D. (2019). Feasibility of off-grid housing under current and future climates. *Appl. Energy* 241, 196–211. <https://doi.org/10.1016/j.apenergy.2019.03.068>.
30. Puranen, P., Kosonen, A., and Ahola, J. (2021). Technical feasibility evaluation of a solar PV based off-grid domestic energy system with battery and hydrogen energy storage in northern climates. *Sol. Energy* 213, 246–259. <https://doi.org/10.1016/j.solener.2020.10.089>.
31. Schmid, F., and Behrendt, F. (2023). Genetic sizing optimization of residential multi-carrier energy systems: the aim of energy autarky and its cost. *Energy* 262, 125421. <https://doi.org/10.1016/j.energy.2022.125421>.
32. Rosenow, J., Gibb, D., Nowak, T., and Lowes, R. (2022). Heating up the global heat pump market. *Nat. Energy* 7, 901–904. <https://doi.org/10.1038/s41560-022-01104-8>.
33. Shivakumar, A., Welsch, M., Taliotis, C., Jakšić, D., Baričević, T., Howells, M., Gupta, S., and Rogner, H. (2017). Valuing blackouts and lost leisure: estimating electricity interruption costs for households across the European Union. *Energy Res. Soc. Sci.* 34, 39–48. <https://doi.org/10.1016/j.erss.2017.05.010>.
34. Ebner, M., Fiedler, C., Jetter, F., and Schmid, T. (2019). Regionalized potential assessment of variable renewable energy sources in Europe. In *2019 16th International Conference on the European Energy Market (EEM) (IEEE Publications)*.
35. IRENA (2022). Global hydrogen trade to meet the 1.5°C climate goal. Part II: technology review of hydrogen carriers. <https://www.irena.org/publications/2022/Apr/Global-hydrogen-trade-Part-II>.
36. Posdziech, O., Schwarze, K., and Brabandt, J. (2019). Efficient hydrogen production for industry and electricity storage via high-temperature electrolysis. *Int. J. Hydrog. Energy* 44, 19089–19101. <https://doi.org/10.1016/j.ijhydene.2018.05.169>.
37. Bianchi, F.R., and Bosio, B. (2021). Operating principles, performance and technology readiness level of reversible solid oxide cells. *Sustainability* 13, 4777. <https://doi.org/10.3390/su13094777>.
38. Castaneda, M., Jimenez, M., Zapata, S., Franco, C.J., and Dyner, I. (2017). Myths and facts of the utility death spiral. *Energy Policy* 110, 105–116. <https://doi.org/10.1016/j.enpol.2017.07.063>.
39. Agnew, S., and Dargusch, P. (2015). Effect of residential solar and storage on centralized electricity supply systems. *Nat. Clim. Change* 5, 315–318. <https://doi.org/10.1038/nclimate2523>.
40. Janko, S.A., Arnold, M.R., and Johnson, N.G. (2016). Implications of high-penetration renewables for ratepayers and utilities in the residential solar photovoltaic (PV) market. *Appl. Energy* 180, 37–51. <https://doi.org/10.1016/j.apenergy.2016.07.041>.
41. Parag, Y., and Sovacool, B.K. (2016). Electricity market design for the prosumer era. *Nat. Energy* 1, 16032. <https://doi.org/10.1038/energy.2016.32>.
42. Schittekatte, T., Mallapragada, D., Joskow, P.L., and Schmalensee, R. (2023). Reforming retail electricity rates to facilitate economy-wide decarbonization. *Joule* 7, 831–836. <https://doi.org/10.1016/j.joule.2023.03.012>.
43. Milojevic-Dupont, N., Wagner, F., Hu, J., Zumwald, M., Nachtigall, F., Biljecki, F., Heeren, N., Kaack, L., Pichler, P.-P., and Creutzig, F. EUBUCCO v0.1: European building stock characteristics in a common and open database for 200+ million individual buildings. *Sci. Data*. <https://doi.org/10.5281/ZENODO.6524780>.
44. EPISCOPE (2016). Energy performance indicator tracking schemes for the continuous optimisation of refurbishment processes in European housing stocks. <http://episcope.eu/iee-project/episcope/>.
45. Steemers, K., and Yun, G.Y. (2009). Household energy consumption: a study of the role of occupants. *Build. Res. Inf.* 37, 625–637. <https://doi.org/10.1080/09613210903186661>.
46. Piao, X., and Managi, S. (2023). Household energy-saving behavior, its consumption, and life satisfaction in 37 countries. *Sci. Rep.* 13, 1382. <https://doi.org/10.1038/s41598-023-28368-8>.
47. Delzendeh, E., Wu, S., Lee, A., and Zhou, Y. (2017). The impact of occupants' behaviours on building energy analysis: a research review. *Renew. Sustain. Energy Rev.* 80, 1061–1071. <https://doi.org/10.1016/j.rser.2017.05.264>.
48. Vögele, S., Poganietz, W.-R., Kleinebrahm, M., Weimer-Jehle, W., Bernhard, J., Kuckshinrichs, W., and Weiss, A. (2022). Dissemination of PV-Battery systems in the German residential sector up to 2050: technological diffusion from multidisciplinary perspectives. *Energy* 248, 123477. <https://doi.org/10.1016/j.energy.2022.123477>.
49. Brockway, A.M., Conde, J., and Callaway, D. (2021). Inequitable access to distributed energy resources due to grid infrastructure

- limits in California. *Nat. Energy* 6, 892–903. <https://doi.org/10.1038/s41560-021-00887-6>.
50. Eriksen, E.H., Schwenk-Nebbe, L.J., Tranberg, B., Brown, T., and Greiner, M. (2017). Optimal heterogeneity in a simplified highly renewable European electricity system. *Energy* 133, 913–928. <https://doi.org/10.1016/j.energy.2017.05.170>.
51. Grams, C.M., Beerli, R., Pfenninger, S., Staffell, I., and Wernli, H. (2017). Balancing Europe's wind power output through spatial deployment informed by weather regimes. *Nat. Clim. Change* 7, 557–562. <https://doi.org/10.1038/nclimate3338>.
52. Kotzur, L., Nolting, L., Hoffmann, M., Groß, T., Smolenko, A., Priesmann, J., Büsing, H., Beer, R., Kullmann, F., Singh, B., et al. (2021). A modeler's guide to handle complexity in energy systems optimization. *Adv. Appl. Energy* 4, 100063. <https://doi.org/10.1016/j.adapen.2021.100063>.
53. Weinand, J.M., McKenna, R., and Fichtner, W. (2019). Developing a municipality typology for modelling decentralised energy systems. *Util. Policy* 57, 75–96. <https://doi.org/10.1016/j.jup.2019.02.003>.
54. Kleinebrahm, M., Weinand, J.M., Naber, E., McKenna, R., and Ardone, A. (2023). Analysing municipal energy system transformations in line with national greenhouse gas reduction strategies. *Appl. Energy* 332, 120515. <https://doi.org/10.1016/j.apenergy.2022.120515>.
55. McKenna, R., Bertsch, V., Mainzer, K., and Fichtner, W. (2018). Combining local preferences with multi-criteria decision analysis and linear optimization to develop feasible energy concepts in small communities. *Eur. J. Oper. Res.* 268, 1092–1110. <https://doi.org/10.1016/j.ejor.2018.01.036>.
56. Lichner, C. (2020). Electrolyzer overview: Lowering the cost of hydrogen and distributing its production. *pv magazine*. <https://pv-magazine-usa.com/2020/03/26/electrolyzer-overview-lowering-the-cost-of-hydrogen-and-distributing-its-production/>
57. Home Power Solution (2022). PICEA—the world's first year-round electricity storage system for your home. www.homepowersolution.de.
58. Way, R., Ives, M.C., Mealy, P., and Farmer, J.D. (2022). Empirically grounded technology forecasts and the energy transition. *Joule* 6, 2057–2082. <https://doi.org/10.1016/j.joule.2022.08.009>.
59. Jaxa-Rozen, M., and Trutnevte, E. (2021). Sources of uncertainty in long-term global scenarios of solar photovoltaic technology. *Nat. Clim. Change* 11, 266–273. <https://doi.org/10.1038/s41558-021-00998-8>.
60. Kleinebrahm, M., Weinand, J., Ardone, A., and McKenna, R. (2018). Optimal renewable energy based supply systems for self-sufficient residential buildings. *IBPSA BauSIM2018*, 7. Deutsch-Österreichische Konferenz. <https://doi.org/10.5445/IR/1000085753>.
61. Perera, A.T.D., Nik, V.M., Chen, D., Scartezzini, J.-L., and Hong, T. (2020). Quantifying the impacts of climate change and extreme climate events on energy systems. *Nat. Energy* 5, 150–159. <https://doi.org/10.1038/s41560-020-0558-0>.
62. Spinoni, J., Vogt, J.V., Barbosa, P., Dosio, A., McCormick, N., Bigano, A., and Füssel, H.-M. (2018). Changes of heating and cooling degree-days in Europe from 1981 to 2100. *Int. J. Climatol.* 38, e191–e208. <https://doi.org/10.1002/joc.5362>.
63. Perera, A.T.D., Javanroodi, K., Mauree, D., Nik, V.M., Florio, P., Hong, T., and Chen, D. (2023). Challenges resulting from urban density and climate change for the EU energy transition. *Nat. Energy* 8, 397–412. <https://doi.org/10.1038/s41560-023-01232-9>.
64. Eurostat (2022). Electricity prices for household consumers – bi-annual data (from 2007 onwards). https://ec.europa.eu/eurostat/databrowser/view/nrg_pc_204/default/map?lang=de.
65. Eurostat (2023). Gas prices for household consumers – bi-annual data (from 2007 onwards). https://ec.europa.eu/eurostat/databrowser/view/NRG_PC_202/default/table?lang=de&category=nrg.nrg_price.nrg_pc.
66. Pedersen, T.T., Gøtske, E.K., Dvorak, A., Andresen, G.B., and Victoria, M. (2022). Long-term implications of reduced gas imports on the decarbonization of the European energy system. *Joule* 6, 1566–1580. <https://doi.org/10.1016/j.joule.2022.06.023>.
67. European Statistical System (2022). CensusHub2. <https://ec.europa.eu/CensusHub2>.
68. Entranze. Enerdata tool. <https://entranze.enerdata.net/>.
69. Enerdata (2022). Odyssee database on the energy consumption drivers by end-use, energy efficiency and CO2 related indicators. <https://odyssee.enerdata.net/database/>.
70. Eurostat (2022). Distribution of population by degree of urbanisation, dwelling type and income group – EU-SILC survey. https://ec.europa.eu/eurostat/databrowser/view/ILC_LVHO01/default/table?lang=en.
71. Eurostat (2022). Local administrative units. <https://ec.europa.eu/eurostat/de/web/nuts/local-administrative-units>.
72. European Commission. EU buildings database. <https://ec.europa.eu/energy/eu-buildings-database/en>.
73. Copernicus Climate Change Service (2017). ERA5: fifth generation of ECMWF atmospheric reanalyses of the global climate. Copernicus climate change service climate data store (CDS). <https://cds.climate.copernicus.eu/cdsapp>.
74. Eurostat (2023). Purchasing power parities (PPPs), price level indices and real expenditures for ESA 2010 aggregates. https://ec.europa.eu/eurostat/web/products-datasets/product?code=PRC_PPP_IND.
75. European Commission (2023). Taxation and information communication. https://ec.europa.eu/taxation_customs/tic/public/vatRates/vatrates.html.
76. European Commission (2021). EU reference scenario 2020. <https://op.europa.eu/en/publication-detail/-/publication/96c2ca82-e85e-11eb-93a8-01aa75ed71a1/language-en/format-PDF/source-219903975>.
77. Liebig, S., Goebel, J., Schröder, C., Grabka, M., Richter, D., Schupp, J., Bartels, C., Fedorets, A., Franken, A., Jacobsen, J., et al. (2019). Sozio-oekonomisches panel (SOEP). <https://doi.org/10.5684/soep-core.v35>.
78. Blocker, A.W. (2022). Fast implementation of the iterative proportional fitting procedure in C. <https://github.com/awblocker/ipfp>.
79. Mainzer, K., Fath, K., McKenna, R., Stengel, J., Fichtner, W., and Schultmann, F. (2014). A high-resolution determination of the technical potential for residential-roof-mounted photovoltaic systems in Germany. *Sol. Energy* 105, 715–731. <https://doi.org/10.1016/j.solener.2014.04.015>.
80. Kotzur, L. (2018). Future grid load of the residential building sector (Forschungszentrum Jülich GmbH).
81. Fath, K., Stengel, J., Sprenger, W., Wilson, H.R., Schultmann, F., and Kuhn, T.E. (2015). A method for predicting the economic potential of (building-integrated) photovoltaics in urban areas based on hourly radiance simulations. *Sol. Energy* 116, 357–370. <https://doi.org/10.1016/j.solener.2015.03.023>.
82. Energy Saving Trust (2008). Measurement of domestic hot water consumption in dwellings. https://assets.publishing.service.gov.uk/government/uploads/system/uploads/attachment_data/file/48188/3147-measure-domestic-hot-water-consump.pdf.
83. George, D., Pearre, N.S., and Swan, L.G. (2015). High resolution measured domestic hot water consumption of Canadian homes. *Energy Build.* 109, 304–315. <https://doi.org/10.1016/j.enbuild.2015.09.067>.
84. EnergieAgenturNRW. (2016). Erhebung Wo im Haushalt bleibt der Strom? <https://docplayer.org/10340556-Erhebung-wo-im-haushalt-bleibt-der-strom-stromverbrauchsanteile-verschiedener-anwendungsbereiche-in-ein-bis-fuenf-personen-haushalten-2015-und-2011.html>.
85. CO2 Online (2018). Bundesweiter Stromspiegel. <https://www.stromspiegel.de/>.
86. Braeuer, F., Kleinebrahm, M., Naber, E., Scheller, F., and McKenna, R. (2022). Optimal system design for energy communities in multi-family buildings: the case of the German Tenant Electricity Law. *Appl. Energy* 305, 117884. <https://doi.org/10.1016/j.apenergy.2021.117884>.
87. Hoffmann, M., Priesmann, J., Nolting, L., Praktikjnjo, A., Kotzur, L., and Stolten, D. (2021). Typical periods or typical time steps? A multi-model analysis to determine the optimal temporal aggregation for energy system models. *Appl. Energy* 304, 117825. <https://doi.org/10.1016/j.apenergy.2021.117825>.

88. Xu, D., and Tian, Y. (2015). A comprehensive survey of clustering algorithms. *Ann. Data Sci.* 2, 165–193. <https://doi.org/10.1007/s40745-015-0040-1>.
89. Richardson, I., Thomson, M., and Infield, D. (2008). A high-resolution domestic building occupancy model for energy demand simulations. *Energy Build.* 40, 1560–1566. <https://doi.org/10.1016/j.enbuild.2008.02.006>.
90. Richardson, I., Thomson, M., Infield, D., and Delahunty, A. (2009). Domestic lighting: a high-resolution energy demand model. *Energy Build.* 41, 781–789. <https://doi.org/10.1016/j.enbuild.2009.02.010>.
91. Richardson, I., Thomson, M., Infield, D., and Clifford, C. (2010). Domestic electricity use: a high-resolution energy demand model. *Energy Build.* 42, 1878–1887. <https://doi.org/10.1016/j.enbuild.2010.05.023>.
92. Destatis. (2006). Zeitbudgeterhebung: Aktivitäten in Stunden und Minuten nach Geschlecht, Alter und Haushaltstyp. *Zeitbudgets - Tabellenband I. 2001/2002*. https://www.statistischebibliothek.de/mir/receive/DEMonografie_mods_00003054.
93. Almeida, A. de, Fonseca, P., Bandeirinha, R., Fernandes, T., Araújo, R., and Nunes, U. (2008). Residential monitoring to decrease energy use and carbon emissions in Europe. https://remodece.isr.uc.pt/downloads/REMODECE_PublishableReport_Nov2008_FINAL.pdf.
94. DIN (2008). Energy Performance of Buildings – Calculation of Energy Use for Space Heating and Cooling (ISO 13790:2008). <https://www.iso.org/standard/41974.html>.
95. Kotzur, L., Markewitz, P., Robinius, M., Cardoso, G., Stenzel, P., Heleno, M., and Stolten, D. (2020). Bottom-up energy supply optimization of a national building stock. *Energy Build.* 209, 109667. <https://doi.org/10.1016/j.enbuild.2019.109667>.
96. Schütz, T., Schiffer, L., Harb, H., Fuchs, M., and Müller, D. (2017). Optimal design of energy conversion units and envelopes for residential building retrofits using a comprehensive MILP model. *Appl. Energy* 185, 1–15. <https://doi.org/10.1016/j.apenergy.2016.10.049>.
97. Hinz, E. (2015). *Kosten energierelevanter Bau- und Anlagenteile bei der energetischen Modernisierung von Altbauten*. BMVBS (Institut Wohnen und Umwelt).
98. Eurostat (2020). Price level indices of investment. https://ec.europa.eu/eurostat/statistics-explained/index.php?title=Comparative_price_levels_for_investment#Construction.
99. Andrews, R.W., Stein, J.S., Hansen, C., and Riley, D. (2014). Introduction to the open source PV LIB for python photovoltaic system modelling package. In 2014 IEEE 40th Photovoltaic Specialist Conference (PVSC) (IEEE), pp. 170–174.
100. Lindberg, K.B., Doorman, G., Fischer, D., Korpås, M., Ånestad, A., and Sartori, I. (2016). Methodology for optimal energy system design of Zero Energy Buildings using mixed-integer linear programming. *Energy Build.* 127, 194–205. <https://doi.org/10.1016/j.enbuild.2016.05.039>.
101. Ruhnau, O., Hirth, L., and Praktiknjo, A. (2019). Time series of heat demand and heat pump efficiency for energy system modeling. *Sci. Data* 6, 189. <https://doi.org/10.1038/s41597-019-0199-y>.
102. Meissner, J.W., Abadie, M.O., Moura, L.M., Mendonça, K.C., and Mendes, N. (2014). Performance curves of room air conditioners for building energy simulation tools. *Appl. Energy* 129, 243–252. <https://doi.org/10.1016/j.apenergy.2014.04.094>.
103. Kotzur, L., Markewitz, P., Robinius, M., and Stolten, D. (2018). Time series aggregation for energy system design: modeling seasonal storage. *Appl. Energy* 213, 123–135. <https://doi.org/10.1016/j.apenergy.2018.01.023>.
104. Kotzur, L., Markewitz, P., Robinius, M., and Stolten, D. (2018). Impact of different time series aggregation methods on optimal energy system design. *Renew. Energy* 117, 474–487. <https://doi.org/10.1016/j.renene.2017.10.017>.
105. Bahl, B., Kümpel, A., Seele, H., Lampe, M., and Bardow, A. (2017). Time-series aggregation for synthesis problems by bounding error in the objective function. *Energy* 135, 900–912. <https://doi.org/10.1016/j.energy.2017.06.082>.
106. Hoffmann, M., Kotzur, L., and Stolten, D. (2022). The Pareto-optimal temporal aggregation of energy system models. *Appl. Energy* 315, 119029. <https://doi.org/10.1016/j.apenergy.2022.119029>.
107. Fett, D., Fraunholz, C., and Keles, D. (2021). Diffusion and system impact of residential battery storage under different regulatory settings. *Energy Policy* 158, 112543. <https://doi.org/10.1016/j.enpol.2021.112543>.

Joule, Volume 7

Supplemental information

**Two million European single-family homes
could abandon the grid by 2050**

**Max Kleinebrahm, Jann Michael Weinand, Elias Naber, Russell McKenna, Armin
Ardone, and Wolf Fichtner**



Supplemental experimental procedures.

S1. Supplemental literature review

S1.1. Real world examples of self-sufficient buildings

The following presents applications of energy self-sufficient residential buildings and building energy system concepts. An overview of the analyzed self-sufficient residential buildings, building concepts, and energy system concepts as well as technical parameters can be found in Table S1. One of the first prominent self-sufficient residential building examples is the single-family “Solar House Freiburg”, a demonstration and research project tested in Germany from 1992 to 1996¹. Electricity was provided by a photovoltaic (PV) system and could be stored in a lead-acid battery to compensate diurnal demand fluctuations and in the form of hydrogen for seasonal storage. Besides reconverting hydrogen to electricity and heat in a fuel cell, the hydrogen was used directly for cooking. Another prominent example is the “first energy self-sufficient multi-family house” in Switzerland, which has been inhabited by nine households since 2016 and can be seen on the left-hand side in Figure S1². The roof and facade are used to produce electricity through integrated PV which is stored by a lithium iron phosphate battery and a hydrogen system with polymer electrolyte membrane electrolyzer, fuel cell, and 30 bar pressurized hydrogen tank (without additional compression after the electrolysis). Heat supply is ensured by two underground heat storages and a heat pump, which uses geothermal probes, the thermal storages and the outside air as heat source. By using efficient demand-side technologies (LED lighting, heat exchanger shower, etc.) and a bonus-malus system in which households are informed about their demand behavior, electrical demand is halved compared to the national average.

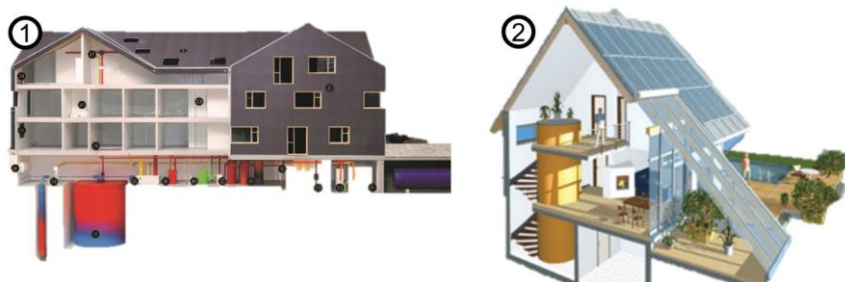


Figure S1. Two examples of applications of self-sufficient residential buildings. (1) The “first energy self-sufficient multi-family building of the world” in Brütten/Swiss³ (image source: Umwelt Arena Schweiz). (2) A self-sufficient single-family building in Freiberg/Germany (image source: Sonnenhaus-Institut⁴, Timo Leukefeld).

The companies Home Power Solutions in Germany and Nilsson Energy in Sweden sell hybrid long-term storage systems for residential buildings⁵.⁶ In Vårgårda, Sweden, a Nilsson Energy system supplies 30 apartments independently of the power grid⁷. In 2021, Home Power Solutions began series production of the PICEA product, which stores PV electricity in hydrogen tanks and a lead-gel battery and uses the excess heat to cover the thermal building demand⁵. The product requires 1.5 m² of space for fuel cell, charging controller, battery, and electrolyzer. The current price depends on the individual design and spans between 70,000 and



100,000 euros^{5, 8}. 80 PICEA products are already installed in 2022 and another 300 are ordered in Germany⁸.

The “Ökohaus Markert” in Carton Wallis, Switzerland, is an example for a self-sufficient residential building without a hydrogen system and has been inhabited since 2012. Freestanding and facade integrated PV is combined with a small wind turbine and battery to cover the electricity demand throughout the year. Heat is provided by solar thermal energy and a heat storage, whereby a wood fired oven is used to cover peak demand⁹. The “VitalSonnenhausPro” and the two self-sufficient single-family houses in Freiberg (see right-hand side Figure S1) optimize the use of the photovoltaic and solar thermal potential in combination with a large building-integrated heat storage system. In Freiberg, a large battery ensures the coverage of the electrical demand in winter. Heat can be generated via a wood stove in peak times. A smaller battery is installed in the “VitalSonnenhausPro” combined with an additional pellet-based Stirling engine for variable electricity and heat generation^{10, 11}.

Table S1. Overview of applications of self-sufficient residential buildings, building concepts and energy system concepts.

PV: photovoltaic; SWT: small wind turbine; ST: solar thermal plant; BS: battery storage; FC: fuel cell; EL: electrolyzer; H₂-S: hydrogen storage; HS: heat storage; HP: heat pump; BIO: biomass; DSM: demand side management; D_{th}: thermal demand; D_{el}: electricity demand; Ctry.: country.

| Real-world applications | Technologies | | | | | | | | | | | | | Year ^a | Ctry. |
|----------------------------------|--------------------------|---------------------------|-------------------------|----------------------------|---------------------------|---------------------------|----------------------------|-------------------------|---------------------------|-------------------------------|------------|----------------------------|----------------------------|-------------------|-------|
| | PV [kW _p] | SWT [kW _p] | ST [m ²] | BS [kWh _{el}] | FC [kW _{el}] | EL [kW _{el}] | H ₂ -S [MWh] | HS [m ³] | HP [kW _{th}] | BIO [kW _{th/el}] | DSM [-] | D _{th} [MWh/a] | D _{el} [MWh/a] | | |
| Solar house ¹ | 4 | | | 20 | 1 | 2 | 1.5 | | | | | 0.15 | 1.4 | 1992 | DE |
| Ökohaus Markert ⁹ | 4 | 1 | 17.5 | 52 | | | | 2.5 | | ✓/0 | | 2.7 | 4.7 ² | 2012 | CH |
| Two SFH Freiberg ¹⁰ | 8.4 | | 46 | 58 | | | | 9.1 | | 25/0 | | 6.7 | 2 | 2014 | DE |
| MFH Brütten ² | 126 | | | 192 | 6.2 | 14.5 | 9.5 ^b | 250 | 28 | | ✓ | ? | 19.8 | 2016 | CH |
| VitalSonnenhausPro ¹¹ | 9.5 | | 80 | 12 | | | | 9 | | .6/17 | | 22 | 2.2 | 2016 | AT |
| Nilsson Energy ⁶ | | | | ✓ | ✓ | ✓ | ✓ | | | | | | | 2014 | SW |
| HPS PICEA ^{5,5} | | | | 25 | 1.5 | 2.5 | .55 ^b | (✓) | | | | | | 2017 | DE |

^aoperation start or product launch, ^bown calculations based on project-specific values and own assumptions, ^cbasic equipment¹²

S1.2. Scientific case studies of self-sufficient buildings

Over the last years, self-sufficient renewable energy-based household supply systems gained interest in the scientific community. An overview of relevant techno-economic articles can be found in Table S2.

Especially in Australia there is a growing interest expressed in public and academic discussions about “living off-grid”, due to favourable conditions in the form of governmental financial support for small scale PV, high rooftop PV potential through low-rise detached buildings, high solar irradiation, high household electricity prices by international standards and high rates of owner-occupied buildings¹³. To find out whether the thought of leaving the grid is an ambition or a real choice, Khalilpour & Vassallo¹⁴ developed a decision support tool for the techno-economic



assessment of the feasibility of leaving the grid with a PV-battery system. After extensive sensitivity analyzes of technology costs, system size, consumer load and feed-in-tariff they conclude that leaving the grid is in most scenarios not the best economic option. Further studies analyze the trade-off between system reliability and system economics by considering different user preferences¹⁵ and the impact of climate change at different locations in Australia¹³ and come to similar conclusions. Particularly in heating dominated regions, PV-battery systems are not economically feasible¹³. However, Goldsworthy & Sethuvenkatraman¹⁶ argue that most studies describe self-sufficient residential buildings as uneconomical compared to grid-connected buildings only because electricity consumption profiles are assumed to stay the same when leaving the grid. They show that the consideration of small demand-side modifications, especially in constraint periods, lead to better economics which can make leaving the grid even economical¹ for some Australian households. To better understand the motivations of off-grid households in Australia, Lovell & Watson¹⁷ conducted a small scale empirical study and identified the desire to make environmental and social decisions, the logistics of arranging new infrastructure, a technology interest in off-grid systems and the sense of self-control as drivers to go off-grid that go beyond economic considerations. They finally define self-sufficient residential buildings as an instance of scarce data, which is the opposite of big data and acts as a barrier to effective governance due to the invisibility of the topic. This favours existing institutions, technologies and cultures and leads to path dependencies as well as making radical innovation difficult to achieve¹⁸.

The economics of off-grid PV-battery systems have also been examined in other countries¹⁹⁻²¹. Quoilin et al.²¹ conclude for multiple countries in the EU that degrees of self-sufficiency cannot exceed 80% without oversizing PV-battery systems. Sabadini & Madlener¹⁹ demonstrate similar results for Germany. Gorman et al.²⁰ analyze the off-grid potential for all owner-occupied single-family buildings (SFBs) in the United States taking into account spatially resolved household electricity demand, solar irradiation and electricity retail cost data from different utilities. They show that grid-defection is not an economic option if no fixed charges in electricity tariffs are in place. However, while technology costs for PV and batteries decline, utilities shift to using fixed charges to bring variable rates closer to their own marginal cost. Therefore, Gorman et al.²⁰ conclude that the change in tariff design could incentivize grid defection but estimate that in most regions of the United States grid defection becomes negligible. These studies show that PV-battery systems under favourable conditions can already be operated economically, but this applies only to a small number of households. However, the above studies only focus on PV-battery systems to cover the electricity demand, which only sometimes includes the electrified energy demand for thermal comfort through, e.g., air conditioning and heat pumps.

The following studies take a more holistic approach by considering the electricity and heat demand directly as input and thereby allow the system to use the flexibility potential of the heating system when dimensioning

¹ Economic feasibility is defined against a reference system in which 100% of the electricity is purchased from the grid.



the local energy system. Lacko et al.²² evaluate the feasibility of a completely renewable energy based heat and electricity supply for an isolated SFB in Slovenia's coastal region using measured demand data. In addition to the PV system, they incorporate a small wind turbine as a second electricity source and a H₂-system consisting of an electrolyzer, fuel cell and hydrogen tank as a seasonal energy storage. The results show that 100% renewable energy supply is technically feasible and can be cost-competitive compared to a fossil fuel based energy supply system. Knosala et al.²³ calculate cost-optimal energy supply systems for a self-sufficient SFB in Germany, focusing on different H₂-storage options. By using a reversible solid oxide cell combined with a liquid organic hydrogen carrier system for long-term storage in combination with advanced heat integration, they show that total annual costs can be reduced by 80% compared to a PV-battery (lithium-ion) system under technological framework conditions in 2030. However, the total annual costs of a 100% grid-dependent system are still 33% lower. Gstöhl & Pfenninger²⁴ show through a case study conducted for 16 residential buildings in Switzerland for the year 2050 that self-sufficient residential buildings could become cost-competitive in temperate climate depending on storage and fossil fuel prices. PV efficiency and available rooftop/façade area are identified as key factors. SFBs with low electricity demand and urban mobility patterns are regarded to achieve self-sufficiency most easily. In contrast multi-family buildings with high electricity demand and rural mobility patterns have a less practical starting position for leaving the grid. Puranen et al.²⁵ demonstrate that self-sufficient residential buildings are technically feasible even under less optimal meteorological conditions in Finland, by analysing a PV-battery system in combination with hydrogen storage and a ground-source heat pump for a zero-energy building. However, a wood fired stove is needed in times of high heat demand. Schmid & Behrendt²⁶ simulate power-flows over a time-frame of 10 years in combination with a technology sizing mechanism to design self-sufficient energy systems for four SFBs across Europe. They conclude that self-sufficient residential buildings at low-seasonality locations can be cost-competitive by 2030.

While existing studies only focus on single individual buildings at specific locations or only take into account PV systems and battery storage systems as technologies, we present the first large scale analysis of all detached owner-owned SFBs in the EU-27, United Kingdom (UK) and Norway (NO) building stock, which tries to identify the technical and economic potential of self-sufficient residential buildings.



Table S2. Overview of techno-economic analysis of 100% renewable energy based self-sufficient residential buildings (geographic focus of studies: Europe, US, Australia).

SFB: single-family building; MILP: mixed-integer linear program; LP: linear program; PV: photovoltaic; SWT: small wind turbine; HS: heat storage; HR: heating rod; BS: battery storage; DSM: demand side management; HP: heat pump; rSOC: reversible solid oxide cell; LOHC: liquid organic hydrogen carrier; GSHP: ground source heat pump; BIO: biomass; ST: solar thermal; BR: building retrofit; el.: electrical demand; th.: thermal demand; appl.: household appliances; SH: space heating; SC: space cooling; DHW: domestic hot water; SI: Slovenia; AU: Australia; BE: Belgium; ES: Spain; DE: Germany; DK: Denmark; HU: Hungary; IT: Italy; RO: Romania; FR: France; UK: United Kingdom; CZ: Czech Republic; CH: Switzerland; US: USA; FI: Finland; NO: Norway.

| Study | Application | Approach | Technologies/ Investments | Energy service demand - (model representation) | Location |
|-------------------|---|---------------------------|--|--|------------------------------------|
| ²² | Techno-economic analysis of one SFB in Slovenia | Heuristic | PV, SWT, H ₂ , HS, HR | el. appl., th. (SH, DHW) - (fixed el. & th. profiles) | SI |
| ¹⁴ | Techno-economic analysis of three SFBs in Australia (w/wo feed in tariff) | MILP | PV, BS | el. appl. - (fixed el. profiles) | AU |
| ²¹ | 894 SFBs across the EU | Heuristic | PV, BS | el. appl. - (fixed el. profiles) | BE, ES, DE, DK, HU, IT, RO, FR, UK |
| ²⁷ | Geospatial analysis with spatial high resolution weather data but highly aggregated demand data (standard load profile – SLP) | LP | PV, BS | el. appl. - (fixed el. profiles) | DE, CZ |
| ¹⁶ | 28 SFBs with demand side flexibility | Heuristic | PV, BS, DSM | el. appl., th. (SH, SC, DHW) - (el. profiles + DSM) | AU |
| ¹³ | Two SFBs at seven locations and multiple weather years | Heuristic | PV, BS | el. appl., th. (SH, DHW) – (fixed el. profiles) | AU |
| ¹⁵ | 54 Australian SFBs, trade-off reliability vs. LCOE | MILP + Heuristic | PV, BS, DSM | el. appl. - (fixed el. profiles) | AU |
| ²⁴ | Analysis of 16 building types with electric mobility | Heuristic | PV, BS, H ₂ , HP | el. appl., th. (SH, SC, DHW), mobility - (fixed el. profiles) | CH |
| ²⁰ | Potential of grid defection of US households | LP | PV, BS | el. appl., th. (SH, SC, DHW) - (fixed el. profiles) | US |
| ¹⁹ | Five households in Germany (w/wo feed in tariff) | Heuristic | PV, BS | el. appl. - (fixed el. profiles) | DE |
| ²³ | One SFB in Germany with advanced heat integration of H ₂ -system | MILP | PV, BS, H ₂ , HP, HS, rSOC, LOHC | el. appl., th. (SH, DHW) - (fixed el. & th. profiles) | DE |
| ²⁵ | Technical feasibility evaluation of one SFB in Finland | Heuristic | PV, BS, H ₂ , GSHP, BIO | el. appl., th. (SH, DHW) - (fixed el. profile) | FI |
| ²⁶ | Ten year power flow simulation and optimal sizing for three building types at four locations | Heuristic | PV, BS, H ₂ , HP, HS | el. appl., th. (SH, DHW) - (fixed el. & th. profiles) | DE, IT, FI, NO |
| This study | Self-sufficient residential building potential for all freestanding SFBs in EU27, UK, NO | MILP+LP+ surrogate | PV, ST, SWT, BS, H₂, HP, HS, BR, DSM | el. appl., th. (SH, SC, DHW) - (fixed el. & DHW profiles + MILP integrated th. model) | EU27 + UK + NO |



S1.3. Archetype buildings and building stock synthesis

To compare the potential of SFBs for complete energy self-sufficiency in Europe, individual energy system optimization problems would have to be solved for these buildings. However, due to the total number of about 78 million single-family homes in the EU-27, United Kingdom and Norway²⁸, individual optimization of all building energy systems is impractical because of computing constraints and time limitations. Established approaches in the scientific literature to handle this problem use building archetypes. This allows investigating a smaller number of archetypes representative for many buildings instead of all buildings while obtaining representative results.

In Mata et al.²⁹, archetype buildings are identified for France, Germany, Spain and the United Kingdom. In three steps, the required number (segmentation step), the technical characteristics (characterization step) and the distribution (quantification step) of the building archetypes are determined. The final energy demands determined with the archetypes deviate only -6% to +2% from official statistics, underlining the suitability of using archetype buildings in energy system analyzes. Sokol et al.³⁰ address the problem of incomplete information in the aggregation to building archetypes in their article. Unknown or uncertain parameters are represented by probability functions, which are updated by Bayesian calibration in the case of available measurement data. For the case study of residential houses in Cambridge, Massachusetts, the methodology shows significantly better performance than traditional deterministic archetype definitions. Kotzur et al.³¹ show that 200 typical buildings are sufficient to represent the diversity of the residential building stock in Germany. To determine these archetype buildings, two iteratively solved optimization problems are used that optimize the representation of previously defined building attributes by archetypes. However, the authors recommend that conventional clustering algorithms for the aggregation should be used in case exact building samples are available. Such clustering methods for determining building archetypes are employed in Hachem-Vermette & Singh³², Fonseca & Schlueter³³, and Borges et al.³⁴. While the clustering method applied in Hachem-Vermette & Singh³² is not specified, the other studies use k-means clustering to determine the spatiotemporal variability of energy services in buildings or to fragment building stocks for urban energy models, respectively.

In the present work, instead of directly deriving archetype buildings from spatially aggregated one-dimensional data as in Kotzur et al.³¹, we first use spatial micro-simulation to combine individual level microdata with aggregated one-dimensional target data, aggregated on NUTS-3 level. In this way, correlations between the individual features are adequately represented in the synthetic population (e.g. household size correlates with building area). In a second step, we apply k-means clustering, which is applicable to the huge amount of data analyzed in this study (all ~78 million SFBs of the EU-27, United Kingdom and Norway building stock).

S2. Supplemental scenarios

Table 3 provides an overview of all scenarios considered in this study. In Section S2.1 scenarios 6-11 are presented, which, in contrast to scenarios 1-5 (discussed in the main document), only take into account the household appliances electrical demand and neglect the thermal



demand side. The influence of complexity reduction strategies for determining the optimal trade-off between calculation time and error is discussed in Section S2.2 and a heuristic is introduced for the determination of scenario specific calculation strategies. Section S2.3 discusses the influence of multiple weather years on the dimensioning of weather-robust self-sufficient energy systems. The impact of the uncertainties with regard to future price, weather, building stock, and energy demand developments on the presented results are discussed in a sensitivity analysis in Section S2.4.

Table S3. Overview of energy system design scenarios and respective energy system technology options.

Scenarios 1-5 are described in the main document. In comparison to the scenarios 1-5, scenarios 6-11 only consider the electricity demand of household devices and exclude the thermal demand for domestic hot water and space heating and cooling (P2H: power-to-heat; el.: electrical demand; th.: thermal demand for domestic hot water and space heating and cooling). Parameter settings used for the calculation strategies in scenarios 1-5 are shown in the last column (see Section S2.2; Td: typical days; ϵ_{ip} : error iterative process). Due to the lower complexity of the optimization problem, scenarios 6-11 can be optimized in reasonable time using the full time series (see Figure S14).

| No. | Scenario | Electrical grid ² | Free-standing PV&ST | Small wind turbines | Rooftop PV&ST, battery, H ₂ | Retrofit, P2H, heat storage | Generator | Demand | Td/ ϵ_{ip} /time |
|-----|---------------------------|------------------------------|---------------------|---------------------|--|-----------------------------|-----------|----------|---------------------------|
| 1 | NoGrid _{ref} | - | - | - | ✓ | ✓ | - | el., th. | 2/34/3000 |
| 2 | NoGrid _{pv} | - | ✓ | - | ✓ | ✓ | - | el., th. | 8/26/4800 |
| 3 | NoGrid _{wind} | - | - | ✓ | ✓ | ✓ | - | el., th. | 4/26/3600 |
| 4 | Grid _{opt} | ✓ | - | - | ✓ | ✓ | - | el., th. | 2/8/1200 |
| 5 | Grid _{ref} | ✓ | - | - | - | ✓ | - | el., th. | 8/8/1200 |
| 6 | NoGrid _{ref-el} | - | - | - | ✓ | - | - | el. | 365/-/- |
| 7 | NoGrid _{pv-el} | - | ✓ | - | ✓ | - | - | el. | 365/-/- |
| 8 | NoGrid _{wind-el} | - | - | ✓ | ✓ | - | - | el. | 365/-/- |
| 9 | NoGrid _{gen-el} | - | - | - | ✓ | - | ✓ | el. | 365/-/- |
| 10 | Grid _{opt-el} | ✓ | - | - | ✓ | - | - | el. | 365/-/- |
| 11 | Grid _{ref-el} | ✓ | - | - | - | - | - | el. | 365/-/- |

S2.1. Optimal energy system design for electricity grid independent buildings

System costs for renewable energy based electricity grid independent SFBs could half by 2050 compared to 2020 (see NoGrid_{ref-el} scenario in Figure S2a). In the exemplary German SFB shown in Figure S2b the costs can even be reduced by 60% in the NoGrid_{ref-el} scenario. Even if the waste heat from the H₂-system cannot be used when considering the electrical demand side in isolation in contrast to scenarios 1-5, investments are made in a hybrid H₂-Battery storage system in the NoGrid_{ref-el} and NoGrid_{wind-el} scenarios. On the other hand, in the NoGrid_{pv-el} scenario, in which the PV potential is not limited to the rooftop area, investments are made in a larger PV system (11 kW_p → 21 kW_p) instead of a hybrid storage system. However, due to the lower robustness of the NoGrid_{pv-el} system against longer periods of low solar radiation, which arise during the robustness scaling with 30 historical weather years, the

² Electricity can be obtained for the national household electricity price and fed into the grid for a feed-in premium of 3 cents/kWh. A constant household electricity price is assumed between 2020 and 2050.



NoGrid_{pv-el} leads to higher costs from 2030 onwards. With a dispatchable diesel backup generator, system costs can be further reduced compared to the 100% renewable energy based scenarios. However, even when future technology improvements in 2050 are considered the costs of electricity grid independent energy supply is still 90% higher, for the exemplary SFB, than in the Grid_{ref-el} scenario.

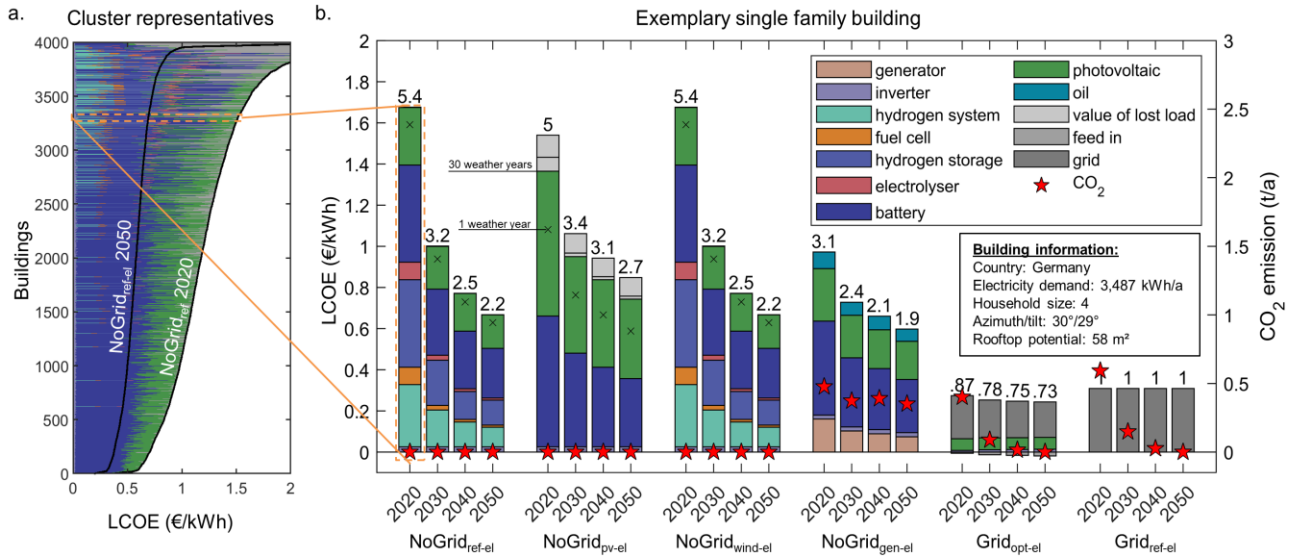


Figure S2. The left-hand section (a) visualizes the energy system cost composition for 4000 representative single-family buildings in the EU-27, United Kingdom and Norway for the NoGrid_{ref-el} scenario. System costs are halved by 2050 compared to 2020. The right-hand section (b) presents the progression of the energy system cost composition of an exemplary single-family building in Germany over time till 2050 for all scenarios.

Relevant characteristics of the residential building, the composition of the levelized cost of electricity and energy system related CO₂ emissions are presented. System costs are calculated using 30 years of historical weather, with the black crosses indicating the system cost if only one weather year is used for the system design. Relative cost differences with regard to the Grid_{ref-el} scenario are shown above the bars.

While 94% of the SFBs considered in this study can already cover their electricity demand in the NoGrid_{ref-el} scenario by using the locally available renewable potential under technological framework conditions in 2020, the proportion of buildings could increase to 98% in 2050 when future technological developments are taken into account (see Figure S3). While in more southern regions such as Malta (MT), Cyprus (CY), Italy (IT), and Spain (ES) almost exclusively PV-battery systems are installed to cover the electricity demand, optimal energy systems in more northern regions use a H₂-storage system due to the more pronounced seasonality of solar radiation (see Figure S3b and d). In contrast to scenarios 1-5, the waste heat from the electrolyzer and fuel cell cannot be used in scenarios 6-11, which makes investing in a H₂ system less attractive.

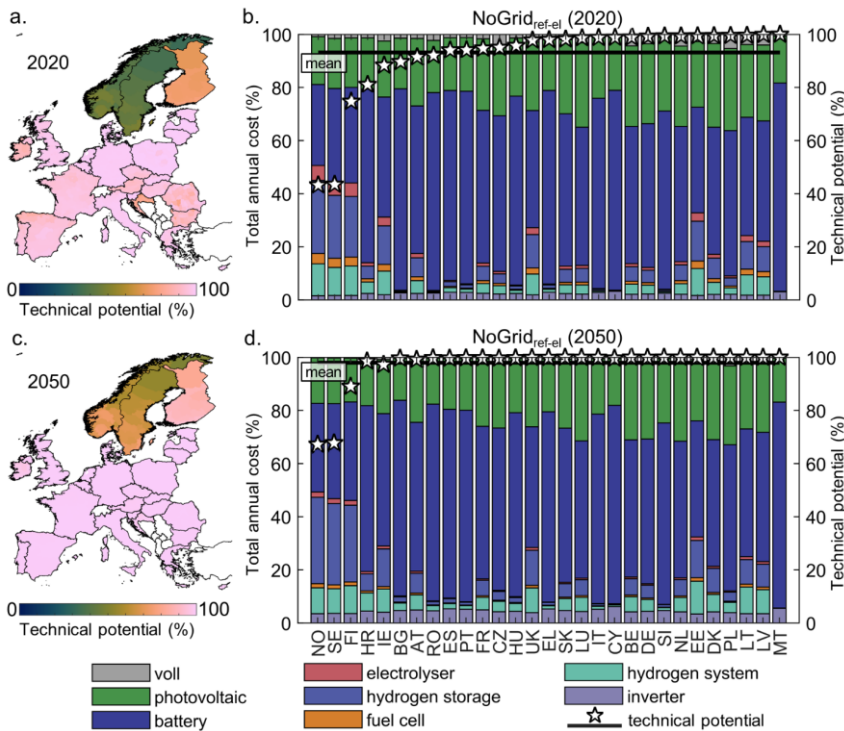


Figure S3. Visualization of the share of technical feasible self-sufficient residential buildings in the NUTS3 regions in Europe for 2020 (a) and 2050 (c) for the NoGrid_{ref-el} scenario. On the right-hand side of the figure (b and d), the building-weighted average composition of the total annual costs (TAC) by energy system components and value of lost load (VoLL) is shown together with the country-specific technical potential.

Each technical feasible self-sufficient residential building of the synthetic building stock is assigned the TAC composition of the corresponding cluster representative and based on that the average composition per country is calculated. Countries are sorted in ascending order of share of their technical potential in 2020. The LCOE composition for the years 2020 and 2050 for 4000 cluster representative SFB are presented for all system configurations in Figure S14.

In Figure S4, the system costs of the SFBs in the NoGrid_{ref-el} scenario are compared with system costs of the Grid_{ref-el} scenario. The LCOE in the Grid_{ref-el} scenario correspond to the country-specific household electricity price (Figure S4a). It is not economically advantageous for any of the buildings considered in this study to be supplied with electricity independently of the electrical grid under techno-economic framework conditions in 2020. In 2050 however, it could be economically beneficial for a minority of SFBs in Cyprus (~1800) to leave the electricity grid and supply themselves independently instead of purchasing 100% of the electricity from the grid. There is an extended economic potential for around half a million SFBs from Cyprus, Spain, Italy, Portugal and Germany. For these buildings, maximum additional costs of 50% compared to the Grid_{ref-el} need to be paid to leave the electricity grid. Compared to the NoGrid_{ref} scenario, in which more than two million SFBs have an extended economical potential, the potential decreases when considering the electrical demand side alone in the NoGrid_{ref-el} scenario.



This can be attributed primarily to the lack of heat integration options in of the H₂-system and the lack of flexibility on the heat demand side. The SFB with the lowest LCOE in the NoGrid_{ref-el} scenario in Cyprus uses a 7 kW_p photovoltaic system in combination with a 33 kWh battery to cover a yearly electricity demand of 6,543 kWh. In this way, LCOE of 0.20 €/kWh can be achieved, which is below the grid procurement costs of 0.22 €/kWh. Further results for scenarios 7-11 can be found in Figure S22, Figure S23, Figure S24, Figure S25 and Figure S26.

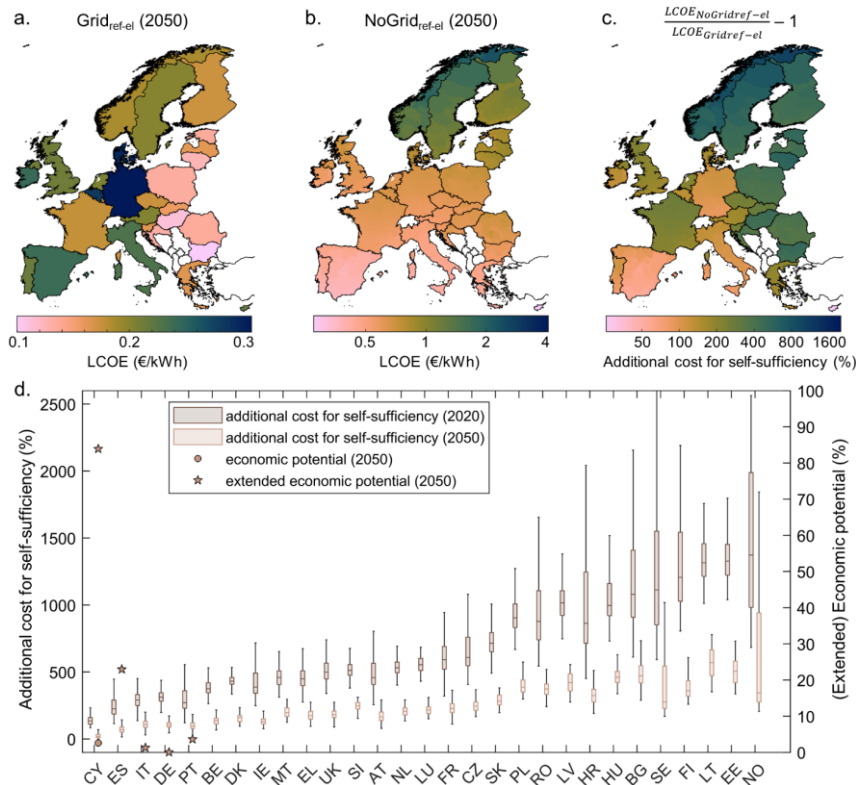


Figure S4. The geospatial distribution of the average levelized cost of electricity (LCOE) for all NUTS3 regions are presented for the Grid_{ref-el} (a) and NoGrid_{ref-el} (b) scenarios. The geospatial distribution of additional costs for self-sufficiency can be found in c. In d, the distribution of the additional costs by country in 2020 and 2050 are shown. Countries are sorted by mean additional costs.

S2.2. Optimal trade-offs: calculation time vs. error

The individual building energy system optimizations in scenario 6-11 can be calculated in hourly resolution in reasonable time considering the full time series over one year. However, by considering the thermal demand side through a linearized capacity-resistance model (5R1C) in combination with discrete retrofit and investment decisions in energy supply and conversion technologies, the complexity of the optimization problem increases significantly. The energy system optimization model cannot be solved in reasonable time using the full time series over one year in hourly resolution for scenarios 1-5 (for one building and MIP Gaps <1% the model needs >24h). Therefore, and to use the computing capacity as efficiently as possible an iterative calculation process (ip) is



presented (see Figure S5) which reduces the computation time and identifies optimal trade-offs between calculation time and optimization error (see Figure S6). The identification of an optimal trade-off between computing time and optimization error enables the generation of a large data set (low computing time) of high-quality individual samples (low optimization error) and thereby capturing the heterogeneity in the EU-27, United Kingdom and Norway building stock.

The basis of the iterative process is the two-stage optimization approach presented in Kotzur³⁵. In the first optimization step, an aggregated representation of the time series in the form of typical days is used to select the technologies of the energy system. In the second optimization step, the technology selection is fixed and the operation and the technology size are optimized using the full time series over one year in hourly resolution. Since the second optimization step is only a linear optimization problem (LP) in contrast to the first optimization step (MILP), the optimization problem can be solved quickly (see Figure S6b). The optimization error (ε_{td}) decreases with an increasing amount of typical days (td) in the first optimization step, while the calculation time increases (see Figure S6d). The optimization error is calculated according to equation (1) in relation to the best solution achieved over all typical days calculated (see equation (2)). Figure S6b visualizes the absolute optimization error exemplarily for a SFB in the NoGrid_{ref} scenario using two typical days in the first optimization step.

$$\varepsilon_{td} = \frac{|TAC_{td,step=2} - TAC_{min,step=2}|}{TAC_{min,step=2}} \quad (1)$$

$$TAC_{min,step=2} = \min\{TAC_{td,step=2}\} \quad td \in [2,4,8,12,16,24] \quad (2)$$

In addition to the observation that the mean optimization error across the 347 SFBs³ examined decreases with an increasing amount of typical days, Figure S6 d. and e. reveals that the optimization error for a large part of the examined buildings is almost zero even when a small amount of typical days is used. This is particularly the case when the difference between the solutions of the first and second optimization step (Δ_{td}) is small (see Figure S6 e.). This difference is referred to below as optimization delta and defined according to equation (3) (see also visualization in Figure S6 a. and b.).

$$\Delta_{td} = \frac{|TAC_{td,step=2} - TAC_{td,step=1}|}{TAC_{td,step=2}} \quad (3)$$

A low optimization delta is therefore a sign that the aggregated time series representation is a sufficiently good approximation of the full time series for the design of the scenario-specific energy system. Figure S6e shows for the NoGrid_{ref} scenario that none of the 347 SFBs has an optimization error greater than 16% if the optimization delta is lower than 34%. The optimization delta is therefore used as an estimator for the optimization error in the iterative process (see Figure S5a).

³200 cluster representatives all over the EU27, United Kingdom and Norway, plus a minimum of 10 country representatives.

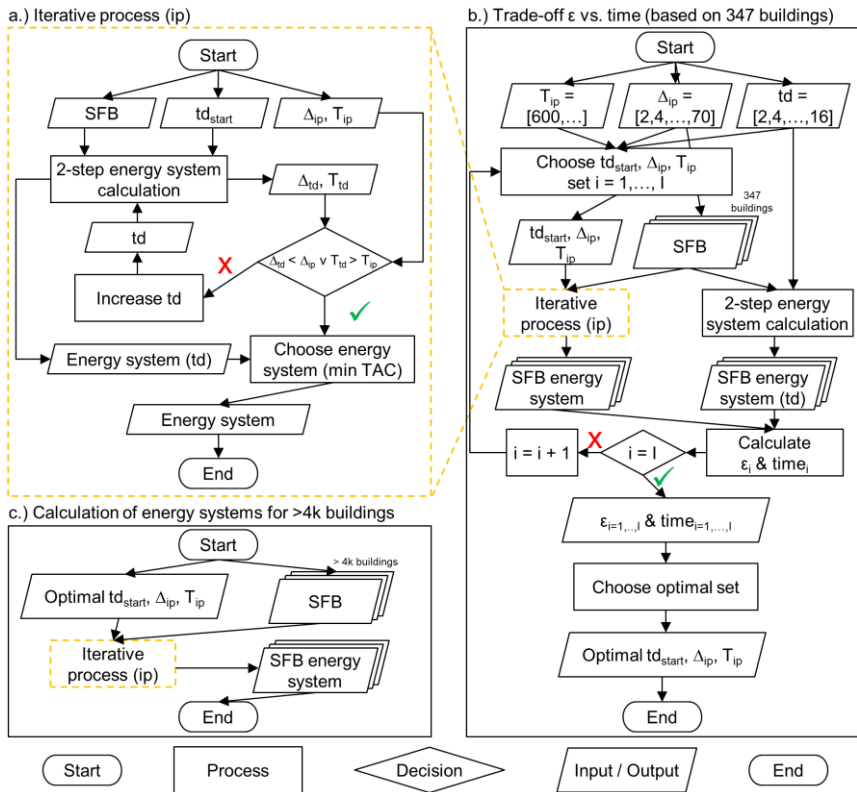


Figure S5. In a, an overview of the iterative process (ip) for the calculation of the energy system design and dispatch of a SFB is given. In b, the procedure for the identification of optimal input parameters for the iterative process presented in a is visualized. In c, the procedure for calculating the energy systems of over 4000 SFBs is presented.

td_{start} : initial amount of typical days; Δ_{ip} & T_{ip} : benchmark for optimization delta and time; Δ_{td} : optimization delta (see equation (3)); T_{td} : optimization time; ϵ : optimization error (see equation (1))

The input required for the iterative process is the initial amount of typical days (td_{start}), a benchmark for the optimization delta (Δ_{ip}), and a benchmark for the optimization time of the first optimization step (T_{ip}). Based on the initial amount of typical days, the two-stage-energy system optimization is carried out. If the optimization delta (Δ_{td}) exceeds the specified benchmark (Δ_{ip}) and the optimization time (T_{td}) is lower than the specified benchmark, the amount of typical days is increased and the two-step energy system calculation is carried out until one of the two termination criteria is met. Finally, the energy system with the lowest total annual cost is selected.

The scenario specific input parameters for the iterative process used in this study are given in Table S3 and are based on the procedure presented in Figure 5b. The derivation of the Pareto optimal parameters (see Figure S6f) is based on 347 representative buildings, for which energy systems are calculated for various amounts of typical days ($td = [2, 4, 8, 12, 16, 24]$). Based on the results of these calculations (ϵ, T) multiple settings of input parameters ($td_{start}, \Delta_{ip}, T_{ip}$) for the iterative process are tested and optimal settings with regard to optimization error



and optimization time are identified (uniform weighting and normalization). Finally, the identified settings are used to calculate the results for >4000 SFBs across EU27, United Kingdom and Europe, which form the basis for the results presented in this study.

Future work could further examine the interdependencies between energy system optimization error, optimization time and the error of the surrogate model. A fixed time budget could be specified in which the goal would be to generate an optimal dataset for training a surrogate model. Depending on the structure of the surrogate model, there should be an optimal trade-off between optimization time (size/diversity of the dataset) and optimization error (accuracy of the dataset).

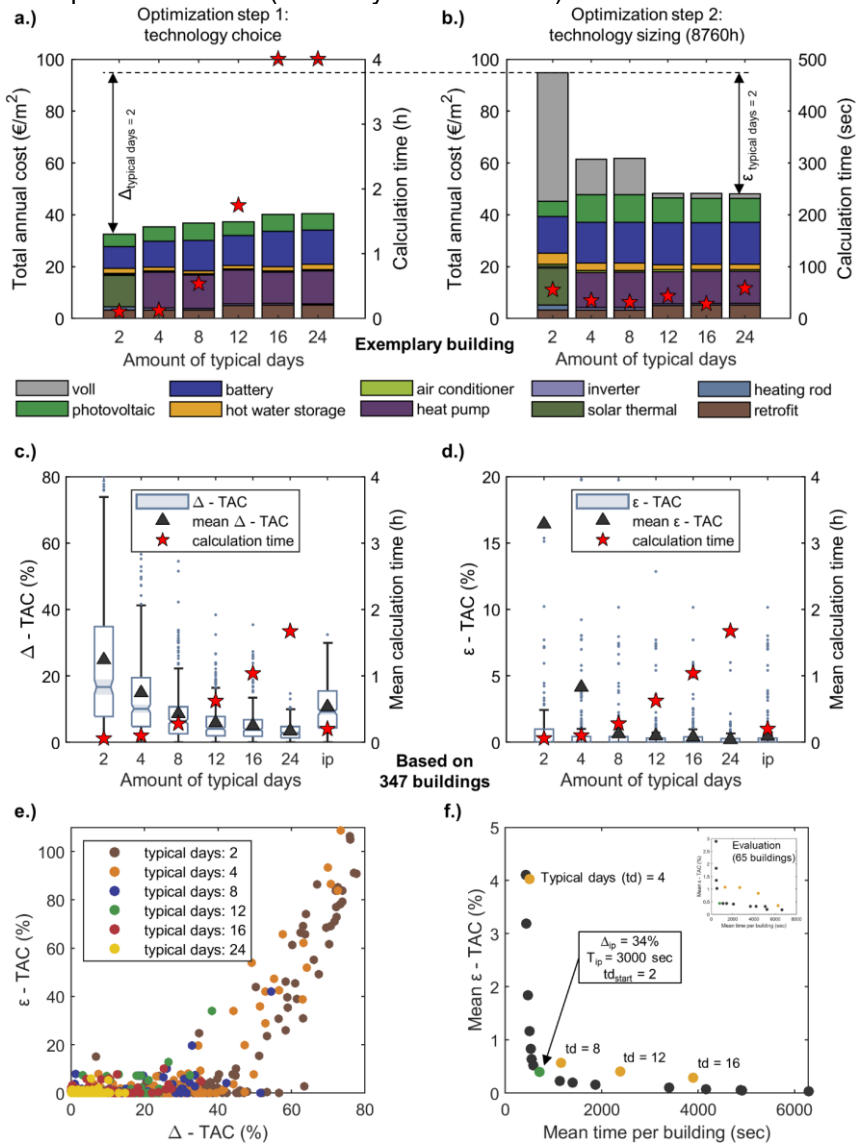


Figure S6. Overview of the results for the identification of the optimal trade-off between optimization error and time.

(a) and (b) present the composition of the total annual cost (TAC) and optimization time in optimization step one (a) and two (b) for a representative SFB. Furthermore, the absolute optimization delta Δ_{td} and error ϵ_{td} are visualized. Figure c and d present the development of



optimization delta, error and time for 347 representative SFBs over an increasing amount of typical days. In e, the optimization delta is plotted against the optimization error whereby every point represents an energy system optimization result with a specific amount of typical days. Finally, (f) presents the trade-off between mean optimization error and optimization time for Pareto optimal configurations of the iterative process (black) and fixed amounts of typical days. Parameters are derived based on 347 SFBs and evaluations of the procedure are conducted based on 65 SFBs.

S2.3. Weather robust energy system design

The majority of previous studies compare self-sufficient energy supply systems against grid connected supply systems on the basis of only one weather year. In our analysis, we take multiple historical weather years into account. This is especially important when comparing self-sufficient residential buildings with grid connected SFBs, as the system design of a self-sufficient residential building should ensure security of supply even under extreme weather periods, while security of supply in a grid-connected SFB is normally ensured by the external infrastructure in combination with a local heat supply system. The capacity of the heat supply system is usually defined on the basis of a standard outside temperature which is calculated using 20 weather years³⁶. Therefore, a representative/average weather year in combination with a standard outside temperature is suitable for techno-economic optimal energy system layout of a grid connected system. For self-sufficient residential buildings, on the other hand, it must not only be ensured that the power component of the energy system is sufficiently sized to cover demand peaks, but also that enough energy is available to ensure security of supply even over longer periods with high demand and low energy feed-in from local renewable energy sources.

Figure S7 presents the average composition and increase in total annual system costs that occur during the robust energy system design process described in the methodology and data section of the main document. The technology selection and the initial technology dimensioning is based on the weather year with the highest number of heating degree days (scenarios 1-3) or the lowest amount of solar irradiation (scenarios 6-8) between 1991 and 2020. The average shares of the total annual system costs from the initial technology dimensioning are calculated according to eq. (4) and can be found in the left part of Figure S7.

$$as_i^{TAC} = \frac{1}{SFB} \sum_{sfb=1}^{SFB} \frac{c_{i,sfb,wy=1}^{init} \cdot ann(l_i) + c_{i,sfb,wy=1}^{o\&m}}{TAC_{sfb,wy=1}} \quad \forall i \in Inv \quad (4)$$

The average increase in total annual system costs (ΔTAC) when considering the additional 29 weather years are calculated year by year according to eq. (5) and can be seen in the right part of Figure S7. The additional weather years are sorted in ascending order by the number of heating degree days.

$$as_{i,n}^{\Delta TAC} = \frac{1}{SFB} \sum_{sfb=1}^{SFB} \frac{c_{i,sfb,wy=n}^{init} \cdot ann(l_i) + c_{i,sfb,wy=n}^{o\&m} - c_{i,sfb,wy=1}^{init} \cdot ann(l_i) - c_{i,sfb,wy=1}^{o\&m}}{TAC_{sfb,wy=1}} \quad (5)$$

$\forall i \in Inv, n = [2,30]$



The results for the NoGrid_{ref} scenario show that the TAC increase on average by more than 5% compared to the initial system design based on the year with the highest number of heating degree days. The more robust system design is achieved by a larger dimensioning of the storage systems, with the hydrogen system being the main contributor to the TAC increase. Since the PV rooftop area potential is already fully exploited in the initial design step for the majority of the considered SFBs, significant further expansion is not possible. Compared to the NoGrid_{ref} scenario, the energy systems of the SFBs in the NoGrid_{pv} and NoGrid_{wind} scenarios are less robust to additional weather years, which is particularly evident in the NoGrid_{pv} scenario, in which TAC increase on average by 10% if 30 weather years are taken into account (see Figure S7). When considering the electrical demand side in isolation, the TACs increase by an average of between 9-13%, depending on the scenario und consideration (see Figure S8).

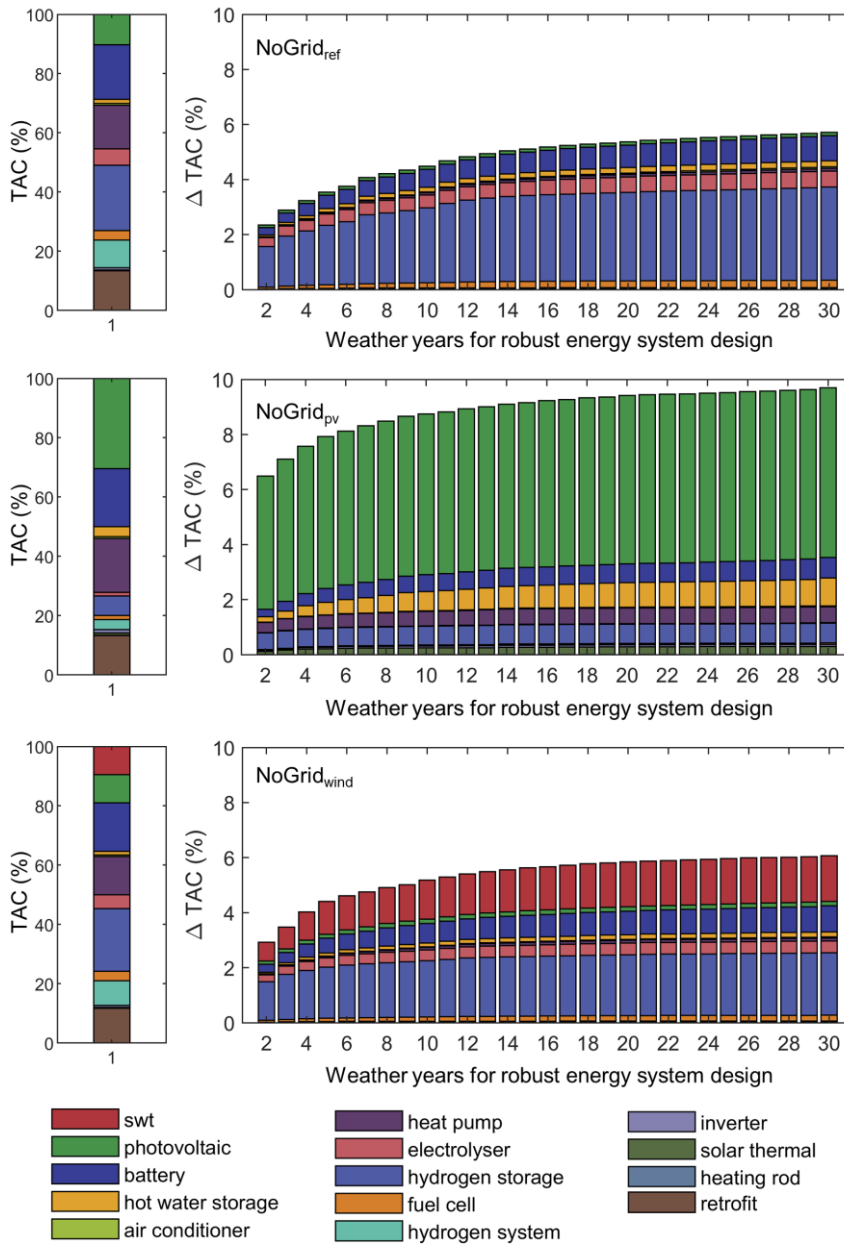


Figure S7. Average composition of total annual system costs (TAC) for the NoGrid_{ref}, NoGrid_{pv} and NoGrid_{wind} scenario under economic framework conditions from the year 2020 (left). Composition of the average additional total annual system costs (Δ TAC) depending on the number of weather years considered for the design of the robust energy system (right). Calculations are based on over cluster representative 4000 SFBs.

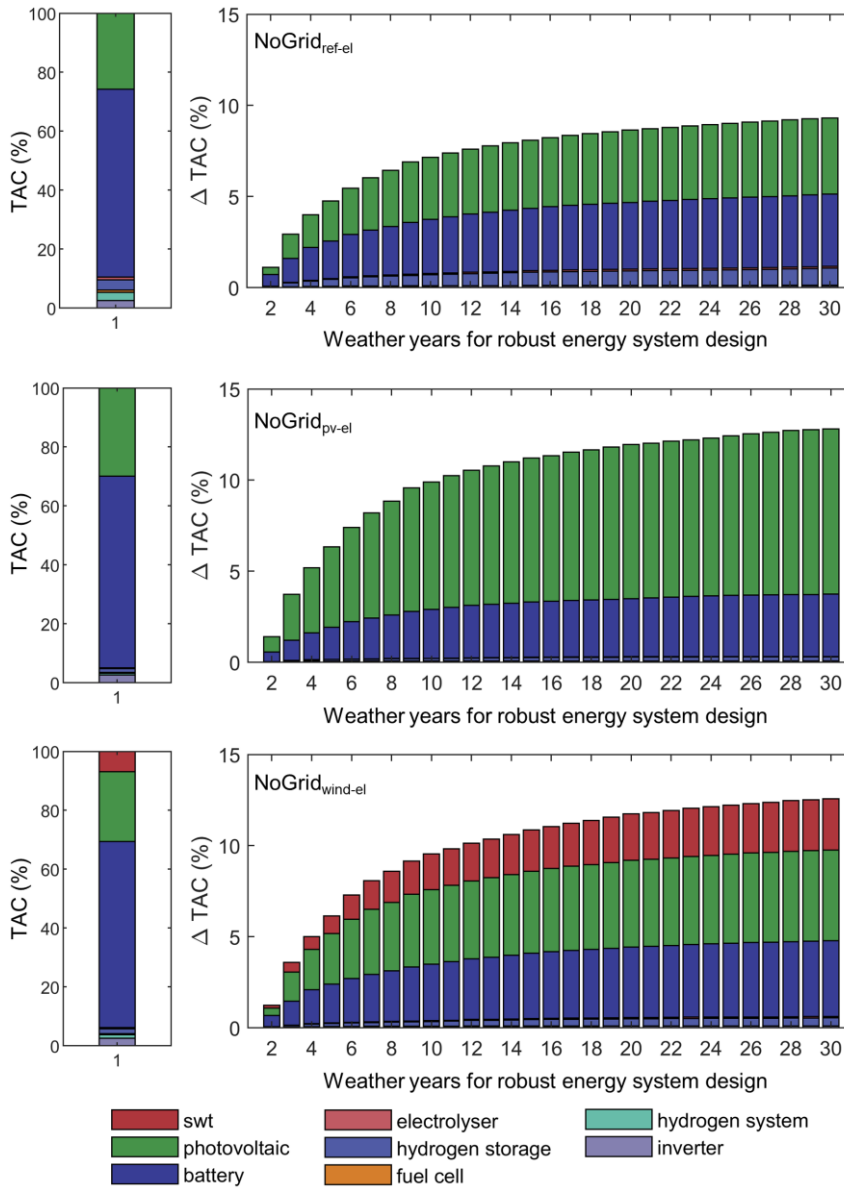


Figure S8. Average composition of total annual system costs (TAC) for the $\text{NoGrid}_{\text{ref-el}}$, $\text{NoGrid}_{\text{pv-el}}$ and $\text{NoGrid}_{\text{wind-el}}$ scenario under economic framework conditions from the year 2020 (left). Composition of the average additional total annual system costs (Δ TAC) depending on the number of weather years considered for the design of the robust energy system (right). Calculations are based on over cluster representative 4000 SFBs.



S2.4. Sensitivity analysis

The impact of the uncertainties with regard to future price, weather, building stock, and energy demand developments on the results of the NoGrid_{ref} and NoGrid_{ref-el} scenarios are discussed in the following. To calculate the sensitivity of the results depending on changes in technology costs, the technology specific cost components of the 4000 cluster centers shown in Figure S13 were varied between -20% and +20%. Further on, a regression model was trained for each cost variation to transfer the impact of the cost changes to the entire synthetic building stock. Regression model configurations are shown in Figure S15. No new energy system optimizations were carried out taking into account the adjusted price structures, since an optimization run of 4000 representative buildings per cost scenario would take several days on 50 servers used in parallel. Consequently, the extended economic potential shown in Figure S9a represents a lower limit, which would be shifted upwards by an optimized energy system design, considering the adjusted cost structures. For the calculation of the impact of changes in the synthetic residential building stock shown in Figure S9b, c and d, each feature of all 41 million SFBs was varied between -20% and +20% in order to examine the effects of, for example, changes in electricity prices or assumptions about roof area potential. The impact of the variation of the three most cost-sensitive features on the spatial distribution of the extended economic potential is shown in Figure S10.

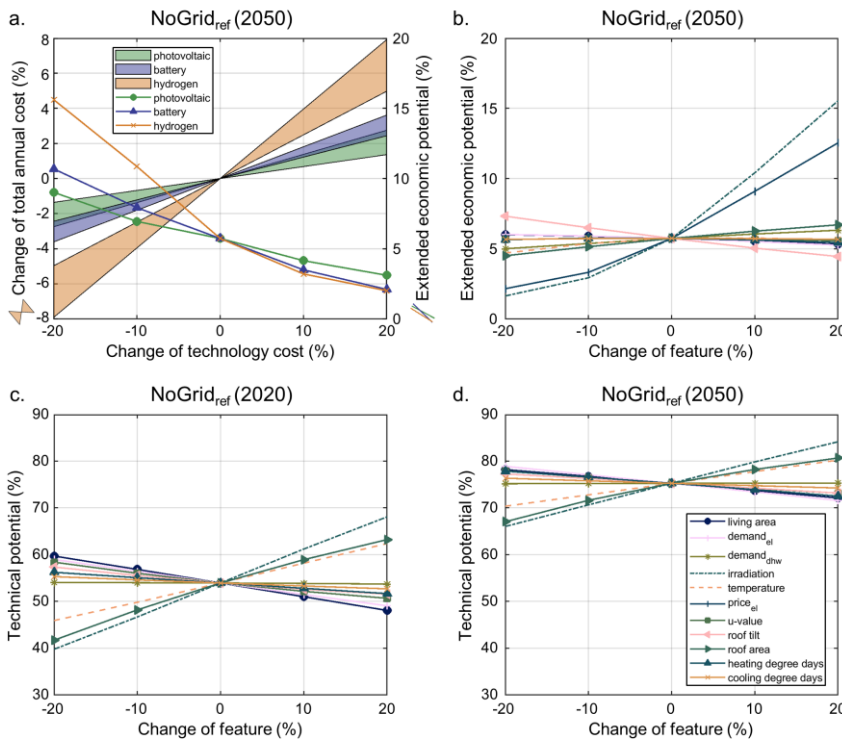


Figure S9: Results of the sensitivity analysis regarding the impact of the uncertainties of future price, weather, building stock, and



energy demand developments. Results are presented for the NoGrid_{ref} scenario.

In a, the influence of the uncertainties of future cost developments of photovoltaic, battery and hydrogen systems on the total annual cost and the extended economic potential is presented. The changes in the total annual cost of the 4000 cluster centers depending on the adjusted cost structures are shown by the colored areas (interquartile range of the 4000 cluster centers). The colored lines represent the extended economic potential. In b, c and d the influence of changing parameters of the investigated synthetic building stock on the extended economic potential (b: 2050) and the technical potential (c: 2020, d: 2050) is shown.

Variations in future cost developments of photovoltaic, battery and hydrogen systems (see Figure S9a) together with changes in household electricity prices and solar irradiation (see Figure S9b) have the greatest impact on the extended economic potential of self-sufficient SFBs in the NoGrid_{ref} scenario in 2050. While a 20% cost increase of the hydrogen system leads to a reduction of the extended economic potential from 5.9% to 2.4%, a 20% cost reduction would lead to an increase of the potential to over 15% of the investigated SFBs. Figure S10 shows, that especially in Germany the extended economic potential would increase significantly with falling hydrogen system prices, due to the high electricity purchase prices. Over 75% of the SFBs analyzed would be able to supply themselves self-sufficient by paying less than 50% more compared to the Grid_{ref} scenario.

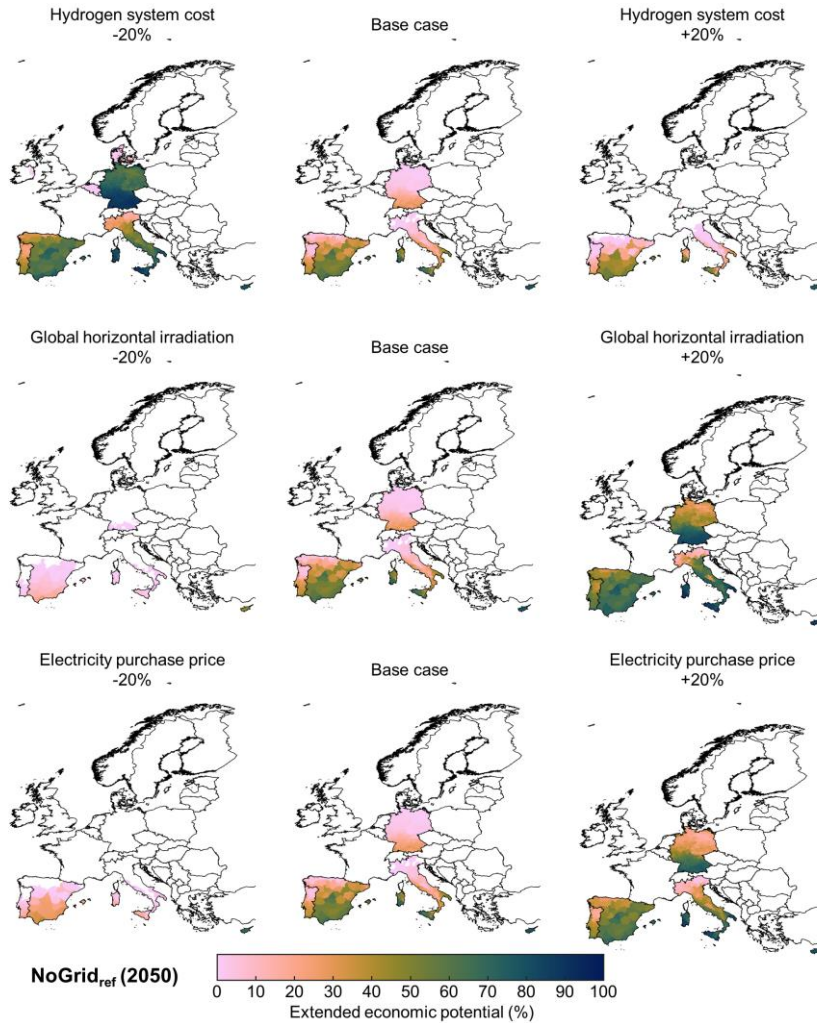


Figure S10: Change in the spatial distribution of the extended economic potential for self-sufficiency as a function of the hydrogen system cost, the global horizontal irradiation, and the electricity purchase price. Results are presented for the NoGrid_{ref} scenario.

The results of the sensitivity analysis of the NoGrid_{ref-el} scenario can be found in Figure S11 and Figure S12. In contrast to the NoGrid_{ref} scenario, in which the thermal demand side is taken into account, the results of the NoGrid_{ref-el} do not show strong dependencies with regard to the cost developments of the hydrogen system. In addition to battery and photovoltaic price developments, changes in global horizontal irradiation and electricity demand have an impact on the extended economic potential. The roof area potential for solar systems, the electricity demand and the locally available solar irradiation have the strongest impact on the technical potential for self-sufficiency.

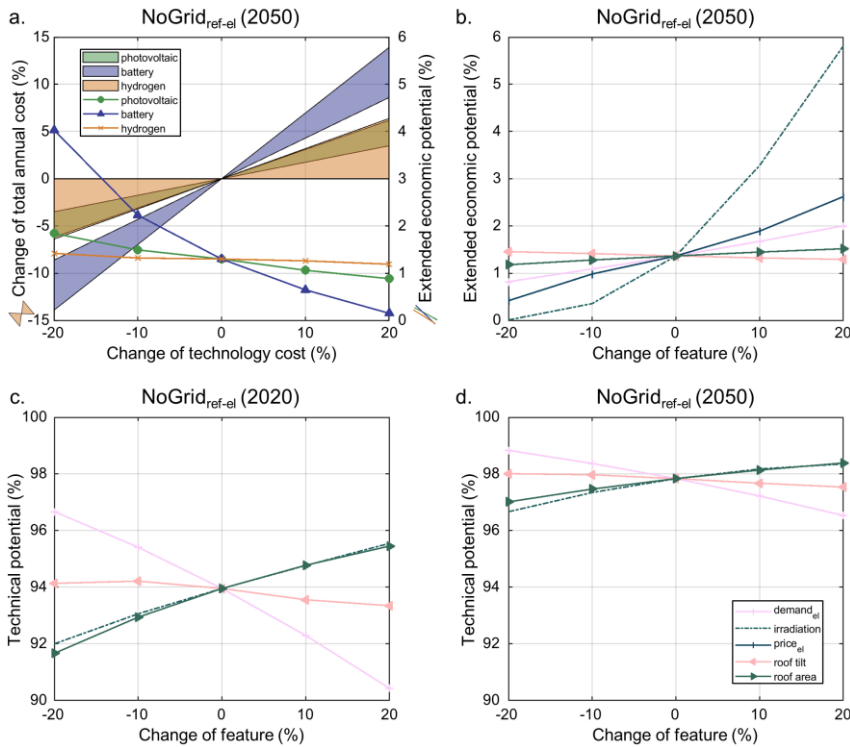


Figure S11: Results of the sensitivity analysis regarding the impact of the uncertainties of future price, weather, building stock, and energy demand developments. Results are presented for the NoGrid_{ref-el} scenario.

In a, the influence of the uncertainties of future cost developments of photovoltaic, battery and hydrogen systems on the total annual cost and the extended economic potential is presented. The changes in the total annual cost of the 4000 cluster centers depending on the adjusted cost structures are shown by the colored areas (interquartile range of the 4000 cluster centers). The colored lines represent the extended economic potential. In b, c and d the influence of changing parameters of the investigated synthetic building stock on the extended economic potential (b: 2050) and the technical potential (c: 2020, d: 2050) is shown.

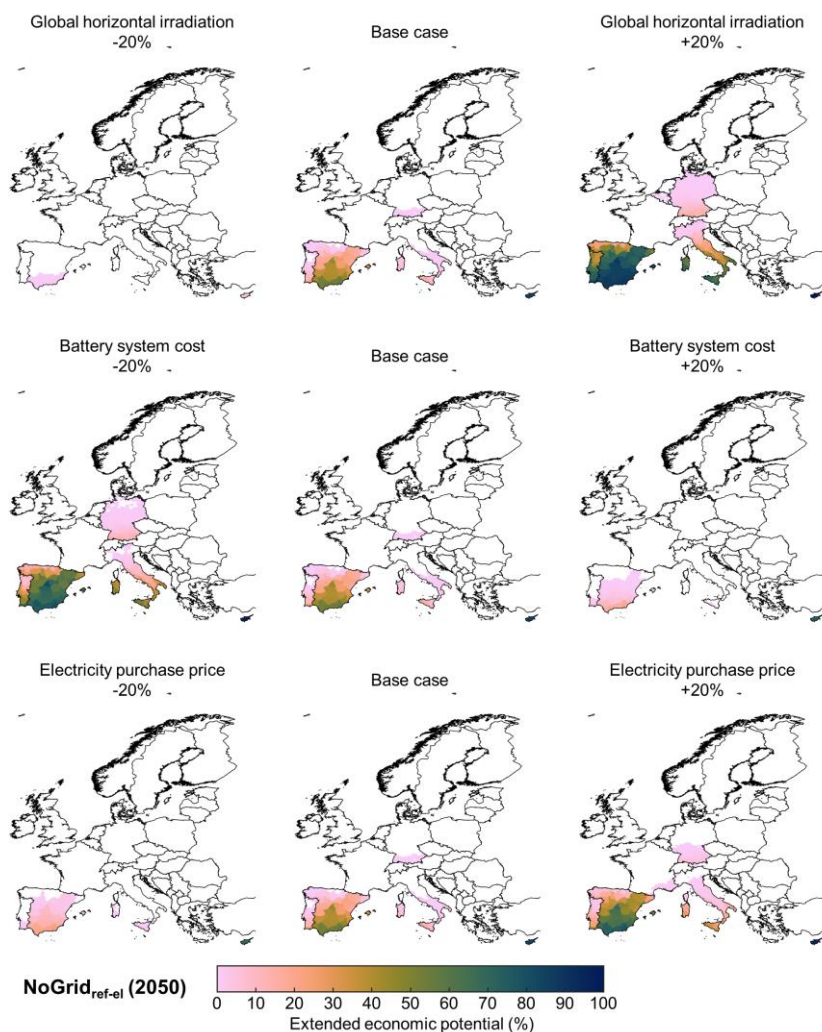


Figure S12: Change in the spatial distribution of the extended economic potential for self-sufficiency as a function of the global horizontal irradiation, the battery system cost, and the electricity purchase price. Results are presented for the NoGrid_{ref-el} scenario.



Supplemental items.

Table S4 and Table S5 present details on the system configurations from Figure 2a and b in the main document for different degrees of self-sufficiency.

Table S4: Results of the technology dimensioning and the selection of the retrofit states depending on the degree of self-sufficiency (DSS) for the selected energy system configurations highlighted in Figure 2a in the main document.

PV: photovoltaic; BS: battery storage; EC: electrolyzer; H₂-S: hydrogen storage; FC: fuel cell; LCOE: levelized cost of electricity

| No. | PV kW _p | BS kW | EC kWh | EC kW | H ₂ -S MWh _{LHV} | FC kW | LCOE €/kWh | DSS % | Feed in kWh | Lost load kWh |
|------------------------|-----------------------|----------|-----------|----------|---|----------|---------------|----------|----------------|------------------|
| Grid _{ref-el} | - | - | - | - | - | - | 0.305 | 0 | - | - |
| 1 | 1.1 | - | - | - | - | - | 0.278 | 20 | 170 | - |
| Grid _{opt-el} | 2.1 | - | - | - | - | - | 0.270 | 29.4 | 511 | - |
| 2 | 7.5 | 0.9 | 5.7 | - | - | - | 0.505 | 75.7 | 2,529 | - |
| 3 | 11.4 | 1.5 | 8.2 | 0.5 | 913 | 0.5 | 1.491 | 99.7 | 102 | - |
| p=20 €/kWh | 11.4 | 3.3 | 8.8 | 0.5 | 898 | 0.5 | 1.617 | 100 | - | 0.08 |

Table S5. Results of the technology dimensioning and the selection of the retrofit states depending on the DSS for the selected energy system configurations highlighted in Figure 2b in the main document.

Three retrofit options are differentiated for each retrofit component: initial state (1), conventional retrofit (2), and advanced retrofit (3). (HR: heating rod; AC: air conditioner; th. dist.: thermal distribution system (old: 0, new: 1); HP: heat pump (~air source, *ground source); PV: photovoltaic; HS: heat storage; BS: battery storage; EC: electrolyzer; H₂-S: hydrogen storage; FC: fuel cell)

| No. | HR kW _{th} | AC kW _{th} | Retrofit | | | | | HP kW _{th} | PV kW _p | HS kWh | BS kW | EC kWh | EC kW | H ₂ -S MWh _{LHV} | FC kW |
|---------------------|------------------------|------------------------|----------|------|-------|--------|-----------|------------------------|-----------------------|-----------|----------|-----------|----------|---|----------|
| | | | Wall | Roof | Floor | Window | th. dist. | | | | | | | | |
| 1 | 9.1 | 2 | 1 | 1 | 1 | 1 | 0 | - | - | - | - | - | - | - | - |
| 2 | - | 2 | 2 | 1 | 1 | 1 | 0 | 9.1~ | - | - | - | - | - | - | - |
| Grid _{ref} | - | 2 | 3 | 3 | 1 | 1 | 0 | 6.8~ | - | - | - | - | - | - | - |
| 3 | - | 2 | 2 | 3 | 1 | 1 | 0 | 6.9~ | 1.6 | - | - | - | - | - | - |
| Grid _{opt} | - | 2 | 3 | 3 | 1 | 1 | 0 | 6.2~ | 5.3 | 15 | - | - | - | - | - |
| 5 | - | 2 | 3 | 3 | 3 | 3 | 0 | 4.3~ | 6.8 | 14 | - | - | - | - | - |
| 6 | - | 2 | 2 | 3 | 3 | 3 | 1 | 4.8* | 10.9 | 14 | - | - | - | - | - |
| 7 | - | 2 | 3 | 3 | 3 | 3 | 1 | 4.4* | 11.4 | 20 | 1.1 | 7.2 | - | - | - |
| 8 | - | 2 | 3 | 3 | 3 | 3 | 1 | 4* | 11.4 | 32 | 1.9 | 16 | 1.3 | 2.1 | 0.5 |
| p=20 €/kWh | - | 2 | 3 | 3 | 3 | 3 | 1 | 4.3* | 11.4 | 26 | 3.3 | 26 | 1.9 | 2.3 | 0.5 |



Table S6. Technology parameter and price developments used in this study. Prices are real prices with reference to 2015.

| | 2020 | 2030 | 2040 | 2050 | Source |
|---|--------|-------|-------|-------|--------|
| Inverter | | | | | |
| Capex (€/kW) | 250 | 250 | 250 | 250 | |
| Lifetime (a) | 15 | 15 | 15 | 15 | |
| Efficiency (%) | 95 | 95 | 95 | 95 | |
| Photovoltaic | | | | | |
| Capex variable (€/kW _p) | 1,111 | 753 | 631 | 574 | |
| Opex (%/a) | 1.1 | 1.3 | 1.4 | 1.5 | |
| Lifetime (a) | 35 | 40 | 40 | 40 | 37 |
| Area (m ² /kW _p) | 5.1 | 4.6 | 4.3 | 4.0 | |
| System loss (%) | 14 | 5 | 4 | 3 | |
| Lithium-ion Battery^a | | | | | |
| Capex (€/kWh) | 264 | 116 | 101 | 87 | |
| Capex (€/kW) | 1,372 | 1,017 | 891 | 763 | |
| Capex (€) | 4,656 | 3,590 | 3,141 | 2,693 | 38 |
| Opex (%/a) | 2.5 | 2.5 | 2.5 | 2.5 | |
| Lifetime (a) | 15 | 15 | 15 | 15 | |
| Charge-/discharge-efficiency (%) | 95 | 95 | 95 | 95 | |
| Self-discharge (%/h) | 0.003 | 0.003 | 0.003 | 0.003 | 39 |
| Small wind turbine | | | | | |
| Capex (€/kW) | 3,800 | 3,600 | 3,500 | 3,400 | |
| Opex (%/a) | 2.6 | 2.5 | 2.5 | 2.4 | 37 |
| Lifetime (a) | 20 | 20 | 20 | 20 | |
| System losses (%) | 10 | 10 | 10 | 10 | 40 |
| Boiler | | | | | |
| Capex (€) | 2,800 | 2,800 | 2,800 | 2,800 | 35 |
| Capex (€/kW) | 100 | 100 | 100 | 100 | |
| Opex (€/kW) | 13 | 13 | 13 | 13 | |
| Efficiency (%) | 97 | 97 | 98 | 99 | 37 |
| Lifetime (a) | 20 | 20 | 20 | 20 | |
| Micro CHP plant | | | | | |
| Capex (€) | 10,500 | 8,333 | 6,167 | 4,000 | |
| Capex (€/kW _{el}) | 3,000 | 2,500 | 2,000 | 1,500 | |
| Opex (%/a) | 1 | 1 | 1 | 1 | 35 |
| Lifetime (a) | 20 | 20 | 20 | 20 | |
| Efficiency el. (%) | 35 | 35 | 35 | 35 | |
| Efficiency th. (%) | 60 | 60 | 60 | 60 | |
| Diesel generator | | | | | |
| Capex (€/kW) | 1,000 | 1,000 | 1,000 | 1,000 | |
| Opex (%/a) | 1.5 | 1.5 | 1.5 | 1.5 | |
| Lifetime (a) | 20 | 20 | 20 | 20 | |
| Max. full load hours (h/a) | 100 | 100 | 100 | 100 | |
| Diesel price (€/kWh) | 0.13 | 0.16 | 0.21 | 0.27 | 41 |
| Warm water storage | | | | | |
| Capex (€) | 800 | 800 | 800 | 800 | |
| Capex (€/kWh) | 35 | 35 | 35 | 35 | 35 |
| Lifetime (a) | 25 | 25 | 25 | 25 | |
| Efficiency (%) | 99 | 99 | 99 | 99 | 42 |
| Self-discharge (%/h) | 0.6 | 0.6 | 0.6 | 0.6 | 43 |
| Heat pump | | | | | |
| Capex (€) | 5,000 | 5,000 | 5,000 | 5,000 | |
| Capex (€/kW _{th}) | 600 | 600 | 600 | 600 | 35 |
| Opex (%/a) | 2 | 2 | 2 | 2 | |
| Lifetime (a) | 20 | 20 | 20 | 20 | |
| Heating rod | | | | | |



| | | | | | |
|---|-------|-------|-------|-------|--------------------------|
| Capex (€/kW) | 850 | 850 | 850 | 850 | |
| Opex (€/kW/a) | 8 | 8 | 8 | 8 | |
| Lifetime (a) | 30 | 30 | 30 | 30 | 37 |
| Efficiency (%) | 98 | 98 | 98 | 98 | |
| Electrolyzer | | | | | |
| Capex (€) | 3,000 | 2,500 | 2,000 | 1,500 | |
| Capex (€/kW _{el}) | 4,000 | 1,500 | 1,000 | 8,00 | |
| Opex (%/a) | 1 | 1 | 1 | 1 | 24, 44, 23, 45-47 |
| Lifetime (a) | 10 | 15 | 20 | 20 | |
| Efficiency (%) | 60 | 70 | 70 | 70 | |
| Compressor | | | | | |
| Capex (€) | 2,000 | 1,000 | 800 | 800 | |
| Capex (€/kW _{el}) | 2,500 | 1,800 | 1,300 | 1,000 | 23, 48, 45 |
| Opex (€/a) | 1 | 1 | 1 | 1 | |
| Lifetime(a) | 20 | 20 | 20 | 20 | |
| Hydrogen storage | | | | | |
| Capex (€/kWh) | 18 | 15 | 10 | 9 | 44, 23, 24, 37 |
| Lifetime (a) | 25 | 30 | 30 | 30 | |
| Fuel cell | | | | | |
| Capex (€) | 3,000 | 2,500 | 2,000 | 1,500 | |
| Capex (€/kW _{el}) | 4,000 | 1,500 | 1,000 | 800 | |
| Opex (%/a) | 1 | 1 | 1 | 1 | 23, 24, 49, 47 |
| Lifetime (a) | 10 | 15 | 20 | 20 | |
| Efficiency el. (%) | 47 | 50 | 50 | 50 | |
| Efficiency th. (%) | 47 | 46 | 48 | 48 | |
| Solar thermal plant | | | | | |
| Capex (€) | 4,000 | 4,000 | 4,000 | 4,000 | |
| Capex (€/m ²) | 350 | 350 | 350 | 350 | 35 |
| Lifetime (a) | 20 | 20 | 20 | 20 | |
| Opex (%/a) | 1 | 1 | 1 | 1 | |
| Efficiency (%) | 60 | 60 | 60 | 60 | Model: Aqua Plasma 15/27 |
| Air conditioner | | | | | |
| Capex (€/kW _{th}) | 245 | 245 | 245 | 245 | |
| Opex (%/a) | 2 | 2 | 2 | 2 | |
| Retrofit measures⁴ | | | | | |
| Capex var. wall (€/m ³) | 165 | 165 | 165 | 165 | |
| Capex fix wall (€/m ²) | 10.4 | 10.4 | 10.4 | 10.4 | |
| Capex var. roof (€/m ³) | 237 | 237 | 237 | 237 | 50 |
| Capex fix roof (€/m ²) | 11.3 | 11.3 | 11.3 | 11.3 | |
| Capex var. floor (€/m ³) | 125 | 125 | 125 | 125 | |
| Capex fix floor (€/m ²) | 30.75 | 30.75 | 30.75 | 30.75 | |
| Capex window option 1 (€/m ²) | 313 | 313 | 313 | 313 | 35 |
| Capex window option 2 (€/m ²) | 361.5 | 361.5 | 361.5 | 361.5 | |

^aPrice assumptions for Lithium-ion battery systems are taken from the Annual Technology Baseline³⁸ provided by the National Renewable Energy Laboratory (NREL). The assumptions are based on the “moderate” scenario for residential battery storage. Prices are converted to € for the year 2015 and do not include US sales tax. Since NREL data mostly represent US technology cost, the “moderate” scenario for the US represents a rather “conservative” battery system cost projection scenario for European market conditions, since soft costs are typically much larger in the US⁵¹.

⁴ Investment parameters for retrofit measures are shown for Germany and are adjusted with the country specific construction price index in other countries.

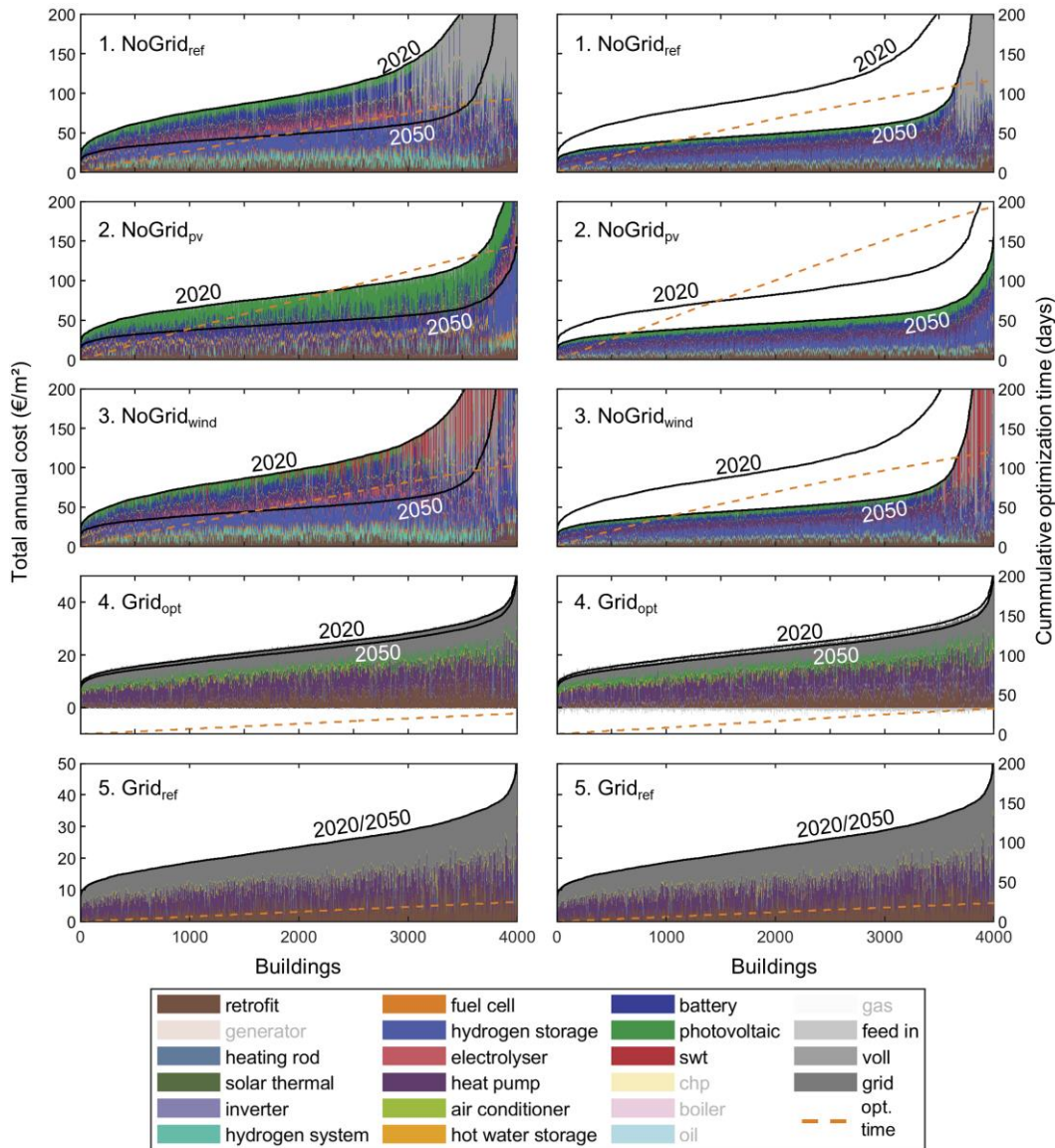


Figure S13. Visualization of the composition of the total annual costs per m² living area for 4000 cluster representative single-family buildings for scenarios 1-5 from Table S3 (left: 2020, right 2050). The orange dashed lines describe the cumulative optimization time. Optimization runs were conducted on 50 servers in parallel.

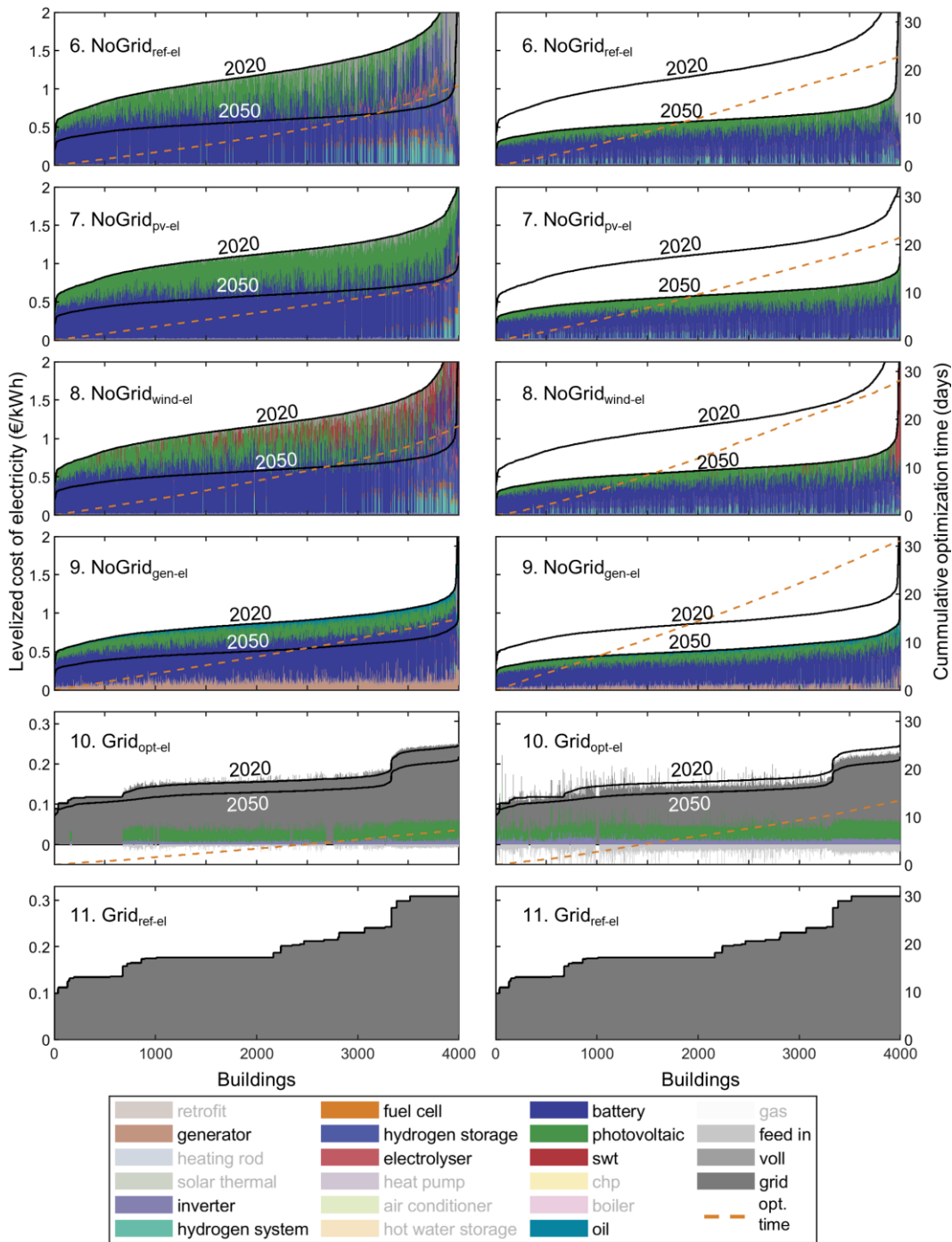


Figure S14. Visualization of the composition of the levelized cost of electricity (LCOE) for 4000 cluster representative single family buildings for scenarios 6-11 from Table S3 (left: 2020, right 2050). The orange dashed lines describe the cumulative optimization time. Optimization runs were conducted on 50 servers in parallel.

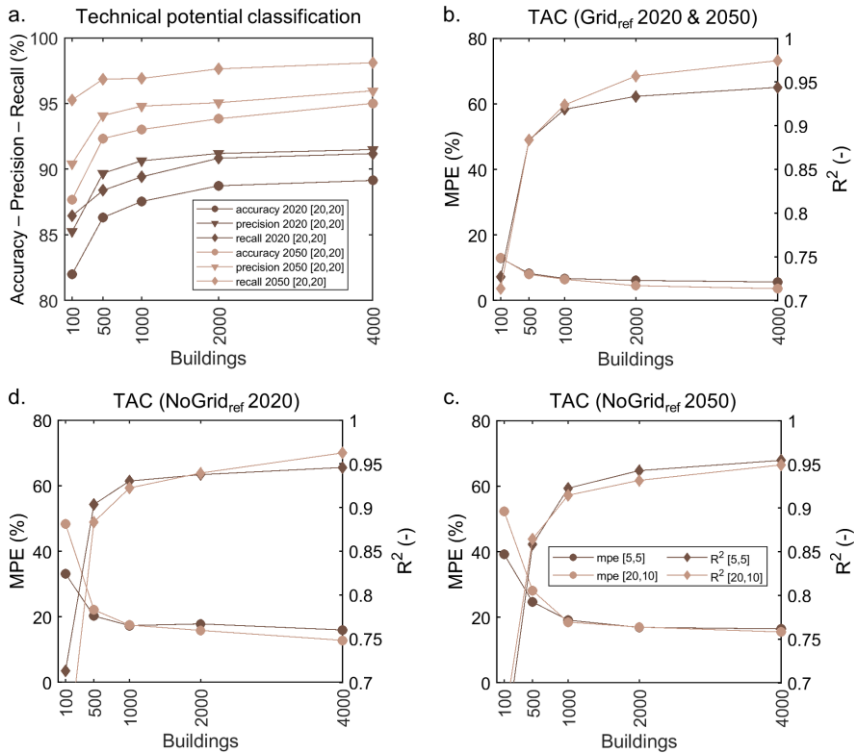


Figure S15. Representation of the performance of the neural networks depending on the training data set size (number of SFBs) and the configuration of the neural networks (number of neurons in the hidden layers, shown in square brackets).

The performance of the neural networks for the classification of the SFBs into potentially technical suitable and unsuitable SFBs is shown in the top left figure (a) using the accuracy, precision (=true positive / (true positive + false positive)) and recall (=true positive / (true positive + false negative)) as evaluation metrics. The bottom two figures and the top right figure show the results of the regression models for determining the TAC for the SFBs in the NoGrid_{ref} scenario in 2020 (c) and 2050 (d) and for the Grid_{ref} scenario (b). The TAC in the Grid_{ref} scenario do not change between 2020 and 2050. The performance of the neural networks is presented using the mean percentage error (MPE) and the coefficient of determination (R^2), which are calculated on the basis of the test data set (training, validation split → 80%/20%, test → 400 samples).

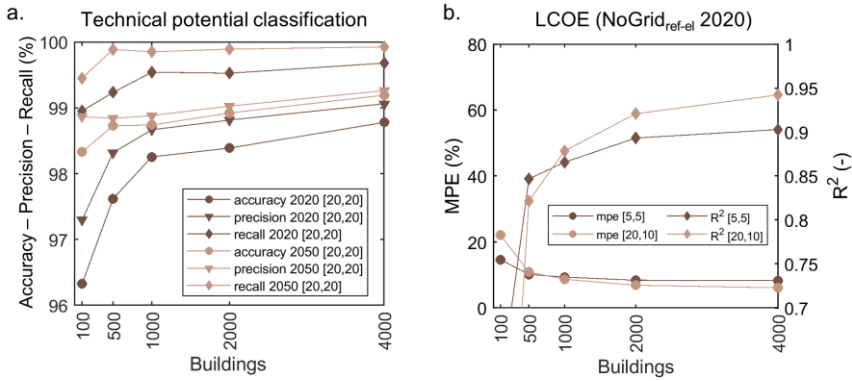


Figure S16. Representation of the performance of the neural networks depending on the training data set size (number of SFBs) and the configuration of the neural networks (number of neurons in the hidden layers, shown in square brackets).

The performance of the neural networks for the classification of the SFBs into potentially technical suitable and unsuitable SFBs is shown in the left figure (a) using the accuracy, precision (=true positive / (true positive + false positive)) and recall (=true positive / (true positive + false negative)) as evaluation metrics. The right figure shows the results of the regression model for determining the LCOE for the SFBs in the NoGrid_{ref-el} scenario in 2020 (b). The performance of the neural networks is presented using the mean percentage error (MPE) and the coefficient of determination (R²), which are calculated on the basis of the test data set (training, validation split → 80%/20%, test → 400 samples).

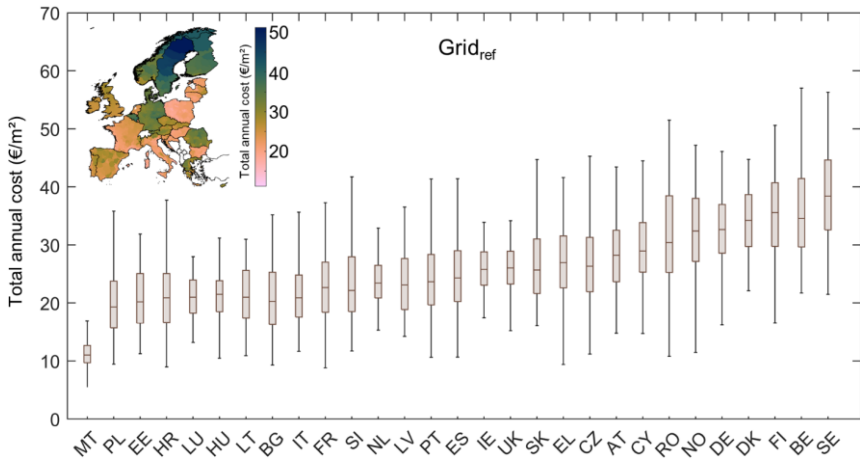


Figure S17. Visualization of the distribution of the total annual costs (TAC) for energy supply by country based on the Grid_{ref} scenario.

The countries are sorted by mean TAC per country in ascending order. The TAC of the reference system do not vary between 2020 and 2050 due to the above mentioned assumptions. The extreme values of the distributions are limited by the country-specific extreme values of the cluster representatives.

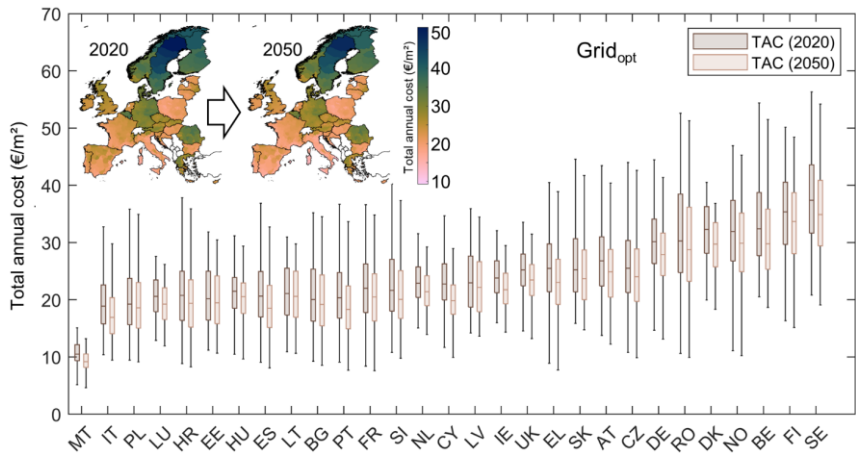


Figure S18. Visualization of the distribution of the total annual costs (TAC) for SFB in the Grid_{opt} scenario by country in 2020 and 2050. The countries are sorted by mean TAC per country in ascending order. The extreme values of the distributions are limited by the country-specific extreme values of the cluster representatives.

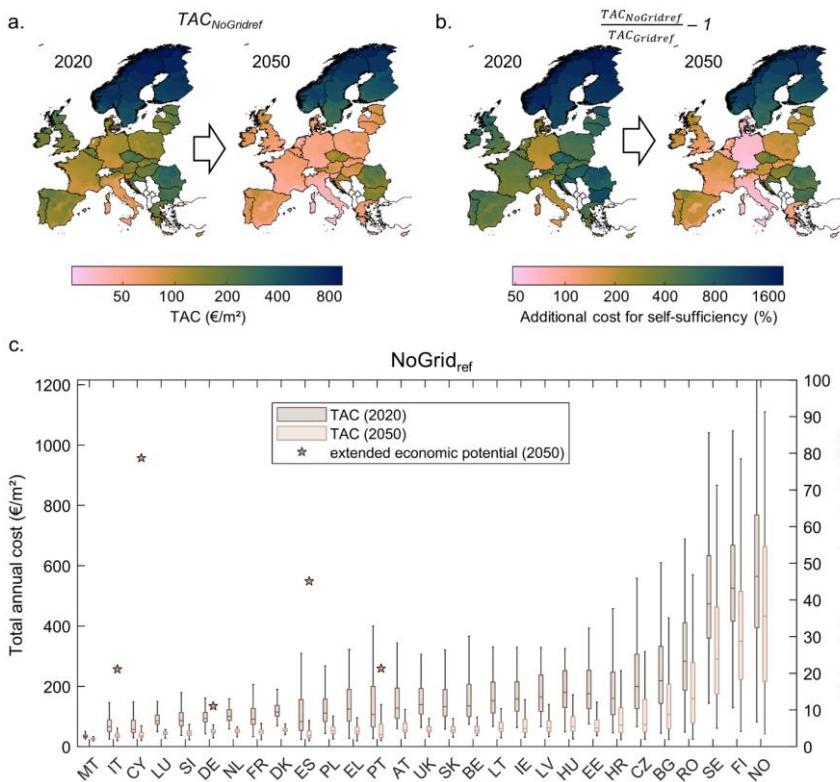


Figure S19. Visualization of the distribution of the total annual costs (TAC) in the NoGrid_{ref} scenario by NUTS3 region (a) and country (c) in 2020 and 2050. Furthermore, the ratio of the costs in the NoGrid_{ref} to the costs in the Grid_{ref} is shown (b), on the basis of which the (extended) technical potential is derived (c).

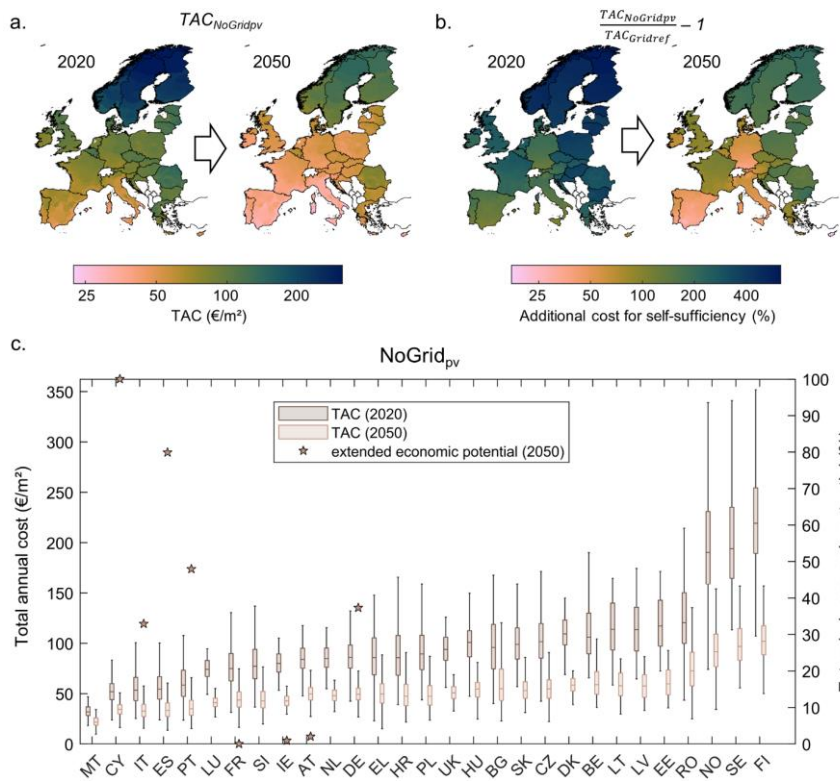


Figure S20. Visualization of the distribution of the total annual costs (TAC) in the NoGrid_{pv} scenario by NUTS3 region (a) and country (c) in 2020 and 2050. Furthermore, the ratio of the costs in the NoGrid_{pv} to the costs in the Grid_{ref} is shown (b), on the basis of which the (extended) technical potential is derived (c).

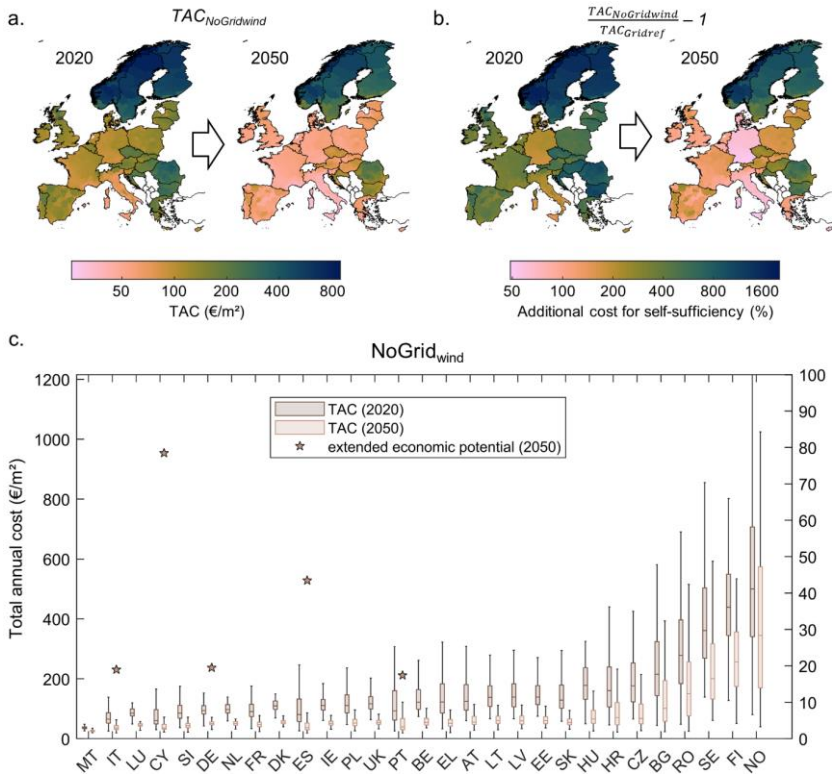


Figure S21. Visualization of the distribution of the total annual costs (TAC) in the NoGrid_{wind} scenario by NUTS3 region (a) and country (c) in 2020 and 2050. Furthermore, the ratio of the costs in the NoGrid_{wind} to the costs in the Grid_{ref} is shown (b), on the basis of which the (extended) technical potential is derived (c).

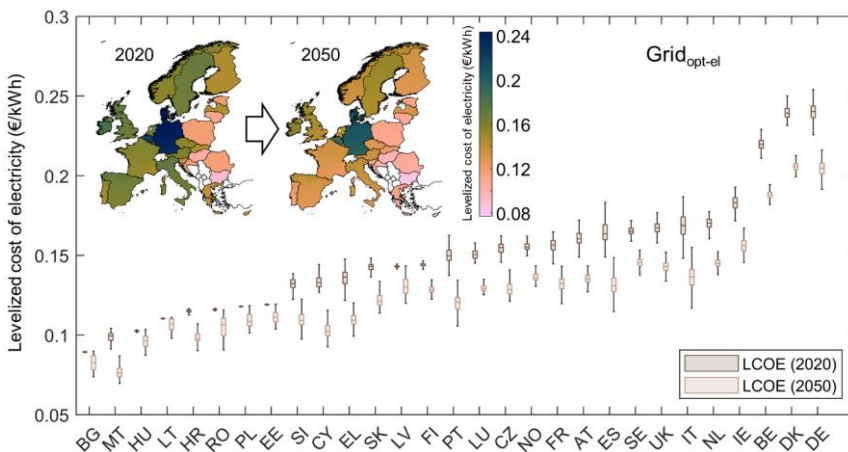


Figure S22. Visualization of the distribution of the levelized cost of electricity (LCOE) for the SFB in the Grid_{opt-el} scenario by country in 2020 and 2050.

The countries are sorted by mean LCOE per country in ascending order. The extreme values of the distributions are limited by the country-specific extreme values of the cluster representatives.

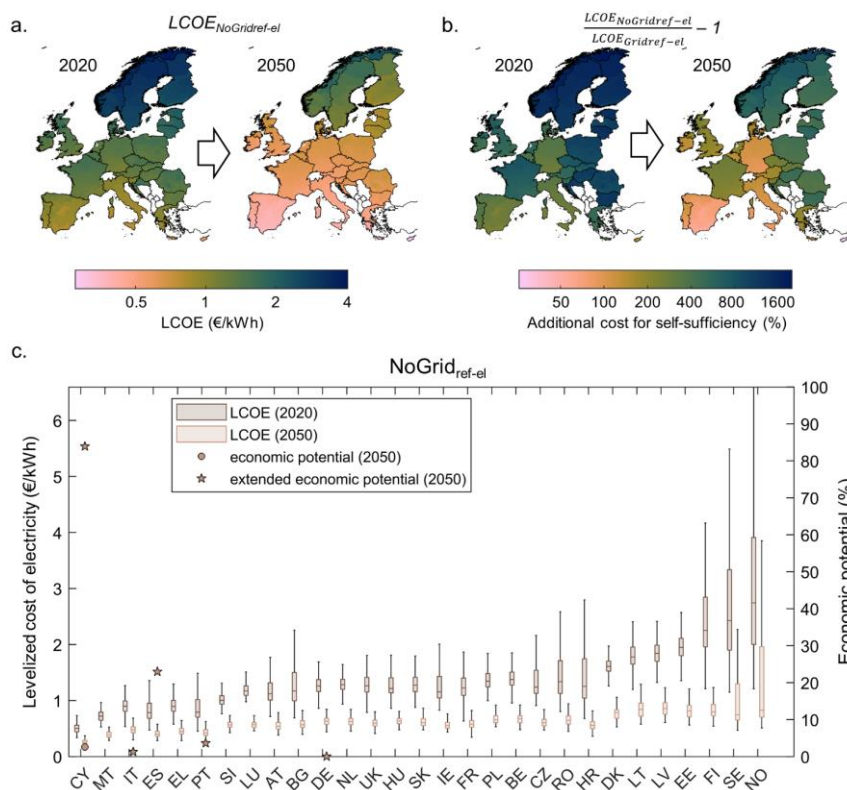


Figure S23. Visualization of the distribution of the levelized cost of electricity (LCOE) in the NoGrid_{ref-el} scenario by NUTS3 region (a) and country (c) in 2020 and 2050. Furthermore, the ratio of the costs in the NoGrid_{ref-el} to the costs in the Grid_{ref-el} is shown (b), on the basis of which the (extended) technical potential is derived (c).

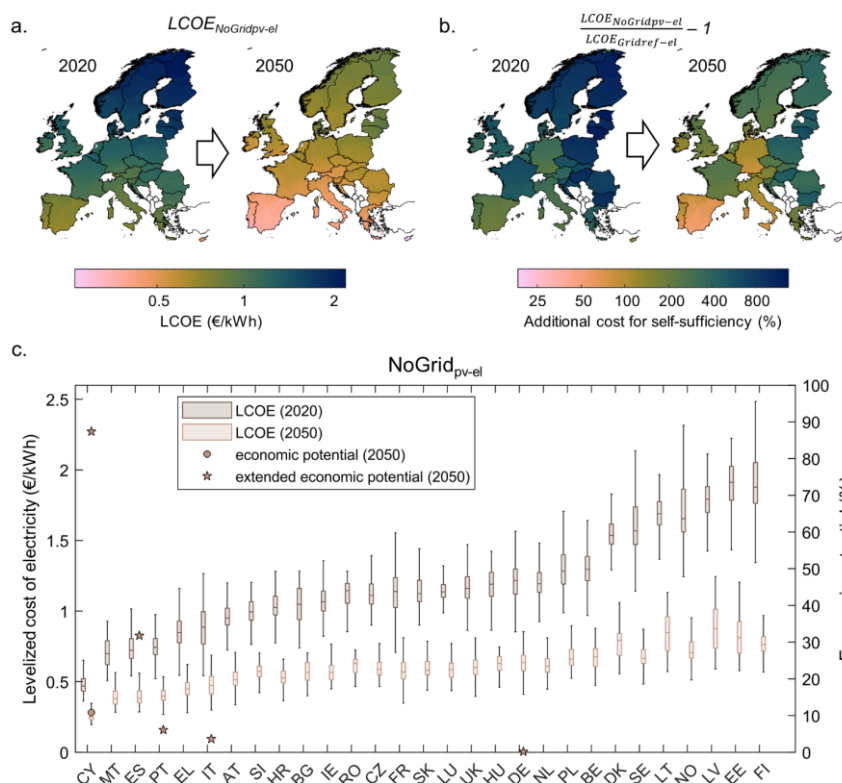


Figure S24. Visualization of the distribution of the levelized cost of electricity (LCOE) in the NoGrid_{pv-el} scenario by NUTS3 region (a) and country (c) in 2020 and 2050. Furthermore, the ratio of the costs in the NoGrid_{pv-el} to the costs in the Grid_{ref-el} is shown (b), on the basis of which the (extended) technical potential is derived (c).

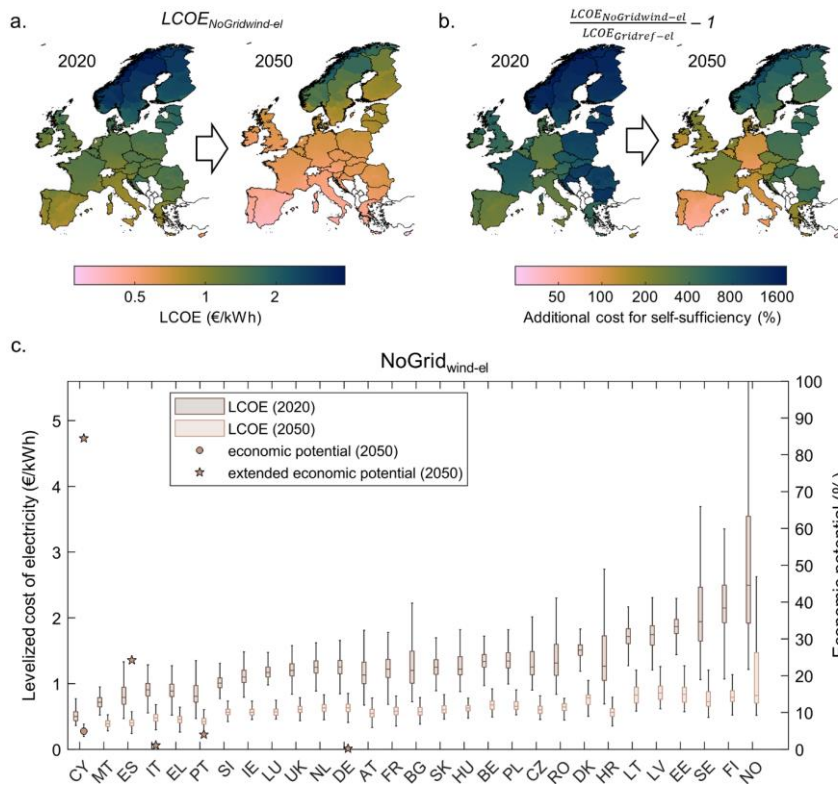


Figure S25. Visualization of the distribution of the levelized cost of electricity (LCOE) in the $NoGrid_{wind-el}$ scenario by NUTS3 region (a) and country (c) in 2020 and 2050. Furthermore, the ratio of the costs in the $NoGrid_{wind-el}$ to the costs in the $Grid_{ref-el}$ is shown (b), on the basis of which the (extended) technical potential is derived (c).

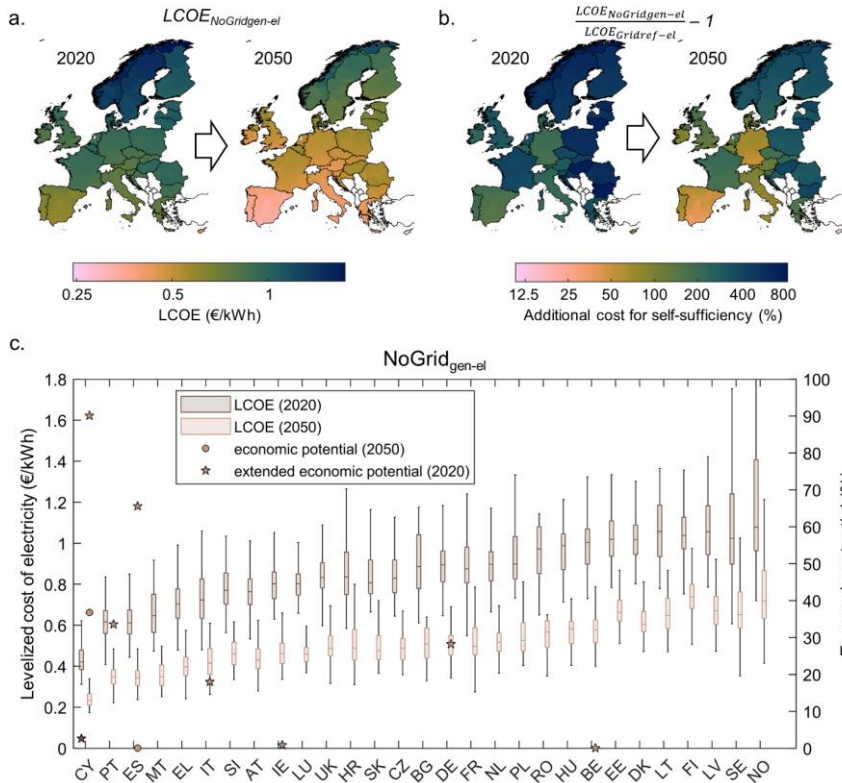


Figure S26. Visualization of the distribution of the levelized cost of electricity (LCOE) in the NoGrid_{gen-el} scenario by NUTS3 region (a) and country (c) in 2020 and 2050. Furthermore, the ratio of the costs in the NoGrid_{gen-el} to the costs in the Grid_{ref-el} is shown (b), on the basis of which the (extended) technical potential is derived (c).

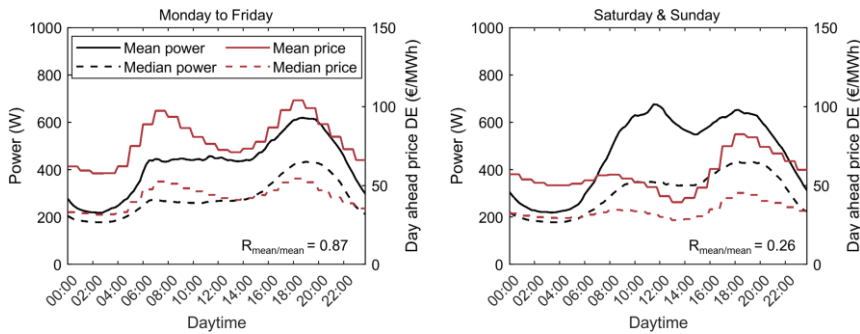


Figure S27. Daily shape of household electricity demand and historical German electricity day-ahead market prices from 2016 till 2022⁵².

The daily shape of household electricity demand is based on 108 German household demand profiles (34 profiles from Schlemminger et al.⁵³ + 74 profiles from Tjaden et al.⁵⁴).

Acknowledgments

This work was supported by the Helmholtz Association under the Joint Initiative, “Energy Systems Integration” (funding reference: ZT-0002) and the program, “Energy System Design”.



Author contributions

Conceptualization, M.K.; Methodology, M.K., E.N., J.W.; Formal Analysis, M.K., J.W., E.N.; Data Curation, M.K., J.W.; Writing – Original Draft, M.K., J.W., E.N.; Writing – Review and Editing, M.K., J.W., R.M., E.N.; Writing – Interactive Feedback, J.W., E.N., R.M. and W.F.; Visualization, M.K.; Project Administration, A.A., and W.F.; Funding Acquisition, A.A. and W.F.

Declarations of interest

The authors declare no competing interests

References

1. Voss, K., Goetzberger, A., Bopp, G., Häberle, A., Heinzel, A., and Lehmberg, H. (1996). The self-sufficient solar house in Freiburg—Results of 3 years of operation. *Solar Energy* 58, 17–23. 10.1016/0038-092X(96)00046-1.
2. Diermann, R. (2016). Ohne Netz: Erstes völlig energieautarkes Mehrfamilienhaus der Welt fertiggestellt, <https://www.wiwo.de/technologie/green/ohne-netz-erstes-voellig-energieautarkes-mehrfamilienhaus-der-welt-fertiggestellt/13883086.html>.
3. Umwelt Arena Schweiz (2023). Erstes energieautarkes Mehrfamilienhaus in Brütten, <https://www.umweltarena.ch/ueberuns/architektur-und-bauprojekte/>.
4. Sonnenhaus Institut e.V. (2022), <https://www.sonnenhaus-institut.de/>.
5. Home Power Solution (2022), www.homepowersolution.de.
6. Nilsson Energy (2022). Nilsson Energy, <https://nilssonenergy.com>.
7. Enkhardt, S. (2019). Schweden: Energieautarker Wohnkomplex wird mit 100 Prozent Photovoltaik und Wasserstoff versorgt. *PV Magazine* 2019.
8. VDI (26.08.2022). CO₂-freier Strom fürs Eigenheim. *VDI* 2022, 25.
9. Schleicher, V. (2014). Passivhaus ganz aktiv. *Energiesparhaus* 1.
10. Storch, T., Leukefeld, T. and Gross, U. (2016). Autonomes Hauskonzept - Ergebnisse aus 2 Jahren Realität, <https://docplayer.org/74043436-Autonomes-hauskonzept-ergebnisse-aus-2-jahren-realitaet-dr-ing-t-storch-1-prof-dipl-ing-t-leukefeld-2-prof-dr-ing-habil-u.html>.
11. Leitl (2016). VitalSonnenHausPro, https://www.vitalsonnenhauspro.at/wp-content/uploads/2016/10/LA_Leitl_Sonnenhauspro_Baureport_A4_EN_161013.pdf.
12. Weber, L. (07.04.2017). Der Traum vom Haus als Selbstversorger. Kombination aus Solarzellen und Brennstoffzelle. *Frankfurter Allgemeine* 2017.
13. Ren, Z., Paevere, P., and Chen, D. (2019). Feasibility of off-grid housing under current and future climates. *Applied Energy* 241, 196–211. 10.1016/j.apenergy.2019.03.068.
14. Khalilpour, R., and Vassallo, A. (2015). Leaving the grid. An ambition or a real choice? *Energy Policy* 82, 207–221. 10.1016/j.enpol.2015.03.005.
15. Liu, H., Azuatalam, D., Chapman, A.C., and Verbič, G. (2019). Techno-economic feasibility assessment of grid-defection. *International Journal of Electrical Power & Energy Systems* 109, 403–412. 10.1016/j.ijepes.2019.01.045.
16. Goldsworthy, M.J., and Sethuvenkatraman, S. (2018). The off-grid PV-battery powered home revisited; the effects of high efficiency air-conditioning and load shifting. *Solar Energy*. 10.1016/j.solener.2018.02.051.
17. Lovell, H., and Watson, P. (2019). Scarce data: off - grid households in Australia. *Energy Policy* 129, 502–510. 10.1016/j.enpol.2019.02.014.
18. Hughes, T.P. (1993). *Networks of power. Electrification in Western society, 1880-1930* (Baltimore: Johns Hopkins University Press). 9780801846144.
19. Sabadini, F., and Madlener, R. (2021). The economic potential of grid defection of energy prosumer households in Germany. *Advances in Applied Energy* 4, 100075. 10.1016/j.adapen.2021.100075.
20. Gorman, W., Jarvis, S., and Callaway, D. (2020). Should I Stay Or Should I Go? The importance of electricity rate design for household defection from the power grid. *Applied Energy* 262, 114494. 10.1016/j.apenergy.2020.114494.
21. Quoilin, S., Kavvadias, K., Mercier, A., Pappone, I., and Zucker, A. (2016). Quantifying self-consumption linked to solar home battery systems. Statistical analysis and economic assessment. *Applied Energy* 182, 58–67. 10.1016/j.apenergy.2016.08.077.

22. Lacko, R., Drobnič, B., Mori, M., Sekavčnik, M., and Vidmar, M. (2014). Stand-alone renewable combined heat and power system with hydrogen technologies for household application. *Energy* 77, 164–170. 10.1016/j.energy.2014.05.110.
23. Knosala, K., Kotzur, L., Röben, F.T., Stenzel, P., Blum, L., Robinius, M., and Stolten, D. (2021). Hybrid Hydrogen Home Storage for Decentralized Energy Autonomy. *International Journal of Hydrogen Energy* 46, 21748–21763. 10.1016/j.ijhydene.2021.04.036.
24. Gstöhl, U., and Pfenninger, S. (2020). Energy self-sufficient households with photovoltaics and electric vehicles are feasible in temperate climate. *PloS one* 15, e0227368. 10.1371/journal.pone.0227368.
25. Puranen, P., Kosonen, A., and Ahola, J. (2021). Technical feasibility evaluation of a solar PV based off-grid domestic energy system with battery and hydrogen energy storage in northern climates. *Solar Energy* 213, 246–259. 10.1016/j.solener.2020.10.089.
26. Schmid, F., and Behrendt, F. (2022). Genetic sizing optimization of residential multi-carrier energy systems: The aim of energy autarky and its cost. *Energy*, 125421. 10.1016/j.energy.2022.125421.
27. Ramirez Camargo, L., Nitsch, F., Gruber, K., and Dorner, W. (2018). Electricity self-sufficiency of single-family houses in Germany and the Czech Republic. *Applied Energy* 228, 902–915. 10.1016/j.apenergy.2018.06.118.
28. Eurostat (2021). Conventional dwellings by occupancy status, type of building and NUTS 3 region, https://ec.europa.eu/eurostat/databrowser/view/CENS_11DWOB_R3_custom_2547371/default/table.
29. Mata, É., Sasic Kalagasidis, A., and Johnsson, F. (2014). Building-stock aggregation through archetype buildings: France, Germany, Spain and the UK. *Building and Environment* 81, 270–282. 10.1016/j.buildenv.2014.06.013.
30. Sokol, J., Cerezo Davila, C., and Reinhart, C.F. (2017). Validation of a Bayesian-based method for defining residential archetypes in urban building energy models. *Energy and Buildings* 134, 11–24. 10.1016/j.enbuild.2016.10.050.
31. Kotzur, L., Markewitz, P., Robinius, M., Cardoso, G., Stenzel, P., Heleno, M., and Stolten, D. (2019). Bottom-up energy supply optimization of a national building stock. *Energy and Buildings*, 109667. 10.1016/j.enbuild.2019.109667.
32. Hachem-Vermette, C., and Singh, K. (2022). Optimization of energy resources in various building cluster archetypes. *Renewable and Sustainable Energy Reviews* 157, 112050. 10.1016/j.rser.2021.112050.
33. Fonseca, J.A., and Schlueter, A. (2015). Integrated model for characterization of spatiotemporal building energy consumption patterns in neighborhoods and city districts. *Applied Energy* 142, 247–265. 10.1016/j.apenergy.2014.12.068.
34. Borges, P., Travasset-Baro, O., and Pageset-Ramon, A. (2022). Hybrid approach to representative building archetypes development for urban models – A case study in Andorra. *Building and Environment* 215, 108958. 10.1016/j.buildenv.2022.108958.
35. Kotzur, L. (2018). Future Grid Load of the Residential Building Sector (Jülich: Forschungszentrum Jülich GmbH, Zentralbibliothek, Verlag). 978-3-95806-370-9.
36. DIN (2017). Energy performance of buildings – Method for calculation of the design heat load – Part 1: Space heating load, Module M3-3; German version EN 12831-1:2017, <https://www.beuth.de/de/norm/din-en-12831-1/261292587>.
37. Danish Energy Agency (2022). Technology Data, <https://ens.dk/en/our-services/projections-and-models/technology-data>.
38. National Renewable Energy Laboratory (2021). 2021 Annual Technology Baseline (ATB) Cost and Performance Data for Electricity Generation Technologies, <https://atb.nrel.gov/>.
39. Malhotra, A., Battke, B., Beuse, M., Stephan, A., and Schmidt, T. (2016). Use cases for stationary battery technologies: A review of the literature and existing projects. *Renewable and Sustainable Energy Reviews* 56, 705–721. 10.1016/j.rser.2015.11.085.
40. Olauson, J., Goude, A., and Bergkvist, M. (2016). Wind energy converters and photovoltaics for generation of electricity after natural disasters. *Geografiska Annaler: Series A, Physical Geography* 97, 9–23. 10.1111/geoa.12052.
41. Prognos, EWI, GWS (2014). Entwicklung der Energiemärkte - Energiereferenzprognose, https://www.prognos.com/sites/default/files/2021-01/140716_kurzfassung_42_seiten_energiereferenzprognose_2014.pdf.
42. Lindberg, K.B., Doorman, G., Fischer, D., Korpås, M., Ånestad, A., and Sartori, I. (2016). Methodology for optimal energy system design of Zero Energy Buildings using mixed-integer linear programming. *Energy and Buildings* 127, 194–205. 10.1016/j.enbuild.2016.05.039.
43. Schütz, T., Streblow, R., and Müller, D. (2015). A comparison of thermal energy storage models for building energy system optimization. *Energy and Buildings* 93, 23–31. 10.1016/j.enbuild.2015.02.031.
44. Beccali, M., Brunone, S., Finocchiaro, P., and Galletto, J.M. (2013). Method for size optimisation of large wind–hydrogen systems with high penetration on power grids. *Applied Energy* 102, 534–544. 10.1016/j.apenergy.2012.08.037.
45. Ulleberg, Ø., and Hancke, R. (2020). Techno-economic calculations of small-scale hydrogen supply systems for zero emission transport in Norway. *International Journal of Hydrogen Energy* 45, 1201–1211. 10.1016/j.ijhydene.2019.05.170.
46. Enapter (2020). H2 View Exclusive – Calculating the Cost of Green Hydrogen, <https://www.enapter.com/newsroom/h2-view-exclusive-calculating-the-cost-of-green-hydrogen>.
47. Grosspietsch, D., Thömmes, P., Girod, B., and Hoffmann, V.H. (2018). How, When, and Where? Assessing Renewable Energy Self-Sufficiency at the Neighborhood Level. *Environmental science & technology* 52, 2339–2348. 10.1021/acs.est.7b02686.
48. Reuß, M., Grube, T., Robinius, M., Preuster, P., Wasserscheid, P., and Stolten, D. (2017). Seasonal storage and alternative carriers. A flexible hydrogen supply chain model. *Applied Energy* 200, 290–302. 10.1016/j.apenergy.2017.05.050.
49. Wei, M., Lipman, T., Mayyas, A., Chien, J., Chan, S., Gosselin, D., Breunig, H., Stadler, M., McKone, T., Beattie, P., Chong, P., Colella, W. and James, B. (2014). A Total Cost of Ownership Model for Low Temperature PEM Fuel Cells in Combined Heat and Power and Backup Power Applications, <https://www.energy.gov/eere/fuelcells/articles/2014-total-cost-ownership-model-low-temperature-pem-fuel-cells-combined>.
50. Hinz, E. (2015). Kosten energierelevanter Bau- und Anlagenteile bei der energetischen Modernisierung von Altbauten. BMVBS (Darmstadt: Institut Wohnen und Umwelt). 9783941140509.

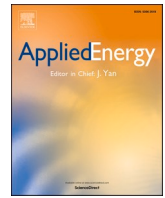
51. Chad, A. and Nate, B. (2021). Storage Futures Study: Storage Technology Modeling Input Data Report, <https://www.nrel.gov/docs/fy21osti/78694.pdf>.
52. Bundesnetzagentur (2023). SMARD Strommarktdaten, SMARD.de.
53. Schlemminger, M., Ohrdes, T., Schneider, E., and Knoop, M. (2022). Dataset on electrical single-family house and heat pump load profiles in Germany. Scientific data 9, 56. 10.1038/s41597-022-01156-1.
54. Tjaden, T., Bergner, J., Weniger, J. and Quaschnig, V. (2015). Repräsentative elektrische Lastprofile für Wohngebäude in Deutschland auf 1-sekündiger Datenbasis, <https://solar.htw-berlin.de/elektrische-lastprofile-fuer-wohngebaeude/>.

Paper C

Analysing municipal energy system transformations in line with national greenhouse gas reduction strategies

Reference

Kleinebrahm, Max; Weinand, Jann Michael; Naber, Elias; McKenna, Russell; Ardone, Armin (2023a): Analysing municipal energy system transformations in line with national greenhouse gas reduction strategies. In Applied Energy 332, Article 120515. DOI: [10.1016/j.apenergy.2022.120515](https://doi.org/10.1016/j.apenergy.2022.120515).



Analysing municipal energy system transformations in line with national greenhouse gas reduction strategies

Max Kleinebrahm^{a,*}, Jann Michael Weinand^b, Elias Naber^a, Russell McKenna^{c,d}, Armin Ardone^a

^a Institute for Industrial Production (IIP), Chair of Energy Economics, Karlsruhe Institute of Technology, Germany

^b Institute of Energy and Climate Research, Techno-economic Systems Analysis (IEK-3), Forschungszentrum Jülich, Germany

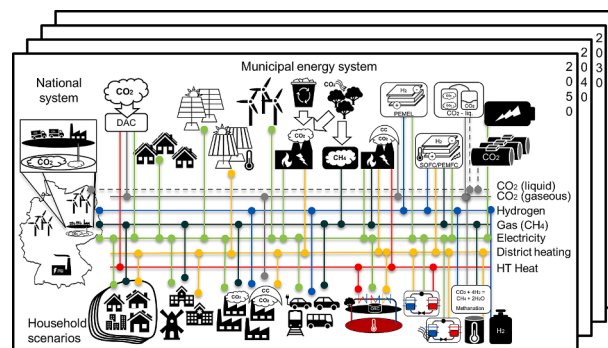
^c Chair of Energy Systems Analysis, Institute of Energy and Process Engineering, Department of Mechanical and Process Engineering, ETH Zürich, Switzerland

^d Laboratory for Energy Systems Analysis, Paul Scherer Institute, Switzerland

HIGHLIGHTS

- Local energy system transformation in line with national GHG reduction strategies.
- Consideration of temporal building stock dynamic and heterogeneity.
- Case study for central European city Karlsruhe.
- 192 stochastic building stock transformation scenarios.

GRAPHICAL ABSTRACT



ARTICLE INFO

Keywords:

Decentralised energy system
Household sector transformation
Climate neutrality
Transferable methods
Renewable energy
Building retrofit
Municipal energy system

ABSTRACT

Climate change mitigation and transformation strategies with expansion targets for renewable energy sources are defined at the national level. Due to the decentralised character of these sources, local energy system planning plays an important role. However, local communities often lack the capacity to develop energy concepts and thus exploit local renewable potentials consistently. This study develops a highly transferable methodology for deriving local energy system transformation scenarios in line with national greenhouse gas reduction strategies. Thus, an energy system optimisation model is substantially extended to collectively optimise the transformation of final energy demand in the residential, industry, tertiary and transport sectors, as well as established and niche greenhouse gas reduction technologies. Here, a focus is set on the building stock transformation, and a stochastic model is presented to better grasp and represent the dynamic developments and heterogeneity of the local building stock. Based on superordinate parameters such as retrofit rates and heating technology diffusion, the stochastic model generates informative building stock scenarios that are used as input for the developed energy system optimisation model. Exemplarily, the model is applied to the central European city of Karlsruhe. The results show that an increase of the retrofit rate to 2 %/a and strong electrification of the heat supply in the building sector is economically and environmentally beneficial. Furthermore, an accelerated expansion of

* Corresponding author.

E-mail address: max.kleinebrahm@kit.edu (M. Kleinebrahm).

photovoltaics compared to the national expansion rate can save costs and CO₂ emissions. Building on the methodology presented, transferable infrastructure models for the electricity, gas and district heating network should be developed that can be used to assess the feasibility of the transformation paths determined by the methodology presented.

Nomenclature

Parameters and Variables

| | |
|----------------------|--|
| A^f | Area potential for freestanding PV, ST |
| ac | Age class of building |
| ann | Annuity factor |
| c | Cost parameter |
| $c_{p,w}$ | Specific heat capacity of water |
| $ctoh$ | Centralisation type of heating |
| cy | Year of construction |
| dc | Weekday category |
| d_{el} | Demand electricity |
| ec | Energy carrier of building |
| EER | Energy efficiency ratio |
| $exp_{PV}^{loc/nat}$ | Local/national PV expansion rate |
| ht | Heating technology |
| loc | Location of building |
| $LCOSH$ | Levelised cost of saved heat |
| ρ_w | Water density |
| $p^{CHP/fPV/HP/ORC}$ | Electrical power CHP/PV/HP/ORC |
| p^{Gas} | Gas consumption |
| $pot_{PV}^{loc/nat}$ | Local/national PV potential |
| $Q^{CHP/HP/GT}$ | Thermal power CHP/HP/GT |
| rm | Retrofit measure |
| rr | Retrofit rate |
| rs | Retrofit share |
| $r_{p/m}$ | Peak to mean ratio |
| ry | Year of retrofit |
| sa | Surface area |
| SH | Space heating demand |
| $temp$ | Temperature |
| $u_{before/after}$ | U-value before/after retrofit |
| \dot{V}_B | Volumetric flow rate |
| x | Optimisation variable |
| λ | Heat conductivity |
| η | Efficiency |

Sets (running index)

| | |
|------------|------------------------------------|
| $A(a)$ | Representative Years |
| $BS(bldg)$ | Building stock |
| $HH(h)$ | Household transformation scenarios |
| $Int(i)$ | Investment intervals |
| $RM(rm)$ | Retrofit measures |
| $T(t)$ | Timesteps |
| $(comp)$ | Building envelope components |

Index

| | |
|------|-------------------|
| ei | Export and import |
|------|-------------------|

| | |
|--------|---------------------------------|
| em | Emission |
| fs | Freestanding |
| GT | Geothermal |
| htr | Historical transition rate |
| HP | Heat Pump |
| inv | Investment |
| op | Operation |
| ORC | Organic Rankine Cycle |
| PW | Production well |
| rt | Rooftop |
| $scen$ | Scenario |
| th | Thermal |
| tor | Time of retrofit |
| tsr | Technology specific requirement |

Acronyms

| | |
|---------|-------------------------------|
| AC | Air conditioner |
| ar | Ambitious retrofit |
| $AS-HP$ | Air source heat pump |
| bio | Biomass |
| CC | Carbon capture |
| CHP | Combined heat and power plant |
| CN | Climate neutral |
| cr | Conventional retrofit |
| DAC | Direct air capture |
| DHW | Domestic hot water |
| DH | District heating |
| el | Electricity |
| GHG | Greenhouse gas |
| $GS-HP$ | Ground source heat pump |
| HRU | Heat recovery unit |
| $LCOE$ | Levelised cost of electricity |
| $LCOSH$ | Levelised cost of saved heat |
| MAE | Mean absolute error |
| MFH | Multi family house |
| $MILP$ | Mixed-integer linear program |
| nc | New construction |
| PV | Photovoltaic |
| $o\&m$ | Operation & maintenance |
| SFH | Single family house |
| SH | Space heating |
| $SOFC$ | Solid oxygen fuel cell |
| ST | Solar thermal plant |
| $TDSC$ | Total discounted system cost |
| $UBEM$ | Urban building energy model |
| wc | Woody combustion |
| wte | Waste to energy |

1. Introduction

At the United Nations Climate Change Conference of the Parties in Glasgow in 2021, the 197 participating countries reaffirmed the Paris Agreement temperature goal. They recognized that limiting global warming to 1.5 °C requires rapid, deep and sustained reductions in

global greenhouse gas emissions [1]. To achieve these goals most cost-effectively, the participating countries are expected to develop long-term greenhouse gas emission reduction strategies, including an early and steady decarbonisation pathway [2]. Accordingly, countries such as Germany have committed to ambitious targets to reduce greenhouse gas emissions by 65 % by 2030 and become climate-neutral by 2045 [3].

Necessary means to achieve these targets include the large-scale

expansion of renewable energies, storage capacities and energy efficiency measures. However, the deployment of renewable energies happens mostly in local communities due to the decentralized character of these sources, and energy efficiency measures like building insulation require the decisions of individuals. Some local movements exist, such as the Covenant of Mayors [4,5], in which local authorities voluntarily commit to a high level of renewable energy deployment, but these local plans are not necessarily in line with national strategies. A direct transfer of national strategies to the local level would be impossible due to the heterogeneity of German municipalities in size, renewable energy potential and energy demand [6,7]. All of this considered, achieving national targets requires a high degree of coordination with local communities [8,9,10], and transferable approaches are needed to determine local energy system transformations in line with national targets.

The majority of the municipal energy system studies in the literature (see Section 2) use an overnight system transformation approach [8,9,11,12,13], which may lack information to policy-makers and energy system planners in terms of how and when to transition to a greenhouse gas (GHG) neutral energy system [14]. Consequently, there is a need for studies that, starting from the existing energy system, show a transformation path consisting of explicit energy system expansion and efficiency measures. While existing municipal energy system transformation studies [10,15,16,17] take into account temporal changes in, e.g., energy carrier and technology prices, they lack the consideration of temporal dynamics with regard to expansion rates of renewable energy technologies and efficiency measures like building retrofits. This can lead to an unrealistically fast spread of measures, compared to the national system transformation, as soon as the measures become economically viable (e.g. [17]). In the transformation studies mentioned, such unrealistically rapid dissemination of, e.g., retrofit measures in the residential building sector is particularly favored by a strongly aggregated depiction of the building stock to reduce computational complexity. To overcome the mentioned issues, the municipal energy system optimisation model RE³ASON [10,15,17,18] is extended in this work to answer the following research questions.

- What are the techno-economically optimal transformation paths of municipal energy systems in the context of national energy system transformations?
 - How can temporally dynamic developments in the residential building stock be appropriately captured in a transferable and open-data-based municipal energy system transformation model?
 - What are optimal local residential building stock transformations regarding key parameters such as retrofit rate, depth, and degree of electrification?
 - What influence do local limitations on expansion rates of renewable energy technologies have on local energy system transformations?
 - What influence does the exclusion/consideration of individual technology options such as biomass, deep geothermal energy, or wind power have on cost and emission developments?

Accordingly, the energy system optimisation model is substantially extended to collectively optimise the transformation of final energy demand in the industry, tertiary, transport sectors, and of the building stock, as well as established and niche greenhouse gas reduction technologies. In order to consider temporal dynamic changes and the heterogeneity in the municipal residential building stock within the energy system optimisation, a stochastic, spatially resolved building stock simulation is introduced in this study and integrated into the energy system optimisation model RE³ASON. To avoid unrealistically high expansion rates of renewable technologies, local maximum yearly expansion rates are defined in accordance with national developments. Furthermore, the overall portfolio of energy system supply technologies is expanded to include all relevant technology options considered in the

respective national energy system transformation scenarios. In order to take into account developments of the energy demand transformation in all sectors, NUTS3-level specific final energy demand developments in the industry, transport and tertiary sectors are temperature corrected and integrated into RE³ASON.

The transferable model is demonstrated for the energy system transformation of the German city Karlsruhe. All methods rely on publicly available data and can be easily used to support local authorities like small scale energy supply system operators, distribution system operators, and public utilities.

In the following, a comparison of the developed approach with the existing literature is given in Section 2. Subsequently, the methodology for municipal energy system planning is presented in Section 3 and its applicability is demonstrated through a case study in Section 4. Section 5 discusses the methodology and results before the article is concluded in Section 6.

2. Literature review

The relevance of the municipal energy system planning research field has increased significantly over the past decades resulting in a total of 1,235 studies in 2019 [5]. Scheller et al. [19] provide an overview of energy system optimisation models with a high spatial, temporal and contextual resolution for the support of local decision makers at the municipal level and define challenges that should be addressed in the development of future models (e.g., integrated view, spatial planning, temporal resolution and uncertainty analysis). Kachirayil et al. [20] reviewed 116 case studies of local, integrated energy system models to identify best-practice approaches to model flexibility and address non-technical constraints. Yazdanie and Orehoung [21] examined gaps in the field of urban energy system planning and showcased the need for more integrated modelling approaches and more comprehensive energy modelling scenarios to represent social factors and system imperfections.

Several studies exist that use overnight modelling approaches to determine energy system target states without analysing the transformation process to reach that state [8,9,11,12,13,22,23,24,25,26]. In Østergaard et al. [11], a scenario for Aalborg (Denmark) entirely based on renewable energy in 2050 is studied. In simulations with the EnergyPLAN model, the scenario is evaluated in terms of the total annual energy balance and the hourly balance between electricity generation and demand. A similar study utilizes the EnergyPLAN model, in this case, to determine a 100 % renewable energy system using low-temperature geothermal energy for district heating in Frederikshavn [12]. Sveinbjörnsson et al. [13] optimize the energy system of the municipality Sønderberg, which aims to reach zero net CO₂ emissions in 2029. Several scenarios show that those with a high degree of electrification perform better than those with a high degree of biomass utilisation. Although these studies make assumptions about the cost development of technologies, the development of energy carrier prices, and emission factors, the municipalities are not explicitly considered in the context of a national energy system transformation scenario. Other municipal energy system analyses exist which analyse the interactions of local and national energy systems. However, these studies are mostly not dealing with the realisation of national scenarios or targets through action at the local level. For example, in Aunedi et al. [22], the interaction with the national level in the cost-efficient supply of local district heating systems is only captured by renewable penetration levels and electricity price volatility. Orehoung et al. [24] use the energy hub concept to manage the relations between energy flows at neighbourhood scale and further extend the concept by the integration of a building simulation tool to be able to evaluate and size urban energy systems according to their energy autonomy, economic and ecological performance. They show that the suggested method can lower peaks in energy demand of neighbourhoods, but no detailed interactions with transformation scenarios of the overarching system are considered. Two

Table 1
Description of the model extensions of the energy system optimisation model RE³ASON.

| No. | RE ³ ASON (before) [18,10,15,17,16] | RE ³ ASON + extensions |
|-----|--|---|
| 1 | Aggregated depiction of building stock by archetype buildings (no consideration of temporal inertia) | Multiple stochastic building stock scenario simulations as a binary decision variable in energy system optimization (Section 3.1 and 3.2.1) |
| 2 | Constant tertiary, industry and transport sector energy demand | Integration of transport, tertiary and industry sector energy demand transformation (Section 3.2.2) |
| 3 | Existing technologies: (see [17,18]) | Existing technologies + freestanding PV&ST, H ₂ infrastructure, CO ₂ -flows and CO ₂ mitigation technologies + consideration of technology expansion rates (Section 3.3) |
| 4 | One-step optimisation solving approach based on four typical weeks per year | Two-step optimisation solving approach taking into account hourly resolution (Section 3.3) |

Table 2
Overview of publicly available sources used in this study to simulate the local residential building stock energy demand.

| Source | Information | Spatial resolution |
|--------|--|-------------------------|
| [29] | Residential building typology (U-values, building geometry, domestic hot water generation) | National level |
| [93] | Census (building age, size, type of heating, type, number of households, household size) | 1 km ² grid |
| [28] | Building location, footprint, height | Individual building |
| [94] | Roof structures, roof orientation | Individual building |
| [30] | Retrofit state, energy carrier, heating technology, ventilation systems, solar-thermal | National level |
| [95] | Solar-thermal installations | Federal state level |
| [34] | New constructions | Municipal level |
| [32] | Buildings under preservation order | National level |
| [35] | Heating technology age | National level |
| [37] | Scenarios for residential air conditioning dissemination | National level |
| [86] | Information about energy-related household activities | National level |
| [85] | Electricity consumption of household devices | National level |
| [57] | Weather data (temperature, irradiation, wind speed) | 30 km ² grid |

exceptions, which are particularly relevant to the present study, are Thellufsen and Lund [9] and Thellufsen et al. [8]. In Thellufsen and Lund [9], a methodology is developed to show how well future local energy systems integrate with the surrounding national energy system by analysing system interactions in a sequential procedure. This methodology is applied in the context of a national scenario for 2030 for the Danish cities of Copenhagen and Sønderberg. In Thellufsen et al. [8], this methodology is extended to investigate a local energy system scenario of the municipality Aalborg in a 100 % renewable energy context of Denmark and Europe. In both articles, the EnergyPLAN model is applied, and thus, a simulation to analyse supply and demand for a specific target state is performed, in contrast to the methodology presented in this study, which analyses transformation paths. Murray et al. [25] present an approach for the comparison of storage systems in neighbourhood decentralized energy system applications from 2015 to 2050. This study is of particular importance, since the authors take into account potential future developments of the overarching energy system based on the Intergovernmental Panel of Climate Change's 'Special Report on Emissions Scenarios'. Based on these scenarios, they project energy demand and renewable potential for a rural and an urban neighbourhood in Switzerland till 2050 and calculate optimal energy system configurations for the years 2015, 2020, 2035 and 2050. In

contrast to the approach presented in this study, Murray et al. [25] focus on neighbourhoods and conduct single optimisations for each respective year (myopic approach) and therefore do not consider the transformation of the energy system in closed form.

In addition to the overnight approaches presented, several studies have examined energy system transformations in municipalities from the point of view of a central municipal planner. McKenna et al. [10] developed a feasible energy concept for the German municipality of Ebhausen by 2030. The results of a mathematical energy system optimisation are evaluated in a multi-criteria decision approach with preferences derived from workshops with municipal decision-makers. The best performing alternatives that emerged showed similarities in installed technologies and measures and thus could be used as robust recommendations for future energy system design. In Weinand et al. [16] and Weinand et al. [17], the costs of energy system transformations by 2030 and 2050, respectively, are optimized for all 11,131 German municipalities. The former study focuses on complete energy autonomy in the municipalities, i.e., complete self-supply of energy demand by local renewable energies. The study shows that energy autonomy is feasible in 56 % of German municipalities and that the Levelised Costs of Electricity (LCOEs) increase on average by 0.41 €/kWh compared to the optimized energy system without autonomy. Weinand et al. [17] investigated the impact of the opposition towards onshore wind due to the influence of landscape beauty on the LCOEs. LCOEs can increase by up to 0.07 €/kWh when the onshore wind is excluded.

In the present article, a techno-economic optimisation of the municipal energy system transformation is presented with a particular focus on the residential building stock. In contrast to previous studies, which use an aggregated household sector energy demand [8,9,12] or a small number of representative archetype buildings to describe the household sector energy demand transformation [15,17], the present study introduces a spatially highly disaggregated stochastic building stock model and combines it with a municipal energy system optimisation approach. In Weinand et al. [15], already a small number of representative buildings (~10 buildings per municipality) lead to long runtimes of the energy system optimisation model (up to multiple days, depending on technologies considered). However, due to the small number of archetype buildings, no restrictions regarding maximum achievable retrofit and technology modernisation rates were imposed in the model. In this way, optimal investment decisions at the building level could be taken into account, but without considering relevant restrictions regarding the temporal dynamics of the building stock. Therefore, the inertia of the building stock transformation process was not considered in previous studies. This study aims to solve this shortcoming by presenting a stochastic building stock transformation model, upstream to the energy system optimisation (no. 1 in Table 1). This way, the high heterogeneity of the residential building stock is captured by considering each residential building. Furthermore, the building stock model can represent the temporal dynamics of the building stock transformation by taking into account core trends regarding future retrofit rates, retrofit depth, technology modernisation, and expansion rates. Through integrating informative and possible building stock transformation scenarios in the sector-coupled municipal energy system optimisation model, optimal transformation pathways of the local energy system can be determined in line with the national energy system. Besides the transformation of the household sector, local final energy demand developments in the industry, tertiary and transport sectors are integrated into RE³ASON to holistically capture the energy demand transformation (no. 2). Additionally, the existing municipal energy system optimisation model is further expanded to include relevant established and novel innovative (niche) technologies for the reduction of greenhouse gas emissions (no. 3). Finally, the optimisation model RE³ASON is extended by a two-stage approach to solving the optimisation problem, which enables the optimisation problem to be solved in hourly resolution (no. 4). All extensions are summarised and contrasted with the former model implementations in Table 1.

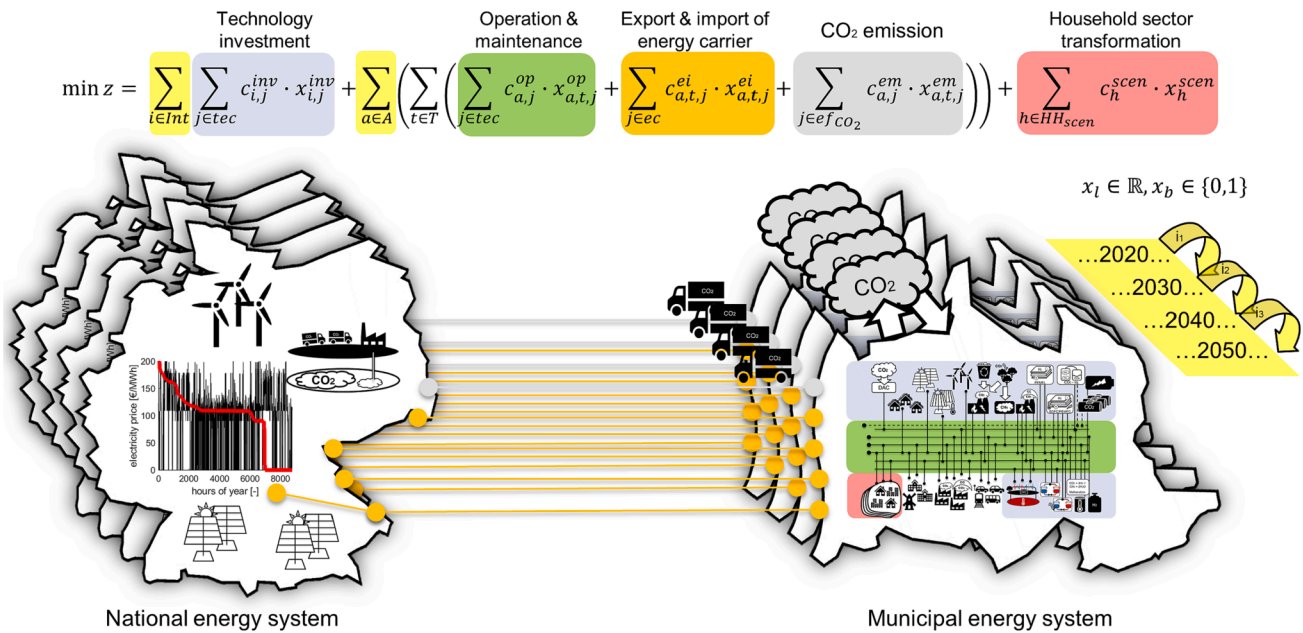


Fig. 1. Visualisation of the objective function to minimise total discounted system cost of the municipal energy system transformation.

3. Methodology

A large amount of data is required to model municipal energy systems (see Table 2). A large part of the data, such as renewable potentials or information on the building stock, is municipality-specific. The base energy system optimisation model RE³ASON [18,15] minimizes the effort involved in data collection to be easily transferable to different German municipalities without additional effort. The only input required is the name of the municipality. Based on the location of the municipality, local weather data, spatially resolved population and building stock information and land use potentials for renewable energy sources are obtained and further processed to derive local energy demand and technology-specific renewable potentials. In a downstream optimisation model, total discounted system costs are calculated from a macroeconomic municipality planner perspective for the optimal energy system transformation. Thereby, the size and dispatch of the energy technologies and demand side measures are optimized. This model is substantially extended in this study.

In Section 3.1, the objective function of the RE³ASON model is shown, and extensions made are introduced. Subsequently, the new and extended approaches for modelling the energy demand side transformation are presented in Section 3.2. Finally, Section 3.3 describes the energy supply side extensions and the new process for solving the municipal energy system optimisation model.

3.1. Objective function

Fig. 1 presents the objective function of the mixed-integer linear program (MILP) optimisation model for minimizing the total discounted system costs from the point of view of a public welfare-oriented municipality planner. The orange and grey connections to the national energy system describe the different energy carriers and CO₂ flows which are considered in the optimization by using long-term energy carrier $c_{a,t,j}^{ei}$ and CO₂ emission $c_{a,j}^{em}$ price developments from the superordinate national scenario. To adequately capture the high variability of the exchange electricity prices and the supply of fluctuating renewable energies, an hourly model resolution is used in contrast to previous studies (see e.g. Weinand et al. [16]). The blue and green highlighted area describes the costs connected to the expansion $c_{i,j}^{inv}$ and operation and maintenance $c_{a,j}^{op}$ of the local energy system. Investments in

technologies $x_{i,j}^{inv}$ take place in the intervals $i \in Int$ in between the representative years of consideration $a \in A$. The algorithm used to solve the MILP optimization problem is presented in Section 3.3.

The consideration of multiple household transformation scenarios is represented by the area highlighted in red. In this study, investment decisions regarding the household sector transformation are made at the level of individual residential buildings outside the optimisation model in an upstream simulation model with a high spatial resolution. This way, the high heterogeneity of the residential building stock is considered without making the model intractable. Furthermore, the dynamics of the building stock can be examined in more detail, taking into account different retrofit rates, retrofit depth, modernisation rates for heating technologies and additional technologies like heat recovery units (HRU) and air conditioners (AC). No optimal decisions are made at the individual building level from the point of view of a central municipal planner. However, transformations at the individual building level are derived based on top-down predetermined national framework conditions. To account for the interaction during the transformation of the local energy system and the local residential building sector in the optimisation model, multiple household scenarios are calculated in the upstream simulation model, between which the optimiser can choose in the form of a discrete decision variable x_h^{scen} . In addition to the development of the final energy demand, the costs associated with the residential building sector transformation c_h^{scen} are calculated in the upstream model.

3.2. Energy demand transformation

A spatially highly resolved stochastic simulation model for the transformation of the local residential building stock is developed in Section 3.2.1, that while considering the framework conditions of the national building stock transformations, determines the change in the local building stock. Furthermore, a top-down approach for the development of the final energy demand in the sectors of industry, tertiary and transport is described in Section 3.2.2.

3.2.1. Bottom-up residential building and household sector transformation

Based on the municipal building stock, Fig. 2 presents the generation of different residential building transformation scenarios using publicly available data and information from national energy system

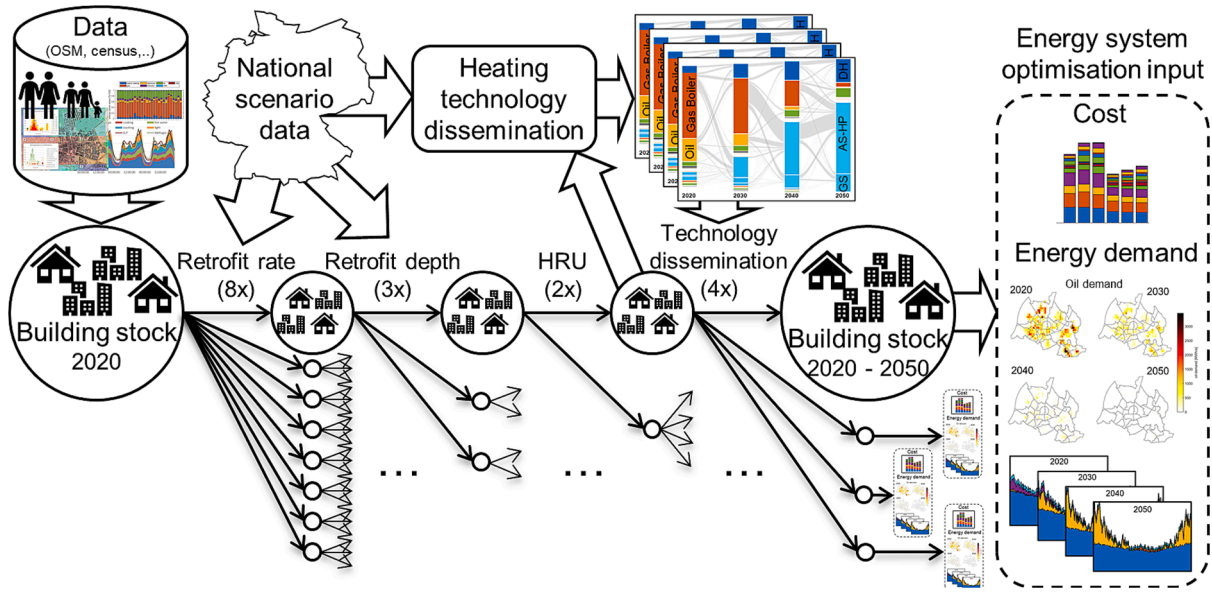


Fig. 2. Generation of different residential building transformation scenarios using transferrable data and information from national energy system transformation studies.

transformation studies. Before the generation of the scenarios is presented, the derivation of the initial building stock is described.

3.2.1.1. Initial building stock. To determine the local building stock in 2020, building stock information about size, age, and type of buildings, as well as the number and size of households in 2011 is derived based on 1 km² spatially resolved census data [27], Open Street Map building information [28] and the German residential building typology [29] by using the procedure presented in Mainzer [18]. A comparison of our approach with current urban building energy modelling developments in literature can be found in the Appendix (see *Urban building energy modelling*). In order to determine the initial retrofit state of the residential buildings, empirically collected building age class-specific retrofit shares rs_{ac} of the German residential building stock are taken from Cischinsky and Diefenbach [30]. Based on these shares, the retrofit state for all buildings $bldg$ of the local residential building stock BS in the year 2016 are sampled by using a Bernoulli distribution according to eq. (1).

$$X_{bldg}^{rs} \sim \text{Bernoulli}\left(P\left(ac_{bldg}\right)\right) \quad \forall bldg \in BS \quad (1)$$

Buildings under preservation order are excluded when sampling the retrofit state. Analogously to [31], 20 % of the Multi-Family Houses (MFH) before 1950, 10 % of the Single-Family Houses (SFH) before 1950 and 5 % of all buildings between 1950 and 1994 are excluded from retrofit measures [32]. The year of retrofit is estimated by assuming that retrofit cycles have been carried out uniformly since 1990 [33]. A piecewise linear dependency between the retrofit probability and the building age is assumed for the probability that a building is renovated in a given year. The relationship is shown in eq. (2), where cy_{bldg} describes the construction year of the building.

$$X_{bldg}^{ry} \sim \text{Bernoulli}\left(P\left(cy_{bldg}, year\right)\right) \quad \forall bldg \in BS, \forall year \in [1990, 2016] \quad (2)$$

Depending on the time of the retrofit, different retrofit depths are assumed. Buildings that were refurbished before 2009 are refurbished to the respective new construction standard of the year of retrofit. From 2009 onwards, the U-values of the refurbished buildings are based on the usual retrofit standard of the IWU building typology for Germany [29]. A retrofit rate of 1 %/a (full retrofit equivalents) between 2016 and

2020 is used to derive the initial building stock state in 2020. Spatially resolved information at the municipality level is used to include new buildings and building demolitions [34]. For the geographic placement of future newly constructed buildings within the municipality, new construction shares of the districts after the year 2000 are used [27]. In this way, unrealistically high growth rates in inner-city areas are avoided. No new locations are set for the exact placement of the buildings, but duplicates of existing buildings are created.

For the allocation of the heating technologies, the spatially resolved information from the census survey on the centralisation type of heating¹ is combined with the Germany-wide information on energy carrier and heating technology distributions depending on the building type and building age [27,30]. In the first step, each building is assigned an energy carrier ec_{bldg} using a multinomial distribution based on the building's construction year cy_{bldg} , building type $type_{bldg}$ and centralisation type of heating $ctoh_{bldg}$ eq. (3).

$$X_{bldg}^{ec} \sim M\left(P\left(cy_{bldg}, type_{bldg}, ctoh_{bldg}\right)\right) \quad \forall bldg \in BS \quad (3)$$

Based on the energy carrier, the specific heating technology ht_{bldg} is assigned to the respective building in a second step eq. (4).

$$X_{bldg}^{ht} \sim M\left(P\left(cy_{bldg}, type_{bldg}, ctoh_{bldg}, ec_{bldg}\right)\right) \quad \forall bldg \in BS \quad (4)$$

The age of the heating technology is estimated based on the building age and the nationally available information on the age distribution of the different heating technologies [35].

Based on the parameterized building stock, the demand for useful energy of household electricity devices, domestic hot water, and space heating is calculated in an hourly resolution based on a combined occupancy and thermal building model described in the Appendix (see *Residential energy demand simulation*).

3.2.1.2. Residential building stock transformation. The transformation of the local building stock is visualized in Fig. 2. In the first step, the buildings to be retrofitted are identified for each simulation year,

¹ Type of heating: district heating, block heating, central heating, room heating, story heating.

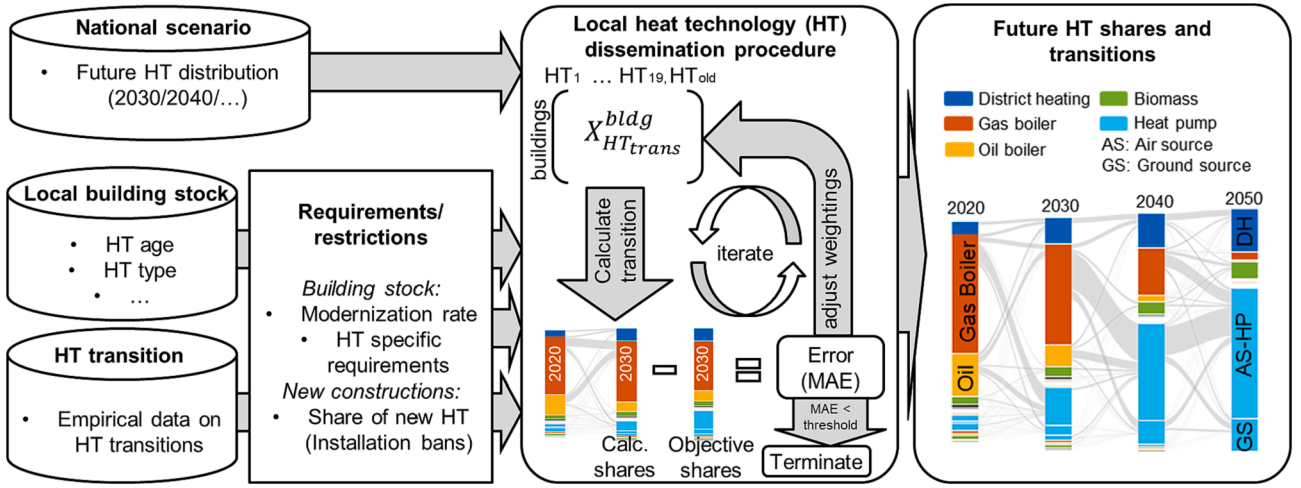


Fig. 3. Visualisation of the iterative process to calculate the dissemination of heating technologies in the local building stock based on overarching changes at the national level.

starting from 2020 until the target year. An annual retrofit rate rr in the form of full retrofit equivalents as well as information on the percentage of deep retrofits rr_{deep} is required as input. For the selection of the buildings to be renovated, the space heating demand after a standard and deep retrofit, as well as the energy-related cost of the retrofit measures c_{rm} are calculated for all buildings of the building stock based on the component-specific surface areas sa_{comp}^{bldg} , U-values u_{comp}^{bldg} , prices c_{comp} and an assumed heat conductivity λ of 0.035 W/(mK) according to Hinz [36] eq. (5).

$$c_{rm}^{bldg} = \sum_{comp} \left(\left(\frac{1}{u_{comp,after}^{bldg,rm}} - \frac{1}{u_{comp,before}^{bldg}} \right) \cdot \lambda \cdot c_{comp,var} + c_{comp,fix} \right) \cdot sa_{comp}^{bldg} + \left(\frac{1 - u_{window,after}^{bldg,rm}}{0.2} \cdot c_{window,var} + c_{window,fix} \right) \cdot sa_{window}^{bldg} \quad (5)$$

$comp \in \{wall, roof, floor\}, \forall bldg \in BS, \forall rm \in RM$

$$LCOSH_{rm}^{bldg} = \frac{c_{rm}^{bldg} \cdot ann}{\Delta SH_{rm}^{bldg}} \quad (6)$$

$\forall bldg \in BS, \forall rm \in RM$

Using the Levelised Cost Of Saved Heat (LCOSH), calculated according to eq. (6), and the amount of saved heat per m^2 ΔSH of the respective retrofit measures, retrofit weightings are calculated. In addition, the age of the building is considered in selecting the buildings to be renovated, analogous to determining the initial residential building stock. Based on these weightings, a multinomial distribution is used to identify the buildings that go through a retrofit cycle in the respective simulation year and to determine the retrofit depth of the measure undertaken eq. (7).

$$X_{rm}^{bldg} \sim M(P_1(LCOSH_{rm1}^{bldg}, \Delta SH_{rm1}^{bldg}, c_{Y_{rm1}^{bldg}}), P_2(\cdot), P_3(\cdot)) \quad (7)$$

$\forall bldg \in BS$

Subsequently, based on the simulated distribution and age of the HRUs in 2020, the future distribution of HRUs is calculated using target shares from selected national scenarios for the future representative years of consideration. For the dissemination of the HRU systems, it is assumed that they are only installed in newly built or well-insulated buildings with a maximum wall U-value of 0.3 W/($m^2 \cdot K$).

The iterative process for simulating the dissemination of heating technologies in the future local building stock is described in Fig. 3.

Information about the local building stock, future heat generation technology shares from national scenarios, historical heating technology transition rates, and assumptions regarding local modernisation rates are required as input parameters. Historical heating technology transition rates are derived from BDEW [35]. The probabilities for a heating technology transition are calculated based on the heating technology type and age (w_{age}) as well as historical transition rates (w_{hr}). In addition, information on the time of retrofit from previous calculation steps (w_{tor}) and technology-specific requirements (w_{tsr}) (e.g. heat pumps can only be installed in buildings with a space heating demand < 120 kWh/ m^2/a) are taken into account. Furthermore, in areas where many buildings already have a district heating connection, the probability of a connection to the district heating network increases in proportion to the number of already installed connections (w_{dh}). Consequently, the probability of a heating technology change $P_{ht,old/new}^{bldg}$ is calculated according to eq. (8) for all buildings and all possible new heating technologies. Based on these transition probabilities and the assumed annual modernisation rate, the multinomial distribution described in eq. (9) is parameterized for each building of the local building stock.

$$P_{ht,old/new}^{bldg} = w_{age} \left(age_{ht,old}^{bldg}, type_{ht,old}^{bldg} \right) \cdot w_{hr} \left(type_{ht,old}^{bldg}, type_{ht,new}^{bldg} \right) \cdot w_{tor} \left(ry_{bldg} \right) \cdot w_{tsr} \left(type_{ht,new}^{bldg}, SH_{bldg}^{bldg} \right) \cdot w_{dh} \left(type_{ht,new}^{bldg}, loc_{bldg} \right) \quad (8)$$

$\forall bldg \in BS, \forall ht_{new} \in HT$

$$X_{ht,old/new}^{bldg} \sim M \left(P_{ht,old/new1}^{bldg}, \dots, P_{ht,old/new19}^{bldg}, P_{ht,old/old}^{bldg} \right) \quad (9)$$

$\forall bldg \in BS$

Starting from the initial heating technology transition distribution parameterized in eq. (9), the iterative process described in Fig. 3 occurs. The heating technologies in the existing building stock and the newly added heating technologies in the newly constructed buildings are calculated in annual steps up to the following reference year (e.g., 2030/40/50 in Fig. 3). The dissemination of the heating technologies in newly constructed buildings follows the trends in the existing building stock. Further, it considers optional higher requirements, e.g., installation bans (e.g., no new heating systems based on fossil fuels). The calculated shares of heating technologies in the reference year are compared with the target distributions of heating technologies in the reference years derived from the national scenarios considering the local initial state. An error in the form of a mean absolute error (MAE) is calculated based on the deviations of the distributions. Based on the heating technology-

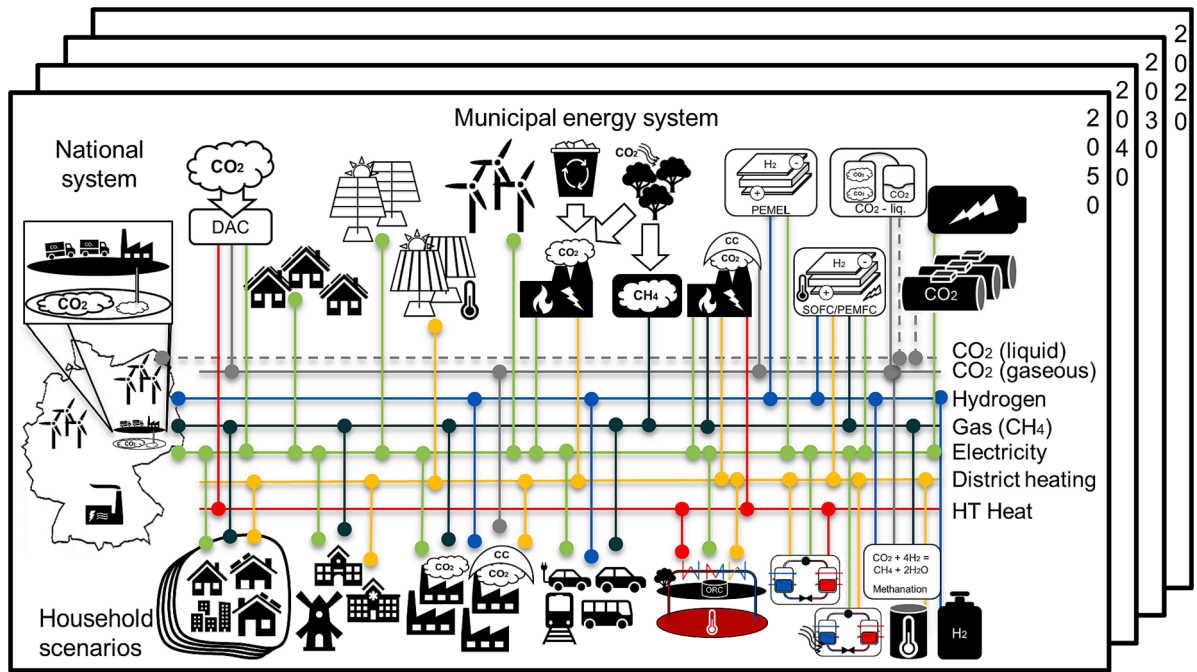


Fig. 4. Visualisation of the technology options and energy carrier flows considered in the municipal energy system optimisation and representation of the exchange flows with the national energy system.

specific deviations, the historical transition rates w_{htr} are adjusted and the heating technology transition is calculated in an iterative way till the MAE reaches a pre-defined threshold. If, due to the local characteristics of the building stock, the MAE does not fall below the specified threshold, the algorithm stops after a certain number of iterations without improvement.

The dissemination of cooling devices in the form of air conditioners in the local residential building stock is implemented in the model based on the scenarios defined by Kenkmann et al. [37]. Two scenarios for the penetration of air conditioning systems in the household sector are analysed (low: ~ 14 %, high: ~25 % of households use ACs). As in Kenkmann et al. [37], the severity of the scenarios depends negatively on the assumed retrofit rate (range of retrofit rate: 1 %/a – 2.5 %/a). Furthermore, it is assumed that ACs are mainly installed in well-renovated buildings and that, on average, 50 % of the living area is cooled [37].

3.2.1.3. Residential building technology design and operation. For the appropriate dimensioning of the heating technologies, the design heat load is calculated based on DIN EN 12831 [38], taking into account the thermal standards of the building envelope. The design heat load ensures the required heat demand can be provided even at the lowest winter temperatures without solar and internal gains. Combined heat and power plants (CHP) and solar thermal plants (ST) are not designed to cover 100 % of the heating demand. The size of the CHP is determined by using a target number of full load hours (5000 h/a) according to BKWK [39], assuming that the CHP is operated in a heat-driven way. The solar thermal systems are designed depending on the available roof area and type of use (combined plant or only for DHW).

Technical parameters from the technical reports of the Danish Energy Agency are used for the simulation of the technology operation [40]. The coefficient of performance of the heat pumps is calculated in hourly resolution depending on the heat source temperature (outside air or geothermal heat) and the heat sink temperature. The heat sink temperature depends on the outside temperature and the feed temperature of the heat distribution system, with the feed temperature being estimated depending on the age of the building [31,41]. The energy efficiency ratio (EER) of the air conditioner is determined in hourly

resolution depending on the outside temperature and is calculated according to the procedure presented by Meissner et al. [42] and Cherem-Pereira and Mendes [43], with the future development of the EER being assumed analogous to Kenkmann et al. [37]. For the simulation of the thermal energy supply of the solar thermal systems, the irradiation is calculated for all roof areas of the local building stock. Therefore, based on satellite data, all useable roof areas are identified using the method presented in Mainzer et al. [98]. Representative area orientations are determined using the k-means method based on azimuth and inclination. Radiation simulations are then carried out for the representative areas with the PV-Lib [97]. The heat supply for all solar thermal systems is calculated based on the method presented by Lindberg et al. [44].

3.2.2. Industry, tertiary and transport sector transformation

For the design of the municipal energy system, the transformation of the final energy demand in the sectors of industry, tertiary and transport needs to be considered. Due to the greater heterogeneity of demand in contrast to the household sector, publicly available data from the SolidEU scenario of the ExtremOS project is used [45]. In contrast to the presented household model in Section 3.2.1 the ExtremOS data are provided by a top-down approach that disaggregates national energy demand to all European NUTS3 regions. The data are available in hourly resolution differentiated by the final energy source and the individual sectors. Furthermore, the demand transformation from the initial state in 2020 to 2050 is provided in five-year steps. The final energy demand is available for the weather year 2012. In order to analyze the energy system transition for different weather years, the final energy demand is adapted to different years based on the daily temperature $temp_d$ and day categories dc of the target year eq. (10, 11). The days are divided into the categories Monday to Thursday, Friday, Saturday, and Sunday/holiday.

$$\min \left(temp_{d_i}^{ref} - temp_{d_i}^{target}, \dots, temp_{d_{365}}^{ref} - temp_{d_i}^{target} \right) \quad (10)$$

$$\forall i \in [1, 365]$$

$$s.t. \quad dc_{d_i} = dc_{d_i} \quad (11)$$

3.3. Energy supply transformation

The base model RE³ASON [18] is further extended to include all relevant technologies considered in the national energy system transformation studies discussed in Section 7.1 in the Appendix (see *National energy system transformation*). Integrated technologies in the base model are wind turbines, rooftop photovoltaic (PV) systems, biomass technologies, natural gas CHPs, lithium-ion batteries, and deep geothermal power plants. The procedure for the transferrable determination of the local renewable potentials for wind turbines, rooftop PV, and biomass systems is based on local land use potentials based on Open Street Map and satellite data and is described in detail in Mainzer [18]. The transferrable methodology for determining the geothermal potential and implementing the simultaneous heat and power generation from geothermal plants is described in Weinand et al. [15,46].

The energy system model is expanded as part of this study to include all technology options and energy carrier flows shown in Fig. 4. Based on the potential for freestanding PV determined at the NUTS3 level in Ebner et al. [47] the available area potential A^f in the respective NUTS3 region is deduced. Thereby, the land use competition is considered for the expansion of freestanding PV and solar thermal plants according to eq. (12). Optimisation variables are presented in bold. $P_{i,a}^{PV}$ describes the capacity of freestanding PV installed in year a , from investment interval i with a specific area consumption of A_i^{PV} . $A_{i,a}^{ST}$ describes the installed solar thermal area in year a from the investment interval i .

$$\sum_i P_{i,a}^{PV} \cdot A_i^{PV} + \sum_i A_{i,a}^{ST} \leq A^f \quad (12)$$

$\forall a \in A$

To cover the future demand for hydrogen in the industrial, transport and energy sectors, the model includes the possibility of importing or generating hydrogen in an electrolyser using locally generated electricity and storing it in pressure storage tanks. Furthermore, investing in a methanation plant to convert hydrogen and CO₂ into synthetic natural gas is possible. The required CO₂ can be captured by investing in carbon capture (CC) systems to upgrade CHPs or directly from the atmosphere by investing in direct air capture systems (DAC). In addition to electricity, heat at a temperature level of ~ 100 °C is required to operate a low-temperature DAC system [48]. Three sources can provide high-temperature heat (>100 °C). The engine exhaust of a CHP can be recovered, which has a higher specific heat content than the engine jacket water, intercooler and lubricating oil [49]. The extraction of heat at high and low-temperature levels ($Q_{t,a}^{CHP, temp, high}$, $Q_{t,a}^{CHP, temp, low}$) and the provision of electricity $P_{t,a}^{CHP, el}$ taking into account the respective efficiencies η of the CHP is shown in eq. (13) for every timestep t in every year a .

$$\begin{aligned} P_{t,a}^{CHP, el} + Q_{t,a}^{CHP, temp, low} + Q_{t,a}^{CHP, temp, high} = \\ P_{t,a}^{Gas} \cdot (\eta^{CHP, el} + \eta^{CHP, temp, low} + \eta^{CHP, temp, high}) \end{aligned} \quad (13)$$

$\forall t \in T, \forall a \in A$

A heat pump can be used to upgrade heat from low-temperature heat sources. If available, the local district heating network can be used so that the inlet temperature $temp_{in}$ of the heat pump would be set equal to the temperature of the district heating network $temp_{dh}$. If there is no district heating network, ambient heat can be used as a heat source ($temp_{in} = temp_{amb}$). According to eq. (14), together with the exergetic efficiency η_{exergy} of the heat pump, the ratio between the electrical power $P_{t,a}^{HP}$ and the thermal output $Q_{t,a}^{HP}$ of the heat pump is defined.

$$Q_{t,a}^{HP} = \frac{temp_{out}}{temp_{out} + temp_{in}} \cdot \eta_{exergy} \cdot P_{t,a}^{HP} \quad (14)$$

$\forall t \in T, \forall a \in A$

Furthermore, a geothermal power plant can be built in municipalities with geothermal potential. For achievable hydrothermal temperature

levels above 100 °C, the implementation of the geothermal power plant presented in Weinand et al. [15] is expanded to include the possibility of extracting high-temperature heat according to eq. (15) and eq. (16). The geothermal heat can be used at different temperature intervals to generate high-temperature heat $Q_{t,a}^{GT, temp, high}$, electricity $P_{t,a}^{GT, ORC}$ and low-temperature heat $Q_{t,a}^{GT, th}$ during operation. For this purpose, the model distinguishes between four different temperature levels ($temp_{t,a}^{GT, pw}$: production well temperature, $temp_{t,a}^{GT, temp, high}$: geothermal high-temperature heat, $temp_{t,a}^{GT, ORC, out}$: organic rankine cycle outlet temperature, $temp_{t,a}^{GT, inject}$: geothermal injection temperature). The energy balance for heat extraction for the district heating network (eq. (17)) is identical to Weinand et al. [15].

$$\frac{Q_{t,a}^{GT, temp, high}}{\eta_{th, temp, high}} = \dot{V}_B \cdot \rho_w \cdot c_{p,w} \cdot (temp_{t,a}^{GT, pw} - temp_{t,a}^{GT, temp, high}) \quad (15)$$

$\forall t \in T, \forall a \in A$

$$\frac{P_{t,a}^{GT, ORC}}{\eta_{el, ORC}} = \dot{V}_B \cdot \rho_w \cdot c_{p,w} \cdot (temp_{t,a}^{GT, temp, high} - temp_{t,a}^{GT, ORC, out}) \quad (16)$$

$\forall t \in T, \forall a \in A$

$$\frac{Q_{t,a}^{GT, th}}{\eta_{th, dh}} = \dot{V}_B \cdot \rho_w \cdot c_{p,w} \cdot (temp_{t,a}^{GT, ORC, out} - temp_{t,a}^{GT, inject}) \quad (17)$$

$\forall t \in T, \forall a \in A$

The maximum volumetric flow rate \dot{V}_B of the geothermal plant, the specific heat capacity of the geothermal water $c_{p,w}$ as well as the water density ρ_w are assumed analogously to Weinand et al. [15].

Due to the large number of technology options in which the optimiser can invest in the representative years and the associated large number of (structural) binary decision variables that are required, for example, for the operation of the geothermal plant (see Weinand et al. [15]), the MILP optimisation model cannot be solved in a reasonable time in closed form over several years in hourly time resolution. To reduce the complexity of the optimisation problem, the time series aggregation method presented in Kotzur et al. [50,51] is integrated into RE³ASON and used in this study, which was specially developed for energy system optimisation problems with time-coupling restrictions. The optimal choice of structure variables is determined in the first optimisation step based on the aggregated time series structure. In a second optimisation step, the operation for the structural design from the first optimisation step is then optimized based on the disaggregated time series structure (similar procedure to Bahl et al. [52] and Kotzur [31]). By integrating the time series aggregation into the workflow of the transferrable methodology presented, the complexity of the optimisation model can be adapted to the available computing resources with little effort, taking into account a slightly reduced computational accuracy (depending on the considered system components [50]). The MILP optimisation problems in this study are solved using the Gurobi solver and a relative MIP gap of 0.5 %. All underlying basic constraints of the RE³ASON optimisation model, such as hourly energy balances, capacity expansion constraints through, e.g., space restriction or state of charge equations of storage technologies can be found in Weinand et al. [17] and Mainzer [18].

4. Case study

To illustrate the methodology presented, an exemplary case study for the Central European city of Karlsruhe in Germany is carried out. Karlsruhe is a city of approximately 308,000 inhabitants whose final energy demand can be divided nearly equally between the household (24 %), industry (26 %), tertiary (24 %) and transport (26 %) sectors [53,54]. A district heating network utilizes waste heat from industrial processes (61 %), CHP (18 %) and a gas-fired heating plant (21 %) to

Table 3

Definition of the parameter ranges for the calculated household sector scenarios. (*: “CN-gas”, **: “CN-electricity”, nc: new construction, cr: conventional retrofit, ar: ambitious retrofit).

| Parameter | Parameter range | | | | | | | | | |
|---------------------------|-----------------|------------------|------------------|-----------------|----------|------|-----|----------------------------------|-----|--|
| Retrofit rate | 20–30 | 1 | 1.33* | 1.66** | 2 | 1.33 | 1.5 | 2 | 2 | |
| [% _{bidg} /a] | 30–40 | 1 | 1.33* | 1.66** | 2 | 1.66 | 2 | 3 | 1.5 | |
| | 40–50 | 1 | 1.33* | 1.66** | 2 | 1.66 | 2 | 3 | 1.5 | |
| | U-values | Roof | 0.15/0.15/0.13** | 0.17/0.17/0.13* | IWU [29] | | | | | |
| (nc/cr/ar) | Wall | 0.16/0.16/0.14** | 0.20/0.20/0.18* | | | | | (building type and age-specific) | | |
| | Window | 0.80/0.80/0.70** | 1.00/1.00/0.80* | | | | | | | |
| | Floor | 0.22/0.22/0.20** | 0.26/0.26/0.23* | | | | | | | |
| HRU | – | 21* | | | | | | 37** | | |
| [% _{bidg,2050}] | | | | | | | | | | |
| Target share heat system | Gas boiler | 2** | | | 12.33 | | | 22.66 | 33* | |
| [% _{bidg,2050}] | Heat pump | 70** | | | 57.66 | | | 45.33 | 33* | |

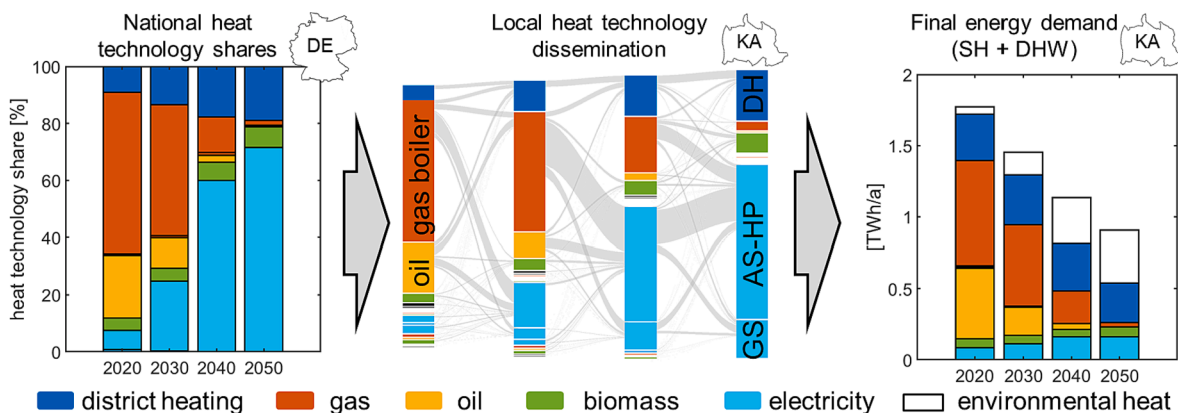


Fig. 5. Visualisation of the calculation steps for simulating the local final energy demand development of the residential building sector for the municipality of Karlsruhe (KA).

supply 25 % of the dwellings in Karlsruhe with district heating in 2020 [55,56]. The energy supply side is characterized by relatively high solar irradiation (1187 kWh/m²/a; German average 1122 kWh/m²/a) and a high potential for geothermal plants due to high achievable hydrothermal temperatures (130–160 °C) [15,57]. Karlsruhe is used as a convenience sample, and further validation of the results of this case study is planned in follow-up work in cooperation with local energy utility companies and infrastructure analysts as part of the research project mentioned in the acknowledgment.

The framework conditions for the case study are presented in Section 4.1. Subsequently, the transformation of the local household sector, a significant model input for the municipal energy system optimisation, is discussed in Section 4.2. Finally, Section 4.3 analyzes the municipal energy system, considering the transformation of sector-specific demand and local renewable potential.

4.1. Economic, environmental and technological framework conditions

The exogenous parameters specified in this study concerning energy carrier import/export price and emission development, CO₂ price development and assumptions regarding grid usage fees for transmission networks have a major impact on the decentralisation or centralisation of future local energy supply. Based on the studies described in the Appendix (see *National energy system transformation*), the framework conditions from Sensfuß et al. [58] are taken for the development of energy carrier prices and emissions as well as for CO₂ emission certificate prices. The reason for choosing the framework parameters of Sensfuß et al. [58] is the high transparency and temporal resolution of, e. g., electricity prices compared to the studies with the target of achieving climate neutrality in 2045. In addition to importing CO₂-emitting energy carriers before achieving climate neutrality in 2050, the local energy

planner is provided with the possibility of importing emission-free carbon-based energy carriers in the form of synthetic methane and Fischer-Tropsch Fuel at import prices according to Hampf et al. [59]. Future developments of technology parameters and price developments are assumed according to the technical reports of the Danish Energy Agency [60]. Size-independent and size-dependent prices for investments in heating technologies are assumed analogous to Kotzur [31].

4.2. Household sector transformation

To illustrate the interactions between the local building sector and the national energy system, 192 transformation scenarios for the local residential building sector of the municipality Karlsruhe in Germany are calculated according to Fig. 2. The scenarios differ in terms of the retrofit rate (8x), the level of the target U-values of retrofit measures (3x), the dissemination of heat recovery units (2x), and the dissemination of the heating system technologies (4x). The definition of the range of the parameters in Table 3 is inspired by the national scenarios “Climate-neutral (CN)-gas” and “CN-electricity” by Sensfuß et al. [58]. In comparison to the “CN-gas” scenario, the “CN-electricity” scenario has a more ambitious yearly retrofit rate and retrofit depth (lower U-values) as well as higher heat pump shares in the future building stock. The future achievable retrofit rate is one of the most frequently discussed parameters in building stock studies, as discussed in the Appendix (see *National energy system transformation*). Consequently, the influence of the retrofit rate is particularly examined by considering a wide range of possible future developments between the investigated representative years. Intermediate heating technology dissemination scenarios are determined by interpolation between the two extreme scenarios. When determining the future retrofit depths (U-values), a distinction is made between three scenarios in which achievable U-values for new

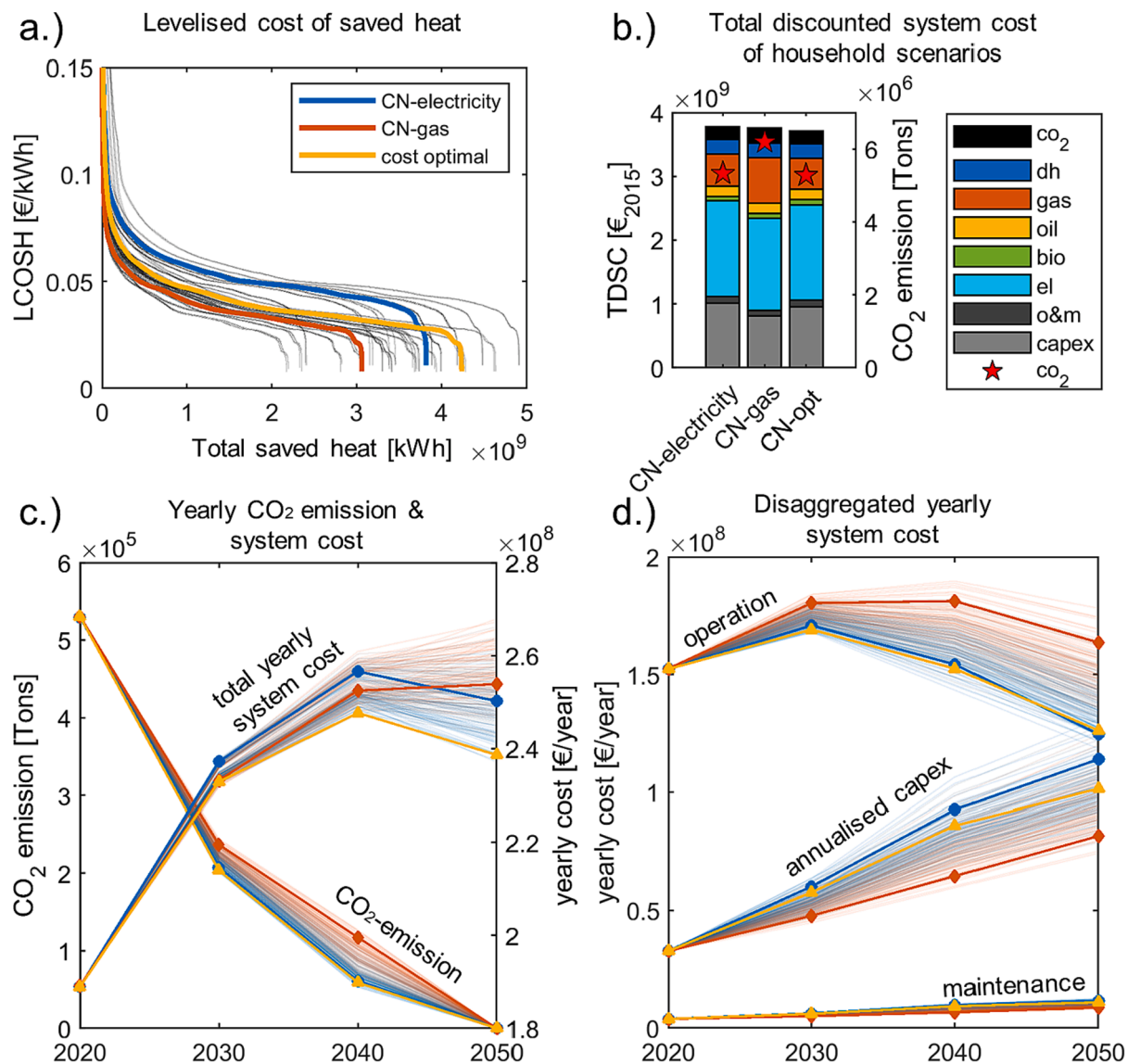


Fig. 6. Comparison of the 192 residential building stock transformation scenarios for the municipality of Karlsruhe regarding a.) the Levelised cost of saved heat, b.) total discounted system cost and CO₂ emission as well as their temporal occurrence c.), d.).

constructions (nc) as well as conventional (cr) and ambitious retrofit (ar) measures are defined (cf. Table 3).

Fig. 5 shows the results of the calculation of the final residential energy demand development for space heating (SH) and domestic hot water (DHW) in Karlsruhe for the “CN-electricity” scenario, one of the 192 different scenarios. Based on the superordinate national transformation of the heating system technology stock, the transformation of the heating technologies in the local building stock is derived. The case study presented here shows a future modernisation rate of 3 %/year between 2020 and 2030, based on empirically derived historical modernisation rates [30], and an increase of 4 %/year between 2030 and 2050 is assumed in all scenarios. The “CN-electricity” scenario shown in Fig. 5 is based on a strong increase in the share of heat pumps in the national building stock, especially between 2030 and 2040, which cannot be fully achieved in the local building stock due to the local conditions and the assumed maximum achievable modernisation rate. Therefore, an increased local expansion of heat pumps is seen between 2040 and 2050. In the described scenario, the final energy demand for space heating and hot water is reduced by 48 % between 2020 and 2050. While oil and gas provided around 69 % of the final energy in the initial state in 2020, in 2050 there is only a small share of gas boilers left in the

local building stock and the majority of the buildings are supplied by heat pumps and district heating systems, which cover for 88 % of final energy demand (environmental heat for heat pumps included).

In contrast to the “CN-electricity” scenario, Fig. A10 describes the developments of the local building stock for the “CN-gas” scenario. The share of heat pumps in 2050 is significantly lower in the “CN-gas” scenario compared to the “CN-electricity” scenario. Due to the lower retrofit rate of 1.33 % per year, the lower requirements for the retrofit measures in the form of less ambitious U-values and an assumed weaker dissemination of heat recovery units in contrast to the “CN-electricity” scenario, a reduction in final energy demand of 36 % is reached in the period from 2020 to 2050. While the share of synthetically produced natural gas in the “CN-electricity” scenario falls to around 3 %, the gas share in the “CN-gas” scenario is significantly higher at 40 % in 2050.

In the following, the scenarios “CN-gas” and “CN-electricity” are compared with the other 190 scenarios. Fig. 6 a.) shows the levelised cost of saved heat (LCOSH) through wall, roof, floor and window retrofit measures against the respective saved heat for space heating over the entire period of consideration (2020 till 2050). The LCOSH is calculated according to eq. (5) and (6) assuming an interest rate of 5 %/a and a retrofit measure lifetime of 40 years for all components. Only energy-

Table 4

Quantification of the effects of individual energy system transformation measures on TDSC and CO₂ emissions. The changes are made exclusively for the individual scenarios and therefore do not affect each other.

| Measure | ΔTDSC [M€] | ΔCO ₂ [kt] | ΔTDSC / ΔCO ₂ | Measure | ΔTDSC [M€] | ΔCO ₂ [kt] | ΔTDSC / ΔCO ₂ |
|------------------------------|------------|-----------------------|--------------------------|----------------------------------|------------|-----------------------|--------------------------|
| b1) 10 % faster PV expansion | -12.7 | -36 | 349 | b5) retrofit rate 2 → 1 %/a | 6.7 | 200 | 34 |
| b2) no wind turbine | 1.0 | 6 | 183 | b6) household elec. → gas | 1.4 | 652 | 2 |
| b3) no biomass | 17.9 | 409 | 44 | b7) -1Mt CO ₂ | 9.2 | -1000 | -9 |
| b4) no geothermal | 7.5 | 61 | 124 | b8) -1Mt CO ₂ w/o DAC | 48.1 | -1000 | -48 |

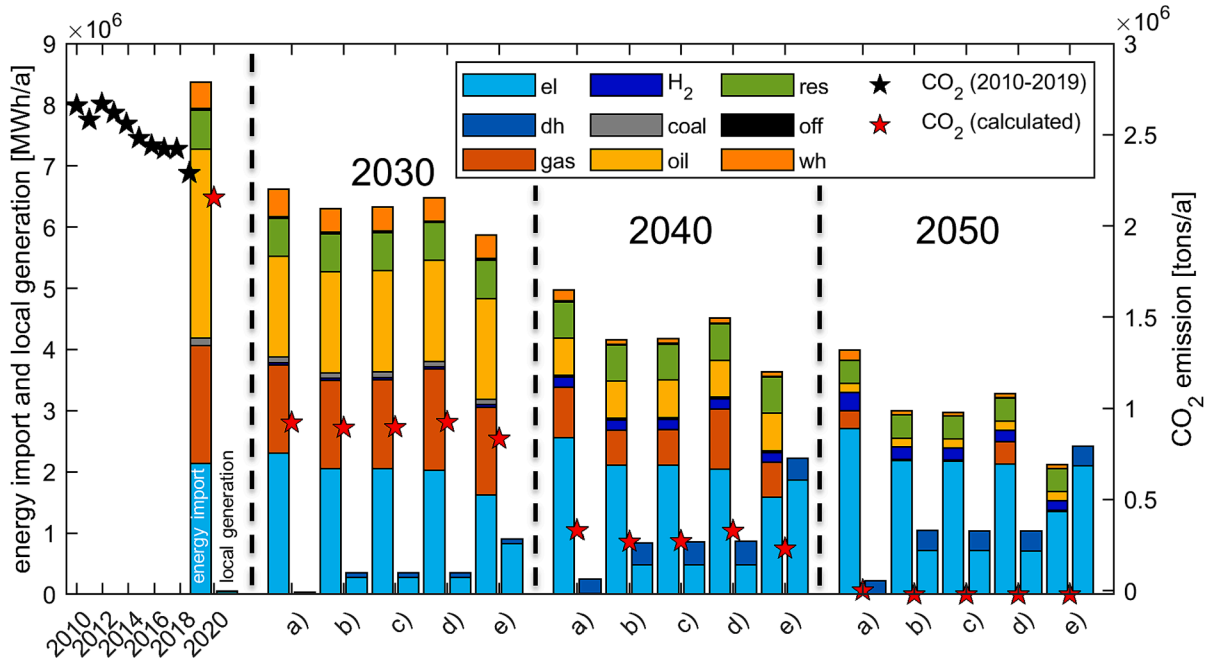


Fig. 7. Visualisation of the development of energy carrier imports, local generation of electricity and district heating, and the development of CO₂ emission for Karlsruhe. Historical CO₂ emissions are shown until 2019 [55,56].

related additional costs are considered, according to Hinz [36]. Due to the low retrofit rate of 1.33 %/a in the “CN-gas” scenario and the less ambitious retrofit depth compared to the “CN-electricity” scenario, the total saved heat is 20 % lower in the “CN-gas” scenario. The energy-weighted average LCOSH in the “CN-gas” scenario (0.039 €/kWh) is 0.014 €/kWh lower in comparison to the LCOSH in “CN-electricity” scenario (LCOSH 0.053 €/kWh). On the one hand, the lower LCOSH can be explained by the selection of the buildings that go through a retrofit cycle (selection according to eq. (7)). Buildings with low LCOSH and high specific heat savings are given preference for retrofit. Therefore, the 0.33 % of the additional buildings retrofitted in the “CN-electricity” scenario tend to have higher LCOSH than the first 1.33 %. On the other hand, the more ambitious U-values in the “CN-electricity” scenario mean that more heat is saved per retrofit. However, the marginal utility of a retrofit decreases with increasing retrofit depth.

Fig. 6 b.) compares the total discounted system cost (TDSC) and the energy-related CO₂ emissions of the local building sector transformation for the “CN-electricity” and “CN-gas” scenarios and the scenario with the lowest TDSC “CN-opt”. The TDSC consists of capital expenditures (CAPEX) in retrofit measures (wall, roof, ...) as well as heating/cooling systems (heat pump, boiler, ...), expenses for the maintenance of the technologies (O&M) and expenses for the procurement of energy carriers and the purchase of CO₂ emission certificates. The prices for the procurement of energy carriers are composed of the market prices and the network charges for transmission and distribution (see Table A6). Further levies and taxes are not taken into account due to the perspective of a central municipal planner. In contrast to the network charges

for gas and electricity grids shown in Table 4, which represent average grid charges across all sectors (industry, tertiary, household), household sector-specific network charges are used here according to BEE [61]. The household-specific charges are further differentiated and reduced network charges for power-to-heat applications are assumed for the heat pump electricity demand [61]. Under the defined framework conditions, the TDSC of the “CN-gas” scenario is 0.6 % lower than the TDSC of the “CN-electricity” scenario, whereas the cumulated CO₂ emissions in the observation period in the “CN-electricity” are over 14 % lower. The composition of the TDSC shows that the capex in the “CN-electricity” scenario is 20 % higher than the capex of the “CN-Gas” scenario due to the higher retrofit activities, the increased expansion of heat pumps and HRU, whereby the costs for the procurement of energy carriers are 7 % higher in the “CN-gas” scenario. The “CN-opt” scenario shows a substantial heat pump expansion as in the “CN-electricity” scenario. In contrast to the “CN-electricity” scenario the retrofit rate is increased from 1.66 %/a to 2 %/a, and the retrofit depth is reduced to the level of the “CN-gas” scenario.

Fig. 6 c.) shows the temporal development of the total annual system costs and the energy-related CO₂ emissions caused by the residential building sector. The color of the background scenarios is chosen depending on the heating technology dissemination (four degrees of differentiation), whereby red is chosen for scenarios with a high proportion of gas boilers (analogous to “CN-gas”) and blue for scenarios with a high proportion of heat pumps (analogous to “CN-electricity”). Fig. 6 d.) presents the development of the annual total costs of the residential building sector, differentiated according to cost type. The three

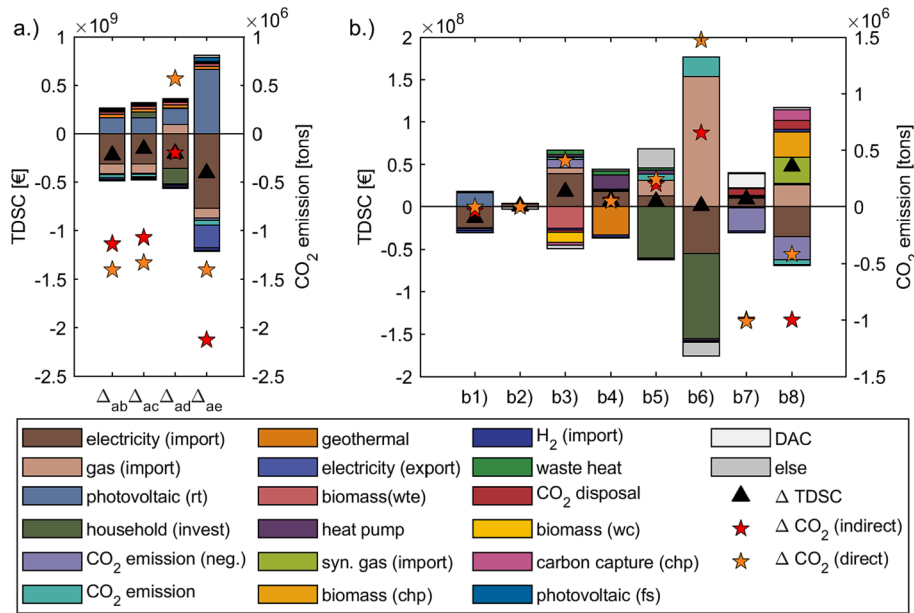


Fig. 8. a.) Illustration of the differences in TDSC and CO₂ emissions without local energy system expansion (a) and with local energy system expansion (b,c,d,e). b.) Visualisation of the differences in TDSC and CO₂ emissions of the measures presented in Table 4. When balancing indirect CO₂ emissions, the emissions from the upstream chain are taken into account, while direct emissions describe emissions caused by local combustion of carbon-based energy carriers.

Table A5

Comparison of studies from 2021 to achieve climate neutrality at the German and European level (GHG: greenhouse gas, CN: climate neutrality).

| Study | Scenario name | Objective | Scope | Openly available data resolution |
|-------|-------------------------------|-----------|-------|----------------------------------|
| [45] | solidEU | GHG -95 % | EU | High (spatial/temporal/sectoral) |
| [58] | TN-PtG/PtL, TN-Strom, TN-H2-G | CN 2050 | DE | High (temporal/sectoral) |
| [74] | KN2045 | CN 2045 | DE | Aggregated (sectoral) |
| [75] | KN100 | CN 2045 | DE | Aggregated (sectoral) |
| [76] | Zielpfad | CN 2045 | DE | - |
| [77] | KSG 2045 | CN 2045 | DE | Aggregated (sectoral) |

exemplary scenarios are highlighted in the foreground, while the spread of the 192 scenarios is shown in the background. All scenarios show an increase in costs between 2020 and 2040. The main reasons for the increase are: On the one hand, the increase in procurement prices for energy sources (including CO₂ emission price) (see operation in Fig. 6 d.) and on the other hand, the increase in costs associated with investments in the building envelope and heating technology

modernisation. While the increase in procurement prices is mainly reflected in the scenarios with a high proportion of gas boilers and a lower retrofit rate, the increase in the scenarios with a high proportion of heat pumps and higher retrofit rates is more driven by the capital expenditures, especially between 2030 and 2040. The difference in the course of the total system costs between the “CN-opt” scenario and the “CN-electricity” scenario can be explained by the lower renovation depth and the less extensive expansion of HRUs and the energy carrier costs saved due to the higher retrofit rate. The delta in saved CO₂ emissions is particularly evident in the year 2040 between the scenarios and can be explained by the faster reduction of the CO₂ emission factor of the electricity mix (30 g/kWh CO₂ emission) compared to the gas mix (150 g/kWh CO₂ emission) of the national energy system in 2040.

4.3. Municipal energy system transformation

The transformation of the local energy system is based on the sector-specific final energy carrier demand developments and the local potential for the expansion of renewable energies. The energy demand development of the four demand sectors in Karlsruhe up to the year 2050 can be found in Fig. A11. While the optimisation model for the

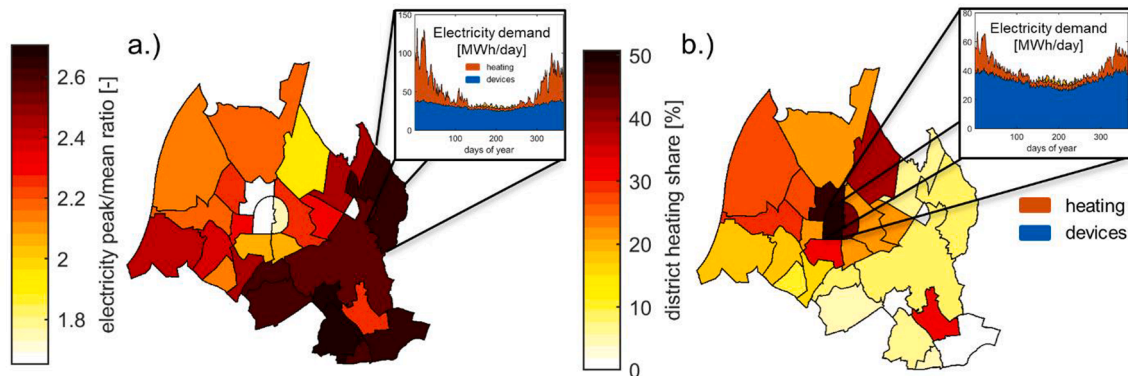


Fig. A9. Exemplary visualisation of the spatial and temporal resolution of the residential demand for electricity and district heating in the “CN-electricity” scenario in 2050.

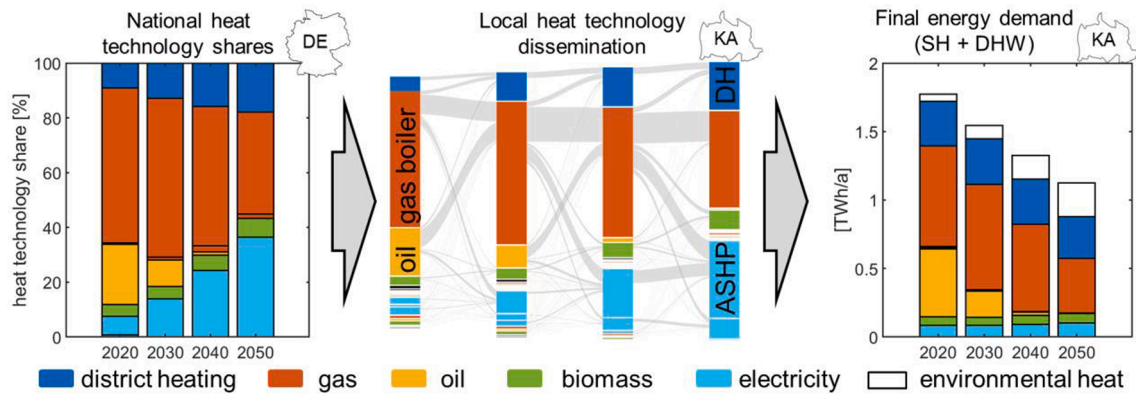


Fig. A10. Visualization of the calculation steps for the simulation of the local final energy demand development of the residential building sector for the municipality of Karlsruhe.

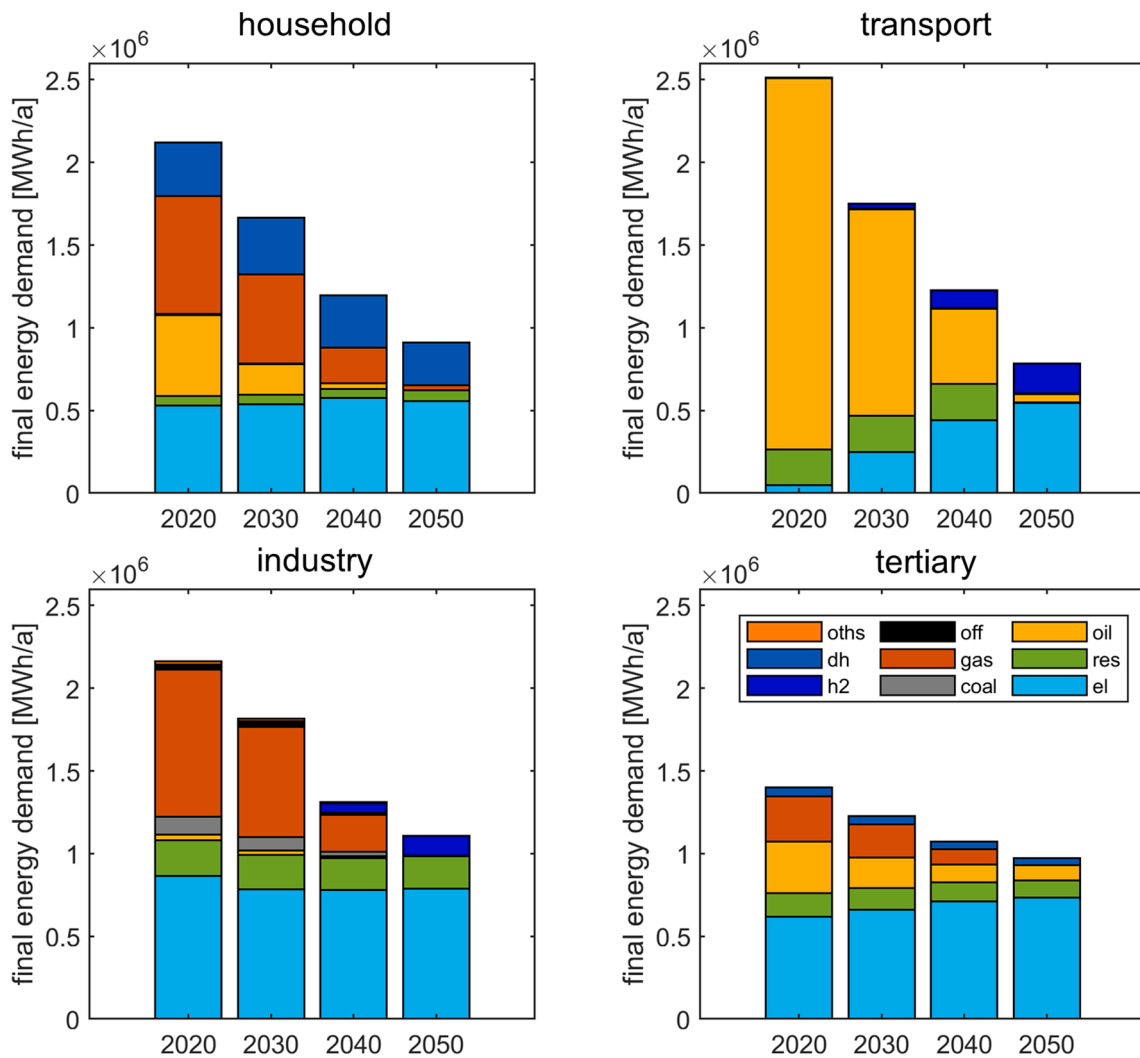


Fig. A11. Sector-specific final energy demand development for the municipality of Karlsruhe. The developments for the industrial, tertiary and transport sectors are based on [90–92] and were adapted to the weather conditions of the weather year (2017) on which this study is based, by using the procedure presented in Section 3.2.2. As an example for the 192 transformation scenarios of the household sector, the development of the final energy demand of the “CN-electricity” scenario is presented.

transformation of the household sector is given a choice between one of the 192 transformation scenarios, the demand developments in the industrial, tertiary and transport sectors are fixed.

To cover the final energy demand, energy carriers can be imported

from the higher-level national energy system, or locally self-generated electricity, heat and renewable gases can be used. The local potentials for biomass plants and rooftop photovoltaic systems can be found in Fig. A12 and Fig. A13 in the Appendix. Besides the fully transferable

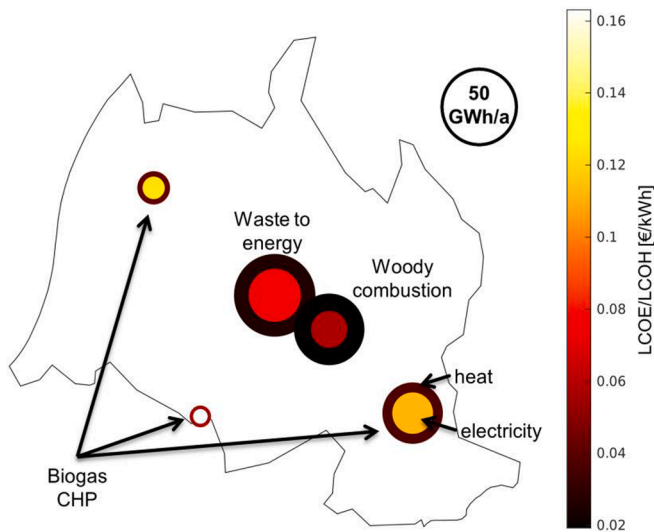


Fig. A12. Spatial representation of the biomass plant locations and the potentials for electricity and heat generation, as well as the LCOE and LCOH associated with the generation for the municipality of Karlsruhe. The calculation of the LCOE and LCOH is based on an interest rate of 5 %/a and an assumed system lifetime of 20 years. The potentials are calculated based on the procedure presented in [18].

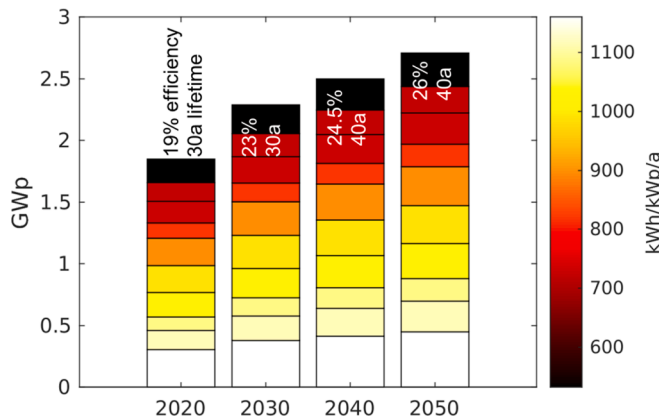


Fig. A13. Development of the potential for rooftop photovoltaic systems in the municipality of Karlsruhe, calculated based on the procedure described in Section 3.2.1.

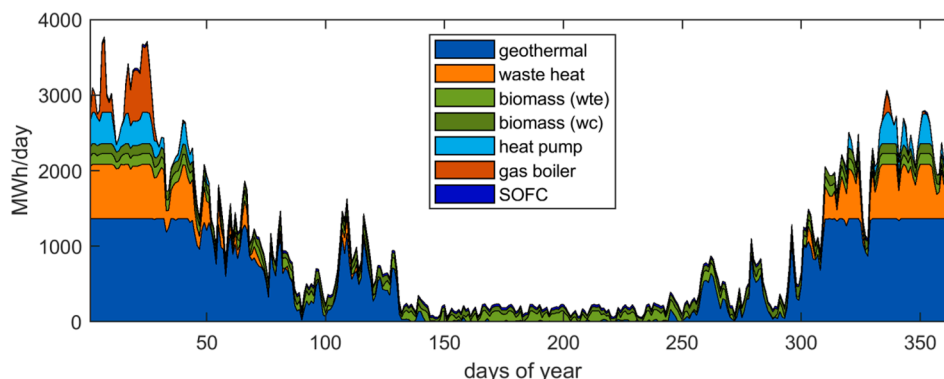


Fig. A14. Daily composition of district heating supply in the year 2050 in scenario b) of Fig. 7.

methods, one manual specification is made to consider the local waste heat supply. Local sources of waste heat can be integrated into the model by specifying the heat output and the temporal availability of the waste heat sources. Karlsruhe’s primary sources of waste heat are a refinery with a waste heat potential of 90 MW and the waste heat from a coal-fired power plant with a waste heat potential of 220 MW [55,56]. In this study, it is assumed that both waste heat sources will be available until 2035. From 2022, the waste heat from a paper factory is also considered in the model with an assumed heat output of 30 MW and availability over the entire observation period of the study [55,56].

Furthermore, Karlsruhe is located in the Upper Rhine Graben and has a high geothermal potential. Hydrothermal temperatures between 130 and 160 °C can be reached at a drilling depth below 5000 m [15]. Furthermore, a technical potential for the installation of one wind turbine exists.

Five different transformation scenarios a)-e) are discussed in detail in the following (Fig. 7). In scenarios b), c) and d) the yearly expansion capacity of photovoltaics is restricted to avoid unrealistic high expansion rates compared to nationwide photovoltaic expansion. Therefore, local expansion rates for rooftop and freestanding photovoltaics are derived from the PV expansion rates calculated in the national scenarios $exp_{PV,i}^{nat}$ from Section 7.1 in the Appendix (rooftop (rt) PV: 6 GW/a, freestanding (fs) PV: 10 GW/a). The locally required expansion rate $exp_{PV,i}^{loc}$ is derived as a function of the share of the technical photovoltaic potential $pot_{PV,i}^{loc}$ of the municipality to be examined in comparison to the national potential $pot_{PV,i}^{nat}$ according to eq. (18).

$$exp_{PV,i}^{loc} = \frac{pot_{PV,i}^{loc}}{pot_{PV,i}^{nat}} \cdot exp_{PV,i}^{nat} \quad (18)$$

$i \in \{rt, fs\}$

In scenario e) the upper boundary for the rooftop and freestanding photovoltaic expansion is removed.

Starting from 2020, Fig. 7 presents five transformation scenarios (a-e). In scenario a) the local renewable expansion of the energy system is permitted. In scenarios b), c) and d) the local energy system is expanded in a cost-optimal way, but the household scenarios are predetermined (b) “CN-opt”, c) “CN-electricity”, d) “CN-gas” (regarding Section 4.2)). While in scenarios b), c) and d) the yearly expansion capacity of photovoltaic plants is restricted, this restriction is removed in scenario e) in comparison to scenario b). All transformation scenarios shown in Fig. 7 reach zero or negative CO₂ emissions in 2050. Even in scenario a) without local energy system expansion, zero CO₂ emissions are achieved since energy carrier imports are CO₂ neutral in 2050 (see Table A6). The TDSC associated with scenario a) are higher than scenarios b) to e) with local energy system expansion. By expanding the local energy system, the TDSC and CO₂ emissions can be reduced by 222 M€ and 1.14 kt over the observation period (see Δ_{ab} in Fig. A10 a.). While the energy imports and CO₂ emissions differ in scenarios b) to d) due to the different

Table A6

Overview of the framework conditions for energy carrier procurement prices, grid charges and emission factors based on [58,61,59,96]. A cost increase of 2 %/a is assumed for the grid charges of the gas network.

| Procurement [€/MWh] | Electricity | Gas | H ₂ | Coal | Oil | Biomass | Synthetic gas | Fischer Tropsch Fuel | CO ₂ [€/ton] |
|---|-------------|-----|----------------|------|-----|---------|---------------|----------------------|-------------------------|
| 2020 | 34 | 37 | 111 | 3.6 | 32 | 50 | 140 | 260 | 25 |
| 2030 | 65 | 36 | 101 | 6.4 | 35 | 70 | 120 | 230 | 75 |
| 2040 | 68 | 36 | 91 | 6.25 | 40 | 100 | 110 | 180 | 125 |
| 2050 | 56 | 31 | 81 | – | – | 130 | 94 | 162 | – |
| Grid charges [€/MWh] | | | | | | | | | |
| 2020 | 37 | 10 | 10 | – | – | – | 10 | – | – |
| 2030 | 36 | 12 | 12 | – | – | – | 12 | – | – |
| 2040 | 36 | 15 | 15 | – | – | – | 15 | – | – |
| 2050 | 31 | 18 | 18 | – | – | – | 18 | – | – |
| CO₂ emission factor [g/kWh] | | | | | | | | | |
| 2020 | 430 | 190 | 0 | 374 | 260 | 0 | 0 | 0 | – |
| 2030 | 110 | 170 | 0 | 374 | 230 | 0 | 0 | 0 | – |
| 2040 | 30 | 150 | 0 | 374 | 190 | 0 | 0 | 0 | – |
| 2050 | 0 | 0 | 0 | – | – | 0 | 0 | 0 | – |

household transformation scenarios, local electricity and district heating generation expansion is comparable. In all three scenarios, the potential for wind power and photovoltaics is fully exploited considering the maximum yearly expansion rates explained above (PV (rt): 16.7 MW_p/a, PV (fs): 1.8 MW_p/a).

Furthermore, investments in biomass plants for the energetic use of waste and wood residues are undertaken in the first investment period between 2020 and 2030 and are further equipped with carbon capture devices from 2040 on. On the other hand, biogas upgrade plants are only built in the last investment period between 2040 and 2050. While the generated biogas is used directly to cover the gas demand in scenario d), in scenarios b) and c) a Solid Oxygen Fuel Cell (SOFC) CHP plant is built to provide heat to the district heating network and electricity to the local grid. After discontinuing the two primary waste heat sources, from 2035 scenarios b) to e) rely on geothermal energy, waste heat from biomass plants and local waste heat from the paper factory to cover the base load of the district heating network. A heat pump in combination with a gas boiler is used to cover the heat peaks (see Fig. A14). By removing the annual maximum expansion capacity in scenario e), the optimal local average expansion rate between 2020 and 2050 is 3.3 times faster than the photovoltaic expansion rate of the national system. To increase self-consumption, Lithium-ion batteries are installed from 2040 on. Through the extreme expansion of photovoltaics, TDSC and indirect CO₂ emissions can be further reduced by reducing external electricity purchases in 2030 and 2040 (see Fig. 8 a)).

In other scenarios, the effects of individual measures on the TDSC and CO₂ emissions of the local energy system transformation are quantified in Table 4 and visualized in Fig. 8b.). Scenario b) is taken as the initial scenario (see Fig. 8) and additional measures are defined or excluded based on this scenario. The ratio between Δ TDSC and Δ CO₂ describes the economic and ecological efficiency of the individual measures. If the ratio is positive, the measure has a clear positive or negative impact on TDSC and CO₂ emissions. If the ratio is negative, no clear statement can be made about both factors. The impacts of measures b1) to b6) are unambiguous. Increasing the local expansion rate of photovoltaics by 10 % compared to the national expansion rate lowers costs and CO₂ emissions. The photovoltaic expansion has high economic efficiency when comparing the efficiency ratio of measure b1) with the other measures. On the other hand, measure b6) which describes the change from a heat supply in the household sector with high proportions of heat pumps (see Fig. 5) to a scenario with higher proportions of gas boilers (see Fig. A10) is particularly ecologically efficient, but does not make a big difference when considering the TDSC. When biomass plants are excluded, these are partly replaced by heat pumps and gas-fired CHPs, while large-scale heat pumps exclusively replace the geothermal plant. If, in comparison to scenario b), additional 1 Mt CO₂ emissions have to be reduced, this is done as in measure b7) by a low-

temperature direct air capture (DAC) plant. The DAC plant is installed in 2050 and captures CO₂ out of the atmosphere by using high-temperature heat (100 °C) from the geothermal plant and electricity as input. Subsequently, the captured CO₂ is liquefied, transported and stored long-term. The basis for the economic evaluation is a CO₂ price of 150 €/t and costs of 40 €/t for the transport and final storage of CO₂ in 2050 [62]. If DAC is excluded as an investment option (measure b8)), synthetic carbon-neutral gas imports achieve the reduction in CO₂ emissions in 2040 and increased carbon capture of exhaust gases from the SOFC plant in 2050.

5. Discussion and outlook

To adequately account for temporal dynamic developments in municipal energy system transformation scenarios, the present study extends an existing municipal energy system optimization approach by a stochastic bottom-up residential building stock model. In contrast to the adopted approach from [18,15,16,17], in which investment decisions in retrofit and other efficiency measures for individual representative buildings are determined within the energy system optimisation model, the investment decisions in the present study are determined outside of the municipal optimisation in a stochastic simulation for every residential building of the municipality. While the approach presented in [18,15,16,17] allows to make optimised investment decisions for individual representative buildings, it is not possible to adequately consider the dynamic changes in the residential building stock, as already a small number of representative buildings leads to long model runtimes. Due to the simplified representation of only a few representative buildings, the model does not consider upper limits for maximum practicable retrofit and technology modernization rates, which means that the entire building stock can be modernized from one year to the next. In our approach, dynamic processes are considered in an upstream simulation model in the form of annually feasible retrofit and technology modernization rates. Furthermore, future heating technology transformations are implemented, taking into account the characteristics of the local residential building stock and future target states from national scenarios. By shifting the optimization decision away from representative buildings to choosing between different residential building stock transformation scenarios, temporal dynamic transformation processes are now considered in the optimization model. As a result of the simulation, the building retrofit status and the technological equipment are available for each building and each simulation year so that infrastructure simulations for electricity, gas or district heating networks can be carried out based on the results of this study.

The simulation decision as to whether a building undergoes a retrofit cycle in a specific year is based on technical parameters such as building age and potentially saved heat and economic parameters such as the

LCOSH of the retrofit measure. Thereby, the aim is to assist local decision-makers in identifying buildings in need of retrofit from a techno-economic point of view to develop support measures depending on the building owner structures. Another approach would be to consider the ownership structure when selecting the buildings that go through a retrofit cycle [63]. Similar factors could also be considered in future work when deciding to modernize heating technologies. However, this would require further spatially high-resolution information on ownership structures and empirical information about owner dependent investment preferences.

The residential building stock scenarios presented in this study are derived based on four core trends regarding the retrofit rate, depth, technology dissemination and HRU uptake. Other potentially relevant trends, such as changes in behavior, e.g., in the form of increased work from home, such as in the COVID-19 pandemic, or the impact of climate change on future heating and cooling demand are not considered in this work. While short-term changes in behaviour during the COVID-19 pandemic led to shifts in energy demand [64,65], long-term behavioural changes are uncertain. Therefore, the simulation of the occupant behavior of the individual households, which is the basis for the simulation of the household appliances and the thermal building demand, is based on historical time-use survey data (see *Residential energy demand simulation* in the Appendix). In future analyses, the potential influence of behavioral changes on the structure of the energy demand profile could be examined by adjusting the underlying time-use survey data based on projected socio-demographic scenarios. In contrast to long-term behavioral changes, the influence of climate change on energy demand, energy generation and energy infrastructure is undisputed [66,67,68]. However, in this study we decided to analyze the effects of the four core trends mentioned above independently of climate change based on an average historical weather year (2017). In follow-up studies, the impact of climate change could be integrated by using high resolution climate projection datasets from, e.g., the EURO-CORDEX project [69]. Especially, high-probability, low-impact conditions should be considered in future energy system design studies since they can significantly impact renewable energy integration levels and system cost [67].

The results of the household sector transformation of the case study for the municipality of Karlsruhe show that under the assumed economic framework conditions, a substantial electrification of the heat supply with a high proportion of heat pumps and an annual retrofit rate of 2 %/a together with less ambitious U-value requirements lead to the lowest TDSC and CO₂ emissions. Scenarios with high U-value requirements and high proportions of HRU lead to higher TDSC. This means that the marginal cost of saving the last few kWh is higher than the cost per kWh of heat supplied. It must be considered here that only energy-related additional costs are used for the economic evaluation of the efficiency measures (full cost considerations would increase the effects described) and only the costs for generation, transport and CO₂ certificates are included for the purchase of energy carriers. Microeconomic assessments of the efficiency measures from a building owner perspective can come to different conclusions if household procurement costs for energy carriers are considered. A real interest rate of 5 %/a is used for all investment decisions in this study. Investments in retrofit measures with high initial costs and long lifetimes would be valued even more favourably if interest rates were assumed to be lower. Furthermore, when interpreting the results, it must be considered that they are subject to many uncertainties with regard to assumptions about the development of energy carrier prices, technology efficiency and price developments.

The results of the municipal energy system optimisation show that, from the point of view of a central social planner, the expansion of local renewable energies is advantageous for reducing overall system costs and minimizing local emissions: a significantly faster expansion of local photovoltaic potentials compared to national expansion scenarios leads to reductions in TDSC. This could be partly explained due to the

optimistic assumptions regarding the development of the technological efficiency of photovoltaics (see Fig. A13), which is based on the [60]. Furthermore, it should be considered that this study does not examine any effects of the local energy system transformation on the national energy system and that, therefore, the local feed-in has no influence on market pricing. If many municipalities would increase variable renewable expansion, the market value of renewable feed-in could be reduced, which could have a feedback on investment decisions. Since network restrictions in the energy distribution networks are not considered in this study, further analysis should be conducted to determine whether the energy system expansion determined in this work can be implemented, taking local infrastructures into account.

While most of the analysed technologies are already established on the market, technologies such as direct air capture are still in the development stage and should therefore be viewed critically when planning future energy systems. The model presented in this work optimizes the local energy system transformation under perfect foresight. Thus, anticipated certain future developments by the optimizer, which are based on assumptions with a high degree of uncertainty, can lead to misleading decisions. Technologies that are still under development, such as direct air capture technologies, should not be used as an excuse to emit more emissions today to offset these emissions in the future.

In Karlsruhe, after the waste heat from the local refinery and the coal-fired power plant is taken out of the system in 2035, a geothermal power plant is built, which, together with the waste heat from the paper factory and the biomass plants, covers the base load of the district heating demand. While the local waste heat sources still have to be provided manually, methods for the automated identification of waste heat potentials should be integrated in the future. While waste heat potentials are currently only considered in the form of available power, in the future, different temperature levels should also be included in the model for more efficient heat integration. A useful database for this is the district heating atlas [70], which tries to collect scarce public information on district heating systems to provide it on a central platform. While scenario independent district heating transmission costs are assumed in the current study, the existing model could also be expanded to include various district heating expansion scenarios with different grid fees. For this, however, approaches for the industrial and tertiary sectors would first have to be developed that assign the process-dependent useful heat demand of the sectors to the respective locations of the non-residential buildings, as is the case in the residential building sector. Furthermore, future studies could analyse the impact of low temperature district heating networks in combination with booster heat pumps in order to use heat sources more efficiently and to minimize heat transfer losses in the district heating network [71,72].

In addition, for the industrial, tertiary and transport sectors, only developments with a high degree of electrification based on the solidEU scenario from Guminski et al. [45] are taken into account in this study. Scenarios with higher shares of hydrogen or synthetic hydrocarbons in the future final energy demand of the respective sectors could lead to different expansion strategies of the local energy system and should be analysed in the future.

While a holistic validation of energy system optimizations for future developments is challenging, we have performed plausibility checks and validations of interim results. For example, the amount of residential buildings in the single districts from OpenStreetMap deviates by about 10 % from empirical data. Furthermore, the final energy demand of this study's household sector simulation of 2.1 TWh/a in 2020 is comparable to results from other studies, with 2.0 TWh/a [54] and 2.5 TWh/a [45]. The difference to the higher value of Guminski et al. [45] can be explained by the different balancing approach, which also incorporates environmental heat. In addition, as presented in Fig. 7, the initial calculated CO₂ emissions in 2020 are in line with historical data [55,56]. The future development of the total final energy demand across all sectors deviates from the local climate protection concept by only about 5 % in the reference years considered [54]. In order to further improve

the accuracy of the initial state of the spatial heating system distributions in future studies, updated data from the 2021 census should be used as soon as it is published. The restriction to purely publicly available input data can lead to buildings being assigned to grid-dependent energy carriers without having a connection to the respective grid infrastructure since detailed information about the energy supply networks is not publicly accessible. Additional location specific information about the energy carriers used for heating in the upcoming census [73] will help reduce incorrect assignments. When further using the results of this study in downstream analysis, the accuracy of the publicly available data basis should be considered with regard to the question to be examined. If necessary, the underlying data should be enriched with expert data, e.g., in the case of detailed power flow calculations.

6. Conclusion

Given the constantly changing political framework conditions for achieving increasingly ambitious climate protection goals, decision support tools are needed that can easily identify local conditions and support local decision-makers in the formulation of energy system transformation strategies.

This study extends the highly transferable energy system optimisation model RE³ASON to consider temporally dynamic transformation processes of the local energy system supply and demand side in line with national greenhouse gas mitigation strategies. To capture dynamic temporal developments and the high heterogeneity of the local residential building stock, an existing energy system model is extended by an upstream dynamic building stock transformation model. By considering higher-level framework parameters from national scenarios and local initial building stock conditions, multiple household transformation scenarios can be calculated and further used as input in an energy system optimisation. To comprehensively consider the transformation of local energy demand and supply transformation, RE³ASON is further extended to include the final energy demand transformation of the industry, tertiary, and transport sectors and a variety of additional greenhouse gas reduction technologies in combination with maximum yearly expansion rates. By the integration of a two-step optimisation approach we demonstrated that the formulated optimisation problem can be solved in hourly resolution.

192 building stock transformation scenarios are calculated for an exemplary case study of the German city of Karlsruhe. The results show that for the cost-minimal transformation of the local building sector, the retrofit rate should be increased to 2 %/a and that, in addition to significantly lower CO₂ emissions, scenarios with high shares of heat pumps can be economically advantageous compared to scenarios with

Appendix

National energy system transformation

In 2021 alone, a large number of studies on the transformation of the German energy system in order to reach climate-neutrality were published (Table A5). The first two studies were published before the amendment of the German Climate Protection Act in 2021 and are therefore not aiming for the goal of climate neutrality in 2045. The solidEU (solidarity in the EU) scenario is a holistic European energy system scenario to reduce greenhouse gas emissions in Europe by 95 % compared to 1990 levels [45]. Sectoral, national, or interim targets in 2030 are not taken into account in this scenario. In contrast to all other studies, the results of the European scenarios are presented in a scenario explorer and relevant interim results, such as final energy demand or CO₂ emissions of the individual sectors with high temporal and spatial resolution are provided. The study by Sensfuß et al. [58] compares three alternative scenarios intending to reach climate neutrality in the year 2050. The three scenarios differ in terms of their pronounced use of the main energy sources, electricity, hydrogen, and synthetic hydrocarbons. A large number of detailed results for the three scenarios, such as electricity price time series, and year-specific costs and emission factors of energy carriers are provided via an extensive scenario explorer.

The bottom four scenarios in Table A5 all aim to achieve GHG neutrality in Germany by 2045 [74,75,76,77]. They agree regarding the massively accelerated expansion of renewable energies on- and offshore and a rapid increase in energy efficiency, especially in the building sector. However, there is disagreement about what level of insulation needs to be reached to become climate neutral. Furthermore, technologies for capturing and geological storage of CO₂ are used in all scenarios to achieve negative GHG emissions. In contrast to the first two studies, the results of the latter studies are not openly available with high temporal and geographical resolution.

high shares of gas boilers, despite higher capital expenditures. The municipal energy system transformation results show that an accelerated expansion of photovoltaics compared to the national reference system can be economically advantageous and leads to lower CO₂ emissions. By considering anticipated transformations, e.g., the discontinuation of local waste heat sources, it is shown that local biomass and geothermal potentials are used to cover the base load of district heating demand, while large-scale heat pumps and gas boilers are used during peak times.

In future work, the integration of the process-specific useful energy demand in the industry, tertiary and transport sectors is planned to better take into account local flexibility and waste heat potentials. Furthermore, transferable infrastructure models for the electricity, gas and district heating networks are developed to verify the feasibility of the calculated scenarios.

CRedit authorship contribution statement

Max Kleinebrahm: Conceptualization, Methodology, Formal analysis, Visualization, Project administration, Data curation, Software, Validation, Writing - original draft, Writing - review & editing. **Jann Weinand:** Conceptualization, Methodology, Formal analysis, Funding acquisition, Writing - original draft, Writing - review & editing. **Elias Naber:** Formal analysis, Writing - review & editing. **Russell McKenna:** Writing - review & editing, Formal analysis. **Armin Ardone:** Funding acquisition, Writing - review & editing.

Declaration of Competing Interest

The authors declare that they have no known competing financial interests or personal relationships that could have appeared to influence the work reported in this paper.

Data availability

Data will be made available on request.

Acknowledgement

This work was supported by the German Federal Ministry for Economic Affairs and Climate (BMWK) through the TrafoKommune project (funding reference: 03EN3008F). We gratefully acknowledge the contributions of Sebastian Soldner, who further developed the presented energy system optimisation model as part of his Master's Thesis at KIT.

Urban building energy modelling

Urban building energy models (UBEM) can be categorized into top-down and bottom-up approaches, while bottom-up models can be further classified into physics-based, data-driven, and reduced-order methods [78,79]. Bottom-up models, are needed to assess the impact of certain retrofit measures among groups of (archetype) buildings [78]. Reduced-order models contain a physical representation of the building while being computationally efficient and easy to parameterise based on archetype information [80]. Therefore, this study uses a reduced-order bottom-up approach, since it fits best the requirements of a highly transferable approach, which is operating in a low data environment. The use of more advanced physics-based models, which require more advanced input data and more computational power, would only lead to a higher pseudo-accuracy due to the initial data situation. In comparison to physics- and reduced-order based approaches, data-driven bottom-up approaches do not contain a physical representation of the building to estimate the energy consumption, but learn a function for the prediction of energy consumption based on information such as available building stock data, billing data or socio-economic indicators [80]. Data-driven methods therefore require a training data set, on the basis of which they can learn the connection between building properties, local weather conditions and energy demand. Since such a dataset is not available, data-driven methods are not suitable for the approach presented in this study.

Residential energy demand simulation

Based on the parameterized building stock, the demand for useful energy for household electricity devices, domestic hot water and space heating is calculated in an hourly resolution based on a similar approach to Kotzur et al. [81]. Therefore, the CREST model developed for the UK for simulating residential electricity demand based on occupant behavior is parameterized with data on the behavior of German residents and German household device information [82,83,84,85,86]. Considering the local weather conditions based on ERA5 reanalysis data [57], occupancy profiles, domestic hot water and electrical appliance demand profiles are generated for 1000 households of different household sizes in the municipality under consideration. The marginal utility of each additional profile decreases as the average profile of the individual households comes very close to the H0 standard load profile (representative electricity demand profile for German households) between 100 and 1,000 households [87,31,88]. The 1,000 households are then assigned to the households in the municipality by stochastic sampling, taking into account the household size.

The thermal demand for space heating is calculated based on a 5R1C model from DIN EN ISO 13790 [89], using the internal gains from the household simulation and the thermal building parameters of the TABULA residential building typology [29]. Since municipalities can be composed of a large number of residential buildings and the simulation of each individual building can take a lot of time and computational resources, it is possible to identify representative buildings based on the k-means cluster method before performing the thermal simulation of each individual building. For this purpose, the residential buildings are divided into clusters based on the features of building type, building age, living space, number of apartments, number of occupants and state of retrofit. Thermal simulations are only carried out for the buildings closest to the respective cluster centers.

Spatiotemporal household energy demand development

The bottom-up structure of the simulation of the energy demand development in the residential building sector enables spatiotemporal analysis within the municipality. To calculate the results shown in Fig. A9, the final energy demand of the geo-allocated residential buildings is aggregated at the district level. Fig. A9 a.) shows the peak to mean ratio ($r_{p/m}$) of the daily electricity demand d_{el} for the individual districts, which is calculated according to eq. (19).

$$r_{p/m} = \frac{\max(d_{el,1}, \dots, d_{el,T})}{(\sum_{t=1}^T d_{el,t})/T} \quad T = 365 \quad (19)$$

It can be seen that the electrical demand increases in winter due to the increased dissemination of heat pumps, especially in parts of the municipality where a small proportion of the buildings can be supplied with district heating (see Fig. 7 b.)). On average, across all districts, the $r_{p/m}$ increases from 1.4 in 2020 to 2.3 in 2050 in the “CN-electricity” scenario. In the “CN-gas” scenario, an $r_{p/m}$ of 1.9 is reached in 2050.

Additional tables and graphs

See Figs. A10-13.

See Table A6.

References

- [1] UNFCCC: Glasgow Climate Pact. Glasgow Climate Change Conference - October/November 2021; 2021. Available online at <https://unfccc.int/documents/311127>.
- [2] Victoria M, Zhu K, Brown T, Andresen GB, Greiner M. Early decarbonisation of the European energy system pays off. *Nature Commun* 2020;11(1):6223. <https://doi.org/10.1038/s41467-020-20015-4>.
- [3] Bundesregierung (Ed.). Klimaschutzgesetz 2021. Generationenvertrag für das Klima; 2021. Available online at <https://www.bundesregierung.de/breg-de/themen/klimaschutz/klimaschutzgesetz-2021-1913672>.
- [4] Marinakis V, Doukas H, Xidonas P, Zopounidis C. Multicriteria decision support in local energy planning: An evaluation of alternative scenarios for the Sustainable Energy Action Plan. *Omega* 2017;69:1–16. <https://doi.org/10.1016/j.omega.2016.07.005>.
- [5] Weinand JM. Reviewing Municipal Energy System Planning in a Bibliometric Analysis: Evolution of the Research Field between 1991 and 2019. *Energies* 2020; 13(6):1367. <https://doi.org/10.3390/en13061367>.
- [6] Weinand JM, McKenna R, Mainzer K. Spatial high-resolution socio-energetic data for municipal energy system analyses. *Sci Data* 2019;6(1):243. <https://doi.org/10.1038/s41597-019-0233-0>.
- [7] Weinand JM, McKenna R, Fichtner W. Developing a municipality typology for modelling decentralised energy systems. *Utilities Policy* 2019;57:75–96. <https://doi.org/10.1016/j.jup.2019.02.003>.
- [8] Thellufsen JZ, Lund H, Sorknæs P, Østergaard PA, Chang M, Drysdale D, et al. Smart energy cities in a 100% renewable energy context. *Renew Sustain Energy Rev* 2020;129:109922. <https://doi.org/10.1016/j.rser.2020.109922>.
- [9] Thellufsen, Jakob Zinck; Lund, Henrik. Roles of local and national energy systems in the integration of renewable energy. *Appl Energy* ; 2016;183:pp.419–429. <https://doi.org/10.1016/j.apenergy.2016.09.005>.
- [10] McKenna R, Bertsch V, Mainzer K, Fichtner W. Combining local preferences with multi-criteria decision analysis and linear optimization to develop feasible energy concepts in small communities. *Eur J Oper Res* 2018;268(3):1092–110. <https://doi.org/10.1016/j.ejor.2018.01.036>.
- [11] Østergaard, Poul; Mathiesen, Brian Vad; Möller, Bernd; Lund, Henrik. A renewable energy scenario for Aalborg Municipality based on low-temperature geothermal heat, wind power and biomass. *Energy* 2010;35(12):4892–4901. <https://doi.org/10.1016/j.energy.2010.08.041>.

- [12] Østergaard, Poul Alberg; Lund, Henrik. A renewable energy system in Frederikshavn using low-temperature geothermal energy for district heating. *Appl Energy* 2011;88(2):479–487. <https://doi.org/10.1016/j.apenergy.2010.03.018>.
- [13] Sveinbjörnsson, Dadi; Ben Amer-Allah, Sara; Hansen, Anders Bavnhøj; Algren, Loui; Pedersen, Allan Schröder. Energy supply modelling of a low-CO₂ emitting energy system: Case study of a Danish municipality. *Appl Energy* 2017;195: 922–941. <https://doi.org/10.1016/j.apenergy.2017.03.086>.
- [14] Hansen K, Breyer C, Lund H. Status and perspectives on 100% renewable energy systems. *Energy* 2019;175:471–80. <https://doi.org/10.1016/j.energy.2019.03.092>.
- [15] Weinand, Jann Michael; McKenna, Russell; Kleinebrahm, Max; Mainzer, Kai. Assessing the contribution of simultaneous heat and power generation from geothermal plants in off-grid municipalities. *Appl Energy* 2019d;255:113824. <https://doi.org/10.1016/j.apenergy.2019.113824>.
- [16] Weinand, Jann Michael; Ried, Sabrina; Kleinebrahm, Max; McKenna, Russell; Fichtner, Wolf. Identification of Potential Off-Grid Municipalities with 100% Renewable Energy Supply for Future Design of Power Grids. *IEEE Trans Power Syst* 2020;1. <https://doi.org/10.1109/TPWRS.2020.3033747>.
- [17] Weinand, Jann; McKenna, Russell; Kleinebrahm, Max; Scheller, Fabian; Fichtner, Wolf. The impact of public acceptance on cost efficiency and environmental sustainability in decentralized energy systems; 2021. Cell Press Patterns.
- [18] Mainzer, Kai.: Analyse und Optimierung urbaner Energiesysteme - Entwicklung und Anwendung eines übertragbaren Modellierungswerkzeugs zur nachhaltigen Systemgestaltung; 2019, checked on 4/23/2019.
- [19] Scheller F, Bruckner T. Energy system optimization at the municipal level: An analysis of modeling approaches and challenges. *Renew Sustain Energy Rev* 2019; 105:444–61. <https://doi.org/10.1016/j.rser.2019.02.005>.
- [20] Kachirayil, Febin; Weinand, Jann Michael; Scheller, Fabian; McKenna, Russell. Reviewing local and integrated energy system models: insights into flexibility and robustness challenges. *Appl Energy* 2022;324:119666. <https://doi.org/10.1016/j.apenergy.2022.119666>.
- [21] Yazdanie M, Orehoung K. Advancing urban energy system planning and modeling approaches: Gaps and solutions in perspective. *Renew Sustain Energy Rev* 2021; 137:110607. <https://doi.org/10.1016/j.rser.2020.110607>.
- [22] Aunedj, Marko, Pantaleo, Antonio Marco, Kuriyan, Kamal, Strbac, Goran; Shah, Nilay (2020): Modelling of national and local interactions between heat and electricity networks in low-carbon energy systems. *Appl Energy* 276:115522. <https://doi.org/10.1016/j.apenergy.2020.115522>.
- [23] Trutnevte E, Stauffacher M, Scholz RW. Supporting energy initiatives in small communities by linking visions with energy scenarios and multi-criteria assessment. *Energy Policy* 2011;39(12):7884–95. <https://doi.org/10.1016/j.enpol.2011.09.038>.
- [24] Orehoung K, Evins R, Dorer V. Integration of decentralized energy systems in neighbourhoods using the energy hub approach. *Appl Energy* 2015;154:277–89. <https://doi.org/10.1016/j.apenergy.2015.04.114>.
- [25] Murray P, Orehoung K, Grosspietsch D, Carmeliet J. A comparison of storage systems in neighbourhood decentralized energy system applications from 2015 to 2050. *Appl Energy* 2018;231:1285–306. <https://doi.org/10.1016/j.apenergy.2018.08.106>.
- [26] Orehoung K, Mavromatidis G, Evins R, Dorer V, Carmeliet J. Towards an energy sustainable community: An energy system analysis for a village in Switzerland. *Energy Build* 2014;84:277–86. <https://doi.org/10.1016/j.enbuild.2014.08.012>.
- [27] Destatis. Mikrozensus - Zusatzserhebung 2010, Bestand und Struktur der Wohneinheiten, Wohnsituation der Haushalte - Fachserie 5 Heft 1 – 2010; 2012.
- [28] OSM. OpenStreetMap. Unter Mitarbeit von OpenStreetMap-Contributors; 2022. Available online at <http://www.openstreetmap.org>, checked on 3/16/2022.
- [29] Loga, Tobias; Stein, Britta; Diefenbach, Nikolaus; Born, Rolf. Deutsche Wohngebäudetypologie. Beispielhafte Maßnahmen zur Verbesserung der Energieeffizienz von typischen Wohngebäuden; erarbeitet im Rahmen der EU-Projekte TABULA - "Typology approach for building stock energy assessment", EPISCOPE - "Energy performance indicator tracking schemes for the continuous optimisation of refurbishment processes in European housing stocks". 2., erw. Aufl. Darmstadt: IWU; 2015. Available online at http://www.building-typology.eu/downloads/public/docs/brochure/DE_TABULA_TypologyBrochure_IWU.pdf.
- [30] Cischinsky H, Diefenbach N. Datenerhebung Wohngebäudebestand 2016. Datenerhebung zu den energetischen Merkmalen und Modernisierungsraten im deutschen und hessischen Wohngebäudebestand. Stuttgart: Fraunhofer IRB Verlag; 2018. Forschungsinitiative Zukunft Bau, F 3080.
- [31] Kotzur L. Future Grid Load of the Residential Building Sector. Jülich: Forschungszentrum Jülich GmbH, Zentralbibliothek, Verlag (Schriften des Forschungszentrums Jülich. checked on 4/4/2022 Reihe Energie & Umwelt, Band/volume 442) Available online at 2018. <https://user.fz-juelich.de/record/858675..>
- [32] UBA. Klimaneutraler Gebäudebestand 2050 - Energieeffizienzpotenziale und die Auswirkungen des Klimawandels auf den Gebäudebestand; 2017. Available online at https://www.umweltbundesamt.de/sites/default/files/medien/1410/publikationen/2017-11-06_climate-change-26-2017_klimaneutraler-gebäudebestand-ii.pdf.
- [33] Singhal, Puja; Stede, Jan. Wärmemonitor 2018: Steigender Heizenergiebedarf, Sanierungsrate sollte höher sein; 2019.
- [34] GENESIS. Baufertigstellungen: Errichtung neuer Wohngebäude sowie Wohnungen in Wohngebäuden – Jahresumme; 2018. Available online at URL <https://www.regionalstatistik.de/genesis/online/loqon>.
- [35] BDEW. Wie heizt Deutschland 2019? BDEW-Studie zum Heizungsmarkt; 2019.
- [36] Hinz, Eberhard. Kosten energierelevanter Bau- und Anlagenteile bei der energetischen Modernisierung von Altbauten. BMVBS. 1. Auflage. Darmstadt: Institut Wohnen und Umwelt; 2015.
- [37] Kenkmann T, Stieß I, Winger C. Entwicklung des Energiebedarfs für die Wohngebäudeklimatisierung in Deutschland 2030/2050. In *Internationale Energiewirtschaftstagung an der TU Wien*. 2019.
- [38] DIN. DIN EN 12831-1. Energetische Bewertung von Gebäuden – Verfahren zur Berechnung der Norm-Heizlast –; 2017, checked on 5/15/2018.
- [39] Bundesverband Kraft-Wärme-Kopplung e.V. (Ed.). Neue Festlegung für Vollbenutzungsstunden im KWK. Zukünftige Auslegung von KWK als stromerzeugende Heizung in der Wohnungswirtschaft; 2020. Available online at <https://www.bkww.de/auslegung-kwk/>, checked on 3/23/2022.
- [40] Danish Energy Agency. Technology Data for Heating installations (06/2021); 2021. Available online at https://ens.dk/sites/ens.dk/files/Analyser/technology_data_catalogue_for_individual_heating_installations.pdf.
- [41] Ruhnau O, Hirth L, Praktijnjo A. Time series of heat demand and heat pump efficiency for energy system modeling. *Scientific data* 2019;6(1):189. <https://doi.org/10.1038/s41597-019-0199-y>.
- [42] Meissner JW, Abadie MO, Moura LM, Mendonça KC, Mendes N. Performance curves of room air conditioners for building energy simulation tools. *Appl Energy* 2014;129:243–52. <https://doi.org/10.1016/j.apenergy.2014.04.094>.
- [43] Cherem-Pereira G, Mendes N. Empirical modeling of room air conditioners for building energy analysis. *Energy Build* 2012;47:19–26. <https://doi.org/10.1016/j.enbuild.2011.11.012>.
- [44] Lindberg, Karen Byskov; Doorman, Gerard; Fischer, David; Korpås, Magnus; Ånestad, Astrid; Sartori, Igor. Methodology for optimal energy system design of Zero Energy Buildings using mixed-integer linear programming. *Energy Build* 2016;127:194–205. <https://doi.org/10.1016/j.enbuild.2016.05.039>.
- [45] Guminski, Andrej; Fiedler, Claudia; Kigle, Stephan; Pellingner, Christoph; Dossow, Patrick; Ganz, Kirstin et al. (2021): xTremOS Summary Report. Available online at https://extremos.ffe.de/#model_landscape.
- [46] Weinand, Jann Michael; Kleinebrahm, Max; McKenna, Russell; Mainzer, Kai; Fichtner, Wolf. Developing a combinatorial optimisation approach to design district heating networks based on deep geothermal energy. *Appl Energy* 2019c; 251:113367. <https://doi.org/10.1016/j.apenergy.2019.113367>.
- [47] Ebner M, Fiedler C, Jetter F, Schmid T. Regionalized Potential Assessment of Variable Renewable Energy Sources in Europe. 18–20 September 2019. Ljubljana, Slovenia. Piscataway, NJ: IEEE; 2019. Available online at.
- [48] Deutz, Sarah, Bardow, André. Life-cycle assessment of an industrial direct air capture process based on temperature-vacuum swing adsorption. *Nat Energy*; 2021.
- [49] Rolls Royce (Ed.). Improving Energy Efficiency with CHP: How to Evaluate Potential Cost Savings; 2021. Available online at https://www.mtu-solutions.com/content/dam/mtu/download/technical-articles/21162_Improving%20Energy%20Efficiency_TA.pdf_jcr_content/renditions/original/21162_Improving%20Energy%20Efficiency_TA.pdf, checked on 3/24/2022.
- [50] Kotzur L, Markewitz P, Robinius M, Stolten D. Impact of different time series aggregation methods on optimal energy system design. *Renew Energy* 2018;117: 474–87. <https://doi.org/10.1016/j.renene.2017.10.017>.
- [51] Kotzur L, Markewitz P, Robinius M, Stolten D. Time series aggregation for energy system design. Modeling seasonal storage. *Appl Energy* 2018;213:123–35. <https://doi.org/10.1016/j.apenergy.2018.01.023>.
- [52] Bahl B, Kümpel A, Seele H, Lampe M, Bardow A. Time-series aggregation for synthesis problems by bounding error in the objective function. *Energy* 2017;135: 900–12. <https://doi.org/10.1016/j.energy.2017.06.082>.
- [53] BBSR (Ed.). Bevölkerungsprognose: Ergebnisse und Methodik. Raumordnungsprognose 2040; 2021. Available online at https://www.bbsr.bund.de/BBSR/DE/veroeffentlichungen/analysen-kompakt/2021/ak-03-2021-dl.pdf;jsessionid=0E7CFEDDC576AB5F68DF90635DB1ABEE.live21302?_blob=publicati onFile&v=4, checked on 4/21/2022.
- [54] Heinz, Matthias. Klimaschutzkonzept 2030 Karlsruhe. Zusammenfassung Potenziale und Szenarien; 2017.
- [55] Stadtwerke Karlsruhe (Ed.). Umwelterklärung 2021. Karlsruhe; 2021. Available online at https://www.stadtwerke-karlsruhe.de/wMedia/docs/service/infomaterial/publikationen/umwelterklaerungen/Umwelterklaerung_2021.pdf, checked on 4/12/2022.
- [56] Stadt Karlsruhe (Ed.). Klimaschutzkonzept 2030 – Anpassung der Klimaschutzziele. Beschlussvorlage; 2021. Available online at <https://web1.karlsruhe.de/ris/oparl/bodies/0001/downloadfiles/00634089.pdf>, checked on 4/10/2022.
- [57] Copernicus Climate Change Service. ERA5: Fifth generation of ECMWF atmospheric reanalyses of the global climate. Copernicus Climate Change Service Climate Data Store (CDS); 2017. Available online at <https://cds.climate.copernicus.eu/cdsapp>.
- [58] Sensfuß, Frank; Lux, Benjamin; Bernath, Christiane; Kiefer, Christoph; Pflüger, Benjamin; Kleinschmitt, Christoph et al. Langfristszenarien für die Transformation des Energiesystems in Deutschland 3. Kurzbericht: 3 Hauptszenarien; 2021.
- [59] Hampp, Johannes; Düren, Michael; Brown, Tom. Import options for chemical energy carriers from renewable sources to Germany; 2021. Available online at <http://arxiv.org/pdf/2107.01092v1>.
- [60] Danish Energy Agency (Ed.) (2022): Technology Data. Available online at <https://ens.dk/en/our-services/projections-and-models/technology-data>, checked on 3/25/2022.
- [61] BEE (Ed.). Neues Strommarktdesign. Neues Strommarktdesign für die Integration fluktuierender Erneuerbarer Energien. With assistance of Holger Becker, Alexander Dreher, Helen Ganal, David Geiger, Norman Gerhardt, Yannic Harms, Dr. Carsten Pape, Maximilian Pfennig, Richard Schmitz, Andrea Schön, Dr. Seba; 2021. Available online at http://klimaneutrales-stromsystem.de/pdf/Strommarktdesignstudie_BEE_final_Stand_14_12_2021.pdf, checked on 5/13/2022.

- [62] Smith E, Morris J, Khesghi H, Teletzke G, Herzog H, Paltsev S. The cost of CO₂ transport and storage in global integrated assessment modeling. *Int J Greenhouse Gas Control* 2021;109:103367. <https://doi.org/10.1016/j.ijggc.2021.103367>.
- [63] Stengel, Julian. Akteursbasierte Simulation der energetischen Modernisierung des Wohngebäudebestands in Deutschland. Zugl.: Karlsruhe, KIT, Diss., 2014. Karlsruhe, Hannover: KIT Scientific Publishing; Technische Informationsbibliothek u. Universitätsbibliothek (Produktion und Energie, 6); 2014, checked on 3/16/2018.
- [64] Buechler E, Powell S, Sun T, Astier N, Zanocco Ca, Bolorinos J, et al. Global changes in electricity consumption during COVID-19. *iScience* 2022;25(1):103568. <https://doi.org/10.1016/j.isci.2021.103568>.
- [65] Lorincz, Mate Janos; Ramfrez-Mendiola, José Luis; Torriti, Jacopo. COVID-19 lockdowns in the United Kingdom: Exploring the links between changes in time use, work patterns and energy-relevant activities. In: ECEEE Summer Study; 2022. Available online at <https://centaur.reading.ac.uk/105689/>.
- [66] Spinoni J, Vogt JV, Barbosa P, Dosio A, McCormick N, Bigano A, et al. Changes of heating and cooling degree-days in Europe from 1981 to 2100. In *Int J Climatol* 2018;38:e191–208. <https://doi.org/10.1002/joc.5362>.
- [67] Perera ATD, Nik VM, Chen D, Scartezzini J-L, Hong T. Quantifying the impacts of climate change and extreme climate events on energy systems. *Nat Energy* 2020;5(2):150–9. <https://doi.org/10.1038/s41560-020-0558-0>.
- [68] Stern PC, Sovacool BK, Dietz T. Towards a science of climate and energy choices. *Nature Clim Change* 2016;6(6):547–55. <https://doi.org/10.1038/nclimate3027>.
- [69] Bartók B, Tobin I, Vautard R, Vrac M, Jin X, Levvasseur G, et al. A climate projection dataset tailored for the European energy sector. *Climate Services* 2019;16:100138. <https://doi.org/10.1016/j.cliser.2019.100138>.
- [70] Pelda J, Holler S, Persson U. District heating atlas - Analysis of the German district heating sector. *Energy* 2021;233:121018. <https://doi.org/10.1016/j.energy.2021.121018>.
- [71] Østergaard, Poul Alberg; Andersen, Anders N. Booster heat pumps and central heat pumps in district heating. *Appl Energy* 2016;184:1374–1388. <https://doi.org/10.1016/j.apenergy.2016.02.144>.
- [72] Østergaard, Poul Alberg; Andersen, Anders N. Economic feasibility of booster heat pumps in heat pump-based district heating systems. *Energy* 2018;155:921–929. <https://doi.org/10.1016/j.energy.2018.05.076>.
- [73] Bundesamt. Zensus 2022; 2022. Available online at https://www.zensus2022.de/DE/Aktuelles/PM_Wie_wohnen_wir.html, checked on 10/30/2022.
- [74] Prognos; Öko-Institut; Wuppertal-Institut. Klimaneutrales Deutschland 2045. Wie Deutschland seine Klimaziele schon vor 2050 erreichen kann. Langfassung im Auftrag von Stiftung Klimaneutralität, Agora Energiewende und Agora Verkehrswende 2021; 2021.
- [75] EWI. dena-Leitstudie Aufbruch Klimaneutralität. Klimaneutralität 2045 - Transformation der Verbrauchssektoren und des Energiesystems. Herausgegeben von der Deutschen Energie-Agentur GmbH (dena); 2021. Available online at https://www.ewi.uni-koeln.de/cms/wp-content/uploads/2021/10/211005_EWI-Gutachterbericht_dena-Leitstudie-Aufbruch-Klimaneutralitaet.pdf.
- [76] BCG/BDI. Klimapfade 2.0 - Ein Wirtschaftsprogramm für Klima und Zukunft; 2021. Available online at https://issuu.com/bdi-berlin/docs/211021_bdi_klimapfade_2_0_-_gesamtstudie_-_vorabve.
- [77] Stolten D, Markewitz P, Schöb T, Kullmann F, Kotzur L, et al. Strategien für eine treibhausgasneutrale Energieversorgung bis zum Jahr 2045. (Kurzfassung) Forschungszentrum Jülich GmbH; 2021.
- [78] Swan LG, Ugursal VI. Modeling of end-use energy consumption in the residential sector: A review of modeling techniques. *Renew Sustain Energy Rev* 2009;13(8):1819–35. <https://doi.org/10.1016/j.rser.2008.09.033>.
- [79] Hong T, Chen Y, Luo X, Luo Na, Lee SH. Ten questions on urban building energy modeling. *Build Environ* 2020;168:106508. <https://doi.org/10.1016/j.buildenv.2019.106508>.
- [80] Ali, Usman, Shamsi, Mohammad Haris; Hoare, Cathal; Mangina, Eleni; O'Donnell, James. Review of urban building energy modeling (UBEM) approaches, methods and tools using qualitative and quantitative analysis. *Energy Build* 2021;246:111073. <https://doi.org/10.1016/j.enbuild.2021.111073>.
- [81] Kotzur, Leander; Markewitz, Peter; Robinius, Martin; Cardoso, Gonçalo; Stenzel, Peter; Heleno, Miguel; Stolten, Detlef. Bottom-up energy supply optimization of a national building stock. *Energy Build* 2019;199:667. <https://doi.org/10.1016/j.enbuild.2019.109667>.
- [82] Richardson, Ian; Thomson, Murray; Infield, David; Clifford, Conor. Domestic electricity use. A high-resolution energy demand model. *Energy Build* 2010;42(10):1878–1887. <https://doi.org/10.1016/j.enbuild.2010.05.023>.
- [83] Richardson, Ian; Thomson, Murray; Infield, David; Delahunty, Alice. Domestic lighting. A high-resolution energy demand model. *Energy Build* 2009;41(7):781–789. <https://doi.org/10.1016/j.enbuild.2009.02.010>.
- [84] Richardson I, Thomson M, Infield D. A high-resolution domestic building occupancy model for energy demand simulations. *Energy Build* 2008;40(8):1560–6. <https://doi.org/10.1016/j.enbuild.2008.02.006>.
- [85] BDEW (Ed.). Stromverbrauch im Haushalt; 2016. Available online at https://www.bdew.de/media/documents/BDEW_Stromverbrauch_im_Haushalt_Juli_2016_Charts.pdf, checked on 3/17/2016.
- [86] Destatis. Zeitbudgeterhebung: Aktivitäten in Stunden und Minuten nach Geschlecht, Alter und Haushaltstyp. Zeitbudgets - Tabellenband I. 2001/2002; 2006. Wiesbaden. Available online at https://www.statistischebibliothek.de/mir/recvie/DEMonografie_mods_00003054.
- [87] Hayn, Marian; Bertsch, Valentin; Fichtner, Wolf. Residential bottom-up load modeling with price elasticity. *IAEE*; 2014, checked on 10/24/2018.
- [88] BDEW. Standardlastprofile (SLP); 2011.
- [89] DIN EN ISO 13790, 2008; DIN EN ISO 13790, checked on 5/29/2018.
- [90] Forschungsstelle für Energiewirtschaft e. V. (Ed.). Load Curves of the Industry Sector – eXtremOS solidEU Scenario (Europe NUTS-3); 2021a. Available online at <http://opendata.ffe.de/dataset/load-curves-of-the-industry-sector-extremos-solid-eu-scenario-europe-nuts-3/>, checked on 4/9/2022.
- [91] Forschungsstelle für Energiewirtschaft e. V. (Ed.). Load Curves of the Transport Sector – eXtremOS solidEU Scenario (Europe NUTS-3); 2021c. Available online at <http://opendata.ffe.de/dataset/load-curves-of-the-transport-sector-extremos-solid-eu-scenario-europe-nuts-3/>, checked on 4/9/2022.
- [92] Forschungsstelle für Energiewirtschaft e. V. (Ed.). Load Curves of the Tertiary Sector – eXtremOS solidEU Scenario (Europe NUTS-3); 2021b. Available online at <http://opendata.ffe.de/dataset/load-curves-of-the-tertiary-sector-extremos-solid-eu-scenario-europe-nuts-3/>, checked on 4/9/2022.
- [93] Bundesamt. Zensus 2011; 2011. Available online at https://www.zensus2011.de/DE/Home/home_node.html.
- [94] Microsoft. Bing Aerial Images. Orthographic aerial and satellite imagery; 2017. Available online at <https://www.bing.com/maps/aerial>, checked on 3/17/2022.
- [95] BSW (Ed.). Anteile der Gebäude mit Pelletheuerung, Wärmepumpe oder Solarthermieanlage. Bundesverband Solarwirtschaft, Bundesverband Wärmepumpe, Deutscher Energieholz- und Pelletverband e.V.; 2016. Available online at https://www.solarwirtschaft.de/fileadmin/user_upload/DEPV_Grafik_Anteil_3Heizsysteme_D.pdf, checked on 3/17/2022.
- [96] Koch, Matthias; Hennenberg, Klaus; Hünecke, Katja; Haller, Markus; Hesse, Tilman. Rolle der Bioenergie im Strom- und Wärmemarkt bis 2050 unter Einbeziehung des zukünftigen Gebäudebestandes. Wissenschaftlicher Endbericht. Edited by Öko-Institut e. V; 2018. Available online at <https://www.oeko.de/fileadmin/oekodoc/Rolle-Bioenergie-im-Strom-Waermemarkt-bis-2050.pdf>.
- [97] Andrews, Robert W.; Stein, Joshua S.; Hansen, Clifford; Riley, Daniel. Introduction to the open source PV LIB for python Photovoltaic system modelling package. In: 2014 IEEE 40th Photovoltaic Specialist Conference (PVSC). 2014 IEEE 40th Photovoltaic Specialists Conference (PVSC). Denver, CO, USA, 08.06.2014 - 13.06.2014; IEEE; 2014. p. 170–4.
- [98] Mainzer, Kai; Killinger, Sven; McKenna, Russell; Fichtner, Wolf. Assessment of rooftop photovoltaic potentials at the urban level using publicly available geodata and image recognition techniques. *Solar Energy* 2017;155:561–573. <https://doi.org/10.1016/j.solener.2017.06.065>.